クラスター展開法を利用した新しい波動関数理論の開発とその応用

課題番号　01470008

平成1年度科学研究費補助金　（一般研究B）　研究成果報告書

平成3年3月

研究代表者　平尾公彦
（名古屋大学教養部）

研究組織

研究代表者　　平尾公彦　（名古屋大学教養部）
研究分担者　　中辻　博　（京都大学工学部）

研究経費

平成１年度	３９００千円
平成２年度	２４００千円
計	６３００千円

研究発表

1. K.Hirao, The SCF Orbital Theory. The Cluster Expansion of a Wavefunction Formalism, Self-Consistent-Field (Elsevier) 531-567 (1990)
2. K.Hirao, The Non-Closed-Shell Symmetry Adapted Cluster (SAC) Theory. The Open-Shell SAC Theory and Multi-Reference SAC Theory submitted for publication
3. H.Nakatsuji, K.Hirao and Y.Mizukami, SAC-CI and Full CI Calculations for the Singlet and Triplet Excited States of H2O, Chem.Phys.Lett. in press
4. K.Hirao, Floating Functions Satisfying the Hellmann-Feynman Theorem submitted for publication
5. K.Hirao, Analytic Derivative Theory Based on the Hellmann-Feynman Theorem submitted for publication
6. K.Hirao, Note on an Upper Bound Property of Second Derivatives of the Energy submitted for publication
7. H.Wasada and K.Hirao, Theoretical Study of the Pennta-Coordinated Trigonal Bipyramidal Compounds; PH5, PF5, PF4H, PF3H2 PF4CH3 PF3(CH3)2, P(O2C2H4)H3, P(OC3H6)H3 and PO5H4- submitted for publication
8. K.Mogi, H.Komine and K.Hirao, Theoretical Study of the N2O-HF Complexes submitted for publication

THE NON-CLOSED-SHELL SYMMETRY ADAPTED CLUSTER (SAC) THEORY. THE OPEN-SHELL SAC THEORY AND MULTI-REFERENCE SAC THEORY

K.HIRAO
Department of Chemistry, College of General Education,
Nagoya University, Nagoya, Japan
and
Institute for Molecular Science, Okazaki, Japan

ABSTRACT

The non-closed-shell version of the symmetry-adapted-cluster (SAC) theory is presented. We classified the total correlation effects into two groups, the dynamical (transferable) or specific (non-transferable) correlation effects. The specific correlation effects consist of near-degeneracies, the internal and semi-internal correlation and the spin polarization. Once specific correlation effects are included, the remaining effects are just like those in closed-shells. We started with the RHF/CASSCF orbitals but re-defined the reference function which includes the state-specific correlation effects. Specific correlation effects are expressed in the form of the linear operator and the dynamical correlation is treated by means of the exponential operator. The present theory is exact and does not include the non-commutative algebra. There is a very close parallel between the standard single reference SAC theory and its non-closed-shell version. We have discussed the open-shell (excited state) SAC theory and the SAC theory based on a multi-reference function (MRSAC). The theory provides low-lying excited state solutions as well as the ground state solution.

I. Introduction

There are three approaches to the electron correlation problems of molecules. The first method is based on the variational principle. The most commonly used variational method is the method of CI.[1] The CI has conceptual simplicity and generality. However, it suffers from the slow convergenece of the wavefunction. The second approach is the many-body perturbation theory.[2] It is a size-consistent theory. The introduction of diagrammatic analysis is a powerful way of handling and summing various types of terms in a perturbation expansion. However, the use of diagrams is only an aid. It does not alter the fact that we are doing the CI calculation, whose convergence is also slow. There is an approach which is neither variational nor perturbational. The theory is based on the cluster expansion of an exact wavefunction.[3-13] It is a size-extensive theory and the convergence of the wavefunction is much faster than that of the CI expansion.

The cluster expansion method is based on the ansatz[3]

$$\Psi = \exp(T)|0\rangle \qquad (1)$$

where $|0\rangle$ is the Hartree-Fock single determinantal reference function and T is a sum of one- to N-particle excitation operators

$$T = T^{(1)} + T^{(2)} + \ldots + T^{(N)} \qquad (2)$$

We have proposed the symmetry adapted cluster (SAC) theory.[5] The SAC

method, originally designed for closed-shell systems, has been extended to include open-shell systems. It is based on the ansatz

$$\Psi = Q\exp(S)|0> \qquad (3)$$

where S is a sum of symmetry adapted single to N-ple excitation operators

$$S = S^{(1)} + S^{(2)} \ldots S^{(N)} \qquad (4)$$

and Q is a symmetry projector which applies only to the disconnected clusters of the expansion. For singlet closed-shells, Q is not necessary. The Schrodinger equation for closed-shells is given by

$$e^{-S} H e^{S} |0> = E_g |0> \qquad (5)$$

where E_g is the ground state energy. By now the SAC approach has been well tested for numerous closed-shell ground states. The single and double SAC method, which is equivalent to the coupled-cluster method with single and double excitations (CCSD) of Bartlett,[4] recovers about 98% of the total correlation energy of a given basis set.[6]

For open-shell excited states, the SAC-CI method has been proposed.[7] The idea behind the SAC-CI theory is that the majority of the electron correlation in the closed-shell ground state will be transferable to the excited states since the excitation of interest involves only one and/or two electrons. We can express the correlated excited state wavefunction in terms of the SAC function using the excitation operator T

$$\Psi_e = T\Psi_g = T\exp(S)|0> \qquad (6)$$

The T and S operators commute each other since both are defined in the same restriction. The expression of eq.(6) is also exact if T includes all excitations. From the Schrodinger equation, we have the SAC-CI equation

$$e^{-S}[H, T]e^{S}|0> = (E_e - E_g)T|0> \qquad (7)$$

where E_e is the energy of the excited state. The SAC-CI wavefunction can be obtained only by a single diagonalization of the nonsymmetric matrix. There is no iteration involved. It is well tested that the SAC-CI with single and double excitations reproduces electronic excitation energies, ionization potentials and electron affinities within the error of 2%.[8]

The single reference cluster approach, however, breaks down when applied to the states where the restricted Hartree-Fock (RHF) function is not a good starting wavefunction. Such cases occur in many actual systems particularly at non-equilibrium geometries when the chemical bonds are broken. In such situations, the low-lying excited configurations are likely to penetrate into the range of the reference configuration energies and act as intruder states. They also occur, when we study open shells and excited states.

While the single reference cluster expansion approach has been successfully exploited during the past two decades, the extension of this formalism to non-closed-shells cannot be considered to be fully understood even today, despite siginificant theoretical progress made in recent years.[9-13] This is undoubtedly due to the inherent complexity of

the problem involved as well as to our lack of understanding of the cluster structure of general non-closed-shell wavefunctions.

In non-closed-shell systems, there are three, about equally important types of correlation effects. The exact wavefunction is expressed as

$$\Psi = \Phi_{ref} + x_{int} + x_{(semi\text{-}int\ +\ polariz)} + x_{all\text{-}ext} \qquad (8)$$

where Φ_{ref} is the reference function with including quasidegeneracies. The internal correlation x_{int} comes from the mixing of the configurations that can be made from the occupied orbitals. Semi-internal correlation $x_{semi\text{-}int}$ comes from the configurations involving the open-shell orbitals. When two electrons collide, for instance, one electron goes into the virtual space while the other remains in the occupied space. Moreover the occupied orbitals in non-closed-shells are individually polarized in excited states other than the singlet state. The one-electron polarization effect is much smaller than the other correlation effects involving pairs of electrons. The polarization effects $x_{polariz}$ are coupled by symmetry to the semi-internal correlation. Both the internal and semi-internal correlation effects are very specific in their magnitudes to each other. They depend strongly on the symmetry of the state, on the total number of electrons, etc. It is expected that once these specific correlation effects are calculated, the remaining effects become just like those in closed-shells. That is, the remaining are the all-external correlation effects $x_{all\text{-}ext}$.

The another difficulty of the non-closed-shell theory lies on the validity of the commutation property of the excitation operators.

Non-commutative algebra makes the theory very complicated and loses its conceptual simplicity. In order to retain the commutative property of all the operators, the fermion creation and annihilation operators should be defined in the same restriction. In non-closed-shells, however, there are three separate orbital spaces, the closed-shell (core), the open-shell (active) and virtual orbital spaces. The problem is what to treat the open-shell orbitals.

A general formalism of the non-closed-shell/multi-reference cluster expansion theory was given by Mukherjee et al,[9] by Jeziorski and Monkhorst,[10] by Nakatsuji,[11] and by others.[12-13] Mukherjee's theory[9] is based on the ansatz,

$$\Psi = \exp(T)\Phi_M \quad ; \quad \Phi_M = \sum C_i \psi_i \qquad (9)$$

and ψ_i are N-electron determinants. T is an excitation operator given by

$$T = t_i^a a_a^+ a_i + \frac{1}{2!} t_{ij}^{ab} a_a^+ a_b^+ a_i a_j + \ldots \qquad (10)$$

The theory is a straightforward generalization of the single reference theory. However, the theory involves non-commutative algebra for the operators and T is not unique unless some additional conditions are imposed. Jeziorski and Monkhorst[10] proposed a genuine multi-reference coupled cluster theory which is free from such difficulties. They started from the ansatz

$$\Psi_\nu = \sum C_{\nu\mu} \exp(T^\mu)\Phi_\mu \qquad (11)$$

where Φ_μ span a complete reference space within the valence orbitals. T^μ is a sum of one- to N-particle excitation operators as given by eq.(10) and is different for each reference determinant. The theory is unique and does not include the non-commutative algebra bacause of the completeness of the reference space. However, from a practical point of view, the theory seems to be too difficult to be applied, except when some drastic approximations are introduced. Nakatsuji[11] has proposed the following ansatz,

$$\Psi^\nu = \mathcal{B}_0[\ \sum b_k^\nu M_k^+\ ]\ \exp(\ \sum C_i^\nu S_i^+\ )|0> \qquad (12)$$

where $|0>$ is the closed-shell single determinant. The M_k^+ and S_i^+ are both symmetry adapted operators and defined by the excitations from the occupied orbitals to the virtual orbitals. The $\mathcal{B}_0$ is an artificial operator and deletes the coefficient b_0^ν in the disconnected terms to avoid the possible divergence in the case of b_0^ν being close to zero. He divided the orbital space into two parts, occupied or virtual and defined the excitation operators. Therefore, all the excitation operators can be chosen as to ensure the commutation relation. However, some important internal correlation effect cannot be included.

In this paper we will present the non-closed-shell version of the SAC theory. The theory is required to be exact. It is also required that the excitation operators can be defined uniquely and the theory does not involve any non-commutative algebra. In the next section, we will first present the open-shell (excited state) SAC theory. Then, the multi-reference SAC theory will be discussed in Sec.III. In the final section, some conclusions will be summarized.

II. The open-shell SAC theory

First, we will consider the open-shell system with a high spin state repesented by only a single determinantal RHF function Φ_0

$$\Phi_0 = \mathcal{A}(\Phi_{closed}\Phi_{open}) = |\varphi_1\alpha\varphi_1\beta\ldots\varphi_q\alpha\varphi_q\beta\varphi_{(q+1)}\alpha\ldots\varphi_p\alpha| \qquad (13)$$

where Φ_{closed} and Φ_{open} are the closed-shell and open-shell parts of Φ_0 and $\mathcal{A}$ is an antisymmetrizer. Thus, the system has 2s unpaired α spins, namely, s=(p-q)/2. In such a case, the RHF wavefunction provides a good zeroth order representation and the open-shell system affords similar simplicity as the closed-shell system.

We will classify the correlation effects into two groups, the dynamical (transferable) correlation or the specific (non-transferable) correlation. The essential characteristic of the present approach is to re-define the reference function composed of RHF orbitals. Our open-shell SAC wavefunction is given by

$$\Psi = \exp(\ R\ )\Phi_{ref}\ ;\ \Phi_{ref} = T\Phi_{closed} \qquad (14)$$

The e^R represents the dynamical correlation and the linear operator T describes the specific non-dynamical correlation. Intermediate normalization is assumed

$$\langle\Phi_0\ |\Phi_0\rangle = \langle\Phi_0\ |\Psi\rangle = 1 \qquad (15)$$

Here, $\Phi_{ref} = T\Phi_{closed}$ is the newly defined reference function which includes the state-specific correlation effects. Thus, T operator generates the open-shell part Φ_{open} when operated on Φ_{closed} and also describes the internal/semi-internal correlation effect and spin polarization effect. The T operator is expressed as a sum of one- to N-particle symmetry adapted excitation operators

$$T = \sum C_I T_I^+ = T^{(1)} + T^{(2)} + \ldots + T^{(N)} \qquad (16)$$

Thus T generates the 2s-electron attached state when applied to Φ_{closed} with the simultaneous spin eigenfunctions of S^2 and S_z

$$S^2\Phi_{ref} = s(s+1)\Phi_{ref} , \quad S_z\Phi_{ref} = s\Phi_{ref} \qquad (17)$$

Although T depends on the system, T is defined uniquely if the system is given. The R operator describes all-external excitations from the closed-shell to virtual orbitals, which is more or less transferable among different states of the system

$$R = \sum C_J R_J^+ = R^{(1)} + R^{(2)} \ldots + R^{(N)} \qquad (18)$$

Thus, T_I^+ and R_J^+ operators are defined exclusively and they commute each other. The theory is exact since any excitation operator can be included in the present formalism. A symmetry projector Q is unnecessary since T is linear and R is a sum of singlet-type excitation operators.

In practical applications we will introduce some approximations. In the present work we consider only one- and two-body parts of T and R,

i.e. $T=T^{(1)}+T^{(2)}$ and $R=R^{(1)}+R^{(2)}$. Let us consider first the T operator. The T operator depends on the systems of interest. Retaining up to double excitation, we have

$$T = \sum C_I T_I^+ = T_0 + \sum C_i^m T_i^m + \sum C_m^a T_m^a + \sum {}^pC_i^a \, {}^pT_i^a +$$

$$+ \sum C_{ij}^{ma} T_{ij}^{ma} + \sum {}^pC_{ij}^{ma} \, {}^pT_{ij}^{ma} + \sum C_{im}^{ab} T_{im}^{ab} + \sum {}^pC_{im}^{ab} \, {}^pT_{im}^{ab} \qquad (19)$$

where C_i^m are the cluster amplitudes to be determined and T_i^m are the symmetry adapted excitation operators (represented by generic symbols C_I and T_I^+, respectively) defined in terms of the fermion creation and annihilation operators. In eq.(19) and throughout we follow the convention that the subscripts (superscripts) i,j refer to the closed-shell orbitals, m, n to open-shell orbitals and a, b to virtual orbitals. The T_0 operator reproduces the RHF wavefunction Φ_0 when applied to Φ_{closed}. The T_i^m, T_m^a and ${}^pT_i^a$ are single excitation operators and others are double excitation operators involving the open-shell orbitals

$$T_0 = a^+_{(q+1)\alpha} \cdots a^+_{m\alpha} \cdots a^+_{p\alpha} \qquad (20a)$$

$$T_i^m = a^+_{(q+1)\alpha} \cdots a^+_{m\alpha} \cdots a^+_{p\alpha} a^+_{m\beta} a_{i\beta} \qquad (20b)$$

$$T_m^a = a^+_{(q+1)\alpha} \cdots a^+_{a\alpha} \cdots a^+_{p\alpha} \qquad (20c)$$

$${}^pT_i^a = [1/2s(s+1)]^{1/2} [s\,(a^+_{a\alpha} a_{i\alpha} - a^+_{a\beta} a_{i\beta}) a^+_{(q+1)\alpha} \cdots a^+_{m\alpha} \cdots a^+_{p\alpha}$$

$$+ a^+_{a\alpha}a^+_{i\beta} \sum_m a^+_{(q+1)\alpha}\cdots a^+_{m\beta}\cdots a^+_{p\alpha}] \qquad (20d)$$

$$T^{am}_{ij} = (a^+_{a\alpha}a_{i\alpha} + a^+_{a\beta}a_{i\beta})a^+_{(q+1)\alpha}\cdots a^+_{m\alpha}\cdots a^+_{p\alpha}a^+_{m\beta}a_{j\beta}/\sqrt{2} \qquad (20e)$$

$$^pT^{am}_{ij} = [1/2s(s+1)]^{1/2} [\, s\,(a^+_{a\alpha}a_{i\alpha} - a^+_{a\beta}a_{i\beta})a^+_{m\alpha}a^+_{m\beta}\, a^+_{(q+1)\alpha}\cdots a^+_{p\alpha}a_{j\beta}$$

$$- a^+_{a\alpha}a_{i\beta}a^+_{m\alpha}a^+_{m\beta} \sum_n \sigma_n\, a^+_{(q+1)\alpha}\cdots a^+_{p\alpha}a_{j\beta}\,] \qquad (20f)$$

$$T^{ab}_{im} = (a^+_{a\alpha}a_{i\alpha} + a^+_{a\beta}a_{i\beta})a^+_{(q+1)\alpha}\cdots a^+_{b\alpha}\cdots a^+_{p\alpha}\, /\sqrt{2} \qquad (20g)$$

$$^pT^{ab}_{im} = [1/2s(s+1)]^{1/2} [s\,(a^+_{a\alpha}a_{i\alpha} - a^+_{a\beta}a_{i\beta})a^+_{(q+1)\alpha}\cdots a^+_{b\alpha}\cdots a^+_{p\alpha}$$

$$- a^+_{a\alpha}a_{i\beta} \sum_n \sigma_n\, a^+_{(q+1)\alpha}\cdots a^+_{b\alpha}\cdots a^+_{p\alpha}] \qquad (20h)$$

The creation operators are defined in the open-shell and virtual orbital spaces and annihilation operators are defined in the closed-shell orbital space. Thus, T^+_I are commutative for each other. The σ_n in eqs.(20f) and (20h) is the spin-flip operator to change the spin of $a^+_{n\alpha}$ to $a^+_{n\beta}$, namely $\sigma_n a^+_{n\alpha} = a^+_{n\beta}$. The T are the usual singlet-type excitation operators while the ^pT are the spin polarization excitation operators which include real excitations and spin-flips. Among them, the single excitation operators $^pT^a_i$ play the most important role in the spin correlation problems.[14] As to the double excitation, there are (2s+1) independent spin eigenfunctions corresponding to the excitation from (φ_i, φ_j) to (φ_a, φ_b). Two types of spin eigenfunctions corresponding to the all-external excitations will be considered in the R operator. The remaining (2s-1)

spin eigenfunctions are neglected in the present approximation since they are expected to make a small contribution to the energy. Then, the reference function in the present approximation becomes as

$$\Phi_{ref} = T\Phi_{closed} = |\varphi_1\alpha\varphi_1\beta \ \ldots \ \varphi_q\alpha\varphi_q\beta\varphi_{(q+1)}\alpha\ldots\varphi_m\alpha\ldots\varphi_p\alpha|$$

$$- \sum C_i^m \ |\varphi_1\alpha\varphi_1\beta \ \ldots \ \varphi_q\alpha\varphi_q\beta\varphi_m\alpha\varphi_m\beta\varphi_{(q+1)}\alpha\ldots\varphi_i\alpha\ldots\varphi_p\alpha|$$

$$+ \sum C_m^a|\varphi_1\alpha\varphi_1\beta \ \ldots \ \varphi_p\alpha\varphi_p\beta\varphi_{(q+1)}\alpha\ldots\varphi_a\alpha\ldots\varphi_p\alpha|$$

$$+ \sum {}^pC_i^a[1/2s(s+1)]^{1/2}|\ldots\varphi_a\varphi_i\varphi_{(q+1)}\cdots\varphi_p\{s(\alpha\beta+\beta\alpha)\alpha\ldots\alpha$$

$$- \alpha\alpha \sum_m \alpha\ldots\beta\ldots\alpha\} \ |$$

$$+ \sum C_{ij}^{am}|\ldots\varphi_{m\alpha}\varphi_{m\beta}\varphi_a\varphi_i(\alpha\beta-\beta\alpha)/\sqrt{2} \ \varphi_{(q+1)}\alpha\ldots\varphi_p\alpha|$$

$$+ \sum {}^pC_{ij}^{am}[1/2s(s+1)]^{1/2}|\ldots\varphi_{m\alpha}\varphi_{m\beta}\varphi_a\varphi_i\varphi_{(q+1)}\cdots\varphi_p\{s(\alpha\beta+\beta\alpha)\alpha\ldots\alpha$$

$$- \alpha\alpha \sum_n \alpha\ldots\beta\ldots\alpha\} \ |$$

$$+ \sum C_{im}^{ab}|\ldots \ \varphi_a\varphi_i(\alpha\beta-\beta\alpha)/\sqrt{2} \ \varphi_{(q+1)}\alpha\ldots\varphi_b\alpha\ldots\varphi_p\alpha|$$

$$+ \sum {}^pC_{im}^{ab}[1/2s(s+1)]^{1/2}|\ldots\varphi_a\varphi_i\varphi_{(q+1)}\cdots\varphi_b\ldots\varphi_p\{s(\alpha\beta+\beta\alpha)\alpha\ldots\alpha\ldots\alpha$$

$$- \alpha\alpha \sum_n \alpha\ldots\beta\ldots\alpha\} \ | \qquad (21)$$

Thus, Φ_{ref} consists of singly and doubly excited configurations involving the open-shell orbitals relative to Φ_0 in addition to Φ_0 itself. Namely, Φ_{ref} includes the semi-internal and spin polarization effects which are specific to the state of interest.

Let us consider next the R operator. Once the state-specific correlation effects are included, the remaining effects are just like those in closed-shells. The R_J^+ operators represent the all-external excitation operators defined by the excitation from the closed-shell orbitals to the virtual orbitals. The R_J^+ operators do not involve any open-shell orbital. Thus, the R_J^+ operators commute each other and also commute with the T_I^+ operators since both are chosen exclusively. The R operator is formally identical with the corresponding operator of the single reference SAC approach. The explicit expressions for the $R^{(1)}$ and $R^{(2)}$ are

$$R = \sum C_J R_J^+ = \sum C_i^a R_i^a + \sum {}^{(1)}C_{ij}^{ab} {}^{(1)}R_{ij}^{ab} + \sum {}^{(2)}C_{ij}^{ab} {}^{(2)}R_{ij}^{ab} \qquad (22)$$

with

$$R_i^a = (a_{a\alpha}^+ a_{i\alpha} + a_{a\beta}^+ a_{i\beta})/\sqrt{2} \qquad (23a)$$

$$\begin{aligned} {}^{(1)}R_{ij}^{ab} &= (R_i^a R_j^b + R_j^a R_i^b)/2 \\ &= (a_{a\alpha}^+ a_{i\alpha} a_{b\beta}^+ a_{j\beta} + a_{a\beta}^+ a_{i\beta} a_{b\alpha}^+ a_{j\alpha} + a_{b\alpha}^+ a_{i\alpha} a_{a\beta}^+ a_{j\beta} + a_{b\beta}^+ a_{i\beta} a_{a\alpha}^+ a_{j\alpha})/4 \end{aligned} \qquad (23b)$$

$${}^{(2)}R_{ij}^{ab} = (R_i^a R_j^b - R_j^a R_i^b)/2$$

$$= (2a^{+}_{a\alpha}a_{i\alpha}a^{+}_{b\alpha}a_{j\alpha} + 2a^{+}_{a\beta}a_{i\beta}a^{+}_{b\beta}a_{j\beta} + a^{+}_{a\alpha}a_{i\alpha}a^{+}_{b\beta}a_{j\beta} + a^{+}_{a\beta}a_{i\beta}a^{+}_{b\alpha}a_{j\alpha}$$

$$- a^{+}_{b\alpha}a_{i\alpha}a^{+}_{a\beta}a_{j\beta} - a^{+}_{b\beta}a_{i\beta}a^{+}_{a\alpha}a_{j\alpha})/4\sqrt{3} \qquad (23c)$$

The R generates the following excited configurations when operating on Φ_0

$$R\Phi_0 = \sum C_i^a |\ldots \varphi_a\varphi_i(\alpha\beta-\beta\alpha)/\sqrt{2}\ldots|$$

$$+ \sum^{(1)} C_{ij}^{ab} |\ldots \varphi_i\varphi_j\varphi_a\varphi_b(\alpha\beta-\beta\alpha)(\alpha\beta-\beta\alpha)/4\ldots|$$

$$+ \sum^{(2)} C_{ij}^{ab} |\ldots \varphi_i\varphi_j\varphi_a\varphi_b(2\alpha\alpha\beta\beta+2\beta\beta\alpha\alpha-\alpha\beta\alpha\beta-\alpha\beta\beta\alpha-\beta\alpha\alpha\beta-\beta\alpha\beta\alpha)/\sqrt{12}\ldots| \qquad (24)$$

The exponential operator e^R produces triply, quadruply,... excited configurations in addition to the singly and doubly excited configurations.

The total wavefunction is given by

$$\Psi = (1 + \sum_J C_J R_J^{+} + \frac{1}{2}\sum_J\sum_K C_J C_K R_J^{+} R_K^{+} + \ldots)\Phi_{ref}$$

$$= \Phi_0 + \sum_I{}' C_I T_I^{+}\Phi_{closed} + \sum_J C_J R_J^{+}\Phi_0 + \sum_I\sum_J{}' C_J C_I R_J^{+} T_I^{+}\Phi_{closed}$$

$$+ \frac{1}{2}\sum_J\sum_K C_J C_K R_J^{+} R_K^{+}\Phi_0 + \ldots \qquad (25)$$

Here summation is done over all orbitals and $\sum'$ indicates that the terms involving T_0 are excluded from the summation. The second terms on the

r.h.s. of eq.(25) represent the specific correlation effects and the third terms describe the dynamical correlation effect. The coupling of the all-external excitation with the semi-internal and spin polarization excitations are also included through the disconnected terms in the form of the products of R_J^+ and T_I^+ operators. The fifth terms correspond to the disconnected clusters of the all-external excitations.

Let us turn now the Schrodinger equation

$$(H - E)\Psi = (H - E)e^{R}\Phi_{ref} = (H - E)e^{R}T\Phi_{closed} = 0 \qquad (26)$$

Left-multiplying eq.(26) by e^{-R}, we have

$$e^{-R}H\ e^{R}\Phi_{ref} = E\Phi_{ref} \qquad (27)$$

Eq.(27) is then projected against a sufficient set of excited functions to generate a series of equations

$$\langle\Phi_{closed}T_I|e^{-R}H\ e^{R}|\Phi_{ref}\rangle = E\langle\Phi_{closed}T_I|\Phi_{ref}\rangle \qquad (28a)$$

$$\langle\Phi_0\ R_J|e^{-R}H\ e^{R}|\Phi_{ref}\rangle = 0 \qquad (28b)$$

where $(T_I^+)^\dagger = T_I$ and $(R_J^+)^\dagger = R_J$. Eq.(28a) are a set of linear equations for T_I^+ while eq.(28b) are a set of nonlinear coupled equations for R_J^+. The resultant set of equations are equal in number to the number of symmetry adapted excitation operators to be determined. Eq.(28b) are formally identical to the corresponding closed-shell SAC equations and eq.(28a) to the SAC-CI equations. The eq.(28a) are reduced to an eigenvalue problem

of the nonsymmetric matrix while eq.(28b) to a system of linear equations. The solution is performed iteratively until the self-consistent is achieved. That is, Φ_{ref} is also determined through the optimization process. This is actually possible and quite straightforward. The total energy is given by projecting the Schrodinger equation onto the RHF function Φ_0

$$\langle\Phi_0|e^{-R}H\ e^{R}|\Phi_{ref}\rangle = E \qquad (29)$$

Thus, the non-closed-shell SAC theory can be obtained with a slight modification of the closed-shell SAC theory.

Now let us examine the relation to the SAC-CI theory. For the sake of simplicity, we will consider the doublet state

$$\Phi = \mathcal{A}(\Phi_{closed}\varphi_m) \qquad (30)$$

The SAC equation for the closed-shell Φ_{closed} is reduced to

$$e^{-S}H\ e^{S}\Phi_{closed} = E_g\Phi_{closed} \qquad (31)$$

where E_g is the energy of $e^{S}\Phi_{closed}$. Also the SAC-CI equation for the electron attached states is given by

$$e^{-S}[H,\ T]e^{S}\Phi_{closed} = (E_e - E_g)T\Phi_{closed} \qquad (32)$$

where $(E_e - E_g)$ gives the electron affinity. If the difference between R and S is defined by S' (S'=R-S), then eq.(27) leads to

$$e^{-S}[H,\ e^{S'T}]e^{S}\Phi_{closed} = (E_e - E_g)e^{S'T}\Phi_{closed} \qquad (33)$$

We see that the T in the SAC-CI equation of eq.(32) is replaced by $e^{S'}T$. This means that the present theory takes account of the reorganization effect of the electron correlation due to the excitation. The frozen correlation approximation in the SAC-CI theory is now relaxed in the present open-shell SAC theory. When S' is small, i.e. dynamical correlations are transferable, the SAC-CI method becomes a good approximation. Thus, the present theory is a straightforward generalization of the SAC-CI theory for the excited states.

III. Multi-reference SAC theory

We now turn to discuss the multi-reference SAC theory (MRSAC). The idea behind the open-shell SAC theory can easily be applied to the multi-reference cases. We will start with the multi-configurational function

$$\Phi_0^{\nu} = \sum A_I^{\nu} \Phi_I \qquad (34)$$

Here, ν denotes a state under consideration. The theory is required to be rather immune to intruders, allowing flexibility in choosing the reference space. Thus, quasidegeneracies are fully considered in Φ_0^{ν}. We assume that Φ_0^{ν} is obtained by the CASSCF theory[15] and Φ_I span a complete space among the active orbitals. But this restriction is not serious. We may start with the conventional MCSCF wavefunction. The configuration

coefficients A_I^ν will be reoptimized but we will keep the norm of the corresponding function throughout the calculation

$$<\Phi_0^\nu | \Phi_0^\nu> = <\Phi_0^{\nu\ opt} | \Phi_0^{\nu\ opt}> = 1 \ ; \quad \Phi_0^{\nu\ opt} = \sum C_I^\nu \Phi_I \tag{35}$$

where $\Phi_0^{\nu\ opt}$ is the corresponding optimized function in the final stage. Note here that we only need the CASSCF orbitals.

In this case, orbitals are classified as core (closed-shell), valence (active) or virtual. The core orbitals are always occupied and all possible distributions of the remaining electrons in the valence orbitals give rise to Φ_0^ν. Then the MRSAC wavefunction is defined as

$$\Psi^\nu = \exp(\ R\ )\Phi_{ref}^\nu \ ; \quad \Phi_{ref}^\nu = T^\nu \Phi_{core} \tag{36}$$

Again, the Φ_{ref}^ν is a newly defined reference function and the Φ_{core} is the doubly occupied part of Φ_0^ν. Intermediate normalization is also assumed

$$<\Phi_0^\nu | \Psi^\nu> = 1 \tag{37}$$

Thus, the T^ν operator generates all the configurations appeared in the starting function Φ_0^ν and also includes the internal and semi-internal correlation effects. The R operator represents the dynamical correlation as before. The T^ν and R can be chosen uniquely and they commute each other. The wavefunction given by eq.(36) is unique and exact. Of course, the theory is reduced to the single reference SAC theory in the absence of near-degeneracies.

For the resulting simplicity we will consider the singlet state with two active orbitals. It gives useful insight on the structure of the MRSAC method. The indices m and n are used to refer to specific active orbitals. The CASSCF wavefunction is given by

$$\Phi_0^\nu = \sum A_I^\nu \Phi_I = A_0^\nu |\ldots\varphi_i\alpha\varphi_i\beta\ldots\varphi_m\alpha\varphi_m\beta|$$

$$+ A_1^\nu |\ldots\varphi_i\alpha\varphi_i\beta\ldots\varphi_m\varphi_n(\alpha\beta-\beta\alpha)/\sqrt{2}| + A_2^\nu |\ldots\varphi_i\alpha\varphi_i\beta\ldots\varphi_n\alpha\varphi_n\beta| \quad (38)$$

Two configurations are sufficient to span the complete space but we will start with the general expression given by eq.(38). If we truncate the excitation operators after double excitation, T is given by

$$T^\nu = \sum C_I^\nu T_I^+ = C_0T_0 + C_m^nT_m^n + C_{mm}^{nn}T_{mm}^{nn} + \sum C_i^m T_i^m + \sum C_{ij}^{mn} T_{ij}^{mn}$$

$$+ \sum {}^pC_i^a\, {}^pT_i^a + \sum C_m^a T_m^a + \sum C_{mn}^{ab} T_{mn}^{ab} + \sum C_{ij}^{ma} T_{ij}^{ma} + \sum C_{im}^{ab} T_{im}^{ab} \quad (39)$$

Since all cluster amplitudes considered here correspond to C_I^ν, we can drop the lable ν without ambiguity. The explicit expressions of these excitation operators are

$$T_0 = a_{m\alpha}^+ a_{m\beta}^+ \quad (40a)$$

$$T_m^n = (a_{m\alpha}^+ a_{n\beta}^+ - a_{m\beta}^+ a_{n\alpha}^+)/\sqrt{2} \quad (40b)$$

$$T_{mm}^{nn} = a_{n\alpha}^+ a_{n\beta}^+ \quad (40c)$$

$$T_i^m = a^+_{m\alpha}a^+_{m\beta}(a^+_{n\alpha}a_{i\alpha} + a^+_{n\beta}a_{i\beta})/\sqrt{2} \qquad (40d)$$

$$T_{ij}^{mn} = a^+_{m\alpha}a^+_{m\beta}a^+_{n\alpha}a^+_{n\beta}(a_{i\beta}a_{j\alpha} - a_{i\alpha}a_{j\beta})/\sqrt{2} \qquad (40e)$$

$$T_m^a = (a^+_{a\alpha}a^+_{n\beta} - a^+_{a\beta}a^+_{n\alpha})/\sqrt{2} \qquad (40f)$$

$$T_{mn}^{ab} = (a^+_{a\alpha}a^+_{b\beta} - a^+_{a\beta}a^+_{b\alpha})/\sqrt{2} \qquad (40g)$$

$$^pT_i^a = (-2a^+_{a\alpha}a_{i\beta}a^+_{m\beta}a^+_{n\beta} + 2a^+_{a\beta}a_{i\alpha}a^+_{m\alpha}a^+_{n\alpha} - a^+_{a\alpha}a_{i\alpha}a^+_{m\alpha}a^+_{n\beta} + a^+_{a\beta}a_{i\beta}a^+_{m\beta}a^+_{n\alpha}$$
$$- a^+_{a\alpha}a_{i\alpha}a^+_{m\beta}a^+_{n\alpha} + a^+_{a\beta}a_{i\beta}a^+_{m\alpha}a^+_{n\beta})/\sqrt{12} \qquad (40h)$$

$$T_{ij}^{am} = (2a^+_{a\alpha}a_{i\beta}a^+_{n\beta}a_{j\alpha} + 2a^+_{a\beta}a_{i\alpha}a^+_{n\alpha}a_{j\beta} + a^+_{a\alpha}a_{i\alpha}a^+_{n\alpha}a_{j\alpha} + a^+_{a\beta}a_{i\beta}a^+_{n\beta}a_{j\beta}$$
$$- a^+_{a\alpha}a_{i\alpha}a^+_{n\beta}a_{j\beta} - a^+_{a\beta}a_{i\beta}a^+_{n\alpha}a_{j\alpha})a^+_{m\alpha}a^+_{m\beta}/\sqrt{12} \qquad (40i)$$

$$T_{im}^{ab} = (2a^+_{a\alpha}a_{i\beta}a^+_{n\beta}a_{b\beta} - 2a^+_{a\beta}a_{i\alpha}a^+_{n\alpha}a_{b\alpha} + a^+_{a\alpha}a_{i\alpha}a^+_{n\alpha}a_{bb} - a^+_{a\beta}a_{i\beta}a^+_{n\beta}a_{b\alpha}$$
$$+ a^+_{a\alpha}a_{i\alpha}a^+_{n\beta}a_{b\alpha} - a^+_{a\beta}a_{i\beta}a^+_{n\alpha}a_{b\beta})/\sqrt{12} \qquad (40j)$$

The creation operators are defined in valence and active orbital spaces while annihilation operators defined in the core orbital space. The first three operators on the r.h.s. of eq.(39) reproduce the CASSCF configurations in Φ_0^ν. Then the Φ_{ref}^ν is given by

$$\Phi_{ref}^\nu = T^\nu\Phi_{core} = C_0|\ldots\varphi_m\alpha\varphi_n\beta| + C_m^n|\ldots\varphi_m\varphi_n(\alpha\beta-\beta\alpha)/\sqrt{2}| +$$

$$+ C^{nn}_{mm}|\ldots\varphi_n\alpha\varphi_n\beta| + \sum C^{m}_{i}\,|\ldots\varphi_{m\alpha}\varphi_{m\beta}\varphi_n\varphi_i(\alpha\beta-\beta\alpha)/\sqrt{2}|$$

$$+ \sum C^{mn}_{ij}|\ldots\ \varphi_i\varphi_j(\alpha\beta-\beta\alpha)/\sqrt{2}\ \varphi_m\alpha\varphi_m\beta\varphi_n\alpha\varphi_n\beta|$$

$$+ \sum C^{a}_{m}\,|\ldots\varphi_a\varphi_n(\alpha\beta-\beta\alpha)/\sqrt{2}\,| \pm \sum C^{ab}_{mn}|\ldots\varphi_a\varphi_b(\alpha\beta-\beta\alpha)/\sqrt{2}|$$

$$+ \sum {}^{p}C^{a}_{i}\,|\ldots\varphi_a\varphi_i\varphi_m\varphi_n(2\alpha\alpha\beta\beta+2\beta\beta\alpha\alpha-\alpha\beta\alpha\beta-\beta\alpha\beta\alpha-\alpha\beta\beta\alpha-\beta\alpha\alpha\beta)/\sqrt{12}|$$

$$- \sum C^{am}_{ij}\,|\ldots\varphi_a\varphi_i\varphi_n\varphi_j(2\alpha\alpha\beta\beta+2\beta\beta\alpha\alpha-\alpha\beta\alpha\beta-\beta\alpha\beta\alpha-\alpha\beta\beta\alpha-\beta\alpha\alpha\beta)/\sqrt{12}|$$

$$+ \sum C^{ab}_{im}\,|\ldots\varphi_a\varphi_i\varphi_b\varphi_n(2\alpha\alpha\beta\beta+2\beta\beta\alpha\alpha-\alpha\beta\alpha\beta-\beta\alpha\beta\alpha-\alpha\beta\beta\alpha-\beta\alpha\alpha\beta)/\sqrt{12}| \qquad (41)$$

The Φ_{ref} includes CASSCF configurations and configurations corresponding to the single and double excitations involving the active orbitals. The R operator is a sum of all-external excitation operators and takes the same form as given by eqs.(22) and (23). The commutation relation of all the excitation operators is satisfied. The total wavefunction is given by

$$\Psi^{\nu} = (1 + \sum_J C^{\nu}_J R^{+}_J + \frac{1}{2}\sum_J\sum_K C^{\nu}_J C^{\nu}_K R^{+}_J R^{+}_K + \ldots)\Phi^{\nu}_{ref}$$

$$= \Phi^{\nu\ opt}_0 + \sum_I{}' C^{\nu}_I T^{+}_I\,\Phi_{core} + \sum_J C^{\nu}_J R^{+}_J\,\Phi^{\nu\ opt}_0$$

$$+ \sum_J C^{\nu}_J R^{+}_J\,(\sum_I{}' C^{\nu}_I T^{+}_I\,\Phi_{core}) + \frac{1}{2}\sum_J\sum_K C^{\nu}_J C^{\nu}_K R^{+}_J R^{+}_K\,\Phi^{\nu\ opt}_0 + \ldots \qquad (42)$$

The second terms on the r.h.s. of eq.(42) represent the internal and

semi-internal correlation effects and the third terms all-external correlation effects. The fourth terms are the coupling between the all-external and internal/semi-internal correlation effects.

The solution of the MRSAC approach given here is very similar to the previous case. The Schrodinger equation is projected against a sufficient set of excited functions to generate a series of equations

$$\langle \Phi_{core} T_I | e^{-R} H e^{R} | \Phi_{ref} \rangle = E \langle \Phi_{core} T_I | \Phi_{ref} \rangle \qquad (43a)$$

$$\langle \Phi_0^{\nu\ opt} R_J | e^{-R} H e^{R} | \Phi_{ref} \rangle = 0 \qquad (43b)$$

The total electronic energy is also given by

$$\langle \Phi_0^{\nu\ opt} | e^{-R} H e^{R} | \Phi_{ref} \rangle = E \qquad (44)$$

Since the T operator is linear, eq.(43a) leads to an eigenvalue problem of the nonsymmetric matrix. The solution with the lowest eigenvalue corresponds to the ground state. The other solutions correspond to the excited states involving the active orbitals. The situation is similar to the case of the conventional CI method. This will provide a good approximation since the dynamical correlation effect represented by e^R is more or less transferable from the ground state to the excited states. Thus, the MRSAC theory presented so far can give the low-lying excited state solutions as well as the ground state solution.

The present approach can also be applied to the majority of open-shell ground states and molecular excited states having more than a single reference configuration or determinantal function.

IV. Summary

We have presented the non-closed-shell version of the SAC theory. We started with the RHF/CASSCF orbitals but re-defined the reference function which includes the state-specific correlation effects. The transferable dynamical correlation effect is expressed through the exponential operator e^R and the linear operator T is used to represent the state-specific correlation effects such as quasidegeneracies, internal and semi-internal correlation effects, the spin-polarization effect, etc. The R and T operators can be chosen uniquely and they are defined exclusively. The non-closed-shell SAC theory can be obtained with a slight modification of the SAC theory for closed-shells. The theory is exact since any excitation can be included in the present formalism. In addition, the theory does not involve any non-commutative algebra. Furthermore, the present theory gives the low-lying excited state solutions as well as the ground state solution.

We would like to stress a very close parallel between the standard single reference closed-shell SAC and its non-closed-shell version. The present theory has practical and conceptual simplicity. This approach is particularly suitable for the evaluation of potential energy surfaces, the excited states and open-shell systems, where allowance for mixing of electronic configurations is often necessary. Applications are now being investigated in order to check the generality and the accuracy of the present theory.

Acknowledgment

This study has partially been supported by the Grant-in-Aid for Scientific Research from the Ministry of Education, Science and Culture.

References

1. I.Shavitt, in Methods of Electronic Structure Theory, ed by H.F.Schaefer (1977, Plenum Press).
2. H.P.Kelly, Adv.Chem.Phys.,**14**,129 (1969);Phys.Rev.,**152**,62 (1966).
3. F.Coester, Nucl.Phys., **7**, 421 (1966); F.Coester and H.Kummel, Nucl.Phys., **17**, 477 (1960);J.Cizek, J.Chem.Phys.,**45**, 4256 (1969); J.Paldus, J.Cizek and I.Shavitt, Phys.Rev., **A5**, 50 (1972).
4. B.J.Bartlett, Ann.Rev.Phys.Chem., **32**, 359 (1981).
5. H.Nakatsuji and K.Hirao, J.Chem.Phys., **68**, 2053 (1978).
6. K.Hirao and Y.Hatano, Chem.Phys.Lett., **100**, 519 (1983); K.Hirao, Theor. Chim.Acta, **71**, 231 (1987).
7. H.Nakatsuji, Chem.Phys.Lett., **59**, 362 (1978); **67**, 329, 334 (1979); K.Hirao, J.Chem.Phys.,**79**, 5000 (1983).
8. K.Hirao and Y.Hatano, Chem.Phys.Lett., **111**, 533 (1984); H.Nakatsuji, K. Hirao and Y.Mizukami, Chem.Phys.Lett., in press.
9. D.Mukherjee, R.K.Moitra and A.Mukhopadhyay, Mol.Phys., **30**, 1861 (1975);**33**, 955 (1977); A.Mukhopadyay, R.K.Moitra and D.Mukherjee, J.Phys. **B12**, 1 (1979); D.Mukherjee, Pramana, **12**,203 (1979);A.Haque and D.Mukherjee, J.Chem.Phys., **80**, 5058 (1984).
10. B.Jeziorski and J.H.Monkhost, Phys.Rev. **A24**, 1668 (1981).
11. H.Nakatsuji, J.Chem.Phys., **83**, 713, 5743 (1985).

12. G.Hose and U.Kaldor, Phys.Scr., **21**, 357 (1981); U.Kaldor, J.Chem.Phys., **81**, 2406 (1984).
13. B.Jeziorski and J.Paldus, J.Chem.Phys., **88**, 5673 (1988); Intern.J.Quantum Chem., **18**, 1243 (1980).
14. H.Nakatsuji and K.Hirao, J.Chem.Phys., **68**, 4279 (1978).
15. P.E.M.Siegbahn, A.Heiberg, B.O.Roos and B.Levy, Phisica Scripta, **21**, 323 (1980); B.O.Roos, P.R.Taylor and P.E.M.Siegbahn, Chem.Phys.,**48**, 157 (1980);B.O.Roos, Intern.J.Quantum Chem.,**S14**, 175 (1980).

SAC-CI AND FULL CI CALCULATIONS FOR THE SINGLET AND TRIPLET EXCITED STATES OF H_2O

Hiroshi NAKATSUJI

Department of Synthetic Chemistry, Faculty of Engineering,
Kyoto University, Kyoto 606, Japan

Kimihiko HIRAO

Department of Chemistry, College of General Education,
Nagoya University, Nagoya, Japan, and
Institute for Molecular Science, Okazaki, Japan

and

Yoshihiro MIZUKAMI

Division of Molecular Engineering, Graduate School of Engineering,
Kyoto University, Kyoto 606, Japan

Abstract

The accuracy of the SAC-CI (symmetry adapted cluster-configuration interaction) method is examined for the singlet and triplet excited states of H_2O by comparing with the full CI results for the [4s2p] basis set. The SAC-CI results for the excitation energy agree to within 1.4 % of the full CI results.

The SAC (symmetry adapted cluster)[1] and SAC-CI [2] methods were proposed for calculations of the ground and excited states, ionized states and electron attached states of a molecule. Through many applications, the SAC/SAC-CI method has been proved to be very useful for reliable and effective calculations of the ground, excited, and ionized states of molecules[3].

Some years ago, the accuracy of the SAC/SAC-CI method has been examined for the ground state[4] and the triplet excited, ionized and electron attached states[5] of H_2O by comparing with the full CI results. The basis set was [4s2p] set of Huzinaga[6] and Dunning[7]. The purpose of this paper is to examine the accuracy of the *singlet* excited states of H_2O calculated by the SAC-CI method, since this examination was missing in the previous paper[5]. We carry out comparative full CI calculations and compare their total energies and excitation energies with the SAC-CI results. Some additional results are also reported for the triplet excited states.

The ground state of H_2O is calculated by the SAC method. The Hartree-Fock (HF) orbitals are calculated by the program GAMESS [8] and used as the reference orbitals in the SAC/SAC-CI calculations. Linked terms in SAC include all single (S_1) and double (S_2) excitation operators and the unlinked terms include quadruple excitation operators as products of double excitation operators (S_2S_2).

The excited states are calculated by the SAC-CI theory. Linked terms in SAC-CI include all single (R_1) and double (R_2) excitation operators. For unlinked terms, we use two different approximations. The first one, called SAC-CI(A), includes only R_1S_2 operators and the second one, called SAC-CI(B), includes both R_1S_2 and R_2S_2 operators. No configuration selection is performed in both SAC and SAC-CI calculations. We used the

program package SAC85 [9].

The full CI calculations for the singlet and triplet excited states of H_2O are carried out with the use of the modified version of the determinant integer full CI program of Handy[10].

The total energy of the ground state is -76.156254 hartree by SAC and -76.157866 hartree by full CI. These are the same as those reported previously [5]. The energy difference is only 1.6×10^{-3} hartree (1.0 kcal/mol), so that the SAC method is proved to be very reliable.

The results for the singlet ground and excited states of H_2O are summarized in table 1. The dimensions of the matrices involved in SAC/SAC-CI are the same as those of SDCI and are three-orders-of-magnitude smaller than those of full CI. The excitation energies of both SAC-CI(A) and SAC-CI(B) are in good agreement with those of full CI. The differences are to within 1.2 %. There is a trend that SAC-CI(A) gives larger excitation energies and, in contrast, SAC-CI(B) gives smaller ones in comparison with full CI. Refined unlinked terms in SAC-CI(B) lower the energies of the excited states and give smaller excitation energies. Total energies of SAC-CI are also in very good agreement with those of full CI. However, we note that the SAC-CI(B) results sometimes overshoot the exact full-CI energies, though the differences are less than 2.1×10^{-3} hartree. This arises from the non-variational nature in the solution of SAC-CI. Variational solution always gives an upper bound for full CI, but it is very difficult to obtain it for the SAC/SAC-CI expansion[2]. For the $^1A_1$ and $^1B_2$ symmetries, we also give the results for the second excited states. Both total energies and excitation energies of SAC-CI (especially, SAC-CI(B)) compare very well with those of full CI. We list the timing data in table 1. The CPU time for SAC-CI is much shorter than that for full CI.

The results of the triplet excited states of H_2O are shown in table 2. Here we also show the previous result of SAC-CI by Hirao and Hatano [5]. We call it SAC-CI(H). The dimensions of SAC-CI(H) are smaller than those of SAC-CI(A) and SAC-CI(B), because SAC-CI(H) does not include spin polarization type double excitation operators for triplet excited states. We also show the results of the second excited states for the $^3A_1$ and $^3B_2$ states. Total energies and excitation energies of SAC-CI(A) and SAC-CI(B) are in very good agreement with those of full CI. The SAC-CI excitation energies differ from the full-CI ones only to within 1.4 %, though the dimensions of SAC-CI are much less than those of full CI. Results of SAC-CI(H) are also comparable and agree well with those of full CI.

In conclusion, the SAC-CI method is confirmed to be quite accurate for the singlet and triplet excited states of H_2O. The excitation energies calculated by the SAC-CI method agree to within 1.4 % with those of full CI, though the dimensions of SAC-CI are three-orders-of-magnitude smaller than those of full CI. The CPU time for SAC-CI is also much shorter than that for full CI. The total energies of SAC-CI(B) sometimes overshoot the full CI energies because of the non-variational nature of the solution, though the energy differences between SAC-CI(B) and full CI are very small. We conclude that the SAC/SAC-CI method is quite reliable and effective for the study of ground, excited and ionized states of molecules.

Acknowledgments

This study has partially been supported by the Grant-in-Aid for Scientific Research from the Ministry of Education, Science and Culture. Calculations were carried out at the Nagoya University Computational Center, and at the Data Processing Center of Kyoto University.

References

1 H. Nakatsuji and K. Hirao, J. Chem. Phys. 68 (1978) 2053.

2 H. Nakatsuji, Chem. Phys. Letters 59 (1978) 362; 67 (1979) 329, 334.

3 H. Nakatsuji, Theor. Chim. Acta 71 (1987) 201;
H. Nakatsuji, M. Komori, and O. Kitao, *Lecture Note in Chemistry*, 50, edited by D. Mukherjee, Springer, Berlin, pp. 101-122, 1989;
H. Nakatsuji, Reports in Molecular Theory, CRC Press, in press.

4 K. Hirao and Y. Hatano, Chem. Phys. Letters 100 (1983) 519.

5 K. Hirao and Y. Hatano, Chem. Phys. Letters 111 (1984) 533.

6 S. Huzinaga, J. Chem. Phys. 42 (1965) 1293.

7 T. H. Dunning, Jr., J. Chem. Phys. 53 (1970) 2823.

8 B. R. Brooks, P. Saxe, W. D. Laidig, and M. Dupuis, Program Library Gamess(No.481), Computer Center of the Institute for Molecular Science, Okazaki, Japan.

9 H. Nakatsuji, Program system for SAC and SAC-CI calculations, Program Library No.146(Y4/SAC), Data Processing Center of Kyoto University, 1985;
H. Nakatsuji, Program Library SAC85 (No.1396), Computer Center of the Institute for Molecular Science, Okazaki, Japan, 1986.

10 N. C. Handy, Chem. Phys. Letters 74 (1980) 280.

Table 1. Total energies and the excitation energies for the singlet ground and excited states of H_2O calculated by the full CI and SAC/SAC-CI methods.

State	Orbital picture		Dimension	Total energy (au)	Excitation energy (eV)	Error from full CI (%)	CPU time[a] (min)
$^1A_1$	ground state	SAC	361	-76.156254	0.0	0.002	1.8
		Full-CI	256474	-76.157866	0.0		55
	$3a_1(n)\rightarrow 4a_1$	SAC-CI(A)	360	-75.754848	10.9229	0.8	0.6[b]
		SAC-CI(B)	360	-75.761163	10.7511	-0.8	2.0[b]
		Full CI	256474	-75.759512	10.8399		190[b]
	$1b_2(\sigma)\rightarrow 2b_2$	SAC-CI(A)	360	-75.450371	19.2082	0.8	
		SAC-CI(B)	360	-75.454417	19.0981	0.2	
		Full CI	256474	-75.457584	19.0558		
$^1A_2$	$1b_1(\pi)\rightarrow 2b_2$	SAC-CI(A)	192	-75.756082	10.8893	0.8	0.1
		SAC-CI(B)	192	-75.761966	10.7292	-0.6	0.6
		Full CI	245000	-75.761050	10.7980		82
$^1B_1$	$1b_1(\pi)\rightarrow 4a_1$	SAC-CI(A)	216	-75.833910	8.7715	0.9	0.2
		SAC-CI(B)	216	-75.840435	8.5940	-1.2	0.8
		Full CI	245776	-75.838288	8.6962		82
$^1B_2$	$3a_1(n)\rightarrow 2b_2$	SAC-CI(A)	312	-75.664680	13.3765	0.8	0.4
		SAC-CI(B)	312	-75.670341	13.2225	-0.4	1.5[b]
		Full CI	254752	-75.670141	13.2718		193[b]
	$1b_2(\sigma)\rightarrow 4a_1$	SAC-CI(A)	312	-75.564611	16.0996	0.9	
		SAC-CI(B)	312	-75.568589	15.9913	0.2	
		Full CI	254752	-75.571512	15.9556		

[a]Due to FACOM M780 computer.
[b]This timing data is for the two excited-state solutions belonging to the same symmetry.

Table 2. Total energies and excitation energies for the triplet excited states of H_2O calculated by the full CI and SAC-CI methods.

State	Orbital picture		Dimension	Total energy (au)	Excitation energy (eV)	Error from full CI (%)	CPU time[a] (min)
$^3A_1$	$3a_1(n)\rightarrow 4a_1$	SAC-CI(A)	417	-75.794396	9.8467	0.3	1.1[b]
		SAC-CI(B)	417	-75.799083	9.7192	-1.0	4.0[b]
		SAC-CI(H)	315	-75.791190	9.934	1.2	
		Full CI	440475	-75.797174	9.8150		246[b]
	$1b_2(\sigma)\rightarrow 2b_2$	SAC-CI(A)	417	-75.566185	16.0567	0.3	
		SAC-CI(B)	417	-75.568723	15.9877	-0.1	
		Full CI	440475	-75.569523	16.0098		
$^3A_2$	$1b_1(\pi)\rightarrow 2b_2$	SAC-CI(A)	274	-75.775095	10.3720	0.9	0.3
		SAC-CI(B)	274	-75.780262	10.2314	-0.5	1.8
		SAC-CI(H)	192	-75.776939	10.322	0.4	
		Full CI	437640	-75.779926	10.2844		114
$^3B_1$	$1b_1(\pi)\rightarrow 4a_1$	SAC-CI(A)	294	-75.864292	7.9448	0.6	0.4
		SAC-CI(B)	294	-75.869963	7.7904	-1.4	2.1
		SAC-CI(H)	216	-75.868314	7.835	-0.8	
		Full CI	437520	-75.867507	7.9011		113
$^3B_2$	$3a_1(n)\rightarrow 2b_2$	SAC-CI(A)	410	-75.718219	11.9196	0.4	0.9[b]
		SAC-CI(B)	410	-75.722134	11.8131	-0.5	3.7[b]
		SAC-CI(H)	312	-75.711568	12.101	1.9	
		Full CI	441120	-75.721626	11.8708		269[b]
	$1b_2(\sigma)\rightarrow 4a_1$	SAC-CI(A)	410	-75.631970	14.2666	0.4	
		SAC-CI(B)	410	-75.634992	14.1844	-0.2	
		Full CI	441120	-75.635841	14.2151		

[a]Due to FACOM M780 computer.
[b]This timing data is for the two solutions belonging to the same symmetry.

THE SCF ORBITAL THEORY
THE CLUSTER EXPANSION OF A WAVEFUNCTION FORMALISM

K.HIRAO
Department of Chemistry, College of General Education,
Nagoya University, Nagoya, Japan

1. INTRODUCTION

In the simplest possible description of an N-electron systems, one-electron function is associated with each electron and the N-electron wavefunction is a Slater determinant built up from these one-electron functions. This independent particle model, which has been developed in forms of the SCF scheme, constitutes the basis upon which the language of quantum chemistry is founded. This review is intended to form a framework for the SCF orbital theory. Our approach is to start with the expression for the N-electron wavefunction in the one-particle cluster expansion of a wavefunction.

Let us consider a wavefunction of the form

$$|\Phi\rangle = \exp[\, T_1]|\Phi_0\rangle$$

$$= (1 + T_1 + \frac{1}{2!}T_1^{\,2} + \frac{1}{3!}T_1^{\,3} + \ldots\ |0\rangle \qquad [1]$$

where the reference function $|\Phi_0\rangle$ is an antisymmetrized product of N one-electron functions and T_1 is the one-particle linked cluster generator

$$|\Phi_0\rangle = a_1^+ a_2^+ \ldots a_N^+ |\rangle$$

$$T_i = \sum_i f_i b_i^+ a_i \qquad [2]$$

The ket $|\rangle$ denotes a vacuum state, a_i^+ and a_i are creation and annihilation operators for single-particle states, b_i^+ are the normalized one-particle cluster generators and the coefficients f_i are complex. Thouless' theorem[1] states that the cluster expansion given by [1] corresponds to a transformation of a single Slater determinant $|\Phi_0\rangle$ to another determinantal function

$$|\Phi\rangle = \prod_i (a_i^+ + f_i b_i^+) |\rangle \qquad [3]$$

As a reference function, we choose a restricted single determinant given by

$$|\Phi_0\rangle = \sum_{k=1}^{n} a_{k\alpha}^+ a_{k\beta}^+ |\rangle$$

$$= \| \varphi_1 \bar{\varphi}_1 \ldots \varphi_k \bar{\varphi}_k \ldots \varphi_n \bar{\varphi}_n \| \qquad [4]$$

for 2n-electron closed-shell systems. Here $\|\ldots\|$ denotes the normalized determinant. A bar above a spin orbital indicates that it is associated with β spin. For open-shell states, the reference function is given by

$$|\Phi_0\rangle = [\sum_{k=1}^{q} a_{k\alpha}^+ a_{k\beta}^+][\sum_{m=q+1}^{p} a_{m\alpha}^+]|\rangle$$

$$= \|\varphi_1\bar{\varphi}_1\cdots\varphi_k\bar{\varphi}_k\cdots\varphi_q\bar{\varphi}_q\varphi_{q+1}\cdots\varphi_m\cdots\varphi_p\| \qquad [5]$$

We define the number of unpaired spins in the system by s

$$s = p - q$$

We assume that the $|\Phi_0\rangle$ or $|0\rangle$ in shorter version is an eigenfunction of the spin operators S^2 and S_z with eigenvalues s/2(s/2+1) and s/2, respectively. We will denote the simultaneous spin eigenfunctions of S^2 and S_z by θ^j_{SM} ($j=1,2,\ldots f$)

$$S^2\theta^j_{SM} = S(S+1)\theta^j_{SM} \ , \quad S_z\theta^j_{SM} = M\theta^j_{SM} \qquad [6]$$

The index j runs over the independent spin eigenfunctions belonging to the same eigenvalues of S^2 and S_z, the number of which is denoted by f. We will construct the spin eigenfunctions through the genealogical scheme,[2] in which a particular N spin eigenfunction is specified in terms of the eigenfunctions of all smaller numbers of spins from which it has been constructed. The basis of the scheme is that an N spin eigenfunction can be obtained by combining a single spin eigenfunction with an (N-1) spin eigenfunction. The possible routes to N spin eigenfunctions are conveniently summarized on a branching diagram.

Throughout the paper, indices k,ℓ refer to the closed-shell orbitals, m,n to open-shell orbitals and i,j to general orbitals. For the sake of convenience, we will separate the spin index and employ the two-component operators. The a_i and b_i are then represented by column matrices,

$$a_i = \begin{matrix} a_{i\alpha} \\ a_{i\beta} \end{matrix} \qquad b_i = \begin{matrix} b_{i\alpha} \\ b_{i\beta} \end{matrix} \qquad [7]$$

The one-particle cluster generator T_1 is written as

$$T_1 = T_c + T_o$$

where T_c and T_o are the one-particle cluster generators for closed-shell and open-shell manifolds, respectively. These are expressed in terms of the excitation operators as

$$T_c = \sum_k [\ f_{0,k} S^+_{0,k} + \sum_\tau f_{\tau,k} S^+_{\tau,k}] \ , \ (\tau = x,y,z)$$

$$T_o = \sum_m [\ f_{0,m} S^+_{0,m} + f_{x,m} S^+_{x,m}\ ] \qquad [8]$$

The closed-shell excitation operators are defined as

$$S^+_{0,k} = \sqrt{2}\ b^+_k\ \sigma_0\ a_k \ , \qquad S^+_{\tau,k} = \sqrt{2}\ b^+_k\ \sigma_\tau\ a_k \quad (\tau=x,y,z) \qquad [9]$$

and the open-shell excitation operators are given by

$$S^+_{0,m} = b^+_m\ \sigma_0\ a_m \ , \qquad S^+_{x,k} = b^+_k\ \sigma_x\ a_k \qquad [10]$$

Here σ_0 and σ_τ (τ=x,y,z) represent 2*2 unit and Pauli matrices, respectively. The f in [8] are complex and their real part is referred to as g and imaginary part to as h, namely $f=g+ih$.

The $S^+_{0,k}$ is called the singlet excitation operator since it generates a singlet-type excited configuration when operating on the reference function $|0\rangle$

$$S^{+}_{0,k}|0> = \|\varphi_1\bar{\varphi}_1 \ldots \chi_k\varphi_k(\alpha\beta-\beta\alpha)/\sqrt{2} \ldots .\| \qquad [11]$$

where χ_k is the spatial orbital created by b^{+}_{k}. Similarly $S^{+}_{\tau,k}$ is named as the triplet excitation operator since it gives a triplet-type excited configuration when operating on the closed-shell reference function, which is an eigenfunction of the operator corresponding to τ component of the total spin angular momentum,

$$S^{+}_{z,k}|0> = \|\varphi_1\bar{\varphi}_1 \ldots \chi_k\varphi_k(\alpha\beta+\beta\alpha)/\sqrt{2} \ldots \varphi_n\bar{\varphi}_n\| \qquad [12]$$

However, when the reference function $|0>$ is an open-shell determinant as in [5], three triplet excitation operators generate the spin contaminating excited states, while the singlet excitation operators preserve the spin symmetry. For instance, the $S^{+}_{z,k}$ operator for open-shell systems can be expressed as a sum of spin-adapted excitation operators,

$$S^{+}_{z,k} = \left(\frac{s}{s+2}\right)^{1/2} {}^{s/2}S^{+}_{p,k} + \left(\frac{2}{s+2}\right)^{1/2} {}^{(s+2)/2}S^{+}_{1,k} \qquad [13]$$

where

$${}^{s/2}S^{+}_{p,k} = (s+2)^{-1/2}\left[\sqrt{s/2}\left(b^{+}_{k\alpha}a_{k\alpha} - b^{+}_{k\beta}a_{k\beta}\right) + \sqrt{2/s}\; b^{+}_{k\alpha}a_{k\beta} \sum_{m} a^{+}_{m\beta}a_{m\alpha}\right]$$

$${}^{(s+2)/2}S^{+}_{1,k} = (s+2)^{-1/2}\left[b^{+}_{k\alpha}a_{k\alpha} - b^{+}_{k\beta}a_{k\beta} - b^{+}_{k\alpha}a_{k\beta} \sum_{m} a^{+}_{m\beta}a_{m\alpha}\right] \qquad [14]$$

The ${}^{s/2}S^{+}_{p,k}$ and ${}^{(s+2)/2}S^{+}_{1,k}$ generate singly excited states of spin eigenfunctions,

$$ {}^{s/2}S^{+}_{p,k}|0> = \|\chi_k\varphi_k\varphi_{q+1}\cdots\varphi_m\cdots\varphi_p\theta^{p}_{s/2\ s/2}\| $$

$$ {}^{(s+2)/2}S^{+}_{1,k}|0> = \|\chi_k\varphi_k\varphi_{q+1}\cdots\varphi_m\cdots\varphi_p\theta^{1}_{(s/2+1)\ s/2}\| \qquad [15] $$

where

$$ \theta^{p}_{s/2\ s/2} = (s+2)^{-1/2}[\sqrt{s/2}\ (\alpha\beta+\beta\alpha)\alpha\ldots\alpha\ldots\alpha-\sqrt{2/s}\ \alpha\alpha\sum_{m}\alpha\ldots\beta\ldots\alpha] $$

$$ \theta^{1}_{(s/2+1)\ s/2} = (s+2)^{-1/2}[(\alpha\beta+\beta\alpha)\alpha\ldots\alpha\ldots\alpha + \alpha\alpha\sum_{m}\alpha\ldots\beta\ldots\alpha] \qquad [16] $$

Note here that the θ^{p} is a linear combination of the spin eigenfunctions constructed by the genealogical scheme

$$ \theta^{p}_{s/2\ s/2} = \left[\frac{s+2}{2(s+1)}\right]^{1/2}\theta^{f-1}_{s/2\ s/2} + \left[\frac{s}{2(s+1)}\right]^{1/2}\theta^{f}_{s/2\ s/2} \qquad [17] $$

These operators in [14] are essentially single excitation operators, although they involve two simultaneous elementary excitations, real excitation and spin flip in the last term, due to the spin-symmetry requirement. The ${}^{s/2}S^{+}_{p,k}$ operator makes an important role in the spin correlation problem and is called as the spin polarization excitation operator.

The ${}^{+}S_{x,k}$ and ${}^{+}S_{y,k}$ excitation operators also generate the spin contaminating excited states when operating on the open-shell reference function.

Let S be the Hermitian conjugate of S^{+}, $S=(S^{+})^{\dagger}$. From the

definition of the excitation operators, we see

$$S|0\rangle = 0 \quad \langle 0|S^{+} = 0 \qquad [17]$$

They satisfy quasiboson commutation relations

$$[S_I, S_J] = [S_J^{+}, S_I^{+}] = 0, \ \langle 0|[S_I, S_J^{+}]|0\rangle = \delta_{IJ} \qquad [18]$$

The unlinked clusters $(S^{+})^2$, $(S^{+})^3$,... generate doubly, triply,... excited states, repectively. The $(S_{0,k}^{+})^2$ and $(S_{\tau,k}^{+})^2$ give the same doubly excited state with a difference of a sign

$$(S_{0,k}^{+})^2|0\rangle = -(S_{z,k}^{+})^2|0\rangle = \|\varphi_1\bar{\varphi}_1 \cdots \chi_k\bar{\chi}_k \cdots \varphi_q\bar{\varphi}_q \cdots\| \qquad [19]$$

2. DETERMINANTAL FUNCTIONS

Let us now examine how the determinantal wavefunction can be expressed in terms of these excitation operators. For simplicity we will consider only the closed-shell case, but the discussion can easily be extended to the open-shell case. Any other Slater determinant, not actually orthogonal to $|\Phi_0\rangle$, can be expressed

$$|\Phi\rangle = \exp[\ iF_\gamma\ ]|\Phi_0\rangle \ ;$$

$$F_\gamma = \frac{1}{i}\sum_k (f_{\gamma,k}S_{\gamma,k}^{+} - f_{\gamma,k}^{*}S_{\gamma,k}) = F_\gamma^{\dagger} \qquad (\gamma = 0,x,y,z) \qquad [20]$$

The exponential operator e^{iF} is unitary due to the Hermitian property of F. Thus, the wavefunction $|\Phi\rangle$ can be obtained from the wavefunction $|\Phi_0\rangle$ by a unitary transformation. If we define a new fermion operator by

$$d^{+}_{\gamma,k} = e^{iF_\gamma} a^{+}_{k} e^{-iF_\gamma} \qquad [21]$$

then we can rewrite the $|\Phi>$ as a determinantal form

$$|\Phi> = \prod_{k} d^{+}_{\gamma,k\alpha} d^{+}_{\gamma,k\beta} |> \qquad [22]$$

These operators satisfy the fermion anticommutation relations.

An alternative prescription may be used to obtain the determinantal wavefunction. Thouless' theorem can be written in terms of the excitation operators as

$$|\Phi> = \mathfrak{N} \exp[\sum_{k} f_{\gamma,k} S^{+}_{\gamma,k}] |0> \qquad [23]$$

The factor $\mathfrak{N}$ assures the normalization. It is apparent that the $|\Phi>$ takes a determinantal form

$$|\Phi> = \prod_{k} c^{+}_{\gamma,k\alpha} c^{+}_{\gamma,k\beta} |> \qquad [24]$$

where

$$c^{+}_{\gamma,k} = (a^{+}_{k} + f'_{\gamma,k} b^{+}_{k} \sigma_\gamma)/(1 + |f'_{\gamma,k}|^2)^{1/2} \qquad [25]$$

Here we denote f' by $f/\sqrt{2}$.

The Hartree-Fock (HF) wavefunction is the optimized one within the space spanned by the determinantal functions generated by the real singlet excitation operators

$$|\Phi> = \mathfrak{N} \exp[\sum_{k} g_{0,k} S^{+}_{0,k}] |0> = \prod_{k} c^{+}_{0,k\alpha} c^{+}_{0,k\beta} |> \qquad [26]$$

where

$$c^{+}_{0,k} = (a^{+}_{k} + g'_{0,k}b^{+}_{k})/[\ 1 + (g'_{0,k})^{2}]^{1\ 2} \qquad [27]$$

The double occupancy of orbitals is preserved. The variational cluster expansion of the wavefunction given by [26] or that of the form

$$|\Phi> = \exp[\ iG_0\ ]|> \ ;\ G_0 = \frac{1}{i}\sum_k g_{0,k}(S^{+}_{0,k} - S_{0,k}) \qquad [28]$$

is the HF wavefunction for the closed-shell systems. Thus, the self-consistency effects can be expressed in the cluster expansion of a wavefunction formalism.

We wish to go further beyond the HF approximation within the framework of the orbital model, that is, within the space spanned by the determinantal functions. However, even if we extend the variational space by introducing the remaining excitation operators, we cannot reach beyond the HF approximation in case the HF solution is stable. This paradox is called the "stability dilemma." It is clearly concerned with the problems of the symmetry dilemma proposed by Lowdin.[3] The stability dilemma can be resolved by projecting the determinantal function onto the correct symmetry space. We can go beyond the HF approximation only when the stability dilemma is resolved. In the next, we will consider the stability condition for the closed-shell HF theory and then discuss the orbital theory including the electron correlation.[4,5]

3. STABILITY CONDITION FOR HARTREE-FOCK SOLUTION

A general condition for the stability problems of the HF state was first formulated by Thouless.[1] Cizek and Paldus[6] and Fukutome[7] have shown that the stability of a closed-shell HF solution involves four different types of stability. We will review the stability condition for the HF solution in terms of the excitation operators.

Consider a small displacement of the HF wavefunction, given by the unitary transformation,

$$|\Phi\rangle = \exp[\ iF\ ]|HF\rangle\ ;$$

$$F = \frac{1}{i}\sum_{\gamma}\sum_{k}(f_{\gamma,k}S^{+}_{\gamma,k} - f^{*}_{\gamma,k}S_{\gamma,k}) = F^{\dagger} \qquad (\gamma=0,x,y,z) \qquad [29]$$

where $|HF\rangle$ is the HF wavefunction. In this case, the excitation operators are defined by the HF orbitals as a basis. The energy expectation is given by

$$E = E_{HF} + i\langle HF|[H,F]|HF\rangle + \frac{i^2}{2!}\langle HF|[[H,F],F]|HF\rangle + \ldots \qquad [30]$$

where E_{HF} is the HF energy. Due to the Brillouin theorem, we have

$$\langle HF|[H,F]|HF\rangle = 0 \qquad [31]$$

This leads to a simple criterion that the energy corresponding to $|HF\rangle$ should be stationary with respect to the type of variation given by [29]. The energy is stable if

$$\frac{i^2}{2!}\langle HF|[[H,F],F]|HF\rangle \geq 0 \qquad [32]$$

This inequality is known as the stability condition for the HF state. Expanding [32] we obtain the stabilty condition

$$\frac{1}{2}\begin{matrix} f_0^\dagger & A_0 & B_0 & f \\ f_0^* & B_0^* & A_0^* & f_0^* \end{matrix} + \frac{1}{2}\sum_\tau \begin{matrix} f_\tau^\dagger & A_t & B_t & f_\tau \\ f_\tau^* & B_t^* & A_t^* & f_\tau^* \end{matrix} \geq 0 \qquad [33]$$

for all coefficients f. Here the f_0 and f_τ are the column vectors formed by $f_{0,k}$ and $f_{\tau,k}$, respectively. The supermatrices A and B are defined as

$$(A_0)_{k\ell} = \langle HF|S_{0,k}HS^+_{0,\ell} - E_{HF}|HF\rangle,$$

$$(B_0)_{k\ell} = \langle HF|S_{0,k}S_{0,\ell}H|HF\rangle,$$

$$(A_t)_{k\ell} = \langle HF|S_{\tau,k}HS^+_{\tau,\ell} - E_{HF}|HF\rangle,$$

$$(B_t)_{k\ell} = \langle HF|S_{\tau,k}S_{\tau,\ell}H|HF\rangle \qquad (\tau=x,y,z) \qquad [34]$$

From the definition we see that A are Hermitian matrices while B are not, since $B^\dagger=B^*$. However, the supermatrices in [33] are again Hermitian. The three identical supermatrices correspond to the triplet-type excitations and the remaining supermatrix is associated with the the singlet-type excitations. Two types of independent stability conditions are called as singlet and triplet (nonsinglet) stability conditions. When the matrices A and B are real matrices, the stability conditions may further be simplified.

First consider the singlet stability condition. The singlet stability condition may be factored into two subproblems

$$g_0^{\dagger}(A_0 + B_0)g_0 + h_0^{\dagger}(A_0 - B_0)h_0 \geq 0 \qquad [35]$$

where g_0 and h_0 are column vectors of real and imaginary parts of the complex column vector $f_0(=g_0+ih_0)$. The matrices $(A_0 \pm B_0)$ are symmetric under the assumption that A_0 and B_0 are real, so unitary matrices (U, V) may be found by which the matrices $(A_0 \pm B_0)$ are diagonalized,

$$U^{\dagger}(A_0 + B_0)U = D_0^{+}$$

$$V^{\dagger}(A_0 - B_0)V = D_0^{-} \qquad [36]$$

Here D are the diagonal matrices. If we further define the unitary transformed excitation operators

$$P_{0,k}^{+} = \sum_k S_{0,k}^{+}U_{\ell k} \quad , \quad Q_{0,k}^{+} = \sum_k S_{0,k}^{+}V_{\ell k} \qquad [37]$$

together with

$$\tilde{g}_0 = U^{\dagger}g_0 \quad , \quad \tilde{h}_0 = V^{\dagger}h_0 \qquad [38]$$

Then, we have from [35] that

$$\sum_k (\tilde{g}_{0,k})^2(D_0^{+})_{kk} + \sum_k (\tilde{h}_{0,k})^2(D_0^{-})_{kk} \geq 0 \qquad [39]$$

where

$$(D_0^{+})_{kk} = \langle HF|P_{0,k}HP_{0,k}^{+} - E_{HF} + P_{0,k}P_{0,k}^{H}|HF\rangle$$

$$(D_0^{-})_{kk} = \langle HF|Q_{0,k}HQ_{0,k}^{+} - E_{HF} + Q_{0,k}Q_{0,k}^{H}|HF\rangle \qquad [40]$$

Thus the singlet stability condition can be classified into real and imaginary conditions,

(a) $(D_0^+)_{kk} \geq 0$, for all k

real singlet stability condition

(b) $(D_0^-)_{kk} \geq 0$, for all k

imaginary singlet stability condition

In the same manner, each triplet stability condition is factored into real and imaginary conditions when A_t and B_t matrices are real. Using the diagonal transformations, we can define the new sets of triplet excitation operators P_τ^+ and Q_τ^+ and coefficients $\tilde{g}_\tau$ and $\tilde{h}_\tau$. Then we have

(c) $(D_t^+)_{kk} = \langle HF|P_{\tau,k}HP_{\tau,k}^+ - E_{HF} + P_{\tau,k}P_{\tau,k}H|HF\rangle \geq 0$

for all k, real triplet stability condition

(d) $(D_t^-)_{kk} = \langle HF|Q_{\tau,k}HQ_{\tau,k}^+ - E_{HF} + Q_{\tau,k}Q_{\tau,k}H|HF\rangle \geq 0$

for all k, imaginary triplet stability condition

These stability conditions ensure that the HF single determinantal wavefunction represents a true minimum of the energy functional within the space spanned by all determinantal functions. As derived above the general variational space is separated into independent subspaces generated by the excitation operators and hence, we obtain an independent stability condition for each subspace. This factorization leads to a useful classification of the orbital theories. We now discuss the instability conditions of the HF solution, suggested by the form of the above stability conditions. For the sake of resulting formal simplicity, we

employ the uncoupled approximation. That is, the unitary transformed excitation operator P^+, Q^+ are replaced by the primitive excitation operators S^+. The uncoupled approximation simplifies the instability conditions to the following forms

(a) $E_{0,k} - E_{HF} + K_{kk}^* < 0$, for all k
real singlet instability condition,

(b) $E_{0,k} - E_{HF} - K_{kk}^* < 0$, for all k
imaginary singlet instability condition,

(c) $E_{t,k} - E_{HF} - K_{kk}^* < 0$, for all k
real triplet instability condition,

(d) $E_{t,k} - E_{HF} + K_{kk}^* < 0$, for all k
imaginary triplet instability condition

where $E_{0,k}$ and $E_{t,k}$ are energies of the singlet and triplet excited states respectively and K_{kk}^* is the usual exchange integral due to the relation of [19]

$$E_{0,k} = \langle HF|S_{0,k}HS_{0,k}^+|HF\rangle$$

$$E_{t,k} = \langle HF|S_{\tau,k}HS_{\tau,k}^+|HF\rangle$$

$$K_{kk}^* = \langle HF|S_{0,k}S_{0,k}H|HF\rangle = -\langle HF|S_{\tau,k}S_{\tau,k}H|HF\rangle \qquad [41]$$

If these instability conditions are satisfied in the HF solution, it means that it does not represent a true minimum with respect to the corresponding fluctuation and that another solution, having

the lower energy than the HF solution, must exist.

In case of the singlet instability problems, the new solutions preserve the double occupancy of the orbitals and therefore preserve the spin symmetry but they violate the space symmetry. The real instability condition is rewritten as

$$E_{HF} - E_{0,k} > K_{kk}^{*} \geq 0 \qquad [42]$$

This implies that the singlet excited state has lower energy than the ground state. Comparing to the real and imaginary singlet instability conditions, we see that the imaginary singlet instability may procede the real singlet instability. In case of the triplet instability problems, the double occupancy, and therefore the singlet character of the HF wavefunction, is not preserved and unrestricted HF (UHF) solutions appear. From the imaginary triplet instability condition we see that the triplet excited state has lower energy than the ground state

$$E_{HF} - E_{t,k} > K_{kk}^{*} \geq 0 \qquad [43]$$

when the HF solution is imaginary triplet unstable.

We start from the reference determinant |HF> built from the HF orbitals. By adding the variational subspace generated by one of the real triplet excitation operators, we have the function

$$|\Phi\rangle = \exp\{\ i G_z\ \}|HF\rangle\ ;$$

$$G_z = \frac{1}{i} \Sigma\ g_{z,k}(S^{+}_{z,k} - S_{z,k}) \qquad [44]$$

where $g_{z,k}$ are real quantities. The energy for |Φ> is

$$E = E_{HF} + i\langle HF|[H,G_z]|HF\rangle + \frac{i^2}{2!}\langle HF|[[H,G_z],G_z]|HF\rangle + \ldots \quad [45]$$

First order correction to the energy vanishes due to the spin symmetry indicating that the energy be stationary. Thus, the subspace added does work as the variational space only if the HF solution is real triplet unstable, namely if

$$\frac{i^2}{2!}\langle HF|[[H,G_z],G_z]|HF\rangle = g_z^{\dagger}(A_t + B_t)g_z < 0 \quad [46]$$

Even if we extend the variational space by introducing the excitation operators, we cannot reach beyond the HF approximation in case the HF solution is stable. This paradox is called the stability dilemma. When the HF solution is unstable, another solution, having lower energy than the HF energy, must exist. Unfortunately the corresponding wavefunction is no longer symmetry-adapted. In this case, the spin-symmetry is not preserved. The release from the stability dilemma results in the symmetry paradox.

Now consider the wavefunction by projecting out the component with the correct symmetry

$$|\Phi'\rangle = \mathbb{O}_S|\Phi\rangle = \mathbb{O}_S \exp[\, iG_z]|HF\rangle \quad [47]$$

where $\mathbb{O}_S$ is the spin projection operator which selects the singlet spin eigenfunctions. We see that the first order energy shift for $|\Phi'\rangle$ vanishes and the stability condition is reduced to

$$g_z^{\dagger}B_t g_z \geq 0 \quad [48]$$

due to the projection operator. The stability condition [48] is

equivalent to requiring that the B_t matrix be positive definite. Since the trace of the B_t matrix is nonpositive,

$$Tr(B_t) = \sum_k \langle HF|S_{z,k}S_{z,k}H|HF\rangle = -\sum_k K_{kk^*} \leq 0 \qquad [49]$$

there always exists at least one negative eigenvalue of the B_t. If the B_t has any negative eigenvalue, it is possible to construct an anti-Hermitian operator iG_z which violates the stability condition [48]. Thus, we can go beyond the HF approximation. The spin-symmetry is also restored. The projection operator introduced preserves the symmetry property by projecting the symmetry adapted components and also resolves the stability dilemma by violating the stability condition.

Noting the sign of the trace of the B_0 and B_t matrices defined by [41],

$$Tr(B_0) = \sum_k \langle HF|S_{0,k}S_{0,k}HF|HF\rangle = \Sigma K_{kk^*} \geq 0$$

$$Tr(B_t) = \sum_k \langle HF|S_{t,k}S_{t,k}HF|HF\rangle = -\Sigma K_{kk^*} \geq 0 \qquad [50]$$

we see that the imaginary singlet and real triplet stability dilemmas can be resolved by applying the appropriate projection operators. That is, the imaginary singlet and three real triplet excitation operators generate the variational space for the improvement of the HF theory.

In general, the closed-shell orbital theories including the electron correlation can be defined as

$$|\Phi\rangle = \mathcal{P} \exp[\ iF\ ]|0\rangle \qquad [51]$$

where the F is the excitation operator to give the variational space and $\mathcal{P}$ is the projection operator to resolve the stability dilemma. By appropriate choice of the excitation operator and the projection operator, we can obtain the various orbital theories proposed so far for improving upon the HF approximation.

For the open-shell systems, we can also derive the stability conditions for the restricted HF (RHF) solution in the same mannar as done in the closed-shell systems. Unlike the closed-shell systems, the UHF wavefunction for open-shell states always leads to lower energy than the RHF wavefunction. The UHF orbitals can be created by making use of the $S^{+}_{z,k}$ excitation operators. Consider the infinitesimal unitary transformation given by

$$|\Phi\rangle = \exp[\ iF_{cz}]|RHF\rangle\ ;$$

$$F_{cz} = \frac{1}{i} \sum_{k} (f_{z,k}S^{+}_{z,k} - f^{*}_{z,k}S_{z,k}) \qquad [52]$$

In this case, the open-shell reference function is a RHF wavefunction. The energy for $|\Phi\rangle$ is

$$E = E_{RHF} + i\langle RHF|[H,\ F_{cz}]|RHF\rangle + \ldots \qquad [53]$$

The relation [13] reduces the first order energy shift to

$$i\langle RHF|[H,F_{cz}]|RHF\rangle = \left(\frac{s}{s+2}\right)^{1\ 2} \sum_{k} f_{z,k}\langle RHF|H\ ^{s/2}S^{+}_{p,k}|RHF\rangle + C.C. \qquad [54]$$

The first order correction to the energy does not vanish, implying

that the RHF solution is not stationary to the variation described by [52]. Thus the open-shell UHF wavefunction always leads to the lower energy than the RHF wavefunction.

The open-shell orbital theory including the electron correlation can be defined as

$$|\Phi\rangle = \mathcal{P} \exp[\, iF_c + iF_o \,]|0\rangle \qquad [55]$$

where F_c and F_o are the closed-shell and open-shell excitation operators respectively. By making use of the imaginary singlet and two types of real triplet (S_x^+ and S_y^+) excitation operators, we can construct the various open-shell orbital theories including the electron correlation.

4. ANALYSIS OF THE ORBITAL THEORY

Now we will analyze the orbital theories including the electron correlation. First, we will consider the alternant molecular orbitals (AMO) for closed-shell systems proposed by Lowdin[8] and examine why one can remove a large part of the correlation error simply by permitting so-called different orbitals for different spins (DODS). The DODS idea is used in the UHF[9] and spin extended HF (SEHF) theories[10] for open-shell states. However, they are poor for both the electron correlation and spin correlation. The SEHF is a good example to understand the importance of resolving the stability paradox. The generalized valence bond (GVB) method[11] and complex molecular orbital (CMO) method[12] will also be discussed.

(a) The DODS Type Wavefunction for Closed-Shell States

We start with the unprojected form of the DODS type wavefunction,

$$|\Phi> = \mathcal{N} \exp[\sum_k g_{0,k} S^+_{0,k} + \sum_k g_{z,k} S^+_{z,k}] \; |0> \qquad [56]$$

When we start from the arbitrary determinant, not from the HF wavefunction, the real singlet excitation operators ($S^+_{0,k}$) are necessary to generate the HF orbitals. If we define the new fermion operators by making a canonical transformation,

$$c^+_{0,k} = (a^+_k + g'_{0,k} b^+_k)/[1 + (g'_{0,k})^2]^{1\ 2}$$

$$c^+_{0,k*} = (b^+_k - g'_{0,k} a^+_k)/[1 + (g'_{0,k})^2]^{1\ 2} \qquad [57]$$

the above wavefunction can be rewritten as

$$|\Phi> = \prod_k c^+_{k\alpha} c^+_{k\beta} |> \qquad [58]$$

where

$$c^+_k = \xi_k c^+_{0,k} + \eta_k c^+_{0,k*} \sigma_z \qquad [59]$$

with

$$\xi_k = 1/[1 + (g'_{z,k})^2]^{1\ 2} \ , \quad \eta_k = g'_{z,k}/[1 + (g'_{z,k})^2]^{1\ 2} \qquad [60]$$

Let us introduce the spatial orbitals for $c^+_{0,k}$ and $c^+_{0,k*}$

$$c^+_{0,k}|> = (\lambda_k \alpha, \lambda_k \beta) \ , \quad c^+_{0,k*}|> = (\nu_k \alpha, \nu_k \beta) \qquad [61]$$

The λ_k and ν_k are spatially orthogonal to each other and the

reduced density matrix for $|\Phi>$ becomes diagonal

$$\rho(1|2) = \sum_k 2\ \xi_k^2\ \lambda_k(1)\lambda_k(2) + \sum_k 2\ \eta_k^2\ \nu_k(1)\nu_k(2) \qquad [62]$$

These functions λ_k, ν_k are therefore the natural orbitals. Due to the relation that $\xi_k^2 + \eta_k^2 = 1$, the ξ_k^2 is the fractional occupation probability for the natural orbital λ_k and η_k^2 is that for the ν_k. In terms of these natural orbitals, we have

$$|\Phi> = \|\varphi_{1a}\varphi_{2a}\cdots\varphi_{na}\bar{\varphi}_{1b}\bar{\varphi}_{2b}\cdots\bar{\varphi}_{nb}\| \qquad [63]$$

where

$$\varphi_{ka} = \xi_k\lambda_k + \eta_k\nu_k$$

$$\varphi_{kb} = \xi_k\lambda_k - \eta_k\nu_k \qquad [64]$$

The new orbitals φ have the property that their spatial overlap integral is diagonal and are called the corresponding orbitals. This expression suggests that the optimized cluster expansion of the wavefunction of the form of [56] is the UHF wavefunction for closed-shell systems.

Since the η_k are small numbers, we can expand $|\Phi>$ in terms of the natural orbitals

$$|\Phi> = C_{rf}|\Phi_{rf}> + C_1|\Phi_1> + C_2|\Phi_2> + \ldots \qquad [65]$$

in the form of the limited CI. Here the Φ_{rf} is the normalized restricted function with doubly occupied orbitals

$$|\Phi_{rf}> = \|\lambda_1\bar{\lambda}_1 \cdots \lambda_k\bar{\lambda}_k \cdots \lambda_n\bar{\lambda}_n\| \qquad [66]$$

with the coefficient given by

$$C_{rf} = \prod_k (\xi_k)^2 \qquad [67]$$

The reference function $|\Phi_{rf}>$ is approximated as the HF determinant but, of course, they will not be identical. The functions $|\Phi_1>$, $|\Phi_2>$, ... are singly, doubly,... excited configurations,

$$C_1|\Phi_1> = \sum_k \sqrt{2}\, C_{rf}(\eta_k/\xi_k)\, \|\lambda_1\bar{\lambda}_1 \cdots \nu_k\lambda_k(\alpha\beta+\beta\alpha)/\sqrt{2} \cdots \lambda_n\bar{\lambda}_n\|$$

$$C_2|\Phi_2> = -\sum_k C_{rf}(\eta_k/\xi_k)^2\, \|\lambda_1\bar{\lambda}_1 \cdots \nu_k\bar{\nu}_k \cdots \lambda_n\bar{\lambda}_n\|$$

$$+ \sum_k C_{rf}(\eta_k/\xi_k)(\eta_\ell/\xi_\ell)\|\lambda_1\bar{\lambda}_1 \cdots \nu_k\lambda_k\nu_\ell\lambda_\ell(\alpha\beta+\beta\alpha)(\alpha\beta+\beta\alpha)/2 \cdots\| \qquad [68]$$

The higher order terms are written in the same manner as above. Note here that the singly and doubly excited configurations include the nonsinglet spin states. The closed-shell UHF theory may exist only when the HF solution is real triplet unstable, which is a striking contrast to the open-shell case. In case the HF state is stable, the coefficients η_k are all zero due to the stability dilemma.

Now we consider the wavefunction by applying the projection operator and selecting the component of the singlet spin eigenfunction

$$|\Phi'\rangle = \mathcal{O}_S|\Phi\rangle \qquad [69]$$

The variational cluster expansion of [69] is the AMO wavefunction.[8] It is called SEHF wavefunction by Kaldor[10] and GF function by Goddard.[13] As the projection operator acts only on the spin part of the wavefunction, we can rewrite $|\Phi'\rangle$ as

$$|\Phi'\rangle = C_{rf}|\Phi_{rf}\rangle + C_2|\Phi_2\rangle + \ldots \qquad [70]$$

The singly excited configurations vanish due to the projection operator. The leading excited configurations are the doubly excited ones. This is the reason why we can cover a large part of the correlation effect simply by permitting the DODS in closed-shell case. The doubly excited configurations take the form

$$C_2|\Phi_2\rangle = -\sum_k C_{rf}(\eta_k/\xi_k)^2 \,\|\lambda_1\bar{\lambda}_1\cdots\nu_k\bar{\nu}_k\cdots\lambda_n\bar{\lambda}_n\|$$

$$-\sum_k (1/\sqrt{3})C_{rf}(\eta_k/\xi_k)(\eta_\ell/\xi_\ell)\|\lambda_1\bar{\lambda}_1\cdots\nu_k\lambda_k\nu_\ell\lambda_\ell\theta^2_{00}\cdots\lambda_n\bar{\lambda}_n\| \qquad [71]$$

where

$$\theta^2_{00} = \{(2\alpha\alpha\beta-\alpha\beta\alpha-\beta\alpha\alpha)\beta-(\alpha\beta\beta+\beta\alpha\beta-2\beta\beta\alpha)\alpha\}/\sqrt{12} \qquad [72]$$

The spin coupling appeared in the AMO wavefunction is θ^f_{00} (f=2) associated with the standard tableaux S_1. This type of spin coupling is not keeping our intuitive idea such as electron-pair bond.

(b) The DODS Type Wavefunction for Open-Shell States

Let us consider the DODS type wavefunction for open-shell systems represented by

$$|\Phi\rangle = \mathfrak{N} \exp[\sum_k g_{0,k} S^+_{0,k} + \sum_k g_{z,k} S^+_{z,k} + \sum_m g_{0,m} S^+_{0,m}]|0\rangle \qquad [73]$$

Here $|0\rangle$ is the open-shell reference function as in [5]. The above wavefunction is expressed as a determinantal function

$$|\Phi\rangle = [\prod_k c^+_{k\alpha} c^+_{k\beta}][\prod_m c^+_{m\alpha}]|\rangle \qquad [74]$$

where

$$\mathbf{c}^+_k = \xi_k \mathbf{c}^+_{0,k} + \eta_k \mathbf{c}^+_{0,k*} \sigma_z$$

$$\mathbf{c}^+_m = (\mathbf{a}^+_m + g'_{0,m} \mathbf{b}^+_m)/[1 + (g'_{0,m})^2]^{1/2} \qquad [75]$$

Now let us define the spatial orbital λ_m for $\mathbf{c}^+_m$. Then the reduced density matrix for $|\Phi\rangle$ becomes

$$\rho(1|2) = \sum_k 2\xi_k^2 \lambda_k(1)\lambda_k(2) + \sum_k 2\eta_k^2 \nu_k(1)\nu_k(2) + \sum_m \lambda_m(1)\lambda_m(2) \qquad [76]$$

The λ_k, ν_k and λ_m are also natural orbitals. If these natural orbitals are replaced by

$$\varphi_{ka} = \xi_k \lambda_k + \eta_k \nu_k$$

$$\varphi_{kb} = \xi_k \lambda_k - \eta_k \nu_k$$

$$\varphi_{ma} = \lambda_m \qquad [77]$$

then we obtain the expression for $|\Phi\rangle$

$$|\Phi\rangle = \|\varphi_{1a}\varphi_{2a}\cdots\varphi_{pa}\bar{\varphi}_{1b}\bar{\varphi}_{2b}\cdots\bar{\varphi}_{qb}\| \qquad [78]$$

Since the η_k are small numbers, we can expand $|\Phi\rangle$ by means of the natural orbitals as in the closed-shell case

$$|\Phi\rangle = C_{rf}|\Phi_{rf}\rangle + C_1|\Phi_1\rangle + C_2|\Phi_2\rangle + \ldots \qquad [79]$$

For open-shell case, the singly excited configuration $|\Phi_1\rangle$ is not a spin eigenfunction and can be expressed as

$$|\Phi_1\rangle = \left(\frac{s}{s+2}\right)^{1/2} \sum_k {}^{s/2}|\Phi_k^p\rangle + \left(\frac{2}{s+2}\right)^{1/2} \sum_k {}^{(s+2)/2}|\Phi_k^1\rangle \qquad [80]$$

where

$${}^{s/2}|\Phi_k^p\rangle = \|\nu_k\lambda_k\cdots\lambda_{q+1}\cdots\lambda_m\cdots\lambda_p\theta^p_{s/2\ s/2}\|$$

$${}^{(s+2)/2}|\Phi_k^1\rangle = \|\nu_k\lambda_k\cdots\lambda_{q+1}\cdots\lambda_m\cdots\lambda_p\theta^1_{(s/2+1)\ s/2}\| \qquad [81]$$

This result is a consequence of the relation given by [13]. Thus the ${}^{(s+2)/2}|\Phi_k^1\rangle$ are the main spin-contaminating configurations of the UHF wavefunction.[9] For example, taking 3-electron doublet spin state (s=1);

$${}^{s/2}\theta^p_{s/2\ s/2} = {}^{1/2}\theta^2_{1/2\ 1/2} = (\alpha\beta\alpha+\beta\alpha\alpha-2\alpha\alpha\beta)/\sqrt{6}$$

$${}^{(s+2)/2}\theta^1_{(s/2+1)\ s/2} = {}^{3/2}\theta^1_{3/2\ 1/2} = (\alpha\beta\alpha+\beta\alpha\alpha+\alpha\alpha\beta)/\sqrt{3} \qquad [82]$$

Thus, the open-shell UHF solution always exists due to the configuration of $^{s/2}|\Phi^{p}>$.

Now consider the SEHF (GF) method.[10,13] The SEHF wavefunction is the optimized one of the form

$$|\Phi^{SEHF}> = \mathcal{O}_S|\Phi^{UHF}> \qquad [83]$$

Expanding $|\Phi^{SEHF}>$ in terms of the natural orbitals, we obtain, instead of [79], that

$$|\Phi^{SEHF}> = C_{rf}|\Phi_{rf}> + C_1\mathcal{O}_S|\Phi_1> + C_2\mathcal{O}_S|\Phi_2> + \ldots \qquad [84]$$

In the closed-shell SEHF wavefunction, the singly excited configurations vanish due to the projection operator. In open shell case, however, the singly excited configurations still remain even if we apply the projection operator. The singly excited configurations in open-shell SEHF wavefunction become

$$\mathcal{O}_S|\Phi_1> = \left(\frac{s}{s+2}\right)^{1/2} \sum_k {}^{s/2}|\Phi_k^{p}> \qquad [85]$$

The improvement from the RHF energy originates from the singly excited configurations, not from the doubly excited configurations. The open-shell SEHF theory takes the orbital correction into account but it does not involve the electron pair correlation through the two-body interactions. We should note that the closed-shell and open-shell SEHF theories are constructed on a quite different approximation.

The $S^{+}_{Z,k}$ operators which give the DODS orbitals are a sum of the spin-adapted excitation operators as shown in [13]. If the

$S^{+}_{z,k}$ operators are replaced by spin polarization operators $^{s/2}S^{+}_{p,k}$ in the SEHF method, the resultant wavefunction constitutes our pseudo-orbital theory,[14]

$$|\Phi\rangle = \mathcal{O}_S\mathfrak{N} \exp[\sum_k g_{0,k}S^{+}_{0,k} + \sum_k g_{z,k}{}^{s/2}S^{+}_{p,k} + \sum_m g_{0,m}S^{+}_{0,m}]|0\rangle$$

$$= \mathcal{O}_S\mathfrak{N} \exp[\sum_k g_{z,k}{}^{s/2}S^{+}_{p,k}]|RHF\rangle \qquad [86]$$

Then the first order correction vanishes to the expectation value of one-electron spin dependent operators. Therefore, the psuedo-orbital theory involves the spin correlation correctly and gives the reasonably accurate spin density within orbital theoretic approach.[14]

On the other hand, if the $^{(s+2)/2}S^{+}_{1,k}$ operators are considered instead of the $S^{+}_{z,k}$, we have

$$|\Phi\rangle = \mathcal{O}_S\mathfrak{N} \exp[\sum_k g_{0,k}S^{+}_{0,k} + \sum_k g_{z,k}{}^{(s+2)/2}S^{+}_{1,k} \sum_m g_{0,m}S^{+}_{0,m}]|0\rangle \qquad [87]$$

The unprojected wavefunction of [87] has the stability dilemma, unlike the SEHF one, and the projection operator resolves the dilemma. Thus, the electron correlation can be included through the unlinked clusters of $^{(s+2)/2}S^{+}_{1,k}$. When the two excitation operators, $^{s/2}S^{+}_{p,k}$ and $^{(s+2)/2}S^{+}_{1,k}$, are treated independently, both the spin and electron correlations can be described correctly. However, when these two operators are combined to yield the $S^{+}_{z,k}$ operator like in UHF and SEHF theories, two effects interfere each other and the method becomes poor for the description of the

energy and the spin density. In the UHF theory, the stability dilemma does not occur due to the existence of the spin polarization operators, ${}^{s/2}S^{+}_{p,k}$, and the self-consistency effects (unlinked terms) of the spin polarization operators should be distorted by the unlinked terms of the ${}^{(s+2)/2}S^{+}_{1,k}$ operators. The pseudo-orbital theory is free from these theoretical defects. A proper inclusion of the (unlinked) self-consistency effect is quite important and the pseudo-orbital theory realizes this requirement in a simple orbital framework.

(c) Complex Molecular Orbitals

Next we consider the complex molecular orbitals (CMO) for closed-shell states described by

$$|\Phi\rangle = \mathcal{O}_R \mathcal{R} \exp[\sum_k f_{0,k} S^{+}_{0,k}]|0\rangle \qquad [88]$$

The $f_{0,k}$ are complex and the unprojected form of [88] leads to the complex HF theory.[12] The $\mathcal{O}_R$ is the projection operator which selects out the real part of the wavefunction. This operator recovers the space symmetry violated by the imaginary singlet excitation operators. It is apparent that

$$|\Phi\rangle = \mathcal{O}_R \prod_k c^{+}_{k\alpha} c^{+}_{k\beta}|\rangle \qquad [89]$$

where

$$\mathbf{c}^{+}_{k} = (\mathbf{c}^{+}_{0,k} + i h'_{0,k} \mathbf{c}^{+}_{0,k*})/[1 + (h'_{0,k})^2]^{1/2} \qquad [90]$$

The $\mathbf{c}^{+}_{0,k}$ and $\mathbf{c}^{+}_{0,k*}$ have the same form as defined by [57]. In a

similar manner, we can define the coefficients ξ_k and η_k by

$$\xi_k = 1/[1 + (h'_{0,k})^2]^{1/2}, \quad \eta_k = h'_{0,k}/[1 + (h'_{0,k})^2]^{1/2} \qquad [91]$$

and spatial orbitals λ_k and ν_k for $\mathbf{c}^+_{0,k}$ and $\mathbf{c}^+_{0,k*}$, respectively. Then, λ_k and ν_k are again the natural orbitals of the unprojected wavefunction of [88]. The CMO wavefunction can be expanded in the limited CI based on its natural orbitals

$$|\Phi\rangle = \mathcal{O}_R \| \ldots (\xi_k\lambda_k + i\xi_k\nu_k)(\xi_k\bar{\lambda}_k + i\eta_k\bar{\nu}_k) \ldots \|$$

$$= C_{rf}|\Phi_{rf}\rangle + C_2|\Phi_2\rangle + \ldots \qquad [92]$$

The reference function is again a restricted wavefunction with doubly occupied orbitals. The singly excited configurations vanish due to their pure imaginary property. The doubly excited configurations have the form

$$C_2|\Phi_2\rangle = -\sum_k C_{rf}(\eta_k/\xi_k)^2 \|\lambda_1\bar{\lambda}_1 \ldots \nu_k\bar{\nu}_k \ldots \lambda_n\bar{\lambda}_n\|$$

$$+ \sum_k C_{rf}(\eta_k/\xi_k)(\eta_\ell/\xi_\ell)\|\lambda_1\bar{\lambda}_1 \ldots \nu_k\lambda_k\nu_\ell\lambda_\ell(\alpha\beta-\beta\alpha)(\alpha\beta-\beta\alpha)/2 \ldots\| \qquad [93]$$

The CMO wavefunction involves the choice of the singlet type spin couplings represented by θ^1. The singlet spin coupling may cause the lower energy than the corresponding spin polarization type spin coupling appeared in SEHF wavefunction since the former might be thought as representing covalent bonds but the latter is not in keeping our intuitive idea such as electron pair bond. Thus the

CMO theory gives the lower energy than the SEHF theory.

Now we define the wavefunction expressed as

$$|\Phi\rangle = \mathfrak{N} \exp\Big[\sum_k g_{0,k} S^{+}_{0,k} + \frac{1}{2} \sum_k (ih_{0,k} {}^{+}S_{0,k}^{2}) \Big] |0\rangle \qquad [94]$$

Then we can rewrite the above wavefunction as

$$|\Phi\rangle = \prod_k c^{+}_{kk} |\rangle \qquad [95]$$

where c^{+}_{kk} is the two-particle creation operator

$$c^{+}_{kk} = [c^{+}_{0,k\alpha} c^{+}_{0,k\beta} - (h'_{0,k})^2 c^{+}_{0,k*\alpha} c^{+}_{0,k*\beta}]/[1 + (h'_{0,k})^4]^{1/2} \qquad [96]$$

Note here that the $(ih_{0,k} S^{+}_{0,k})^2$ are the unlinked terms of the imaginary singlet excitation operators but they generate two-particle cluster functions. If we further define

$$\xi_k = 1/[1 + (h'_{0,k})^2]^{1/2} \ , \ \eta_k = h'_{0,k}/[1 + (h'_{0,k})^2]^{1/2} \qquad [97]$$

and the spatial orbitals λ_k and ν_k for $\mathbf{c}^{+}_{0,k}$ and $\mathbf{c}^{+}_{0,k*}$, we have

$$|\Phi\rangle = \| \varphi_{1a}\varphi_{1b}(\alpha\beta - \beta\alpha)/\sqrt{2} \ \ldots \ \varphi_{na}\varphi_{nb}(\alpha\beta - \beta\alpha)/\sqrt{2} \| \qquad [98]$$

where

$$\varphi_{ka} = \xi_k \lambda_k + \eta_k \nu_k \ , \ \varphi_{kb} = \xi_k \lambda_k - \eta_k \nu_k \qquad [99]$$

The φ_{ka} and φ_{kb} satisfy the strong orthogonality condition that the orbitals are orthogonal each other unless they are singlet paired,

$$\langle\varphi_{ka}|\varphi_{kb}\rangle \neq 0 \quad , \quad \langle\varphi_k|\varphi_\ell\rangle = 0 \qquad [100]$$

Therefore the optimized $|\Phi\rangle$ in [94] is the GVB wavefunction[11] proposed by Goddard. This type of wavefunction was first suggested by Hurley et al.[15] under the name of the paired-electron approximation. The GVB wavefunction is also expanded as a limited CI based on its own natural orbitals. The expansion is analogous to those of the SEHF and CMO wavefunctions. However, the GVB wavefunction only includes the paired-type doubly excited configurations;

$$\|\lambda_1\lambda_1\cdots\nu_k\nu_k\cdots\lambda_n\lambda_n\|$$

The CMO wavefunction for open-shell systems is also defined in a similar manner as in [88]. The wavefunction involves the singlet type spin couplings θ^1 associated with the standard tableux S_f . For example, the spin coupling appeared in the doubly excited configurations for doublet spin state is

$$\theta^1_{1/2\ 1/2} = (\alpha\beta-\beta\alpha)(\alpha\beta-\beta\alpha)\alpha/2 \qquad [101]$$

The spin polarization type spin coupling represented by θ^p does not appear in the CMO method. Thus the CMO is not suitable for the calculation of the spin dependent properties.

(4) Complex DODS Wavefunction

Next consider the wavefunction defined by

$$|\Phi\rangle = \mathcal{O}_R\mathcal{O}_S\mathcal{R}\ \exp[\ \sum_k f_{0,k}S^+_{0,k} + \Sigma\ g_{z,k}S^+_{z,k}\ ]|0\rangle \qquad [102]$$

The $|\Phi\rangle$ can be written in the following determinantal form

$$|\Phi\rangle = \mathcal{O}_R\mathcal{O}_S \prod_k c^+_{k\alpha}c^+_{k\beta}|\rangle \qquad [103]$$

where

$$\mathbf{c}^+_k = \xi_{0,k}\xi_{z,k}[\mathbf{c}^+_{0,k} + (\eta_{z,k}/\xi_{z,k})\mathbf{c}^+_{0,k*}\sigma_z + i(\eta_{0,k}/\xi_{0,k})\mathbf{c}^+_{0,k*}$$

$$-i(\eta_{0,k}/\xi_{0,k})(\eta_{z,k}/\xi_{z,k})\mathbf{c}^+_{0,k}\sigma_z \,] \qquad [103]$$

The $\xi_{0,k}$, $\eta_{0,k}$, $\xi_{z,k}$ and $\eta_{z,k}$ have the same form as defined previously. In terms of the natural orbitals λ_k, ν_k for $\mathbf{c}^+_{0,k}$ and $\mathbf{c}^+_{0,k*}$, we can expand the wavefunction as

$$|\Phi\rangle = C_{rf}|\Phi_{rf}\rangle + C_2|\Phi_2\rangle + \ldots. \qquad [104]$$

mhe reference function is again the restricted wavefunction with 64ubly occupied orbitals. The doubly excited configurations contain possible two independent spin eigenfunctions θ^1 and θ^f $(f=2)$

$$\|\nu_k\lambda_k\nu_\ell\lambda_\ell(\alpha\beta-\beta\alpha)(\alpha\beta-\beta\alpha)/2\|$$

$$\|\nu_k\lambda_k\nu_\ell\lambda_\ell(2\alpha\alpha\beta-\alpha\beta\alpha-\beta\alpha\alpha)\beta-(\alpha\beta\beta+\beta\alpha\beta-2\beta\beta\alpha)\alpha/\sqrt{12}\|$$

The complex DODS method leads to lower energy than the other orbital theories discussed above.

For open-shell systems, the complex general spin orbital (GSO) theory defined by the following cluster expansion

$$|\Phi\rangle = \mathcal{P}\,\mathfrak{N}\exp[\sum_k f_{0,k}S^+_{0,k} + \sum_k g_{x,k}S^+_{x,k} + \sum_m f_{0,m}S^+_{0,m}$$

$$+ \sum_{m} g_{x,m} S^{+}_{0,m} \,]|0> \qquad [105]$$

corresponds to the complex DODS theory for closed-shell systems. The projection operator $\mathcal{P}$, which resolves the stability dilemma, takes the form $\mathcal{P} = \mathcal{O}_R \mathcal{O}_S \mathcal{O}_M$. The $\mathcal{O}_M$ selects out the spin symmetry adapted components of S_z operator characterized by M. We see that doubly excited configurations of $|\Phi>$ involve the two types of independent spin eigenfunctions, that is, the singlet type θ^1 and the spin polarization type θ^f.

We have shown that the stability of the HF solution leads to a concept called stability dilemma. Only when the stability dilemma is resolved, the electron correlation effect can be taken into account through the unlinked terms of the one-electron linked clusters (excitation operators) within the framework of the orbital theory. The stability and symmetry paradox can be resolved by projecting the determinantal wavefunction onto the correct symmetry space. The various orbital theories can be obtained by the appropriate choice of the excitation operators.

The limited CI in terms of natural orbitals can be used to study the internal relationship of various orbital theories.

TABLE 1

The doubly excited configurations in the limited CI based on the natural orbitals of GVB, AMO(SEHF), CMO and Complex DODS wavefunctions for closed-shell states.

GVB	$\|\nu_k\nu_k\alpha\beta\|$
AMO(SEHF)	$\|\nu_k\nu_k\alpha\beta\|$
	$\|\nu_k\lambda_k\nu_\ell\lambda_\ell\{(2\alpha\alpha\beta-\alpha\beta\alpha-\beta\alpha\alpha)\beta-(\alpha\beta\beta+\beta\alpha\beta-2\beta\beta\alpha)\alpha\}/\sqrt{12}\|$
CMO	$\|\nu_k\nu_k\alpha\beta\|$
	$\|\nu_k\lambda_k\nu_\ell\lambda_\ell(\alpha\beta-\beta\alpha)(\alpha\beta-\beta\alpha)/2\|$
Complex DODS	$\|\nu_k\nu_k\alpha\beta\|$
	$\|\nu_k\lambda_k\nu_\ell\lambda_\ell(\alpha\beta-\beta\alpha)(\alpha\beta-\beta\alpha)/2\|$
	$\|\nu_k\lambda_k\nu_\ell\lambda_\ell\{(2\alpha\alpha\beta-\alpha\beta\alpha-\beta\alpha\alpha)\beta-(\alpha\beta\beta+\beta\alpha\beta-2\beta\beta\alpha)\alpha\}/\sqrt{12}\|$

TABLE 2

The leading excited configurations in the limited CI based on the natural orbitals of UHF, SEHF, GVB, CMO and Complex GSO open-shell wavefunctions for doublet spin states.

	singly excited configurations
UHF	$\|\nu_k\lambda_k\lambda_m(\alpha\beta+\beta\alpha)\alpha/\sqrt{2}\|$
SEHF	$\|\nu_k\lambda_k\lambda_m(\alpha\beta\alpha+\beta\alpha\alpha-2\alpha\alpha\beta)/\sqrt{6}\|$
	doubly excited configurations
GVB	$\|\nu_k\nu_k\lambda_m\alpha\beta\alpha\|$

CMO	$\|\nu_k\nu_k\lambda_m\alpha\beta\alpha\|$
	$\|\nu_k\lambda_k\nu_\ell\lambda_\ell\lambda_m(\alpha\beta-\beta\alpha)(\alpha\beta-\beta\alpha)\alpha/2\|$
Complex GSO	$\|\nu_k\nu_k\lambda_m\alpha\beta\alpha\|$
	$\|\nu_k\lambda_k\nu_\ell\lambda_\ell\lambda_m(\alpha\beta-\beta\alpha)(\alpha\beta-\beta\alpha)\alpha/2\|$
	$\|\nu_k\lambda_k\nu_\ell\lambda_\ell\lambda_m\{(2\alpha\alpha\beta-\alpha\beta\alpha-\beta\alpha\alpha)\beta-(\alpha\beta\beta+\beta\alpha\beta-2\beta\beta\alpha)\alpha\}\alpha/\sqrt{12}\|$
	$\|\nu_k\lambda_k\nu_m(\alpha\beta-\beta\alpha)\alpha/\sqrt{2}\|$

The leading excited configurations are most important since the higher order terms arise just from the self-consistency effects. In TABLE 1 and 2, we summarized the leading excited configurations appeared in the limited CI expansion. From these we can expect

$$E_{\text{Complex DODS}} \leq E_{\text{CMO}} \leq E_{\text{AMO}} \leq E_{\text{GVB}}$$

for closed-shell states

$$E_{\text{Complex GSO}} \leq E_{\text{CMO}} \leq E_{\text{GVB}} << E_{\text{SEHF}} < E_{\text{UHF}}$$

for open-shell states

We assumed that natural orbitals defined in each orbital theory are not identical but similar and that the singlet type spin coupling may cause the lower energy than the corresponding spin polarization type spin coupling.

5. BRUECKNER ORBITALS

The HF wavefunction is a best energy wavefunction among all possible determinantal functions. Then the first order correction to the energy vanishes due to the Brillouin theorem and also

vanishing are the first order corrections to the electron density and to the expectation value of the spin-free one-electron operators. Another criteiron of goodness is that of maximum overlap with the exact wavefunction. The best-overlap wavefunction is the determinant with least mean-square deviation from the exact wavefunction. It can be shown that the best-overlap orbitals are identical with Lowdin's exact SCF orbitals.[16] The best-overlap determinant has the very interesting property that if we expand the wavefunction in terms of the best-overlap orbitals to a complete basis, then no singly excited configurations appear in the expansion. The orbitals are also called as the Brueckner orbitals.[17]

The Brueckner orbitals can easily be obtained if one uses a cluster expansion of the wavefunction. Consider the cluster expansion of the wavefunction

$$|\Phi\rangle = \exp[\ S\ ]|0\rangle\ ;$$

$$S = C_1S_1 + C_2S_2 + \ldots + C_NS_N \qquad [106]$$

with

$$\langle\Phi_0|\Phi_0\rangle = \langle\Phi_0|\Phi\rangle = 1 \qquad [107]$$

Here S_i is a linked cluster operator which produces i-fold symmetry-adapted excited configurations when operating on $|0\rangle$ and C_i is an expansion coefficient. The Schrodinger equation

$$(H - E)|\Phi\rangle = (H - E)e^{S}|0\rangle = 0 \qquad [108]$$

is then projected against a sufficient set of the excited functions to generate a series of nonlinear coupled equations

$$\langle S_i | e^{-S} H e^{S} | 0 \rangle = 0 \qquad [109]$$

The total energy is given by projecting of the Schrodinger equation onto the reference state,

$$\langle 0 | e^{-S} H e^{S} | 0 \rangle = E \qquad [110]$$

This is our symmetry-adapted-cluster (SAC) theory for the ground state.[18] Now let us choose single, double and triple excitaions as the linked cluster,

$$|\Phi\rangle = \exp[C_i S_i + C_{ij} S_{ij} + C_{ijk} S_{ijk}] |0\rangle \qquad [111]$$

Here we used a brief notation that the repeated index implies a summation

$$C_i S_i = \sum_i C_i S_i \ , \quad C_{ij} S_{ij} = \sum_{ij} C_{ij} S_{ij} \ , \ \text{etc}$$

Then we have

$$\langle S_i | H | 0 \rangle + \langle S_i | H - E | C_j S_j \rangle + \langle S_i | H | C_{jk} S_{jk} + \frac{1}{2!} (C_j S_j)^2 \rangle$$

$$+ \langle S_i | H | C_{jk\ell} S_{jk\ell} + C_j C_{k\ell} S_j S_{k\ell} + \frac{1}{3!} (C_j S_j)^3 \rangle = 0 \qquad [112]$$

If we use the Thouless' theorem, we get

$$|\Phi\rangle = \exp[C_{ij} S_{ij} + C_{ijk} S_{ijk}] |0'\rangle \qquad [113]$$

Here $|0'\rangle$ is again a determinantal wavefunction. Thus, a stepwise

optimization of [113] is possible by first guessing C_i, then obtaining a new $|0'\rangle$ which can then be the starting point for the calculation of a new C_i with [112], etc. When the iteration is completed, we can always choose orbitals such that all C_i vanish identically. Note that the corresponding variational principle for the HF wavefunction

$$|\Phi\rangle = \exp[\ C_i S_i\ ]|0\rangle \qquad [114]$$

leads to the Brillioun condition

$$\langle S_i|H|0\rangle = 0 \qquad [115]$$

Now, imposing $C_i = 0$, we get from [112]

$$\langle S_i|H|0\rangle + \langle S_i|H|C_{jk}S_{jk}\rangle + \langle S_i|H|C_{jk\ell}S_{jk\ell}\rangle = 0 \qquad [116]$$

This is called as the Brillouin-Brueckner condition and is actually a condition for $|\Phi\rangle$ to be the Slater determinant that has maximum overlap with the exact wavefunction.

The Brueckner orbitals are useful in nuclear theory. But in atomic and molecular problems the Brueckner orbitals have any noteworthy advantage and it is believed that the Brueckner orbitals for closed-shell state do not usually differ much from the HF orbitals. In order to examine this, we have calculated Brueckner orbitals for H_2O. The calculations were performed with a double zeta quality basis, the same as that used in the earlier full CI calculations.[19] These calculations are reported at three C_{2v} geometries, corresponding to stretching of the OH bonds to R_e, $1.5*R_e$ and $2.0*R_e$. Results are summarized in TABLE 3. For

equilibrium geometry, R_e, two sets of orbitals resemble each other. The energy difference is only 0.0007 au and the overlap integral between Brueckner and HF determinants is 0.9997. However, when a single determinantal expression is not a good approximation, the best-energy and best-overlap orbitals differ considerably. For $2.0*R_e$, the energies differ by 0.022 au and the overlap between two wavefunctions is 0.9782. TABLE 3 also includes the correlation energies calculated by the SAC theory based on the Brueckner orbitals. The best-overlap determinant includes no singly excited configurations in the expansion of [106]. This leads to considerable simplification in the SAC theory.

TABLE 3

Comparison of HF orbitals and Brueckner orbitals for H_2O

	R_e	$1.5*R_e$	$2.0*R_e$
$E_{Hartree-Fock}$	-76.009842	-75.809774	-75.595188
$E_{Brueckner}$	-76.009102	-75.797353	-75.573106
$\langle\Phi_{HF}\|\Phi_{Brueckner}\rangle$	0.999679	0.995653	0.978160
Correlation energy (au) based on the Brueckner orbitals			
SAC with S_2	-0.146240	-0.205402	-0.300733
SAC with S_2 and S_3	-0.147391	-0.209178	-0.311659
full CI (ref.19)	-0.147030	-0.210992	-0.310067

6. SUMMARY

We have discussed the SCF orbital theory with the formalism of the cluster expansion of the wavefunction. Especially we stressed on analyzing the structure of the SCF orbital theory including the correlation effect. The stability and symmetry paradox may always be resolved by applying the appropriate projection operator to the determinantal function. The best results obtained if the variational parameters are revaried after projecting out the component of the trial wavefunction with the correct symmetry properties, lead to the various SCF orbital theories proposed previously. However, the procedure is sometimes difficult from the computational point of view.

Although the orbital theory constitutes the basis upon which the language of quantum chemistry is founded, it is certainly necessary to go further and perform a study of postcorrelation if more accurate information is required. The very promising approach to the correlation problem is the theory based on the cluster expansion of the wavefunction. As shown above, the one-particle cluster expansion which corresponds to the HF theory, gives the 99% of the total energy. The orbital theory including correlation effects takes into account the two-particle interaction through the unlinked terms of the one-particle cluster. Thus, the next step for improving upon HF theory is to consider two-particle linked cluster explicitly. This is our SAC[18] and

SAC-CI[20] theories. If we consider one- and two-particle clusters at a time, then we can recover 98% of the correlation error.

REFERENCES

1 D.J.Thouless, Nucl.Phys., 21 (1960) 225.

2 M.Kotani, A.Amemiya, E.Ishiguro and T.Kimura, Tables of Molecular Integrals, Maruzen, Tokyo, 1955.

3 P.O.Lowdin, Rev.Mod.Phys., 35 (1963) 496; Adv.Chem.Phys. 14 (1969) 283.

4 K.Hirao and H.Nakatsuji, J.Chem.Phys., 69 (1978) 4535.

5 K.Hirao and H.Nakatsuji, J.Chem.Phys., 69 (1978) 4548.

6 J.Cizek and J.Paldus, J.Chem.Phys., 47 (1967) 3976; ibid, 53 (1970) 821;Phys.Rev., A3 (1971) 525; J.Paldus and J.Cizek, Phys.Rev., A2 (1970) 2268.

7 H.Fukutome, Prog.Theor.Phys., 40 (1969) 1227.

8 P.O.Lowdin, Phys.Rev., 97 (1955) 1474, 1490, 1509;P.O.Lowdin Rev.Mod.Phys. 34 (1962) 520; R.Pauncz, Alternant Molecular Orbital Method, Saunders, Philadelphia, 1967.

9 J.A.Pople and R.K.Nesbet, J.Chem.Phys., 22 (1954) 571; H.Nakatsuji, J.Chem.Phys., 59 (1973) 2586.

10 U.Kaldor, J.Chem.Phys., 48 (1968) 450.

11 W.J.Hunt, P.J.Hays and W.A.Goddard, J.Chem.Phys., 57 (1972) 738 ; F.W.Bobrowicz and W.A.Goddard in: H.F.Schaefer (Ed.), Methods of Electronic Structure Theory, Plenum Press, New York, 1977, pp79-127.

12 J.Hendekovic, Int.J.Quantum Chem., 8 (1974) 799; 10 (1976)

1025.

13 W.A.Goddard, J.Chem.Phys. 48 (1968) 450.

14 H.Nakatsuji and K.Hirao, J.Chem.Phys., 68 (1978) 4279.

15 A.C.Hurley, J.E.Lennard-Jones and J.A.Pople, Proc.R.Soc. (London) Sect A220 (1953) 446.

16 P.O.Lowdin, J.Math.Phys., 3 (1962) 1171.

17 W.Brenig, Nucl.Phys., 22 (1961) 177; W.Kutzelnigg and V.H.Smith Jr, J.Chem.Phys., 41 (1964) 896.

18 H.Nakatsuji and K.Hirao, J.Chem.Phys., 68 (1978) 2053; K.Hirao, J.Chem.Phys., 79 (1983) 5000.

19 P.Saxe, H.F.Schaefer and N.C.Handy, Chem.Phys.Lett. 79 (1981) 202; R.J.Harrison and N.C.Handy, Chem.Phys.Lett., 95 (1983) 386.

20 H.Nakatsuji, Chem.Phys.Lett., 67 (1979) 329, 334.

FLOATING FUNCTIONS SATISFYING THE HELLMANN-FEYNMAN THEOREM

K.HIRAO

Department of Chemistry, College of General Education, Nagoya University, Nagoya, Japan

and

Institute for Molecular Science, Okazaki, Japan

FILE NO. A0.12.076 (Received 21 Dec 1990)

ABSTRACT

The electrostatic calculation for molecules using approximate wavefunctions leads to well-known difficulties connected with the application of the Hellmann-Feynman theorem. This is due to the basis set inadequacies in the underlying SCF/MCSCF calculations. This defect can easily be remedied by floating functions whose centers are optimized in space. We can keep almost everything of the traditional wavefunction with nuclear fixed basis set, but we apply single floating to ensure the Hellmann-Feynman theorem. Then one can obtain a wavefunction obeying the Hellmann-Feynman theorem. This provides a great conceptual simplification and may lead to practical advantages. The single floating scheme which retains one expansion center per nucleus is successfully applied to a series of small molecules using SCF and CASSCF wavefunctions with sufficiently polarized basis sets.

I. INTRODUCTION

The derivatives of the potential energy hypersurface are of fundamantal importance in studying molecular geometries, vibrations, chemical reactions and dynamics. The analytical calculations of energy derivatives has received much attention in the past decade.[1,2] First and second derivatives can now be calculated analytically for a variety of wavefunctions by direct differentiation of an expectation value of the Hamiltonian. The gradient of total molecular energy with respect to nuclear coordinates, X_a is given by

$$\frac{\partial E}{\partial X_a} = \frac{\partial}{\partial X_a}\langle\Psi|H|\Psi\rangle = \langle\Psi|\frac{\partial H}{\partial X_a}|\Psi\rangle + \langle\frac{\partial\Psi}{\partial X_a}|H|\Psi\rangle + \langle\Psi|H|\frac{\partial\Psi}{\partial X_a}\rangle \qquad (1)$$

The negative gradient equals to the force acting on nucleus a and it is called as the Born-Oppenheimer force.

The Hellmann-Feynman theorem[3] offers an attractive alternative to the direct differentiation. Theorem states that the force holding the nuclei together in a molecule could be given an entirely classical interpretation once the electron density has been computed by quantum mechanics. This electrostatic theorem results in the simple formula for the force on nucleus a

$$f_a = -\langle\Psi|\frac{\partial H}{\partial X_a}|\Psi\rangle \qquad (2)$$

if Ψ and E are exact eigenfunction and eigenvalue of H. This seems a very simplification since the derivative of the Hamiltonian, involving only one-electron operators, is much simpler than the derivative of the expectation value of the Hamiltonian. The so-called Hellmann-Feynman force obtained in this way will agree with the energy derivative.

The Hellmann-Feynman theorem is apparently valid even for optimal variational wavefunctions. However, the application of (2) leads to well-known difficulties connected with the application of the Hellmann-Feynman theorem.[4-8] The error in the Hellmann-Feynman theorem arises essentially from the basis set inadequacies in the underlying calculations. The Hellmann-Feynman force is extremely sensitive to the small error in the wavefunction, particularly near the nuclei of interest. This small error is enough to vitiate any force calculation. In spite of its great theoretical significance, the Hellmann-Feynman theorem has been of surprisingly little value for practical calculations and its value has been largely conceptual.

The validity of the Hellmann-Feynman theorem requires some condition when LCAO approximate wavefunctions are employed. Hurley[9] showed that the Hellmann-Feynman theorem is satisfied by the wavefunction built from floating functions, whose centers are optimized in space. Nakatsuji[10] showed that a sufficient condition for the Hellmann-Feynman theorem is that the basis set includes the derivatives for every basis function. Floating corresponds to the addition of derivative functions. In other words, the addition of the derivative AO gives the freedom of floating to the parent AO. The different point is that the addition of derivative AO gives lower energy

than the floating functions since the basis set space due to the addition of derivative AO becomes much wider than that of floating.

Floating functions make the optimization of wavefunctions more complicated since a new set of variational parameters is introduced. However, the optimization of orbital centers is now trivial with recent developments in second-order technique for optimization of geometries.[11] Clearly, the Hellmann-Feynman theorem is very nice theorem, lending itself to a clear-cut conceptual picture. Furthermore the theorem leads to a considerable reduction of computational work for the higher energy derivatives. In view of these, we decided to reexamine floating functions obeying the Hellmann-Feynman theorem.

Since the introduction of floating functions by Hurley,[9] the calculations of molecular wavefunctions and properties using floating functions have been reported by several authors. Frost[12] introduced floating spherical gaussians in 1967 and Huber[13] has studied the floating orbital geometry optimization method. Nakatsuji and coworkers[14] have carried out the force-theoretical studies. More recently, Helgaker and Almlof[15] calculated properties using floating gaussian orbitals. They used floating for an alternative to adding polarization functions. Hurley reinvestigated the subject and stressed the usefulness of the Hellmann-Feynman theorem.[16]

The floating functions are translationally invariant and satisfy the Hellmann-Feynman theorem but the orbitals may have their cusps off the nuclei.[17] The floating seems simply and conveniently to include the major portion of polarization effects but at the same time floating introduces the less desirable characteristics in the wavefunction, the

discontinuities in the wavefunction in the vicinity of the nuclei. The floating reduces the electron density at the nuclei, as discussed earlier by Shell and Ebbing.[18] Thus, floating produces only minor changes in the energy improvement. Indeed, floating is less effective than adding polarization functions. Other properties, especially in which polarization effects play an important role, are often significantly improved.[15]

The method proposed in this paper is related to the floating functions, but it is presented in a different philosophy. If one wants to satisfy the Hellmann-Feynman theorem, one is inevitably led to floating of basis functions. Having realized this, we want to keep the spirit and logistic of the standard SCF/MCSCF as long as possible. These days we are using the fully polarized basis sets. The conventional SCF or correlated wavefunction with nuclear fixed basis is, on the whole, not really bad, it only has difficulties to represent the electron density in the neighborhood of nuclei and this region is very critical for the electrostatic theorem. We can remedy this by floating a wavefunction. If polarization and related effects due to floating are included sufficiently in advance by other features in the wavefunction, the displacement of the orbital positions from the nucleus and the energy improvement can be expected to approach zero in order to minimize the effect of the discontinuities. The key idea is that we can keep almost everything of the traditional wavefunction with nuclear fixed basis set, but we do apply floating in order to satisfy the Hellmann-Feynman theorem. The floating is carried out only for the Hellmann-Feynman theorem, not for the energy improvement.

We first calculate the equilibrium geometry of a molecule

through the usual geometry optimization procedure according to the criterion that the gradients are zero. Then we detach the expansion centers and optimize the positions, keeping the nuclear positions fixed. Floating makes the wavefunction obey the Hellmann-Feynman theorem, but the wavefunction is improved accordingly and the equilibrium geometry will shift from that before floating. However, if floating has little effect, that is, the improvement due to floating is limited to remedy the wavefunction near the nuclei, the deviation is expected to be small enough that the Hellmann-Feynman force remains in the acceptable error. Then, we can go into the next step, for instance, the calculation of higher energy derivatives.

The main message of this paper is that one can obtain a wavefunction obeying the Hellmann-Feynman theorem simply by floating. This provides a great conceptual simplification and may lead to practical advantages. The main interest of this paper is not in the numerical results but in their analysis and in the conclusions drawn from this analysis.

In Sec.II we present and discuss the results of our calculations on a series of test molecules. In Sec.III some general conclusions are summarized.

II. Results and Discussions

The floating functions required for the Hellmann-Feynman theorem may be obtained by detaching the basis functions from the nuclei and transferring them to new expansion centers. The total energy is minimized with respect to variations of all the expansion centers of basis functions.

In many cases diffuse functions would go wide of their parent atom, often breaking symmetry of the molecule and occasionally coming to rest close to another atomic center. Such behavior is not acceptable and it is often used to attach diffuse orbitals to the same floating center of the less diffuse orbitals. Whenever the expansion centers of orbitals with angular momentum higher than zero are optimized, a combined floating center for all components of the shell should be used in order to preserve the rotational invariance of the shell. The important point is that all the expansion centers whichever they are independent or combined, should be optimized so as to satisfy the Hellmann-Feynman theorem. Although floating of innermost orbitals has a negligible effect on the calculated properties, their positions must be treated as a variational parameter in view of the Hellmann-Feynman theorem. When the bond functions are used, their positions must also be determined variationally.

The standard computer programs for geometry optimization of a molecule can well be adapted to yield floating functions. The basis functions are put on dummy nuclei with zero nuclear charge and bare nuclei with the appropriate nuclear charge at the nuclear positions. The positions of the expansion centers are optimized in the same manner as nuclear positions are optimized in geometry calculations. The Hellmann-Feynman force is very sensitive to the displacement from the nuclei. A convergence criterion of 10^{-7} atomic units was adopted for the gradients.

The Hellmann-Feynman forces were calculated with different basis sets. For each basis set we carried out one calculation with the fixed basis set and one calculation in which the positions of the

orbital centers were variationally optimized. For the first row atoms we used the Huzinaga-Dunning double zeta [4s2p][19] and triple zeta [5s3p][20] basis sets. For hydrogen we used the Huzinaga-Dunning [2s] and [3s] basis with the scale factor of 1.2. Single polarization function is taken from the literature[21] and the exponents of double polarization functions are basically composed of the second and third outermost primitive gaussians of their valence basis functions. All calculations were performed using HONDO7 program system.[22]

A. Floating Schemes

We utilized the floating procedure just for the validity of the Hellmann-Feynman theorem. We don't want to improve the whole wavefunction. We do want to remedy only a poor description of the wavefunction near the nuclei. For this purpose, the single floating scheme is expected to be the most appropriate. To illustrate this we calculated H_2 and CO molecules using various floating schemes at the SCF level.

Table I gives the H_2 results. First we optimized the H-H distance (R_{HH}) with the fixed TZ2p basis set. The gradient becomes less than 10^{-7} au at R_{HH}=1.368658 au. Then at this nuclear separation, we calculated floating functions by various schemes. The single floating means that each atom gives rise to one floating center. This is denoted by {3s2p}; three s orbitals and two p orbitals are combined on each hydrogen atom to the same floating center. In the double floating, {3s,2p}, three s valence basis functions were placed on one floating center and two p polarization

functions on a second floating center. The most flexible scheme is to employ the different expansion centers for different orbitals of an atom, {1s,1s,1s,1p,1p}. We can see from Table I that for the fixed basis, the Hellmann-Feynman force at the minimum energy point is quite large, f_H=0.0011271 au, implying that the fixed basis set fails in obtaining reliable Hellmann-Feynman force. Floating described above ensures the Hellmann-Feynman theorem. However, at the same time floating introduces a new set of variational parameters which leads to the improvement of the wavefunction. The minimum point on the energy hypersurface will shift a little from that with the fixed basis. The Hellmann-Feynman force computed with floating functions is accurate since it obeys the Hellmann-Feynman theorem. The non-zero Hellmann-Feynman force arises from the deviation from the true energy minimum point. Therefore we must reoptimize the molecular geometry to reach the true minimum energy point of the floating functions. The magnitude of the Hellmann-Feynman force computed with the floating function indicates the degree of deviation from the energy minimum point. The floating function which employs different expansion centers for the different orbitals gives the lowest energy and therefore does the largest Hellmann-Feynman force. The decrease of E is $4.65*10^{-4}$ au. This floating scheme is quite an effective way to describe polarization of the basis functions although it is less effective than adding explicit polarization functions. On the other hand, the energy decrease due to single floating is only $0.2*10^{-5}$ au (0.001 kcal/mol). This implies that the single floating function is very close to that with the fixed basis except the region near the nuclei. It is convenient for the present purpose that floating

is used just for validity of the Hellmann-Feynman theorem. The computed Hellmann-Feynman force is $f_H=0.26*10^{-4}$ au. The magnitude is negligibly small. For reference, we obtained the true minimum energy point by applying the energy gradient to the expansion centers and the Hellmann-Feynman forces to the nuclei simultaneously. Optimal single floating function gives the energy minimum at $R_{HH}=1.368600$ au. The deviation is only $0.58*10^{-4}$ au and no energy improvement is gained with 8-digit accuracy through reoptimization. The difference is so small that we believe that it will not influence any further calculations. It is worth mentioning that the magnitude of the energy lowering due to floating is in the same order of that of the Hellmann-Feynman force remained with floating functions.

Table II gives results on CO calculated by various floating schemes with DZp basis set. All calculations were done at $R_{CO}=$ 2.111673 au optimized with the fixed basis set. At this nuclear distance, the gradients with fixed basis are less than 10^{-7} au. However, the computed Hellmann-Feynman forces are $f_C=0.3087$ au and $f_O=-0.7584$ au which indicates the complete breakdown of the Hellmann-Feynman theorem. Here the direction from C to O is taken to be a positive sign. The Hellmann-Feynman force calculated with floating functions shows the degree of deviation of the energy minimum from that with the fixed basis. The better the calculated energy is, the larger the Hellmann-Feynman force remains. The decrease of E due to single floating is $0.46*10^{-4}$ au (0.029 kcal/mol) and the remaining Hellmann-Feynman force is $f_C=-f_O=0.19*10^{-4}$au. Again the effect of single floating is negligibly small. The true minimum internuclear distance with the single floating wavefunction is 2.111686 au. So the discrepancy is

only $0.13*10^{-4}$ au. The displacements of the floating centers from C and O nuclei are $1.054*10^{-4}$ and $-0.7870*10^{-4}$ au, respectively. The displacements are very small but they are completely enough to ensure the Hellmann-Feynman theorem.

The energy lowering and the magnitude of the Hellmann-Feynman force increase as the number of expansion centers. When more flexible floating schemes are used, the newly introduced variational parameters work as to improve not only the region near the nuclei but also other parts of the wavefunction. This can readily be seen also from the computed dipole moment. The calculated dipole moment with single floating wavefunction is -0.07051 au (C^+O^-), which is very close to -0.07053 au calculated with the fixed basis. On the other hand, more flexible floating schemes give quite different values. Note here that the sign of the SCF computed dipole moment has the opposite sign (C^+O^-) to that of experiment (C^-O^+).[27)]

These examples allow us to feel with some confidence that single floating is the most appropriate scheme for our purpose. So we employ the single floating scheme hereafter and all functions on each atom are expanded on the same floating center. With such a scheme, the usual geometry optimization has very good convergence properties to achieve less than 10^{-7} au in gradients.

B. Basis Sets

Now let us examine the effects of the basis sets. All floating functions were obtained by a single floating scheme at the SCF level. Calculated results with the fixed and floating functions for CO, organized according to the types of the basis sets are summarized in

Table III. For each basis set, fixed (upper row) and floating (lower row) results are listed together for comparison. The basis set generally improves from top to bottom. For each basis set, we first optimized the CO distance and then the expansion centers were variationally determined at the same nuclear separation. The largest basis set employed was obtained by contracting Huzinaga's (14s9p) basis set[23] to (10,10,1,1,1,1/5,1,1,1,1) set supplemented by three sets of d polarization functions (EBS). The most accurate computation of the ground state of CO is by McLean and Yoshinime.[24] They used five s-, four p-, one d- and one f-type STO functions. They obtained an energy E=-112.78911 au at R_{CO}=2.132 au, which is 0.00088 au lower than that by the present EBS calculation.

The optimized CO distance generally diminishes as the basis set improves. First consider the Hellmann-Feynman force calculated with the fixed basis sets. As expected unpolarized basis sets such as DZ and TZ give the largest Hellmann-Feynman forces. Adding polarization functions decreases the error but fairly large Hellmann-Feynman forces still remain. Of course, the error decreases as the basis set improves. However, even with EBS, we have f_C=-0.0574 and f_O=-0.1310 au. This shows that the best available approximate wavefunction with fixed basis is too inaccurate to be of much use for the electrostatic calculation. Floating changes the picture of the Hellmann-Feynman force dramatically although the decrease in total energy is quite small. The non-zero Hellmann-Feynman forces with floating functions do not arise from the failure of the Hellmann-Feynman theorem but from the slight deviation from the true minimum energy point. Thus the magnitude of the Hellmann-Feynman force reflects the effect of floating. The larger

the Hellmann-Feynman force is, the greater effect floating has. Floating with unpolarized basis set has considerable effects on the energy and geometry. On the other hand, floating with the sufficiently polarized basis has little effects on both. The energy improvement due to floating with TZ2p and EBS is less than $1.0*10^{-4}$ au and the Hellmann-Feynman forces calculated are fairly close to zero. Values of dipole moment of CO are presented in Table IV. The difference between fixed and floating functions is also very small, less than $1.0*10^{-4}$ au. This also supports that single floating does not affect the wavefunction except in the vicinity of the nuclei.

From these results we conclude that a single floating scheme with sufficiently polarized basis set, at least as large as DZp seems to be adequate for the present purpose. A single floating scheme makes the wavefunction obey the Hellmann-Feynman theorem. Due to the improvement of the wavefunction, we will have the non-zero Hellmann-Feynman force at the equilibrium geometry determined with the fixed basis set. However, the Hellmann-Feynman force still remains within the acceptable error.

The displacement of hydrogen must be the largest when optimized through floating. It can easily be understood since the exponent of hydrogen is the smallest (The displacement from the nucleus is approximately proportional to the $1/\alpha^{1/2}$ where α is an exponent of the gaussian function). Thus, the most difficulty of the present application may be found in a system which has a polar bond involving hydrogen. We used HF as an example. Results are summarized in Table V. The direction from H to F is assumed to be positive. All the computations were performed at the HF internuclear distance optimized with each basis set.

Very accurate SCF calculations on HF have been made by Cade and Huo using STO basis.[25] Their energy is -100.07030 au at the experimental R_{HF}(=1.7328 au), which is only 0.0008 au lower than that by the present EBS. The general trend is similar to that found in CO. But the effect of floating is more significant than that of CO. Particularly the displacement of expansion center of hydrogen is of the order of 10^{-2} au, which is by 10^{2}~10^{3} times larger than that of a heavy atom. Consequently the Hellmann-Feynman force appeared is fairly large even with DZp basis set. This implies deficiency of the polarization functions, which leads to a relatively large geometry change. That is, the DZp basis is not flexible enough to describe such a polar bond.

Two approaches will be suggested to overcome this difficulty. One may insist that the true energy minimum is searched by reoptimization of the geometry. The true minimum point in a DZp floating function is at R_{HF}=1.7053 au. However, no energy improvement was gained through reoptimization, indicating the energy hypersurface is rather flat with respect to stretching of such a polar bond. The difference of the bond distance between fixed and floating functions is $1.5*10^{-3}$ au. Alternatively, one may add the polarization functions to reach a better polarization of hydrogen. If one adds an additional p set to the DZp basis set, which is denoted by the DZp' (double polarization on H), floating yields the Hellmann-Feynman force of the order of 10^{-4} au, which is nontheless tolerable. With floating DZp' we also reoptimized the geometry and found that the deviation from the true minimum is $1.6*10^{-4}$ au, ten times smaller than that of DZp basis. Thus, the DZp' provides sufficient flexibility to polarize the s basis functions of hydrogen. With this basis set one obtains good results with respect to the

Hellmann-Feynman force. Of course if more flexible basis sets such as TZ2p and EBS are used, the Hellmann-Feynman force remains within the acceptable error.

The calculated dipole moments of HF are summarized in Table VI. The fixed as well as floating basis sets give dipole moments which are too large compared to the experiment.[28] Polarization functions reduce their values. We also see that the dipole moments computed with sufficiently polarized basis sets (DZp', TZ2p, EBS) are indeed close to those with the corresponding fixed basis sets.

We also calculated CH_4, C_2H_6, C_2H_4, C_2H_2, NH_3, H_2O and H_2CO molecules and results are listed in Tables VII and VIII. These test calculations confirm the above conclusions. In general, a single floating scheme works well if used with sufficiently polarized basis sets. For hydrocarbons, the single floating DZp basis gives excellent results. For a system involving polar hydrogens a single floating with DZp' gives reasonably good results.

C. Geometry Changes

Energies and forces acting on C at various internuclear distances for CO computed with DZp basis are listed in Table IX. The force computed with fixed functions is taken from the negative gradient (Born-Oppenheimer force). The fixed basis gives the energy minimum at R_{CO}=2.111673 au while the floating function at R_{CO}=2.111686 au. Both functions give very close energies and forces. Energy lowering due to single floating is almost constant over a wide range of internuclear distance, ca. $5*10^{-5}$au (0.03 kcal/mol). Computed forces show the similar tendency as the total energies. The difference between fixed and floating functions lies

within the range of $4.0*10^{-5}$ au. Thus, the potential curve is not affected by floating.

Table X shows results on HF molecule with DZp' basis. The similar trend can be found as the case of CO. The energy lowering due to floating is almost constant in the region of R_{HF}=1.5~3.0 au. However, it increases considerably at R_{HF}=4.0~5.0 au. At this region, the charge transfer occurs from H to F. Inconsistent effect of floating indicates that the present basis set is still not sufficient enough to describe the whole HF potential curve at the same level of accuracy. Thus, single floating can be used to check the adequacy of the basis set, especially the sufficiency of the polarization functions.

D. Correlation Effects

The electron correlation effect is also examined using the complete active space SCF (CASSCF) wavefunction.[26] The Hurley's condition[9] is satisfied by any variationally optimized wavefunction. So the floating MCSCF wavefunction obeys the Hellmann-Feynman theorem. The CI wavefunction satisfies, in principle, the Hellmann-Feynman theorem. However, if one truncates the expansion of the configurations to some order, the Hellmann-Feynman theorem is not satisfied. In a CI treatment, configuration expansion coefficients are determined variationally but orbitals are left unoptimized. Variation of orbitals introduces singly excited configurations relative to the parent CI configurations. For example, triply excited configurations are necessary for the usual single and double CI wavefunction with respect to the Hellmann-Feynman theorem. Thus, we employed here the CASSCF wavefunction to examine the correlation

effect on floating.

Results on H_2 with TZ2p basis are given in Table XI. The 2 and 3 active orbital CASSCF include valence configurations arising from σ bonding and σ antibonding MO, while 5 active orbital CASSCF includes configurations arising from three σ and two π orbitals. We optimized first the H-H distance in each fixed CASSCF theory and then a single floating scheme is applied. Correlation effects increase the H-H bond distance relative to the SCF one. As to single floating, however, the trends as found with the CASSCF theory are the same as found with the SCF theory. That is, the energy difference between fixed and floating CASSCF is very small and the remaining Hellmann-Feynman force of floating wavefunction is also negligible small. In the 5 active orbital CASSCF theory, we allowed excitations from σ to π orbitals. The slight increase of the magnitude of the Hellmann-Feynman force may arise from the disregarding the d function in the present calculations. Of course, it will be improved if we employ the basis set which ensures the d polarization. This is numerically verified by the calculation with the basis set supplemented by d functions (see the final row of Table XI).

Results on CO are given in Table XII. The 2 and 3 active orbital CASSCF include valence configurations arising from excitations from CO σ bonding to σ antibonding MO. In the 6 active orbital CASSCF, the six electrons are distributed within the two active σ and four active π orbitals. The effect of floating is again very similar to that of the SCF case. Table XII also lists the calculated dipole moment. Fixed and floating CASSCF produce a very close dipole moment. Only the 6 active orbital CASSCF gives a dipole moment of 0.12749 au,

of the correct sign with the experiment (C^-O^+).[27] This also supports that the correct result could not be obtained except by including excitations involving π MO.[29]

The single floating scheme can also be applied successfully to the MCSCF wavefunction. It is noted that the error in the Hellmann-Feynman theorem arises essentially from the basis set inadequacies, not from the accuracies of the variational wavefunction.

III. Conclusions

We have systematically investigated the importance of floating functions which satisfy the Hellmann-Feynman theorem. It is demonstrated that the error resulting from the use of the Hellmann-Feynman theorem can be made negligible small by a single floating scheme if used with a sufficiently polarized basis set. In many cases, it is reasonably well described even at the DZp level, although in some cases hydrogen requires double polarization. The current methods for the analytical calculation of energy gradients can be well adapted to yield floating functions. The computation required only about twice of the computing times of conventional geometry optimization and can be performed just as routinely. The floating functions satisfies the electrostatic (Hellmann-Feynman) theorem, which provides a great conceptual simplification and may lead to practical advantages. If we have a wavefunction obeying the Hellmann-Feynman theorem for a molecule, we may talk about geometries, vibrations, chemical reactions, etc, in the language of clear-cut conceptual picture. The simplicity of the Hellmann-Feynman

theorem is appealing. In adiition we can calculate the higher energy derivatives based on the Hellmann-Feynman theorem. The Hurley's condition can be used to obtain approximations to the first-order wavefunction, from which the second, third and fourth energy derivatives can be obtained, leading to quadratic, cubic and quartic force constants. There are several significant advantages over the direct analytic derivative method. The expressions of these higher energy derivatives are much simpler than those of the wave-mechanical method. The electrostatic calculation involves only one-electron integrals. No integrals appear involving derivatives of the basis functions. There is no need of solving the coupled perturbed Hartree-Fock equations to obtain the wavefunction derivatives. One only needs solutions of linear equations. There is no iteration involved. The calculation of the force constants baed on the Hellmann-Feynman theorem will be reported elsewhere.[30]

Acknowledgments

The author wishes to acknowledge the assistance of Mr.K.Mogi in carrying out a portion of these calculations. The calculations were performed on the FACOM M782 at the Nagoya University and on the HITAC S810 at the Institute for Molecular Science. The author is grateful for the supply of computer time. This work was partly supported by a Grant-in-Aid for Scientific Research from the Japanese Ministry of Education, Science and Culture.

References

1. J.Gerratt and I.M.Mills, J.Chem.Phys., **49**, 1719, 1730 (1968).
2. P.Pulay, Mol.Phys.,**17**, 197 (1969);ibid, **18**, 473 (1970); Adv.Chem.Phys. **69**, 241 (1987); in Modern theoretical chemistry, Vol.**4**, ed. H.F.Schaefer,(Plenum, New York 1977); P.Pulay, in The Force Concept in Chemistry, ed. B.M.Deb (Van Nostrand Reinhold Company, New York, 1981)
3. H.Hellmann, Einfuhrung in die Quantenchemie (Deuticke, Leipzig, 1937), 285; R.P.Feynman, Phys.Rev.,**56**, 340 (1939).
4. J.Goodisman, J.Chem.Phys., **39**, 2397 (1963).
5. M.L.Benston and B.Kirtman, J.Chem.Phys.,**44**, 119, 126 (1966).
6. R.K.Nesbet, J.Chem.Phys., **36**, 1518 (1962).
7. B.J.Ransil, Phys.Rev.,**32**, 245 (1960).
8. R.F.Bader, Can.J.Chem., **41**, 2303 (1963).
9. A.C.Hurley, Proc.Roy.Soc.London Ser. **A226**, 179, 193 (1954); A.C.Hurley, in Molecular Orbitals in Chemistry, Physics, and Biology, ed. by Lowdin and Pullman, Academic Press, New York (1964).
10. H.Nakatsuji, K.Kanda and T.Yonezawa, Chem.Phys.Lett., **75**, 340 (1980); H.Nakatsuji, T.Hayakawa and M.Hada, Chem.Phys.Lett., **80**, 94 (1981); See also P.Habitz and C.Votava, J.Chem.Phys., **72**, 5532 (1980).
11. R.Fletcher, Practical Methods of Optimization (Wiley, Chichester, 1980), Vol.1 ; J.E.Dennis, Jr and R.B. Schabel, Numerical Methods for Unconstrained Optimization and Nonlinear Equation (Prentice-Hall, Englewood Cliffs, 1983) ; B.A.Murtagh and R.W.H. Sargent, Comput.J.,**13**, 185 (1970).
12. A.A.Frost, J.Chem.Phys., **47**, 3707 (1967); in Modern theoretical

chemistry, Vol.**3**, ed. H.F.Schaefer (Plenum Press, New York, 1977).

13. H.Huber, Chem.Phys.Lett.,**62**, 95 (1979); ibid, **70**, 353 (1980); Theor.Chim.Acta, **55**, 117 (1980); J.Mol.Struc.Theochem.,**76**, 277, (1981).
14. H.Nakatsuji, K.Matsuda and T.Yonezawa, Chem.Phys.Lett.,**54**, 347 (1978);H.Nakatsuji, S.Kanayama, S.Harada and T.Yonezawa, J.Amer.Chem.Soc., **100**, 7528 (1928).
15. T.Helgaker and J.Almlof, J.Chem.Phys., **89**, 4889 (1988).
16. A.C.Hurley, J.Compt.Chem., **9**, 75 (1988).
17. S.T.Epstein, The Variational Methods in Quantum Chemistry, (Academic Press, New York, 1974); S.T.Epstein, in The Force Concept in Chemistry, ed. B.M.Deb (Van Nostrand Reinhold Company, New York, 1981).
18. H.Shull and D.D.Ebbing, J.Chem.Phys., **28**, 866 (1958).
19. T.H.Dunning, Jr., J.Chem.Phys.,**53**, 2823 (1970).
20. T.H.Dunning, Jr., J.Chem.Phys.,**55**, 716 (1971).
21. T.H.Dunning Jr. and P.J.Hay, in Modern theoretical chemistry Vol.**3**, ed. H.F.Schaefer (Plenum Press, New York, 1977).
22. M.Dupuis, J.D.Watts, H.O.Villar and G.J.B.Hurst, IBM Tech.Rep. KGN-181 (1988), QCPE Program #544, Univ.of Indiana.
23. S.Huzinaga, M.Klobukowski and H.Tatewaki, Can.J.Chem.,**63**, 1812 (1985).
24. A.D.McLean and M.Yoshimine, Tables of linear molecular wave functions.IBM, San Jose (1967).
25. P.E.Cade and W.H.Huo, J.Chem.Phys.,**47**, 614 (1967).
26. P.E.M.Siegbahn, A.Heiberg, B.O.Roos and B.Levy, Phisica Scripta, **21**, 323 (1980); B.O.Roos, P.R.Taylor and P.E.M.Siegbahn,

Chem.Phys., **48**, 157 (1980); P.E.M.Siegbahn, J.Almlof, A.Heiberg and B.O.Roos, J.Chem.Phys., **74**, 2381 (1981); B.O.Roos, Intern.J.Quantum Chem., **S14**, 175 (1980).

27. C.A.Burrus, J.Chem.Phys.,**28**, 427 (1958); J.S.Muenter, J.Mol.Spectrosc.,**55**, 490 (1975).
28. J.S.Muenter and W.Klemperer, J.Chem.Phys.,**52**, 6033 (1970).
29. F.Grimaldi, A.Lecourt and C.Moser, Intern.J.Quantum Chem., **S1** 153 (1967).
30. K.Hirao, J.Chem.Phys., submitted for publication.

Table I

Total energies and Hellmann-Feynman forces acting on H nucleus of H_2 molecule (R_{HH} = 1.368658)[a] calculated with fixed and floating TZ2p basis set (a.u.)

Expansion center per nucleus	Energy	HF force
fixed	-1.128416	0.0011271
floating		
{3s2p} [b]	-1.128418	0.0000256
{3s,2p} [c]	-1.128509	0.0000378
{1s,2s,2p} [d]	-1.128567	0.0001081
{1s,1s,1s,1p,1p} [e]	-1.128881	0.0002986

a) The Born-Oppenheimer force is less than 10^{-7} au at this internuclear distance.

b) Single floating ; one expansion center per nucleus.

c) Double floating; the valence basis functions were placed on one floating center and polarization functions on a second.

d) Triple floating; the innermost orbital is placed on one floating center, the remaining two s functions on a second and polarization functions on a third.

e) Quintuple floating; different expansion center for the different orbitals.

Table II

Total energies and Hellmann-Feynman forces acting on C nucleus of CO molecule (R_{CO} = 2.111673)[a] calculated with fixed and floating DZp basis set (a.u.)

Expansion center per nucleus	Energy	HF force
fixed	-112.759377	0.3087334
floating		
{4s2p1d} [b]	-112.759423	0.0000189
{1s,3s2p1d} [c]	-112.760056	0.0006548
{1s,3s,2p1d} [d]	-112.762330	0.0073079
{1s,3s2p,1d} [e]	-112.762503	0.0108202
{1s,3s,2p,1d} [f]	-112.764590	0.0164709

a) The Born-Oppenheimer force is less than 10^{-7} au at this internuclear distance.

b) Single floating ; one expansion center per nucleus.

c) Double floating; the innermost function is placed on one floating center and the remaining functions on a secend.

d) Triple floating; the innermost orbital is placed on one floating center, the remaining three s functions on a second and two p and one d functions on a third.

d) Triple floating; the innermost orbital is placed on one floating center, the remaining three s and two p functions on a second and polarization functions on a third.

f) Quadruple floating; the innermost orbital, remaining three s, two p and polarizations are placed on the different expansion centers.

Table III

Energies and Hellmann-Feynman forces of CO by various basis sets at the internuclear distance optimized with fixed basis (a.u.)

Basis		R_{CO}	Energy	Hellmann-Feynman Force	
				C	O
DZ	fixed	2.150313	-112.685311	-1.070930	2.300725
	floating		-112.685774	-0.000333	0.000333
TZ	fixed	2.123982	-112.707937	-0.967949	2.094532
	floating		-112.708320	-0.000389	0.000388
DZp	fixed	2.111673	-112.759377	0.308733	-0.758350
	floating		-112.759423	-0.000019	0.000019
DZp+ [a]	fixed	2.107483	-112.762850	0.299029	-0.760322
	floating		-112.762850	0.000014	-0.000014
DZ2p	fixed	2.103270	-112.766560	0.246179	-0.416335
	floating		-112.766579	0.000039	-0.000039
TZ2p	fixed	2.092277	-112.778534	0.323223	-0.504481
	floating		-112.778565	0.000002	-0.000002
EBS [b]	fixed	2.085026	-112.788226	0.057448	-0.130950
	floating		-112.788227	0.000002	-0.000002

a) DZp plus diffuse functions

b) Extended basis set; (10,10,1,1,1,1/5,1,1,1,1/1,1,1). Ref.23.

Table IV

Calculated dipole moment of CO by various basis sets at the CO distance optimized with the fixed basis (a.u.)

Basis	Diple moment	
	fixed	floating
DZ	-0.11407	-0.11418
TZ	-0.09091	-0.09097
DZp	-0.07053	-0.07051
DZp+ [a]	-0.06693	-0.06692
DZ2p	-0.06150	-0.06154
TZ2p	-0.05892	-0.05897
EBS [b]	-0.05549	-0.05549
Exptl [c]	0.0441+0.0020	

a) DZp plus diffuse functions

b) Extended basis set; (10,10,1,1,1,1/5,1,1,1,1/1,1,1). Ref.23.

c) Ref.27.

Table V

Energies and Hellmann-Feynman forces of HF by various basis sets at the internuclear distance optimized with fixed basis (a.u.)

Basis		R_{HF}	Energy	Hellmann-Feynman Force	
				H	F
DZ	fixed	1.737861	-100.021980	-0.112725	2.186379
	floating		-100.027628	0.006160	-0.006160
TZ	fixed	1.737918	-100.036872	-0.107144	1.808263
	floating		-100.042256	0.006099	-0.006099
DZp	fixed	1.706794	-100.047932	-0.016942	0.973120
	floating		-100.048188	0.001145	-0.001145
DZp' [a]	fixed	1.704032	-100.048724	-0.006338	0.999229
	floating		-100.048809	0.000114	-0.000114
DZ2p	fixed	1.702171	-100.050186	-0.007233	0.975888
	floating		-100.050284	0.000143	-0.000143
TZ2p	fixed	1.696589	-100.063476	-0.008407	0.614806
	floating		-100.063551	0.000104	-0.000104
EBS [b]	fixed	1.695666	-100.069497	-0.008354	0.141422
	floating		-100.069565	0.000065	-0.000065

a) Double polarization on H

b) Extended basis set; F(10,10,1,1,1,1/5,1,1,1,1/1,1,1) H(5,1,1,1,1/1,1,1,1). See Ref.23.

Table VI

Calculated dipole moment of HF by various basis sets at the HF distance optimized with the fixed basis (a.u.)

Basis	Diple moment	
	fixed	floating
DZ	-0.88236	-0.88653
TZ	-0.93753	-0.93279
DZp	-0.77797	-0.77916
DZp' [a]	-0.77770	-0.77780
DZ2p	-0.73168	-0.73171
TZ2p	-0.77069	-0.77092
EBS [b]	-0.74383	-0.74389
Exptl [c]	-0.719	

a) Double polarization on H.

b) Extended basis set.

c) Ref.28.

Table VII

Energies and forces acting on C at various internuclear distances for CO molecule calculated with DZp basis set (a.u.)

R_{CO}	Energies		Forces [a]	
	fixed	floating	fixed	floating
	-(E+112.)			
1.8	0.649799	0.649845	-0.848409	-0.848370
2.0	0.748490	0.748540	-0.208468	-0.208477
2.1	0.759272	0.759318	-0.018173	-0.018192
2.111673	0.759377	0.759423	0.0	-0.000019
2.111686	0.759377	0.759423	0.000021	0.0
2.12	0.759325	0.759371	0.012510	0.012490
2.2	0.754015	0.754063	0.115227	0.115206
2.5	0.684845	0.684898	0.305807	0.305801
3.0	0.520183	0.520230	0.317951	0.317983

a) The direction from C to O is positive in sign. Forces in fixed basis are negative gradients and those of floating are Hellmann-Feynman forces.

Table VIII

Energies and forces acting on H at various internuclear distances for HF molecule calculated with DZp' basis set (a.u.)

R_{HF}	Energies		Forces [a]	
	fixed	floating	fixed	floating
	-(E+100.)			
1.5	0.028831	0.028961	-0.223372	-0.223052
1.6	0.044222	0.044324	-0.092624	-0.092398
1.703876	0.048724	0.048809	-0.000114	0.0
1.704032	0.048724	0.048809	0.0	0.000114
1.8	0.045736	0.045836	0.058199	0.058243
2.0	0.026359	0.026433	0.126347	0.126359
3.0	-0.123682	-0.123622	0.136026	0.135959
4.0	-0.233889	-0.233603	0.086692	0.086312
5.0	-0.302811	-0.302115	0.053664	0.053391
10.0	-0.401496	-0.401492	0.005985	0.005988

a) The direction from H to F is positive in sign. Forces in fixed basis are negative gradients and those of floating are Hellmann-Feynman forces.

Table IX

Energies and Hellmann-Feynman forces of CH_4, C_2H_6, C_2H_4 and C_2H_2 at the geometry optimized with fixed basis (a.u.)[a,b]

Basis		Energy	Hellmann-Feynman Force
CH_4			
DZ	fixed	-40.185613	$f_{H_x}=f_{H_y}=f_{H_z}=0.04212$
	floating	-40.193598	$f_{H_x}=f_{H_y}=f_{H_z}=0.00006$
DZp	fixed	-40.207594	$f_{H_x}=f_{H_y}=f_{H_z}=0.00562$
	floating	-40.207860	$f_{H_x}=f_{H_y}=f_{H_z}=-0.00004$
TZ2p	fixed	-40.212172	$f_{H_x}=f_{H_y}=f_{H_z}=0.00194$
	floating	-40.212212	$f_{H_x}=f_{H_y}=f_{H_z}=-0.00001$
C_2H_6			
DZ	fixed	-79.206408	$f_{C_z}=-0.01445$, $f_{H_z}=0.02756$, $f_{H_x}=0.06955$
	floating	-79.218869	$f_{C_z}=0.00119$, $f_{H_z}=-0.00011$, $f_{H_x}=-0.00012$
DZp	fixed	-79.249242	$f_{C_z}=0.01041$, $f_{H_z}=0.00366$, $f_{H_x}=0.00912$
	floating	-79.249644	$f_{C_z}=0.00007$, $f_{H_z}=-0.00002$, $f_{H_x}=-0.00006$
TZ2p	fixed	-79.257119	$f_{C_z}=0.00556$, $f_{H_z}=0.00100$, $f_{H_x}=0.00312$
	floating	-79.257159	$f_{C_z}=0.00001$, $f_{H_z}=-0.00000$, $f_{H_x}=-0.00000$

C_2H_4

DZ	fixed	-78.011990	f_{C_z} = 0.05708, f_{H_z} = 0.03934, f_{H_x} = 0.06531
	floating	-78.020649	f_{C_z} = 0.00209, f_{H_z} =-0.00016, f_{H_x} =-0.00020
DZp	fixed	-78.050575	f_{C_z} =-0.065451 f_{H_z} = 0.00500, f_{H_x} = 0.00827
	floating	-78.058374	f_{C_z} = 0.00007, f_{H_z} =-0.00003, f_{H_x} =-0.00006
TZ2p	fixed	-78.061954	f_{C_z} =-0.02796, f_{H_z} = 0.00189, f_{H_x} = 0.00359
	floating	-78.062012	f_{C_z} = 0.00002, f_{H_z} =-0.00001, f_{H_x} =-0.00001

C_2H_2

DZ	fixed	-76.799232	f_C = 0.12977, f_H = 0.07389
	floating	-76.803606	f_C = 0.00151, f_H =-0.00032
DZp	fixed	-76.832544	f_C =-0.11310, f_H = 0.00960
	floating	-76.832686	f_C = 0.00018, f_H =-0.00012
TZ2p	fixed	-76.848167	f_C =-0.03391, f_H = 0.00460
	floating	-76.848207	f_C = 0.00004, f_H =-0.00002

---

a) The direction from each nucleus to the center of mass is taken to be be a positive sign.

b) Molecular geometry

CH_4 (T_d); the x, y and z are all S_4 axes.

C_2H_6 (D_{2d}), C_2H_4 (D_{2h}) ; 2-fold axis is z and σ_v plane is xz.

Table X

Energies and Hellmann-Feynman forces of NH_3, H_2O and H_2CO [a,b] at the geometry optimized with fixed basis (a.u.)

Basis		Energy	Hellmann-Feynman Force
NH_3			
DZ	fixed	-56.180540	f_{N_z}=-0.69904, f_{H_z}=0.00524, f_{H_x}=0.08514
	floating	-56.189200	f_{N_z}=-0.00217, f_{H_z}=0.00072, f_{H_x}=-0.00129
DZp	fixed	-56.209682	f_{N_z}=-0.47138, f_{H_z}=0.00331, f_{H_x}=0.01476
	floating	-56.210195	f_{N_z}=-0.00047, f_{H_z}=-0.00016, f_{H_x}=-0.00037
DZp'	fixed	-56.210892	f_{N_z}=-0.46139, f_{H_z}=0.00301, f_{H_x}=0.00353
	floating	-56.210961	f_{N_z}=-0.00006, f_{H_z}=0.00002, f_{H_x}=0.00003
TZ2p	fixed	-56.219257	f_{N_z}=-0.36410, f_{H_z}=0.00148, f_{H_x}=0.00406
	floating	-56.219318	f_{N_z}= 0.00006, f_{H_z}=0.00001, f_{H_x}=0.00003
H_2O			
DZ	fixed	-76.011020	f_{O_z}= 1.90398, f_{H_z}=-0.04031, f_{H_x}=-0.09526
	floating	-76.019883	f_{O_z}=-0.00191, f_{H_z}= 0.00096, f_{H_x}= 0.00374
DZp	fixed	-76.046951	f_{O_z}= 0.82209, f_{H_z}=-0.00781, f_{H_x}=-0.01488
	floating	-76.047405	f_{O_z}=-0.00113, f_{H_z}= 0.00057, f_{H_x}= 0.00061

DZp'	fixed	-76.048501	f_{O_z} = 0.82369, f_{H_z} =-0.00142, f_{H_x} =-0.00519
	floating	-76.048613	f_{O_z} =-0.00002, f_{H_z} = 0.00001, f_{H_x} = 0.00000
TZ2p	fixed	-76.060362	f_{O_z} = 0.60174, f_{H_z} =-0.00295, f_{H_x} =-0.00545
	floating	-76.060447	f_{O_z} =-0.00007, f_{H_z} = 0.00003, f_{H_x} = 0.00005

H_2CO

DZ	fixed	-113.830712	f_{C_z} =-0.30027, f_{O_z} = 2.07353, $\|f_H\|$ =0.08629
	floating	-113.836354	f_{C_z} = 0.00007, f_{O_z} = 0.00004, $\|f_H\|$ =0.00011
DZp	fixed	-113.895328	f_{C_z} =-0.10490, f_{O_z} = 0.82985, $\|f_H\|$ =0.01021
	floating	-113.895507	f_{C_z} =-0.00006, f_{O_z} = 0.00001, $\|f_H\|$ =0.00003
TZ2p	fixed	-113.910966	f_{C_z} =-0.07209, f_{O_z} = 0.54429, $\|f_H\|$ =0.00424
	floating	-113.911014	f_{C_z} =-0.00002, f_{O_z} = 0.00001, $\|f_H\|$ =0.00002

---

a) The direction from each nucleus to the center of mass is taken to be a positive sign.

b) Molecular geometry

NH_3; 3-fold axis is z and σ_v plane is xz.

H_2O, H_2CO ; 2-fold axis is z and σ_v plane is yz.

Table XI

Energies and Hellmann-Feynman forces of H_2 by fixed and floating CASSCF theory with TZ2p basis set (a.u.)

Theory		R_{HH}	Energy	Hellmann-Feynman Force
SCF	fixed	1.368658	-1.128416	0.001127
	floating		-1.128418	0.000026
CASSCF				
2-active[a)]	fixed	1.408933	-1.147313	0.000172
	floating		-1.147313	0.000009
3-active[b)]	fixed	1.396635	-1.153941	0.000351
	floating		-1.153942	0.000009
5-active[c)]	fixed	1.383846	-1.163418	0.001230
	floating		-1.163433	0.000048
5-active[c,d)]	fixed	1.386399	-1.164591	0.003125
	floating		-1.164594	0.000027

a) CASSCF with two σ orbitals as active.

b) CASSCF with three σ orbitals as active.

c) CASSCF with three σ orbitals and two π orbitals as active.

d) TZ2p plus d functions (d_α=1.0).

Table XII

Energies and Hellmann-Feynman forces of CO by fixed and floating CASSCF theory with DZp basis set (a.u.)

Theory		R_{CO}	Energy	Hellmann-Feynman Force on C	Dipole Moment
SCF	fixed	2.111673	-112.759377	0.308733	-0.07053
	floating		-112.759423	0.000019	-0.07051
CASSCF					
2-active[a)]	fixed	2.112269	-112.768249	0.305935	-0.06809
	floating		-112.768295	-0.000017	-0.06808
3-active[b)]	fixed	2.112163	-112.771064	0.304618	-0.06541
	floating		-112.771109	-0.000018	-0.06539
6-active[c)]	fixed	2.168402	-112.880197	0.320136	0.12752
	floating		-112.880240	-0.000016	0.12749
Exptl[d)]					0.0441±0.0020

a) CASSCF with two σ orbitals as active.

b) CASSCF with three σ orbitals as active.

c) CASSCF with two σ orbitals and four π orbitals as active.

d) Ref.28.

ANALYTIC DERIVATIVE THEORY BASED ON THE HELLMANN-FEYNMAN THEOREM

K.HIRAO
Department of Chemistry, College of General Education, Nagoya University, Nagoya, Japan
and
Institute for Molecular Science, Okazaki, Japan

ABSTRACT

General formulae for the second, third and fourth derivatives of the energy with respect to the nuclear coordinates of a molecule are derived from the Hellmann-Feynman theorem. The Hurley's condition can be used to obtain approximations to the first-order wavefunction, from which the second, third and fourth energies can be obtained, leading to quadratic, cubic and quartic force constants. The procedure is equivalent to derive higher energy derivatives by the perturbation variation method. There ar several significant advantages over the direct analytic derivative method The expressions of these higher energy derivatives are much simpler than those of the direct analytic derivative method. The electrostatic calculation involves only one-electron integrals. No integrals are necessary involving derivatives of the basis functions. There is no need of solving the coupled perturbed Hartree-Fcok equations to obtain the wavefunction derivatives. One only needs solutions of linear equations. There is no iteration involved. There are intuitive physical pictures

associated with these higher derivatives as the Hellmann-Feynman force picture associated with the first derivatives.

I. Introduction

Many important molecular properties are directly defined as the derivatives of an electronic energy. Electric moments and polarizabilities are property defined as the derivatives of the energy with respect to the applied electric fields. Magnetic properties such as diamagnetic susceptibilities and nuclear magnetic resonance chemical shifts are related to energy derivatives with respect to external and nuclear magnetic fields. Differentiation of the energy with respect to nuclear coordinates corresponds to the calculations of forces and force constants. These nuclear displacement energy derivatives are very important in the exploration of potential surfaces.

The first derivatives of the energy with respect to nuclear coordinates give the force acting on the nucleus and are used to find the stationary points such as equilibrium structures and transition structures. The second derivatives are related to the harmonic force constants as well as the nature of the stationary point. The third and fourth derivatives are related to the cubic and quartic force constants, respectively. The knowledge of these derivatives yields anharmonic spectroscopic constants.

There are two general approaches to the calculation of analytic energy derivatives. The first method is the direct analytic differentiation of the expectation value of the Hamiltonian. The

procedure has been the most commonly used and procedure doing this has been the forcus of many investigations in recent years. The underlying idea behind the direct analytical derivative method is just rigorously differentiating the true quantum mechanical energy. Generally this involves solving a type of eigenfunction equations or a simultaneous system of linear equations. Consequently n differentiations are necessary to reach n-th energy derivatives.

Direct analytic first derivatives of the SCF energy were first derived by Pulay.[1] It is now relatively straightforward to calculate the first derivatives with respect to nuclear coordinates for any method. Pople and coworkers[2] presented the analytical method for the evaluation of SCF second derivatives. To obtain second derivatives it is necessary to solve the coupled perturbed Hartree-Fock equations of Gerratt and Mills.[3] The most severe bottleneck in this approach is the drastic increase of the number of basis molecular integrals to be computed. In spite of this, such second derivative approach is used rather routinely for SCF and some MC-SCF schemes. The formulation of the SCF third derivatives were first given by Gaw, Yamaguchi and Schaefer.[4] Some simplifications in the formula were given by Gaw and Handy.[5] The fourth derivatives were presented by Handy and coworkers.[6] This needs the solution of the second order coupled perturbed Hartree-Fock equations.

Alternative method is possible based on the use of the Hellmann-Feynman theorem.[7,8] The Hellmann-Feynman theorem gives the first derivatives of the energy with respect to the nuclear coordinates as a simple expectation value. Consequently, n-1 differentiations are required to reach the n-th derivatives of the energy. In addition we have the so-called Hurley's condition[9] for the optimal variational

wavefunction, which serves as an auxiliary condition. Thus, the Hellmann-Feynman approach seems to be much superior to the direct differentiation method. However, although there have been isolated successes of the Hellmann-Feynman approach,[10,11] thus far there is no general theoretical understanding of the situation. This is mainly due to the unreliability of the Hellmann-Feynman method for evaluating forces on nuclei. Although the Hellmann-Feynman theorem is valid for true Hartree-Fock wavefunctions, it is found to be of little value for the finite basis sets typically used in molecular calculations. Thus, the error in the Hellmann-Feynman theorem arises essentially from the basis set inadequacies in the underlying calculations. The Hellmann-Feynman forces are extremely sensitive to the small error in the wavefunction particularly near the nuclei of interest. The validity of the Hellmann-Feynman theorem requires some additional condition when the finite basis sets are employed.

Hurley showed that the Hellmann-Feynman theorem is satisfied by the wavefunction built from floating functions, whose centers are optimized in space.[9] The floating functions are translationally invariant and satisfy the Hellmann-Feynman theorem but the orbitals may have their cusps off the nuclei. The conventional SCF or correlated wavefunction with nuclear fixed basis is, on the whole, not really bad, it only has difficulties to represent the electron density in the neighborhood of nuclei and this region is very critical for the Hellmann-Feynman theorem. As shown in the previous paper,[12] this defect can easily be remedied by a single floating scheme and we can obtain the wavefunction obeying the Hellmann-Feynman theorem.

Nakatsuji and coworkers[13] have proposed the basis functions for the

validity of the Hellmann-Feynman theorem. A sufficient condition for the Hellmann-Feynman theorem is that the basis sets include derivative basis functions for every basis function.

The Hellmann-Feynman theorem provides a great conceptual simplification and leads to practical advantages. We will develop here the analytic derivative theory based on the Hellmann-Feynman theorem.

In Sec.II some properties of the Hellmann-Feynman theorem and the sufficient conditions for the Hellmann-Feynman theorem will be reexamined. In Sec.III the second, third and fourth energy derivatives for a diatomic molecule will be derived from the Hellmann-Feynman theorem. In Sec.IV general analytic expressions for these higher energy derivatives will be given. In the final section some conclusion will be summarized.

II. The Hellmann-Feynman Theorem

Let Ψ be a normalized optimal variational wavefunction and E the corresponding energy

$$\langle\Psi|H-E|\Psi\rangle = 0 \qquad (1)$$

By differentiating eq.(1) with respect to a nuclear coordinate λ we obtain

$$E^1 = \langle\Psi|H^1|\Psi\rangle + \langle\Psi^1|H-E|\Psi\rangle + \langle\Psi|H-E|\Psi^1\rangle \qquad (2)$$

Here the derivatives of operators and wavefunctions are designated as

$$H^1 = \frac{\partial H}{\partial \lambda} \quad , \quad \Psi^1 = \frac{\partial \Psi}{\partial \lambda}$$

The variational condition ensures that

$$\langle \Psi^1 | H-E | \Psi \rangle + \langle \Psi | H-E | \Psi^1 \rangle = 0 \qquad (3)$$

whence we have the Hellmann-Feynman theorem

$$E^1 = \langle \Psi | H^1 | \Psi \rangle \qquad (4)$$

The negative energy gradient is called as the Hellmann-Feynman force. Such a condition as eq.(3) was first given by Hurley[9] and is called as the Hurley's condition. True Hartree-Fock approximations (as distinct from the SCF approximations), be they restricted, unrestricted, open-shell, closed-shell, multi-configurational, or whatever, satisfy the Hellmann-Feynman theorem.

For simplicity we will consider the 2n electron closed-shell systems in this paper. The wavefunction is expressed as a Slater determinant

$$\Psi = \| \varphi_1 \alpha \varphi_1 \beta \ \ldots \ \varphi_i \alpha \varphi_i \beta \ \ldots \ \| \qquad (5)$$

The Hartree-Fock orbitals $\varphi_1 \ldots \varphi_n$ are eigenfunctions of the Fock operator, the corresponding eigenvalues being $\varepsilon_1 \ldots \varepsilon_n$

$$F\varphi_i = \varepsilon_i \varphi_i \qquad (6)$$

Orbital labels i,j,k ... denote occupied orbitals, a,b,c... denote

virtual orbitals and p,q,r... denote general orbitals. The Hellmann-Feynman theorem is satisfied if the Hurley's condition of eq.(3) is fulfilled. The wavefunction derivative is given by

$$\Psi^1 = \sum_i^{nocc} \| \varphi_1 \alpha \varphi_1 \beta \ldots \varphi_i^1 \varphi_i (\alpha\beta - \beta\alpha) \ldots \| \qquad (7)$$

Taking account of the one electron property of H^1, we assume that the derivative of the orbital can be expressed as a linear combination of the other orbitals

$$\varphi_i^1 = \varphi_p U_{pi} / \sqrt{2} \qquad (8)$$

where p=i is excluded from the orthogonality condition of orbitals. We used Einstein summation notation for repeated indices. Substituting eq.(8) into eq.(7), we have

$$\Psi^1 = U_{ai} \Psi_{ai} \qquad (9)$$

with

$$\Psi_{ai} = \| \varphi_1 \alpha \varphi_1 \beta \ldots \varphi_a \varphi_i (\alpha\beta - \beta\alpha) / \sqrt{2} \ \ldots \|$$

The Ψ_{ai} are singly excited configurations. Thus the Hurley's condition of eq.(3) is equivalent to the Brillouin theorem

$$\langle \Psi_{ai} | H-E | \Psi \rangle + \langle \Psi | H-E | \Psi_{ai} \rangle = 0 \qquad (10)$$

As known well, the Hellmann-Feynman theorem is satisfied for the optimal wavefunction as a consequence of the variational principle.

The differentiation of the Fock equations $\langle\varphi_j|F-\varepsilon_i|\varphi_i\rangle = 0$ leads to

$$\langle\varphi_j|F^1-\varepsilon_i^1|\varphi_i\rangle + (\varepsilon_j-\varepsilon_i)\langle\varphi_j|\varphi_i^1\rangle = 0 \qquad (11)$$

In the case of i=j we have the Hellmann-Feynman theorem with respect to the orbital energy

$$\varepsilon_i^1 = \langle\varphi_i|F^1|\varphi_i\rangle \qquad (12)$$

Let us now consider the SCF approximation. The molecular orbitals are defined in terms of the finite basis functions $\chi_1 \cdots \chi_m$

$$\varphi_i = \chi_\alpha C_{\alpha i} = XC_i \qquad (13)$$

The X and C_i are the row and column vectors of χ_α and $C_{\alpha i}$, respectively. The derivative of φ_i with respect to λ is given by

$$\varphi_i^1 = X^1 C_i + XC_i^1 \qquad (14)$$

in a matrix representation. The first term on the r.h.s of eq.(14) arises from the fact that the basis functions will generally be defined in such a way that they move with the nucleus. The second term arises from the fact that the coefficients may also depend on λ. The Hurley's

condition is fulfilled if

$$FC_i = \varepsilon_i SC_i \qquad (15a)$$

and

$$F^{(1)}C_i = \varepsilon_i S^{(1)}C_i \qquad (15b)$$

where

$$(F^{(1)})_{\alpha\beta} = \langle \chi_\alpha^1 | F | \chi_\beta \rangle \quad , \quad (S^{(1)})_{\alpha\beta} = \langle \chi_\alpha^1 | \chi_\beta \rangle$$

Eq.(15a) are the Fock equations and hold for any SCF orbital. But eq.(15b) are not fulfilled in general. Thus the Hellmann-Feynman theorem is not necessarily satisfied for the SCF wavefunctions with the finite basis sets. The error in the Hellmann-Feynman theorem arises essentially from the basis functions. The Hellmann-Feynman theorem error in the SCF approximation can be estimated by

$$\Delta = 4 \sum C_i^\dagger (F^{(1)} - \varepsilon_i S^{(1)}) C_i \qquad (16)$$

This is called as the AO error.[13] Note here that the Hurley's condition is inequivalent to the Brillouin theorem in the case of the SCF approximations.

Two approaches have been suggested to overcome this difficulty. One way is to employ the basis set which is invariant to the changes of λ. Evidently the floating functions will do the job. In the floating

functions the individual orbitals are not fixed on the nuclei a priori. Rather the centers are allowed to float, the variational method then determining the optimal centering. If the floating functions are used, the derivative of φ_i is given by

$$\varphi_i^1 = XC_i^1 \qquad (17)$$

and the Hurley's condition becomes identical to the Brillouin theorem. One can easily obtain the wavefunction obeying the Hellmann-Feynman theorem by a single floating scheme if used with the sufficiently polarized basis sets.[12]

The other approach, the use of fixed basis functions, is also applicable. The first method is to describe a molecule by one-center basis sets. Although application is limited, its usefulness is discussed.[14] The second is to employ the basis sets $X = \{\chi, \chi^1, \chi^2, \ldots\}$, where χ^n denotes the n-th derivatives of χ. It is necessary to include the derivative basis functions for every basis function. Then eq.(15b) are fulfilled and the SCF wavefunction obeys the Hellmann-Feynman theorem.[13] If these basis sets are used, the space spanned by derivative basis functions is included in the original basis function space. Thus we can expand the derivative basis functions X^1 in terms of the original basis functions X such as $X^1 = XB$. Then it is possible to represent φ_i in the form of

$$\varphi_i^1 = X(BC_i + C_i^1) \qquad (18)$$

From eq.(15b) we see that XBC_i lies on the virtual manifold. Thus,

the Brillouin theorem is also sufficient to satisfy the Hurley's condition.

In any case if the wavefunction obeys the Hellmann-Feynman theorem, the derivative of the wavefunction can be defined in terms of only the original basis functions. On the other hand, in the usual basis sets used in the molecular calculations, the wavefunction derivative are defined in terms of both X and X^1. This implies that the basis set function space is not flexible enough to cover the space spanned by the derivative basis functions. The introduction of X^1 yields integrals involving basis function derivatives and the iterative coupled perturbed Hartree-Fock equations which constitutes a heavy part of the computations in the calculation of the higher energy derivatives.

The above consideration implies the sufficient condition for the fixed basis functions to satisfy the Hellmann-Feynman theorem is that the space spanned by the derivative basis functions constitutes a partial space of the original basis function space. This suggests the new method to obtain the wavefunction obeying the Hellmann-Feynman theorem. But this is not the subject of this paper and we will not go further on this point.

III. Analytic Energy Derivatives of a Diatomic Molecule

In this section we shall derive the second, third and fourth energy derivatives based on the Hellmann-Feynman theorem. For a sake of resulting formal simplicity, we will first consider the 2n-electron closed-shell SCF wavefunction for a diatomic molecule. The electronic energy is given by

$$\langle\Psi|H-E|\Psi\rangle = 0 \qquad (1)$$

The nuclear coordinates are understood to have been written in terms of the internuclear distance R. Thus only R appears as a parameter. Differentiation of eq.(1) results in the Hellmann-Feynman theorem

$$E^1 = \langle\Psi|H^1|\Psi\rangle \qquad (4)$$

if the Hurley's condition is fulfilled

$$\langle\Psi^1|H-E|\Psi\rangle + \langle\Psi|H-E|\Psi^1\rangle = 0 \qquad (3)$$

Here we used the notation

$$H^n = \frac{\partial^n H}{\partial R^n}$$

and analogous notation for Ψ^n and E^n. We observe that R is real so that the derivative wavefunctions are assumed to be real. This is not a serious restriction. The normalization condition of the wavefunction requires

$$\langle\Psi^1|\Psi\rangle = 0 \qquad (19)$$

(a) Second derivative

Differentiation of the Hellmann-Feynman theorem with respect to R yields

$$E^2 = \langle\Psi|H^2|\Psi\rangle + 2\langle\Psi^1|H^1|\Psi\rangle \qquad (20)$$

The second derivative of the energy requires the knowledge of the first derivative of the wavefunction. The essential difficulty in calculating higher energy derivatives lies in finding a good approximation to the first derivative of the wavefunction. By differentiating the Hurley's condition we have the first-order Hurley's condition

$$\langle\Psi^1|H|\Psi\rangle + \langle\Psi^1|H-E|\Psi^1\rangle + \langle\Psi^2|H-E|\Psi\rangle = 0 \qquad (21)$$

Eq.(21) is the equation to determine the first derivative of the wavefunction. As shown later, finding Ψ^1 based on the use of eq.(21) is equivalent to finding the optimal Ψ^1 by the perturbation variation method.[15] Based on the discussion in Sec.II, we assume that Ψ^1 can be expanded in terms of the singly excited configurations

$$\Psi^1 = U_{ai}^{(1)} S_{ai}^{+} \Psi \qquad (22)$$

Here $U_{ai}^{(1)}$ are expansion coefficients, namely the first-order variational parameters and S_{ai}^{+} are the single excitation operators defined by

$$S_{pq}^{+} = (a_{p\alpha}^{+} a_{q\alpha} + a_{p\beta}^{+} a_{q\beta})/\sqrt{2} \qquad (23)$$

The a_p^+ and a_q are the creation and destruction operators which satisfy

Fermion anticommutation relation. From the orthogonality relations of orbitals, we have

$$U^{(1)}_{pq} + U^{(1)}_{qp} = 0 \qquad (24)$$

The S^{+}_{ai} generates a singlet singly excited configuration when operating on Ψ

$$S^{+}_{ai}\Psi \equiv S^{+}_{ai}|> = \| \ldots \varphi_a\varphi_i(\alpha\beta-\beta\alpha)/2 \ldots \| \qquad (25)$$

Eq.(21) involves the second derivative of the wavefunction Ψ^2. So we must eliminate Ψ^2. The Ψ^2 can be written in general in terms of the excitation operators as

$$\Psi^2 = U^{(1)}_{pq}U^{(1)}_{rs}S^{+}_{pq}S^{+}_{rs}|> \qquad (26)$$

The orbital pairs pq, rs run over all orbitals. Thus Ψ^2 consists of the ground, singly and doubly excited configurations

$$\Psi^2 = [\ U^{(2)} + U^{(2)}_{ai}S^{+}_{ai} + U^{(2)}_{ai,bj}\ S^{+}_{ai}S^{+}_{bj}\ ]|> \qquad (27)$$

The ground state component comes from the excitations $S^{+}_{ia}S^{+}_{ai}|>$ and singly excited configurations arise from $S^{+}_{ab}S^{+}_{bi}|>$ and $S^{+}_{ji}S^{+}_{aj}|>$. The Ψ^2 can be expressed in terms of the first-order parameters as

$$\Psi^2 = [\ U^{(1)}_{ia}U^{(1)}_{ai}S^{+}_{ia}S^{+}_{ai} + U^{(1)}_{ab}U^{(1)}_{bi}S^{+}_{ab}S^{+}_{bj} + U^{(1)}_{ji}U^{(1)}_{aj}S^{+}_{ji}S^{+}_{aj}$$

$$+ U_{ai}^{(1)} U_{bj}^{(1)} S_{ai}^{+} S_{bj}^{+} \;]|> \qquad (28)$$

Comparing eq.(28) and eq.(27) we have

$$U^{(2)} = -|U_{ai}^{(1)}|^2 \qquad (29a)$$

$$U_{ai}^{(2)} = U_{ab}^{(1)} U_{bi}^{(1)} + U_{ji}^{(1)} U_{aj}^{(1)} \qquad (29b)$$

$$U_{ai,bj}^{(2)} = U_{ai}^{(1)} U_{bj}^{(1)} \qquad (29c)$$

The $U^{(2)}$ can be obtained also from the second-order normalization condition

$$<\Psi^2|\Psi> + <\Psi^1|\Psi^1> = 0 \qquad (30)$$

Returning to eq.(21), we see that the last term requires only the knowledge of the doubly excited configurations of Ψ^2. Using the relation given by eq.(29c), we can rewrite eq.(21) as

$$<|S_{ai} H^1|> + [\; <|S_{ai}(H-E)S_{bj}^{+}|> + <|S_{ai}S_{bj}H|> \;] U_{bj}^{(1)} = 0 \qquad (31)$$

These are a set of linear equations, which are sufficient for finding $U_{ai}^{(1)}$. We only need solutions of eq.(31) to obtain Ψ^1. There is no iteration involved. Eq.(31) are known as the coupled perturbed Hartree-Fock equations as discussed by Stevens et al.[16] Note here that once the first-order wavefunction has been determined, the second-order wavefunction Ψ^2 can be obtained except $U_{ai}^{(2)}$. The $U_{ai}^{(2)}$ requires the

knowledge of $U^{(1)}_{ab}$ and $U^{(1)}_{ji}$ which cannot be fixed from the first-order wavefunction.

Finally, the second energy derivative can be written in terms of the excitation operators as

$$E^2 = \langle|H^2|\rangle + 2U^{(1)}_{ai}\langle|S_{ai}H^1|\rangle \qquad (32)$$

Eq.(32) can be formulated in another way. Let us consider the general expression of E^2 obtained by double differentiation of eq.(1)

$$E^2 = \langle\Psi|H^2|\Psi\rangle + 4\langle\Psi^1|H^1|\Psi\rangle + 2\langle\Psi^1|H-E|\Psi^1\rangle + 2\langle\Psi^2|H-E|\Psi\rangle \qquad (33)$$

It can be shown[17] for any approximate Ψ^1, say $\tilde{\Psi}^1$ that

$$\langle\Psi|H^2|\Psi\rangle + 4\langle\tilde{\Psi}^1|H^1|\Psi\rangle + 2\langle\tilde{\Psi}^1|H-E|\tilde{\Psi}^1\rangle + 2\langle\tilde{\Psi}^2|H-E|\Psi\rangle \equiv \tilde{E}^2 \geq E^2 \qquad (34)$$

Thus we may choose an arbitrary trial function with variable parameters and optimize it by minimizing $\tilde{E}^2$. If $\tilde{\Psi}^1$ contains only linear parameters and $\tilde{\Psi}^2$ can be writtes as eq.(27), it is easy to show that the optimized trial function Ψ^1_{opt} satisfies

$$\langle\Psi^1_{opt}|H|\Psi\rangle + \langle\Psi^1_{opt}|H-E|\Psi^1_{opt}\rangle + \langle\Psi^2_{opt}|H-E|\Psi\rangle = 0 \qquad (35)$$

This implies that the Ψ^1_{opt} satisfies eq.(21) derived from the Hurley's condition. Also we have the expression of E^2 for the optimal Ψ^1_{opt}

$$E^2 = \langle\Psi|H^2|\Psi\rangle + 2\langle\Psi^1_{opt}|H^1|\Psi\rangle \qquad (36)$$

which takes the same form as given by eq.(20). Thus, finding approximate Ψ^1 from the Hurley's condition of eq.(21) is equivalent to optimizing Ψ^1 using the perturbation variation technique.[15] Namely, the analytic energy derivatives derived from the Hellmann-Feynman theorem is satisfied for the optimal wavefunction derivative determined by the Hurley's condition. It must be emphasized that the variational perturbation method will lead to successful results only for the wavefunction obeying the Hellmann-Feynman theorem.

Eq.(32) can be expressed in a simple matrix form

$$b + (A + B)U = 0 \qquad (37)$$

The b and U are the column vectors of $<|S_{ai}H^1|>$ and first-order variational parameters $U_{ai}^{(1)}$, respectively. The A and B matrices are defined by

$$(A)_{ai,bj} = <|S_{ai}(H-E)S_{bj}^{+}|> \qquad (38a)$$

$$(B)_{ai,bj} = <|S_{ai}S_{bj}H|> \qquad (38b)$$

Since we are dealing with closed-shell systems, all the integrals can be chosen as real. So the A and B matrices are symmetric. Now let us consider the unitary transformation among singly excited configurations which diagonalizes (A+B) matrix

$$O^{\dagger}(A + B)O = d \qquad (39)$$

Here O is the unitary matrix and d is a diagonal matrix. If we further define the unitary transformed excitation operators by

$$R^{+}_{ai} = S^{+}_{bj} O_{bj,ai} \qquad (40)$$

together with

$$T^{(1)}_{ai} = O_{bj,ai} U^{(1)}_{bj} \qquad (41)$$

Then we have

$$\Psi^{1} = T^{(1)}_{ai} R^{+}_{ai} |> \qquad (42)$$

and

$$T^{(1)}_{ai} = - <|R_{ai} H^{1}|> / \Delta E_{ai} \qquad (43)$$

with

$$\Delta E_{ai} = <|R_{ai} (H-E) R^{+}_{ai}|> + <|R_{ai} R_{ai} H|> \qquad (44)$$

Finally, the second energy derivative can be written as

$$E^{2} = <|H^{2}|> - 2 \, |<|R_{ai} H^{1}|>|^{2} / \Delta E_{ai} \qquad (45)$$

Eq.(45) is derived without any approximation in spite of its simplicity.

Namely by choosing 0 as diagonalizing the matrix (A+B), the second energy derivative can be expressed in the similar form as a simple sum-over-state perturbation method.[18] The similar procedure has been used to analyze the second-order perturbation energy of the coupled Hartree-Foch theory and the unlinked terms of the SCF effect of orbitals.[19] Note here that ΔE_{ai} is not really the excitation energy, it includes the additional term originated from the B matrix. It is called as the generalized exchange integral[19] since $\langle|S_{ai}S_{ai}H|\rangle$ equals to the usual exchange integral (ai|ai). The generalized exchange integral represents the SCF effect of the change in the orbitals due to the displacement of the internuclear distance.

The first term of r.h.s. of eq.(45) is the classical formula for the force constant and corresponds to moving the nuclei while holding the electrons fixed. It is positive. The second terms are often referred to as the relaxation terms since they represent the effect of the changes in charge distribution due to the movement of the nuclei. As can be seen from eq.(45), the relaxation terms are negative. This holds for optimized variational functions as well as for the exact wavefunction.[20]

(c) Third derivative

The third energy derivative is obtained by further differentiating eq.(20) with respect to R

$$E^3 = \langle\Psi|H^3|\Psi\rangle + 4\langle\Psi^1|H^2-E^2|\Psi\rangle + 2\langle\Psi^1|H^1-E^1|\Psi^1\rangle + 2\langle\Psi^2|H^1-E^1|\Psi\rangle \quad (46)$$

This expression of the third energy derivative contains the second derivative of the wavefunction Ψ^2. The unknown quantities of Ψ^2 are the

parameters $U^{(2)}_{ai}$ for the singly excited configurations. So it is necessary to look at the second-order Hurley's condition obtained by differentiating eq.(21)

$$\langle\Psi^3|H-E|\Psi\rangle + 2\langle\Psi^2|H^1-E^1|\Psi\rangle + 3\langle\Psi^2|H-E|\Psi^1\rangle$$

$$+ \langle\Psi^1|H^2|\Psi\rangle + 2\langle\Psi^1|H^1-E^1|\Psi^1\rangle = 0 \qquad (47)$$

However, eq.(47) includes the third derivative of the wavefunction, Ψ^3. Therefore, we shall try to eliminate the third-order wavefunction. This is possible. The general form of Ψ^3 is

$$\Psi^3 = [\, U^{(3)} + U^{(3)}_{ai} S^+_{ai} + U^{(3)}_{ai,bj} S^+_{ai} S^+_{bj} + U^{(3)}_{ai,bj,ck} S^+_{ai} S^+_{bj} S^+_{ck} \,]|\rangle \qquad (48)$$

However, we can express $U^{(3)}_{ai}$, $U^{(3)}_{ai,bj}$, and $U^{(3)}_{ai,bj,ck}$ in terms of the lower order parameters by analyzing the excitations,

$$U^{(3)} = -3U^{(2)}_{ai} U^{(1)}_{ai} \qquad (49a)$$

$$U^{(3)}_{ai,bj} = 3U^{(2)}_{ai} U^{(1)}_{bj} \qquad (49b)$$

$$U^{(3)}_{ai,bj,ck} = U^{(1)}_{ai} U^{(1)}_{bj} U^{(1)}_{ck} \qquad (49c)$$

The relation of eq.(49a) can be derived directly from the third-order normalization condition of the wavefunction

$$\langle\Psi^3|\Psi\rangle + 3\langle\Psi^2|\Psi^1\rangle = 0 \qquad (50)$$

Note here that only the doubly excited configurations of Ψ^3 can contribute to the first term of eq.(47). Thus, eq.(47) contains only unknown parameters $U_{ai}^{(2)}$ if $U_{ai}^{(1)}$ are known. Expressing eq.(47) in terms of $U_{ai}^{(2)}$ and $U_{ai}^{(1)}$, we have the following relations

$$U_{ai}^{(2)}\langle|S_{ai}H|\rangle = U_{ai}^{(1)}[\ \langle|S_{ai}H^2|\rangle + 2\langle|S_{ai}(H^1-E^1)S_{bj}^+|\rangle U_{bj}^{(1)}$$

$$+ \{\ 2\langle|S_{ai}S_{bj}HS_{ck}^+|\rangle + \langle|S_{bj}S_{ck}HS_{ai}^+|\rangle\ \} U_{bj}^{(1)}U_{ck}^{(1)}\ ] \qquad (51)$$

Thus, the $U_{ai}^{(2)}$ can be expressed explicitly in terms of the first-order parameters. The third energy derivative is now rewritten as

$$E^3 = \langle|H^3|\rangle + 6U_{ai}^{(1)}\langle|S_{ai}H^2|\rangle + 6U_{ai}^{(1)}U_{bj}^{(1)}\langle|S_{ai}(H^1-E^1)S_{bj}^+|\rangle$$

$$+ 6U_{ai}^{(1)}U_{bj}^{(1)}U_{ck}^{(1)}\langle|S_{ai}S_{bj}HS_{ck}^+|\rangle \qquad (52)$$

The formula is much simpler than that of the direct analytic derivative method. Note here that the final expression of E^3 contains only the first-order variational parameters. The explicit knowledge of Ψ^2 is not necessary. This point will be discussed later.

If we use the unitary transformed excitation operators, the above expression can be expressed in the form of the sum-over-state perturbation method

$$E^3 = \langle|H^3|\rangle - 6\ \langle|H^1R_{ai}^+|\rangle\langle|R_{ai}H^2|\rangle\ /\ \Delta E_{ai}$$

$$+ 6\langle|H^1R^+_{ai}|\rangle\langle|R_{ai}(H^1-E^1)R^+_{bj}|\rangle\langle|R_{bj}H^1|\rangle/(\Delta E_{ai}\Delta E_{bj})$$

$$- 6\langle|H^1R^+_{ai}|\rangle\langle|H^1R^+_{bj}|\rangle\langle|R_{ai}R_{bj}HR^+_{ck}|\rangle\langle|R_{ck}H^1|\rangle/(\Delta E_{ai}\Delta E_{bj}\Delta E_{ck}) \quad (53)$$

This equation is also exact. There is no approximation employed.

Now let us consider the general analytic expression of E^3 derived by successive differentiations of eq.(1)

$$E^3 = \langle\Psi|H^3|\Psi\rangle + 6\langle\Psi^1|H^2-E^2|\Psi\rangle + 6\langle\Psi^1|H^1-E^1|\Psi^1\rangle + 6\langle\Psi^2|H^1-E^1|\Psi\rangle$$

$$+ 6\langle\Psi^2|H-E|\Psi^1\rangle + 2\langle\Psi^3|H-E|\Psi\rangle \quad (54)$$

Expanding the wavefunction derivatives in terms of the excitation operators as before and minimizing E^3 with respect to the unknown parameteter $U^{(2)}_{ai}$, we have

$$\frac{\partial E^3}{\partial U^{(2)}_{ai}} = \langle|S_{ai}H^1|\rangle + [\ \langle|S_{ai}(H-E)S^+_{bj}|\rangle + \langle|S_{ai}S_{bj}H|\rangle\ ]U^{(1)}_{bj} = 0 \quad (55)$$

Eq.(55) hold automatically if Ψ^1 is chosen optimal, that is if $U^{(1)}_{ai}$ satisfy eq.(31). The E^3 expression for the optimal Ψ^2 takes the same form as given by eq.(46). Thus, the first-order wavefunction suffices to determine the third energy derivatives. This property is also utilized to derive the third energy derivatives of the direct analytic method.[4]

(c) Fourth derivative

The fourth derivative is obtained by differentiating eq.(46) again

with respect to R

$$E^4 = \langle\Psi|H^4|\Psi\rangle + 6\langle\Psi^1|H^3|\Psi\rangle + 6\langle\Psi^2|H^2-E^2|\Psi\rangle + 6\langle\Psi^1|H^2-E^2|\Psi^1\rangle$$

$$+ 6\langle\Psi^2|H^1-E^1|\Psi^1\rangle + 2\langle\Psi^3|H^1-E^1|\Psi\rangle \qquad (56)$$

The last term on the r.h.s. of eq.(56) involves the third derivative of the wavefunction. We need the singly excited components of Ψ^3 to evaluate this term due to the one-electron property of H^1. To determine the unknown quantities, we start with the third-order Hurley's condition

$$\langle\Psi^4|H-E|\Psi\rangle + 3\langle\Psi^3|H^1-E^1|\Psi\rangle + 4\langle\Psi^3|H-E|\Psi^1\rangle + 3\langle\Psi^2|H^2-E^2|\Psi\rangle$$

$$+ 9\langle\Psi^2|H^1-E^1|\Psi^1\rangle + 3\langle\Psi^2|H-E|\Psi^2\rangle + \langle\Psi^1|H^3|\Psi\rangle + 3\langle\Psi^1|H^2-E^2|\Psi^1\rangle = 0 \qquad (57)$$

Again the above condition contains the fourth derivative of the wavefunction. However, the required quantities to evaluate the first term of eq.(57) are only the doubly excited configurations of Ψ^4. From the analysis of the excitation operators, we see that

$$U^{(4)}_{ai,bj} S^+_{ai} S^+_{bj} = (4U^{(3)}_{ai} U^{(1)}_{bj} + 3U^{(2)}_{ai} U^{(2)}_{bj}) S^+_{ai} S^+_{bj} \qquad (58)$$

Thus we can find the unknown parameters $U^{(3)}_{ai}$ from eq.(57). The final expression of $U^{(3)}_{ai}$ becomes

$$U^{(3)}_{ai}\langle|S_{ai}H^1|\rangle = U^{(1)}_{ai}[\ \langle|S_{ai}H^3|\rangle + 3\langle|S_{ai}(H^2-E^2)S^+_{bj}|\rangle U^{(1)}_{bj}$$

$$+ 9\langle|S_{ai}S_{bj}H^1S^+_{kc}|\rangle U^{(1)}_{bj}U^{(1)}_{kc} + \{ 3\langle|S_{ai}S_{bj}(H-E)S^+_{ck}S^+_{dl}|\rangle +$$

$$+ 4\langle|S_{ai}S_{bj}S_{ck}HS^+_{dl}|\rangle \}U^{(1)}_{bj}U^{(1)}_{ck}U^{(1)}_{dl}] + 3U^{(2)}U^{(1)}_{ai}\langle|S_{ai}H^1|\rangle$$

$$+ 3U^{(2)}_{ai}[\langle|S_{ai}H^2|\rangle + 3\langle|S_{ai}(H^1-E^1)S^+_{bj}|\rangle U^{(1)}_{bj}$$

$$+ \{ \langle|S_{ai}(H-E)S^+_{bj}|\rangle + \langle|S_{ai}S_{bj}H|\rangle \}U^{(2)}_{bj}$$

$$+ 2\{ 2\langle|S_{ai}S_{bj}HS^+_{ck}|\rangle + \langle|S_{bj}S_{ck}HS^+_{ai}|\rangle \}U^{(1)}_{bj}U^{(1)}_{ck}] \qquad (59)$$

Note here it is not necessary to solve the second-order coupled perturbed Hartree-Fock equations for the calculation of the third-order parameters. It is also possible to represent $U^{(3)}_{ai}$ in terms of the first-order parameters $U^{(1)}_{ai}$ if we utilize the relations given by eq.(51).

The fourth energy derivative can be expressed in terms of the excitation operators

$$E^4 = \langle|H^4|\rangle + 6U^{(1)}_{ai}\langle|S_{ai}H^3|\rangle + 6U^{(2)}_{ai}\langle|S_{ai}H^2|\rangle + 6U^{(2)}\langle|H^2-E^2|\rangle$$

$$+ 6U^{(1)}_{ai}U^{(1)}_{bj}\langle|S_{ai}(H^2-E^2)S^+_{bj}|\rangle + 6U^{(2)}U^{(1)}_{ai}\langle|S^+_{ai}H^1|\rangle$$

$$+ 6U^{(2)}_{ai}U^{(1)}_{bj}\langle|S_{ai}(H^1-E^1)S^+_{bj}|\rangle$$

$$+ 6U^{(1)}_{ai}U^{(1)}_{bj}U^{(1)}_{ck}\langle|S_{ai}S_{bj}H^1S^+_{ck}|\rangle + 2U^{(3)}_{ai}\langle|S_{ai}H^1|\rangle \qquad (60)$$

Utilizing the relations given in eq.(59) we can eliminate $U^{(3)}_{ai}$ and have

$$E^4 = \langle|H^4|\rangle + 8U_{ai}^{(1)}\langle|S_{ai}H^3|\rangle + 12U_{ai}^{(1)}U_{bj}^{(1)}\langle|S_{ai}(H^2-E^2)S_{bj}^{+}|\rangle$$

$$+ 24U_{ai}^{(1)}U_{bj}^{(1)}U_{ck}^{(1)}\langle|S_{ai}S_{bj}H^1S_{ck}^{+}|\rangle$$

$$+ 6U_{ai}^{(1)}U_{bj}^{(1)}U_{ck}^{(1)}U_{dl}^{(1)}\langle|S_{ai}S_{bj}(H -E)S_{ck}^{+}S_{dl}^{+}|\rangle$$

$$+ 8U_{ai}^{(1)}U_{bj}^{(1)}U_{ck}^{(1)}U_{dl}^{(1)}\langle|S_{ai}S_{bj}S_{ck}H\ S_{dl}^{+}|\rangle$$

$$+ 6U_{ai}^{(2)}U_{bj}^{(2)}\{\ \langle|S_{ai}(H-E)S_{bj}^{+}|\rangle + \langle|S_{ai}S_{bj}H|\rangle\ \}$$

$$+ 12U_{ai}^{(2)}[\ \langle|S_{ai}H^2|\rangle + 2U_{bj}^{(1)}\langle|S_{ai}(H^1-E^1)S_{bj}^{+}|\rangle$$

$$+ \{\ 2\langle|S_{ai}S_{bj}HS_{ck}^{+}|\rangle + \langle|S_{ai}HS_{bj}^{+}S_{ck}^{+}|\rangle\ \}U_{bj}^{(1)}U_{ck}^{(1)}\ ] \qquad (61)$$

Since according to the relations of eq.(51), the last four terms on the r.h.s. of the above equation is

$$12U_{ai}^{(2)}[\ \langle|S_{ai}H^2|\rangle + 2U_{bj}^{(1)}\langle|S_{ai}(H^1-E^1)S_{bj}^{+}|\rangle$$

$$+ \{\ 2\langle|S_{ai}S_{bj}HS_{ck}^{+}|\rangle + \langle|S_{ai}HS_{bj}^{+}S_{ck}^{+}|\rangle\ \}U_{bj}^{(1)}U_{ck}^{(1)}\ ]$$

$$= 12|U_{ai}^{(2)}|^2\langle|S_{ai}H^1|\rangle/U_{ai}^{(1)} \qquad (62)$$

provided that $U_{ai}^{(1)} \neq 0$. If we further use the relations given by eq.(51) we can express E^4 in terms of only the first-order parameters $U_{ai}^{(1)}$. Although the formula looks complicated, it consists only of straightforward combinations of known quantities. There are no algebraic

problems.

The fourth energy derivatives can be expressed in terms of the unitary transformed excitation operators as

$$E^4 = \langle|H^4|\rangle - 8\,\langle|H^1R^+_{ai}|\rangle\langle R_{ai}H^3|\rangle / \Delta E_{ai}$$

$$+ 12\langle|H^1R^+_{ai}|\rangle\langle|R_{ai}(H^2-E^2)R^+_{bj}|\rangle\langle|R_{bj}H^1|\rangle / (\Delta E_{ai}\Delta E_{bj})$$

$$- 24\langle|H^1R^+_{ai}|\rangle\langle|H^1R^+_{bj}|\rangle\langle|R_{ai}R_{bj}H^1R^+_{ck}|\rangle\langle|R_{ck}H^1|\rangle / (\Delta E_{ai}\Delta E_{bj}\Delta E_{ck})$$

$$+ 6\langle|H^1R^+_{ai}|\rangle\langle|H^1R^+_{bj}|\rangle\langle|R_{ai}R_{bj}(H-E)R^+_{ck}R^+_{dl}|\rangle\langle|R_{ck}H^1|\rangle\langle|R_{dl}H^1|\rangle /$$

$$(\Delta E_{ai}\Delta E_{bj}\Delta E_{ck}\Delta E_{dl})$$

$$+ 8\langle|H^1R^+_{ai}|\rangle\langle|H^1R^+_{bj}|\rangle\langle|H^1R_{ck}|\rangle\langle|R_{ai}R_{bj}R_{ck}HR^+_{dl}|\rangle\langle|R_{dl}H^1|\rangle /$$

$$(\Delta E_{ai}\Delta E_{bj}\Delta E_{ck}\Delta E_{dl})$$

$$- 6|T^{(2)}_{ai}|^2\Delta E_{ai} \qquad (63)$$

Here, $T^{(2)}_{ai}$ are the transformed second-order parameters

$$T^{(2)}_{ai} = (\Delta E_{ai})^{-1}[\ \langle|R_{ai}H^2|\rangle - 2\langle|R_{ai}(H^1-E^1)R^+_{bj}|\rangle\langle|R_{bj}H^1|\rangle/\Delta E_{bj}$$

$$+ \{2\langle|R_{ai}R_{bj}HR^+_{ck}|\rangle + \langle|R_{ai}HR^+_{bj}R^+_{ck}|\rangle\}\langle|R_{bj}H^1|\rangle\langle|R_{ck}H^1|\rangle/(\Delta E_{bj}\Delta E_{ck})\ ] \qquad (64)$$

Eq.(63) is also an exact equation.

Let us again consider the general formula for E^4 obtained by successive differentiations of eq.(1)

$$E^4 = \langle\Psi|H^4|\Psi\rangle + 8\langle\Psi^1|H^3|\Psi\rangle + 12\langle\Psi^2|H^2-E^2|\Psi\rangle + 12\langle\Psi^1|H^2-E^2|\Psi^1\rangle$$

$$+ 24\langle\Psi^2|H^1-E^1|\Psi^1\rangle + 8\langle\Psi^3|H^1-E^1|\Psi\rangle + 6\langle\Psi^2|H-E|\Psi^2\rangle$$

$$+ 8\langle\Psi^3|H-E|\Psi^1\rangle + 2\langle\Psi^4|H-E|\Psi\rangle \qquad (65)$$

Taking account of eq.(58), we minimize E^4 with respect to $U_{ai}^{(3)}$. This yields

$$\frac{\partial E^3}{\partial U_{ai}^{(3)}} = \langle|S_{ai}H^1|\rangle + [\ \langle|S_{ai}(H-E)S_{bj}^{+}|\rangle + \langle|S_{ai}S_{bj}H|\rangle\ ]U_{bj}^{(1)} = 0 \qquad (66)$$

This is also satisfied if Ψ^1 is chosen optimal and the E^4 for the optimal Ψ^3 becomes identical to that in eq.(56). Thus, the optimal Ψ^1 is sufficient to evaluate the derivatives of the energy up to fourth-order. Analogous results for E^5, E^6,... may be derived. The only difficulty is that these lower-order wavefunctions must be known exactly.

IV. General Formulae for the Second, Third and Fourth Energy Derivatives

In this section we shall give the general formulae for the second, third and fourth energy derivatives based on the Hellmann-Feynman theorem

We will start with the energy expression given by eq.(1). By differentiating eq.(1) with respect to a nuclear coordinate λ, we obtain the Hellmann-Feynman theorem

$$E^{\lambda} = \langle\Psi|H^{\lambda}|\Psi\rangle \qquad (67)$$

and the Hurley's condition

$$\langle\Psi^{\lambda}|H-E|\Psi\rangle + \langle\Psi|H-E|\Psi^{\lambda}\rangle = 0 \qquad (68)$$

We assume the wavefunction is normalized to unity and have

$$\langle\Psi^{\lambda}|\Psi\rangle + \langle\Psi|\Psi^{\lambda}\rangle = 0 \qquad (69)$$

Second energy derivatives can be obtained by differentiating eq.(67) with respect to μ

$$E^{\lambda\mu} = \langle\Psi|H^{\lambda\mu}|\Psi\rangle + 2\langle\Psi^{\lambda}|H^{\mu}|\Psi\rangle \qquad (70)$$

Here we used the relations, assuming that all the functions are real,

$$\langle\Psi^{\lambda}|H^{\mu}|\Psi\rangle = \langle\Psi^{\mu}|H^{\lambda}|\Psi\rangle \qquad (71)$$

The second derivatives require the first derivative wavefunctions Ψ^{λ}. By differentiating eq.(68) with respect to μ we have the first-order Hurley's condition

$$\langle\Psi^{\lambda}|H^{\mu}|\Psi\rangle + \langle\Psi^{\lambda}|H-E|\Psi^{\mu}\rangle + \langle\Psi^{\lambda\mu}|H-E|\Psi\rangle = 0 \qquad (72)$$

As shown in the previous section, Ψ^{λ} may be expanded in terms of the singly excited configurations

$$\Psi^{\lambda} = U_{ai}^{\lambda} S_{ai}^{+}|\rangle \qquad (73)$$

Then $\Psi^{\lambda\mu}$ can be expressed as

$$\Psi^{\lambda\mu} = [\ -|U_{ai}^{\lambda}|^2 + U_{ai}^{\lambda\mu} S_{ai}^{+} + U_{ai}^{\lambda}U_{bj}^{\mu} S_{ai}^{+}S_{bj}^{+}\ ]|\rangle \qquad (74)$$

Eq.(72) with $\lambda=\mu$ gives

$$\langle|S_{ai}H^{\lambda}|\rangle + [\ \langle|S_{ai}(H-E)S_{bj}^{+}|\rangle + \langle|S_{ai}S_{bj}H|\rangle\ ]U_{bj}^{\lambda} = 0 \qquad (75)$$

By solving a set of linear equations we can obtain Ψ^{λ} and then $E^{\lambda\mu}$,

$$E^{\lambda\mu} = \langle|H^{\lambda\mu}|\rangle + 2U_{ai}^{\lambda}\langle|S_{ai}H^{\mu}|\rangle \qquad (76)$$

The third energy derivatives are derived by further differentiating eq.(70) with respect to ν. It is not symmetrized with respect to λ, μ, ν. It can be recast in a symmetrical form. The third energy derivatives are given by

$$E^{\lambda\mu\nu} = \langle\Psi|H^{\lambda\mu\nu}|\Psi\rangle + \frac{4}{3} P_1^{(3)}\langle\Psi^{\lambda}|H^{\mu\nu}-E^{\mu\nu}|\Psi\rangle + \frac{2}{3} P_2^{(3)}\langle\Psi^{\lambda\mu}|H^{\nu}-E^{\nu}|\Psi\rangle$$

$$+ \frac{2}{3} P_3^{(3)}\langle\Psi^{\lambda}|H^{\mu}-E^{\mu}|\Psi^{\nu}\rangle \qquad (77)$$

The notation $P_1^{(3)}$, $P_2^{(3)}$, $P_3^{(3)}$ means the permutation of the superscripts

$$P_1^{(3)} = (\lambda)(\mu\nu) + (\mu)(\nu\lambda) + (\nu)(\lambda\mu)$$
$$P_2^{(3)} = (\lambda\mu)(\nu) + (\mu\nu)(\lambda) + (\nu\lambda)(\mu)$$
$$P_3^{(3)} = (\lambda)(\mu)(\nu) + (\mu)(\nu)(\lambda) + (\nu)(\lambda)(\mu)$$

This implies there are three terms from each $P^{(3)}$. The third energy derivatives require the second-order parameters, $U_{ai}^{\lambda\mu}$. The second-order Hurley's condition is given by

$$\langle\Psi^{\lambda\mu\nu}|H-E|\Psi\rangle + \frac{2}{3} P_2^{(3)}\langle\Psi^{\lambda\mu}|H^{\nu}-E^{\nu}|\Psi\rangle + P_2^{(3)}\langle\Psi^{\lambda\mu}|H-E|\Psi^{\nu}\rangle$$

$$+ \frac{1}{3} P_1^{(3)}\langle\Psi^{\lambda}|H^{\mu\nu}-E^{\mu\nu}|\Psi\rangle + \frac{2}{3} P_3^{(3)}\langle\Psi^{\lambda}|H^{\mu}-E^{\mu}|\Psi^{\nu}\rangle = 0 \qquad (78)$$

Using the relations

$$U_{ai,bj}^{\lambda\mu\nu} = P_2^{(3)} U_{ai}^{\lambda\mu} U_{bj}^{\nu} \qquad (79)$$

we can express $U_{ai}^{\lambda\mu}$ in terms of U_{ai}^{λ} from eq.(78) as

$$\frac{1}{3} P_2^{(3)} U_{ai}^{\lambda\mu} \langle|S_{ai}H^{\nu}|\rangle = \frac{1}{3} P_1^{(3)} U_{ai}^{\lambda}\langle|S_{ai}H^{\mu\nu}|\rangle$$

$$+ \frac{2}{3} P_3^{(3)} U_{ai}^{\lambda}\langle|S_{ai}(H^{\mu}-E^{\mu})S_{bj}^{+}|\rangle U_{bj}^{\nu} + P_2^{(3)} U_{ai}^{\lambda}\langle|S_{ai}S_{bj}HS_{ck}^{+}|\rangle U_{bj}^{\mu} U_{ck}^{\nu} \qquad (80)$$

In the case of $\lambda=\mu=\nu$, eq.(80) are reduced to

$$U^{\lambda\lambda}_{ai}\langle|S^{+}_{ai}H^{\lambda}|\rangle = U^{\lambda}_{ai}[\ \langle|S_{ai}H^{\lambda\lambda}|\rangle + 2\langle|S_{ai}(H^{\lambda}-E^{\lambda})S^{+}_{bj}|\rangle U^{\lambda}_{bj}$$

$$\{\ 2\langle|S_{ai}S_{bj}HS^{+}_{ck}|\rangle + \langle|S_{ai}HS^{+}_{bj}S^{+}_{ck}|\rangle\ \}U^{\lambda}_{bj}U^{\lambda}_{ck}\ ] \qquad (81)$$

Also we have the following relations by putting $\lambda=\nu$ in eq.(80)

$$2U^{\lambda\mu}_{ai}\langle|S_{ai}H^{\lambda}|\rangle + U^{\lambda\lambda}_{ai}\langle|S_{ai}H^{\mu}|\rangle =$$

$$2U^{\lambda}_{ai}\langle|S_{ai}H^{\lambda\mu}|\rangle + U^{\mu}_{ai}\langle|S_{ai}H^{\lambda\lambda}|\rangle + 4U^{\lambda}_{ai}\langle|S_{ai}(H^{\lambda}-E^{\lambda})S^{+}_{bj}|\rangle U^{\mu}_{bj}$$

$$+ 2U^{\lambda}_{ai}\langle|S_{ai}(H^{\mu}-E^{\mu})S^{+}_{bj}|\rangle U^{\lambda}_{bj} + 3U^{\lambda}_{ai}\langle|S_{ai}S_{bj}HS^{+}_{ck}|\rangle U^{\lambda}_{bj}U^{\mu}_{ck}$$

$$+ 6U^{\lambda}_{ai}\langle|S_{ai}S_{bj}HS^{+}_{ck}|\rangle U^{\mu}_{bj}U^{\lambda}_{ck} \qquad (82)$$

So once $U^{\lambda\lambda}_{ai}$ have been determined by eq.(81), the remaining $U^{\lambda\mu}_{ai}$ can be obtained from eq.(82). Now the third energy derivatives given in eq.(77) can be rewritten in terms of the excitation operators as

$$E^{\lambda\mu\nu} = \langle|H^{\lambda\mu\nu}|\rangle + 2\ P^{(3)}_{1}U^{\lambda}_{ai}\langle|S_{ai}H^{\mu\nu}|\rangle$$

$$+ 2\ P^{(3)}_{3}U^{\lambda}_{ai}U^{\mu}_{bj}\langle|S_{ai}(H^{\nu}-E^{\nu})S^{+}_{bj}|\rangle$$

$$+ 2\ P^{(3)}_{2}U^{\lambda}_{ai}U^{\mu}_{bj}U^{\nu}_{ck}\langle|S_{ai}S_{bj}HS^{+}_{ck}|\rangle \qquad (83)$$

Thus, we only need solutions of linear equations of eq.(75) to evaluate the third energy derivatives.

The fourth energy derivatives are given in a symmetrical expression

by

$$E^{\lambda\mu\nu\kappa} = \langle\Psi|H^{\lambda\mu\nu\kappa}|\Psi\rangle + \frac{3}{2} P_1^{(4)}\langle\Psi^{\lambda}|H^{\mu\nu\kappa}|\Psi\rangle + P_2^{(4)}[\langle\Psi^{\lambda\mu}|H^{\nu\kappa}-E^{\nu\kappa}|\Psi\rangle$$

$$+ \langle\Psi^{\lambda}|H^{\mu\nu}-E^{\mu\nu}|\Psi^{\kappa}\rangle + \frac{1}{2}\{\langle\Psi^{\lambda\mu}|H^{\nu}-E^{\nu}|\Psi^{\kappa}\rangle + \langle\Psi^{\lambda\mu}|H^{\kappa}-E^{\kappa}|\Psi^{\nu}\rangle\}]$$

$$+ \frac{1}{2} P_1^{(4)}\langle\Psi^{\lambda\mu\nu}|H^{\kappa}-E^{\kappa}|\Psi\rangle \qquad (84)$$

with

$$P_1^{(4)} = (\lambda)(\mu\nu\kappa) + (\mu)(\nu\kappa\lambda) + (\nu)(\kappa\lambda\mu) + (\kappa)(\lambda\mu\nu)$$

$$P_2^{(4)} = (\lambda\mu)(\nu\kappa) + (\mu\nu)(\kappa\lambda) + (\nu\kappa)(\lambda\mu) + (\kappa\lambda)(\mu\nu) + (\mu\kappa)(\lambda\nu)$$
$$+ (\lambda\nu)(\mu\kappa)$$

The above expression includes third derivatives of the wavefunction which requires the knowledge of the singly excited configurations of $\Psi^{\lambda\mu\nu}$. The variational parameters $U_{ai}^{\lambda\mu\nu}$ of $\Psi^{\lambda\mu\nu}$ can be determined by the third-order Hurley's condition obtained by differentiating eq.(78) and the relations

$$U_{ai,bj}^{\lambda\mu\nu\kappa} S_{ai}^{+} S_{bj}^{+} = (P_3^{(4)} U_{ai}^{\lambda\mu\nu} U_{bj}^{\kappa} + \frac{1}{2} P_2^{(4)} U_{ai}^{\lambda\mu} U_{bj}^{\nu\kappa}) S_{ai}^{+} S_{bj}^{+} \qquad (85)$$

with

$$P_3^{(4)} = (\lambda\mu\nu)(\kappa) + (\mu\nu\kappa)(\lambda) + (\nu\kappa\lambda)(\mu) + (\kappa\lambda\mu)(\nu)$$

Then we have the following relations

$$\frac{1}{4}\,P_3^{(4)}U_{ai}^{\lambda\mu\nu}\langle|S_{ai}H^{\kappa}|\rangle = \frac{1}{4}\,P_1^{(4)}U_{ai}^{\lambda}\langle|S_{ai}H^{\mu\nu\kappa}|\rangle$$

$$+\frac{1}{4}\,P_2^{(4)}U_{ai}^{\lambda}U_{bj}^{\mu}\langle|S_{ai}(H^{\nu\kappa}-E^{\nu\kappa})S_{bj}^{+}|\rangle$$

$$+P_3^{(4)}U_{ai}^{\lambda}U_{bj}^{\mu}U_{ck}^{\nu}U_{dl}^{\kappa}\Big[\frac{9}{4}\langle|S_{ai}S_{bj}(H-E)S_{ck}^{+}S_{dl}^{+}|\rangle + 2\langle|S_{ai}S_{bj}S_{ck}HS_{dl}^{+}|\rangle\Big]$$

$$+\frac{1}{4}\,P_2^{(4)}\big[U_{ai}^{\lambda}\langle|S_{ai}H^{\mu}|\rangle U^{\nu\kappa} + U_{ai}^{\mu}\langle|S_{ai}H^{\lambda}|\rangle U^{\nu\kappa}\big]$$

$$+\frac{1}{2}\,P_2^{(4)}U_{ai}^{\lambda\mu}\Big[\langle|S_{ai}H^{\nu\kappa}|\rangle + \frac{3}{2}\{\langle|S_{ai}(H^{\nu}-E^{\nu})S_{bj}^{+}|\rangle U_{bj}^{\kappa}$$

$$+\langle|S_{ai}(H^{\kappa}-E^{\kappa})S_{bj}^{+}|\rangle U_{bj}^{\nu}\}$$

$$+\{\langle|S_{ai}(H-E)S_{bj}^{+}|\rangle + \langle|S_{ai}S_{bj}H|\rangle\}\,U_{bj}^{\nu\kappa}$$

$$+2\{\,2\langle|S_{ai}S_{bj}HS_{ck}^{+}|\rangle + \langle|S_{ai}HS_{bj}^{+}S_{ck}^{+}|\rangle\,\}U_{bj}^{\nu}U_{ck}^{\kappa}\Big] \qquad (86)$$

In the case of $\lambda=\mu=\nu=\kappa$, the above relations are reduced to eq.(59). Once $U_{ai}^{\lambda\lambda\lambda}$ have been determined, $U_{ai}^{\lambda\lambda\mu}$ can be obtained by putting $\lambda=\nu=\kappa$ in eq.(86). Finally we can determine the remaining $U_{ai}^{\lambda\mu\nu}$ using the known $U_{ai}^{\lambda\lambda\lambda}$ and $U_{ai}^{\lambda\lambda\mu}$. Now the fourth derivatives can be evaluated in terms of the known quantities. Although the equations are rather complicated, there are no algebraic problems. Finally, the fourth energy derivatives can be written as

$$E^{\lambda\mu\nu\kappa} = \langle|H^{\lambda\mu\nu\kappa}|\rangle + 2\,P_1^{(4)}U_{ai}^{\lambda}\langle|S_{ai}H^{\mu\nu\kappa}|\rangle$$

$$+2\,P_2^{(4)}U_{ai}^{\lambda}U_{bj}^{\mu}\langle|S_{ai}(H^{\nu\kappa}-E^{\nu\kappa})S_{bj}^{+}|\rangle$$

$$+ 6\ P_3^{(4)} U_{ai}^{\lambda} U_{bj}^{\mu} U_{ck}^{\nu} \langle | S_{ai} S_{bj} H^{\kappa} S_{ck}^{+} | \rangle$$

$$+ 8\ U_{ai}^{\lambda} U_{bj}^{\mu} U_{ck}^{\nu} U_{dl}^{\kappa} \langle | S_{ai} S_{bj} S_{ck} H S_{dl}^{+} | \rangle$$

$$+ 6\ U_{ai}^{\lambda} U_{bj}^{\mu} U_{ck}^{\nu} U_{dl}^{\kappa} \langle | S_{ai} S_{bj} (H-E) S_{ck}^{+} S_{dl}^{+} | \rangle$$

$$+ P_2^{(4)} U_{ai}^{\lambda\mu} U_{bj}^{\nu\kappa} \{ \langle | S_{ai} (H-E) S_{bj}^{+} | \rangle + \langle | S_{ai} S_{bj} H | \rangle \}$$

$$+ 2\ P_2^{(4)} U_{ai}^{\lambda\mu} [\langle | S_{ai} H | \rangle + \langle | S_{ai} (H^{\nu} - E^{\nu}) S_{bj}^{+} | \rangle U_{bj}^{\kappa}$$

$$+ \langle | S_{ai} (H^{\kappa} - E^{\kappa}) S_{bj}^{+} | \rangle U_{bj}^{\nu}$$

$$+ \{ 2 \langle | S_{ai} S_{bj} H S_{ck}^{+} | \rangle + \langle | S_{ai} H S_{bj}^{+} S_{ck}^{+} | \rangle \} U_{bj}^{\nu} U_{ck}^{\kappa} \ ] \qquad (87)$$

Of course we can express $E^{\lambda\mu\nu\kappa}$ in terms of only the first-order parameters by eliminating $U_{ai}^{\lambda\mu}$ with the help of eq.(80).

V. Conclusion

We have derived equations which provide the second, third and fourth derivatives of the energy of a molecule based on the Hellmann-Feynman theorem. The Hurley's condition can be used to obtain approximations to the first-order wavefunction, from which the second, third and fourth energies can be obtained. There are several significant advantages over the direct analytic derivative method. First the anlytic expressions of

these higher derivatives are much simpler compared to those of the direct analytic method. Second the electrostatic calculation involves only one-electron integrals. Since the wavefunction derivatives can be expanded in the excited configurations in terms of the basis functions, there appear no integrals involving derivatives of the basis functions. This leads to drastic simplification since the fully ab initio evaluation of higher energy derivatives of the conventional method requires large amounts of computer time and storage primarily because of the derivatives of the integrals. Third there is no need of solving the coupled perturbed Hartree-Fock equations to obtain the derivatives of the wavefunction. We only need solutions of a set of linear equations. There is no iteration involved. Only the first derivative wavefunction is sufficient to determine these higher order derivatives. Fourth there are intuitive physical pictures associated with these higher derivatives as the Hellmann-Feynman force picture associated with the first derivatives.

We have also shown that the present procedure of deriving higher energy derivatives based on the Hellmann-Feynman theorem with the auxiliary Hurley's condition is equivalent to minimizing the derivative energy by the perturbation variation techniques. Thus the derived formulae can be applicable to any real one-electron perturbation such as electric properties. Also it is easy to modify the formulae for the pure imaginary perturbed wavefunctions in the case of magnetic properties. If the spin-dependent perturbations are treated, the singlet excitation operators defined in eq.(23) should be replaced by the triplet excitation operators

$$S^{+}_{pq} = (a^{+}_{p\alpha}a_{q\alpha} - a^{+}_{p\beta}a_{q\beta})/\sqrt{2}$$

We have also derived these higher derivatives in the similar form of the sum-over-state perturbation method without any approximation. These expressions may help our understanding of various terms of these higher energy derivatives.

In this paper explicit formulae are derived only for the closed-shell SCF wavefunction. But the present procedure can easily be extended to other variational wavefunctions obeying the Hellmann-Feynman theorem.

Acknowledgement

This work was partly supported by a Grant-in-Aid for Scientific Research from the Japanese Ministry of Education, Science and Culture.

References

1. P.Pulay, Mol.Phys., **17**, 197 (1969); ibid **18**, 473 (1970); Adv.Chem.Phys., **69**, 241 (1987).
2. J.A.Pople, K.Raghavachari, H.B.Schlegel and J.S.Binkley, Int.J.Quantum Chem., **S13**, 225 (1979).
3. J.Gerratt and I.M.Mills, J.Chem.Phys., **49**, 1719, 1730 (1968).
4. J.F.Gaw, Y.Yamaguchi and H.F.Schaefer, J.Chem.Phys., **81**, 6395 (1984).
5. J.F.Gaw and N.Handy, Chem.Phys.Lett., **121**, 321 (1985).
6. S.M.Colwell, D.Jayatilaka, P.E.Maslen, R.D.Amos and N.Handy, private communication.
7. H.Hellmann, Einfuhrung in die Quantenchemie (Deuticke, Leipzig, 1937), 285; R.P.Feynman, Phys.Rev.,**56**, 340 (1939).
8. S.T.Epstein, The Variational Methods in Quantum Chemistry, (Academic Press, New York, 1974); S.T.Epstein, in The Force Concept in Chemistry, ed. B.M.Deb (Van Nostrand Reinhold Company, New York, 1981).
9. A.C.Hurley, Proc.Roy.Soc.London Ser. **A226**, 179, 193 (1954); A.C.Hurley, in Molecular Orbitals in Chemistry, Physics, and Biology, ed. by Lowdin and Pullman, Academic Press, New York (1964).
10. T.Berlin, J.Chem.Phys., **19**, 208 (1951); L.Salem, J.Chem.Phys.,**38**, 1227 (1963); R.H.Schwendeman, J.Chem.Phys., **44**, 556 (1966); H.Kim, J.Chem.Phys., **48**, 301 (1968); H.Nakatsuji, K.Kanda and T.Yonezawa, J.Chem.Phys., **77**, 1961 (1982); H.Nakatsuji, K.Kand and T.Yonezawa, Intern.J.Quantum Chem., **23**, 387 (1983); See also review J.Goodisman, in The Force Concept in Chemistry, ed. B.M.Deb (Van Nostrand Reinhold Company, New York, 1981).

11. Other formulations are possible based on the use of the virial theorem to define $\partial E/\partial\lambda$, see for example, W.L.Clinton,J.Chem.Phys., 33 1603 (1960) and P.Phillipson, ibid, 39, 3010 (1963);44, 633 (1966).
12. K.Hirao, submitted for J.Chem.Phys.
13. H.Nakatsuji, K.Kanda and T.Yonezawa, Chem.Phys.Lett., 75, 340 (1980); H.Nakatsuji, T.Hayakawa and M.Hada, Chem.Phys.Lett., 80, 94 (1981).
14. R.Moccia, Theoret.Chim.Acta(Berlin), 8,8 (1967); D.M.Bishop and A.Macias, J.Chem.Phys., 51, 4997 (1969);ibid, 53, 3515 (1970); D.M.Bishop and M.Randic, J.Chem.Phys., 44, 2480 (1966).
15. I.M.Mills, Mol.Phys., 1, 107 (1957); M.L.Benson and B.Kirtman, J.Chem. Phys.,44, 126 (1966).
16. A.Dalgarno, Adv.Phys., 11, 281 (1962); R.M.Stevens, R.M.Pitzer and W.N.Lipscomb, J.Chem.Phys., 38, 550 (1963); R.M.Stevens and W.N.Lipscomb, J.Chem.Phys., 40, 2238 (1964); K.Thomsen and P.Swanstrom, Mol.Phys., 26, 735 (1973).
17. J.O.Hirschfelder, W.B.Brown and S.T.Epstein, Adv.Quantum Chem., 1, 255 (1964); J.H.Epstein and S.T.Epstein, J.Chem.Phys., 42, 3630 (1965)
18. A.Unsold, Z.Physik, 43, 569 (1927).
19. H.Nakatsuji, J.Chem.Phys.,61, 3728 (1974); K.Hirao and H.Nakatsuji, J.Chem.Phys., 69, 4535, 4548 (1978).
20. J.N.Silverman and J.C. van Leuven, Chem.Phys.Lett., 7, 37 (1979); B.M.Deb, Chem.Phys.Lett., 17, 78 (1972); K.Hirao, Chem.Phys.Lett., submitted for publication.

NOTE ON AN UPPER BOUND PROPERTY OF SECOND DERIVATIVES OF THE ENERGY

K.HIRAO

Department of Chemistry, College of General Education, Nagoya University, Nagoya, Japan

and

Institute for Molecular Science, Okazaki, Japan

ABSTRACT

An alternative proof is given for the upper bound relation of second derivatives of the energy

$$(\partial^2 E/\partial\lambda^2)\langle\Psi|\Psi\rangle \leq \langle\Psi|\partial^2 H/\partial\lambda^2|\Psi\rangle$$

The relation is proved to be equivalent to the stability condition of a variational wavefunction.

Silverman and Leuven[1] have used perturbation variational theory to derive the upper bound relation for second derivatives of the energy

$$(\partial^2 E/\partial\lambda^2)\langle\Psi|\Psi\rangle \leq \langle\Psi|\partial^2 H/\partial\lambda^2|\Psi\rangle \qquad (1)$$

Here H is the Hamiltonian, λ is any parameter in H (coordinate of a nucleus, charge of a nucleus, etc.), Ψ and E are either the exact eigenfunction and eigenvalue of the Schrodinger equation or some optimal variational counterparts to them. An alternative proof is provided by Deb[2] for the exact solution. The curvature theorem (1) provides insight into the behavior of exact and optimum variational solutions to the Schrodinger equation when these solutions are treated as functions of a real parameter occuring in the Hamiltonian. For instance, when the coordinates of nucleus in a molecule are taken as λ, then the second derivatives of the energy give the force constants. In this case, the relation (1) indicates the relaxation terms are negative.

In this note we wish to show that there is an easier way to derive (1) for the optimized variational wavefuctions (all variational parameters chosen to minimize the expectation value of $H(\lambda)$ for each $\{\lambda\}$) as well as for the exact wavefunction.

Let Ψ be a normalized optimal variational wavefunction and E the corresponding optimal energy

$$\langle\Psi|H-E|\Psi\rangle = 0 \qquad (2)$$

and let λ be a real parameter in H. Here, we first differentiate (2) with respect to λ to find

$$(\partial E/\partial\lambda)\langle\Psi|\Psi\rangle = \langle\Psi|\partial H/\partial\lambda|\Psi\rangle + \langle\partial\Psi/\partial\lambda|H-E|\Psi\rangle + \langle\Psi|H-E|\partial\Psi/\partial\lambda\rangle \quad (3)$$

However, the variational condition ensures that

$$\langle\partial\Psi/\partial\lambda|H-E|\Psi\rangle + \langle\Psi|H-E|\partial\Psi/\partial\lambda\rangle = 0 \quad (4)$$

whence we have the Hellmann-Feynman theorem[3]

$$(\partial E/\partial\lambda)\langle\Psi|\Psi\rangle = \langle\Psi|\partial H/\partial\lambda|\Psi\rangle \quad (5)$$

The condition (4) is called as the Hurley's condition.[4]
Differentiating (5) again with respect to λ yields

$$(\partial^2 E/\partial\lambda^2)\langle\Psi|\Psi\rangle = \langle\Psi|\partial^2 H/\partial\lambda^2|\Psi\rangle + \langle\partial\Psi/\partial\lambda|\partial H/\partial\lambda|\Psi\rangle + \langle\Psi|\partial H/\partial\lambda|\partial\Psi/\partial\Psi\rangle \quad (6)$$

Similarly by differentiating the Hurley's condition we obtain

$$\langle\partial\Psi/\partial\lambda|\partial H/\partial\lambda|\Psi\rangle + \langle\Psi|\partial H/\partial\lambda|\partial\Psi/\partial\lambda\rangle = -2[\langle\partial\Psi/\partial\lambda|H-E|\partial\Psi/\partial\lambda\rangle + \mathrm{Re}\langle\partial^2\Psi/\partial\lambda^2|H-E|\Psi\rangle] \quad (7)$$

Substitution in (6) leads to the result

$$(\partial^2 E/\partial\lambda^2) - \langle\Psi|\partial^2 H/\partial\lambda^2|\Psi\rangle = -2[\langle\partial\Psi/\partial\lambda|H-E|\partial\Psi/\partial\lambda\rangle + \mathrm{Re}\langle\partial^2\Psi/\partial\lambda^2|H-E|\Psi\rangle] \quad (8)$$

Hence what we want is a condition which will ensure that

$$\langle \partial\Psi/\partial\lambda | H-E | \partial\Psi/\partial\lambda \rangle + \mathrm{Re}\langle \partial^2\Psi/\partial\lambda^2 | H-E | \Psi \rangle \geq 0 \qquad (9)$$

as a consequence of the variational principle.

Now let us consider a small displacement of an optimal wavefunction by replacing λ to $\lambda+\delta\lambda$. From Taylor's theorem we can expand the wavefunction as

$$\Psi(\lambda+\delta\lambda) = \Psi(\lambda) + (\partial\Psi/\partial\lambda)\delta\lambda + (1/2!)(\partial^2\Psi/\partial\lambda^2)(\delta\lambda)^2 + \ldots \qquad (10)$$

Here $\Psi(\lambda+\delta\lambda)$ is assumed to be normalized also to unity. The first differential of Ψ is the first order change in Ψ produced by changing λ. Similarly the second differential of Ψ is the second order change of Ψ. Then the energy is given by

$$E(\Psi(\lambda+\delta\lambda)) = E + [\langle \partial\Psi/\partial\lambda | H-E | \Psi \rangle + \langle \Psi | H-E | \partial\Psi/\partial\lambda \rangle]\delta\lambda + (1/2!)[\langle \partial\Psi/\partial\lambda | H-E | \partial\Psi/\partial\lambda \rangle + \mathrm{Re}\langle \partial^2\Psi/\partial\lambda^2 | H-E | \Psi \rangle](\delta\lambda)^2 + \ldots \qquad (11)$$

The first order term in $\delta\lambda$ is zero due to the Hurley's condition (4). This leads to a simple criterion that the energy corresponding to Ψ be stationary with respect to the variation given by (10). Once one has located a stationary point, a natural question to ask is, is it a minimum, a maximum or just a saddle point? The way to answer this question is to look at the second order term in $\delta\lambda$. The second order term is expressed as a quadratic form in the $|\partial\Psi/\partial\lambda\rangle$ and $\langle\partial\Psi/\partial\lambda|$. Thus the question to be answered is, is the form positive (local minimum),

negative (local maximum) or indefinite (saddle point)? The energy is stable if

$$(1/2!)[\langle \partial\Psi/\partial\lambda | H-E | \partial\Psi/\partial\lambda \rangle + \mathrm{Re}\langle \partial^2\Psi/\partial\lambda^2 | H-E | \Psi \rangle] \geq 0 \qquad (12)$$

This inequality is known as the stability condition for the optimized variational wavefunction. The stability condition ensures that the wavefunction represents a true minimum or a saddle point of the energy functional. Thus if the energy is stable we arrive at the required upper bound relation from (8)

$$(\partial^2 E/\partial\lambda^2)\langle \Psi | \Psi \rangle \leq \langle \Psi | \partial^2 H/\partial\lambda^2 | \Psi \rangle \qquad (13)$$

That is, the upper bound condition is equivalent to the stability condition. The upper bound condition provides additional criterion to that of the variational principle for judging the quality and stability of an approximate wavefunction. A general condition for the stability problems of a Hartree-Fock solution was first formulated by Thouless[5]. Cizek and Paldus[6], Fukutome[7] and Hirao and Nakatsuji[8] have discussed the concept of the stability of a variational wavefunction. But we will not go further on this point. If the equality of (12) and therefore of (13) is satisfied, the critical point is a saddle point and we must go to higher order terms to examine the critical point.

If E is the exact energy, $(H-E)\Psi=0$, then the last term of r.h.s. in (8) vanishes. The E is the true lowest bound state energy and an expectation value of a positive semidefinite operator (H-E) gives

$$\langle \partial\Psi/\partial\lambda | H-E | \partial\Psi/\partial\lambda \rangle \geq 0 \qquad (14)$$

which leads to the required upper bound relation.[2)]

There is an alternative to the choice of (10) for Ψ, namely

$$\Psi' = \exp[\, ihD \,]\Psi \quad ; \quad D = (1/i)(\partial/\partial\lambda) \qquad (15)$$

Here D is a given differentiation operator and h is an arbitrary real number not contained in H. Since the D is Hermitian, Ψ' is related to Ψ by a unitary transformation. The energy $E'=\langle\Psi'|H|\Psi'\rangle$ is given by

$$E' = E + h[\langle \partial\Psi/\partial\lambda | H-E | \Psi\rangle + \langle\Psi | H-E | \partial\Psi/\partial\lambda\rangle] + h^2[\langle \partial\Psi/\partial\lambda | H-E | \partial\Psi/\partial\lambda\rangle + \mathrm{Re}\langle \partial^2\Psi/\partial\lambda^2 | H-E | \Psi\rangle] + \ldots \qquad (16)$$

Now consider the transformation of the Hamiltonian expressed as

$$e^{-ihD} H e^{ihD}$$

Then the exponential series can easily be expanded using Hausdorff formula to yield

$$E' = E + ih\langle\Psi|[H-E,D]|\Psi\rangle + (ih)^2/2!\langle\Psi|[[H-E,D],D]|\Psi\rangle + \ldots$$
$$= E - h\langle\Psi|\partial H/\partial\lambda - \partial E/\partial\lambda|\Psi\rangle + (h^2/2!)\langle\Psi|\partial^2 H/\partial\lambda^2 - \partial^2 E/\partial\lambda^2|\Psi\rangle + \ldots \qquad (17)$$

By comparing (16) with (17), we can see that the first order energy term gives the Hellmann-Feynman theorem and the second order term with the stability condition leads to the upper bound relation.

References

1. J.N.Silverman and J.C.van Leuven, Chem.Phys.Lett., **7**, 37 (1970).
2. B.M.Deb, Chem.Phys.Lett., **17**, 78 (1972).
3. H.Hellmann, Einfuhrung in die Quantenchemie (deuticke, Vienna, 1937); R.P.Feynman, Phys.Rev., **56**, 340 (1939).
4. A.C.Hurley, Proc.Roy.Soc., **A226**, 179 (1954).
5. D.J.Thouless, Nucl.Phys., **21**, 225 (1960).
6. J.Cizek and J.Paldus, J.Chem.Phys., **47**, 3976 (1967); ibid, **53**, 821 (1970); Phys.Rev.,**A3**, 525 (1971); J.Paldus and J.Cizek, Phys.Rev.,**A2**, 2268 (1970).
7. H.Fukutome, Prog.Theor.Phys., **40**, 1227 (1969).
8. K.Hirao and H.Nakatsuji, J.Chem.Phys., **69**, 4535, 4548 (1978).

Theoretical study of the reactions of penta-coordinated trigonal bipyramidal compounds; PH_5, PF_5, PF_4H, PF_3H_2, PF_4CH_3, $PF_3(CH_3)_2$, $P(O_2C_2H_4)H_3$, $P(OC_3H_6)H_3$ and $PO_5H_4^-$

H. Wasada
Department of Chemistry, Faculty of Science, Nagoya University, Nagoya, Japan
and
K. Hirao
Department of Chemistry, College of General Education, Nagoya University, Nagoya, Japan
and
Institute for Molecular Science, Okazaki, Japan

Abstract

We have studied pseudorotation reactions of some penta-coordinated phosphorous compounds {PH_5, PF_5, PF_4H, PF_3H_2, PF_4CH_3, $PF_3(CH_3)_2$, $P(O_2C_2H_4)H_3$, $P(OC_3H_6)H_3$ and $PO_5H_4^-$} to elucidate the reaction mechanisms by using ***ab initio*** SCF and MP4 methods. We have calculated the potential surface for the lowest pass of pseudorotation reactions. The geometries of the transition state connecting them have been determined theoretically. The ligands which form the covalent bond with the central phosphorus atom such as Hydrogen, methyl and methylene groups prefer to coordinate in the equatorial position. This

nature of the ligands is called as the ***equatoriphilicity*** . It is possible to predict whether the pseudorotation reaction can occur or not, based on the number of the equatoriphilic ligands in the penta-coordinated molecules. The normal coordinate analyses have been carried out at the stationary points of PH_5 and PF_5. The mechanism of pseudorotation is discussed and explained on the theoretical basis.

1. Introduction

The different behavior in the hydrolysis reactions between DNA and RNA is an interesting fact that is related to their different roles in the biochemical system. DNA molecules which work as tapes for the storage of genetic informations show very strong resistance to the decomposition by the hydrolysis. Even after one hour reaction at 100°C in 1N NaOH (aq.) DNA molecules don't show any changes.[1] On the other hand, 2-hydroxyethyl methyl phosphate, which is a model molecule of RNA, easily undergoes the hydrolysis reaction. The half-life of the hydrolysis reaction of this molecule at 25°C in 1N NaOH (aq.) is 25 minutes.[1] Indeed RNA molecules have high turnover rates and are easily hydrolized. The difference to the hydrolysis reaction between DNA and RNA which functions as a carrier of genetic informations comes from these chemical characteristics. The behavior of phosphate ester to the hydrolysis reaction is closely related to the nature of phosphorus atom. The high reactivity comes from the penta-coordinated intermediate formed by the attack of the vicinal hydroxyl group through the hydrolysis reaction. The group-15 elements in the second and succeeding rows of the periodic table can show higher valence numbers. One of the possible

structures of penta-coordinated compounds is trigonal bipyramid. The hypervalent character of elements in higher rows of the periodic table is quite different from that of the first row elements. For example, CH_5^- is in a high energy transition state of the S_N2 reaction, while SiH_5^- is a stable intermediate. Recently, as theoretical techniques have been expanded, it becomes possible to predict the existence of compounds from the theoretical background. Though it has been assumed that hypervalent compounds of first-row elements such as nitrogen cannot exist, a recent study of Ewig et al. suggested the existence of three nitrogenous penta-coordinated compounds, i.e. NF_3H_2, NF_4H and NF_5.[53]

In relation to the phosphorus penta-coordinated compounds, Westheimer[2] has proposed the mechanism of the hydrolysis of phosphate esters. He has postulated that the nucleophilic displacement reactions of phosphorous compounds proceeds through penta-coordinated intermediates. (see Figure 1-(a)) He also assumed that an axial entry of the nucleophile takes place in forming a trigonal bipyramidal intermediate and that an axial departure of a leaving group occurs in forming products. If the activated states have sufficiently long lifetime, it is further assumed that ligand rearrangement, that is pseudorotation reaction, may be encountered before product formation. The Berry's pseudorotation[4] process, which rapidly exchange axial and equatorial ligands in the trigonal bipyramidal intermediate (Figure 1-(b)), has a strong basis in phosphorous chemistry where NMR studies have established intramolecular ligand exchange process for many phosphorane molecules. (see Figure 2) Many studies of the bonding nature, structures of phosphorous molecules and relative reaction energies of pseudorotation

reaction have been performed experimentally and theoretically.[3]-[32],[46]-[50] Particularly, Holmes has contributed to developments of the understanding of penta-coordinated phosphorous compounds.[32] In theoretical treatments some models are adopted; valence electron pair repulsion model[24], a three-center four-electron bonding model.[25]-[27] Furthermore there are many ***ab initio*** or semiempirical molecular orbital calculations.[27]-[31],[50] Strich et al.[7] studied PH_5 and supported Berry's pseudorotation. Marsden[12] calculated PF_5 and estimated the energy barrier of the pseudorotation to be 3.8 kcal/mol. Schleyer[45] studied first and second row substituents of phosphoranes in a systematic way. Recently, Dieters and Holmes[14] studied a series of substituted phosphorous compounds. The pseudorotation reaction is not confined to only phosphorus compounds. Recently Gordon et al.[50] have performed theoretically an extensive study of the pseudorotation reaction of SiH_5^-.

There has been much interest in the pseudorotation mechanism in view of the important role of the phosphorus chemistry. As the pseudorotation reaction is a ligand exchange isomerization reaction between the apical part and the equatorial part, the reaction mechanism is closely related to the relative stabilities between the isomers which are interconverted through the pseudorotation isomerization reaction. The relative stability of apical and equatorial substituted isomers have been discussed by the substituent electronegativities, steric interaction and ring strain. It is very difficult to observe directly the pseudorotation process as it is a reaction in the intermediate. And it is necessary to study the transition state of the reaction to understand the process of pseudorotation reaction. ***Ab initio*** calculations are nowadays widely accepted as a

legitimate way of getting informations that are experimentally inaccessible. The theory can describe the mechanism and provide some correct explanations of the pseudorotation hypothesis.

We have carried out ***ab initio*** molecular orbital calculations on pseudorotation profiles of some phosphorous compounds in this study. The computational methods in this study are described in Section 2. The results are present and discussed in Section 3. The emphasis of the discussion is put on the pseudorotation mechanism. We also discussed the relative stability of isomers. The equatorial substituent effects in the apical bond formation are also discussed. Some general conclusions are summarized in Section 4.

2. Computational details

In this study all geometries of penta-coordinated compounds were fully optimized at the SCF level. Because of the fact pointed out by Magnusson[44] that relative energies of singly substituted phosphoranes vary considerably with different basis set, it is necessary to use basis set at least as large as 6-31G*. So for all molecules except PH_5, the basis sets are used at the double-zeta level[33),(35)] which are augmented with polarization functions. The polarization functions (α_P=0.43, α_C=0.75, α_O=0.85, α_F=0.90, α_H=1.00) are added to phosphorus atom and other ligands which are directly connected to the central phosphorus atom. We have also added a diffuse function (α_O=0.059) on the phosphoryl oxygen atom in the calculation of $PO_5H_4^-$. We used a triple-zeta[33] plus polarization (TZP) basis set for PH_5 calculations. The correlation energies are calculated by the fourth-order Møller-Plesset perturbation

method (MP4) at SCF optimized geometries.

3. Results and discussions

In Section **3A** we discuss the pseudorotations of some penta-coordinated phosphorous compounds. We discuss the relation between the stability and the structure of penta-coordinated phosphorous compound in Section **3B**, i.e. equatoriphilicity. We discuss the apical bond character by using the orbital energy correlation diagrams in Section **3C**. Some discussions on the equatorial substituent effects are given in Section **3D**.

3A. Pseudorotation

PH_5

The optimized structures of the ground (D_{3h}) and transition (C_{4v}) states are shown in Figure 3-(a) and (b), respectively. The ligand at the apex position of the C_{4v} structure is called as the pivotal ligand.

The energy relation between the ground state and the transition state is shown in the energy diagram. (see Figure 4) The broken line shows result of the SCF calculation and the solid shows that of the MP4 calculation. The individual electron pairs are separated as far as possible in the ground state. These electrons become closer each other in the transition state. Thus the electron correlation effect becomes more significant in the transition state. The energy barrier of the pseudorotation reaction is about 2 kcal/mol with and without the electron correlation. We can say, therefore, the Berry's pseudorotation occurs very easily in this molecule.

The electronic structure of phosphorane PH_5 is

$$(core)^{10}(1a_1')^2(1e')^2(2e')^2(1a_2'')^2(2a_1')^2(3e')^0(4e')^0(3a_1')^0 \text{ -----}$$

The highest occupied molecular orbital (HOMO) is shown in Figure 5-(a). The apical bond has a three-center character and is weaker than the normal single bond. The electronic structure of the transition state is

$$(core)^{10}(1a_1)^2(1e)^2(2e)^2(2a_1)^2(1b_1)^2(3a_1)^0(4a_1)^0 \text{ -----}$$

The changes of the bond length of PH_5 through the reaction are shown in Table III-(a), in which the bond length before the reaction is put as 100. The pivotal ligand stays in the equatorial plane before and after the pseudorotation reaction. The pivotal bond length is shortest in the transition state. Its change is also smallest in the reaction. The orbital mainly related to the pivot is $1a_1$ MO which is the deepest one in the valence molecular orbitals of the ground state. In the transition state two apical orbitals and two equatorial orbitals mixes-up to form four equivalent ligand orbitals. The bond brought to the apical position is lengthened. The electron density moves to the overlap region between phosphorus and the pivotal hydrogen from other parts of the molecule in course of the reaction. So the pivotal bond becomes shorter than the corresponding equatorial bonds in the ground state.

The symmetry of the transition density[36)-(39)] from the HOMO to the LUMO of the ground state PH_5 is

$$a_1' \times e' = e'$$

The intramolecular vibration mode inducing the pseudorotation is e′ symmetry. The transition densities with 3-21G* basis set are shown in Figure 5-(b) and (c), in which (b) is one along the apical axis and (c) is one in the equatorial plane. The intramolecular displacement of

individual atoms is expected to occur along the arrows. The results of the vibrational analysis of the ground state with TZP basis set are shown in Figure 6-(a) and (b). There are two modes of e′ symmetry with the frequencies of 629.0 cm^{-1} and 1373.8 cm^{-1}. We can see that the equatorial bond is more flexible than the apical one and the opening motion of the equatorial ligands (629.0 cm^{-1}) initiates the pseudorotation reaction. We also performed the vibrational analysis calculation for the transition state. There is one vibrational mode with the imaginary frequency. The transition vector is shown in Figure 6-(c). One of the <HPH angles closes down and the other angle opens up simultaneously. The transition vector shows that the molecule returns to the ground state along this mode of the vibration.

PF_5

The optimized structures of PF_5 are shown in Figure 7. This molecule has a D_{3h} symmetry at the ground state and a C_{4v} at the transition state. The values in the parentheses are the experimental ones.[16] The calculated apical and equatorial bond lengths are in good agreement with the experiment. The calculated energies at several levels of approximation for ground and transition states are shown in Table I. From these results, the MP2 level of correlation correction seems to be adequate for the calculation of the potential energy barrier. The potential energy barrier in the reaction has 4.24-5.07 kcal/mol (see Figure 8), so the pseudorotation reaction proceeds easily. The change of the bond length is least for the pivotal ligand as shown in Table III-(b). The bond length of the pivotal ligand is shortest in the transition state like PH_5 case.

The results of the vibrational analysis are shown on Figure 9. Berry's pseudorotation reaction begins with e′ vibration and the transition state has C_{4v} symmetry. The opening motion of the equatorial ligand is easier (185.3 cm^{-1}) than the bending of the apical bond (559.9 cm^{-1}) for this molecule as well as PH_5.

PF_4H and PF_3H_2

The total and relative energies are summarized in Table I for PF_4H and PF_3H_2.

The energy diagram of PF_4H in course of the reaction is drawn in Figure 10-(a). The hydrogen atom is in the equatorial position in the ground state. This atom occupies the apex (pivotal position) of C_{4v} structure in the transition state. There are 7.38 and 5.70 kcal/mol of potential energy barriers for PF_4H pseudorotation reaction at SCF and MP4 levels, respectively.

The most stable isomer of PF_3H_2 has two hydrogens in the equatorial position. The results of the calculated potential energy are summarized in Table II. The potential energy surface of this reaction is shown in Figure 10-(b). The isomerization product is fairly unstable because of the very small energy difference between the transition state and the product. The barrier height to the pseudorotation of PF_3H_2 is calculated to be 12.16 kcal/mol and 10.43 kcal/mol by the SCF and MP4, respectively. The relative energies of the pseudorotated isomer to the ground state are calculated to be 12.03 kcal/mol and 10.82 kcal/mol at the SCF and MP4 levels, respectively. The pseudorotation reaction does not proceed because of the high potential energy barrier. We can also say

that there is no stable energy minimum structure for the pseudorotation products from the MP4 results. Through the process of the pseudorotation reaction both of two equatorial hydrogen atoms cannot remain in the equatorial plane. One hydrogen is brought inevitably to the apical position and its bond is lengthened leading to the instabilization of the molecular system.

PF_4CH_3 and $PF_3(CH_3)_2$

Westheimer discussed the pseudorotation reaction of PF_4CH_3 and $PF_3(CH_3)_2$.[2] If the pseudorotation reaction occurs, the only one type of F-NMR peak is expected for PF_4CH_3. The NMR experiment verified that the pseudorotation is expected to occur in PF_4CH_3 molecule. On the other hand, no evidence of the pseudorotation reaction is obtained in the case of $PF_3(CH_3)_2$.

Our results on PF_4CH_3 are shown in Figure 11-(a). One methyl group is in the equatorial plane at the ground state. The methyl group occupies the pivotal position in the transition state structure. As the pseudorotation proceeds, two apical fluorines and two equatorial fluorines interchange. The energy barrier for the pseudorotation reaction is calculated to be 5.26 kcal/mol (SCF) and 3.95 kcal/mol (MP4). The easy proceeding of the pseudorotation reaction is expected for PF_4CH_3, which verifies experimental results.

We also studied on $PF_3(CH_3)_2$. In the ground state two methyl groups occupy the equatorial positions. One of two methyl groups takes the apical position in the isomerization product. The other apical position is occupied by the fluorine atom. As the reaction proceeds, the bond

brought to the apical position from the equatorial one is stretched, and the stability of the molecule decreases. The potential energy curve of the reaction is shown in Figure 11-(b). There is only one stable minimum structure for $PF_3(CH_3)_2$ reaction. The energies of the isomerized product are calculated to be 15.04 kcal/mol (SCF) and 14.01 kcal/mol (MP4) higher relative to the stable isomer. Thus the pseudorotation reaction cannot proceed as shown in the experiment because of the high energy barrier and the shape of the potential energy curve. The high barrier comes mainly from the fact that one of CH_3 group occupies the apical position.

$P(O_2C_2H_4)H_3$ and $P(OC_3H_6)H_3$

Westheimer[2] also discussed the compounds having ring structures shown in Figure 2-(c),(d).

As a model of the cyclic intermediate in a RNA hydrolysis reaction we studied the ethyleneglycoxyphosphorane ($P(O_2C_2H_4)H_3$). One end of the ring of this molecule occupies the apical position and the other end forms one end of the equatorial plane in the ground state. The angle between apical PO and PH bonds comes close as the pseudorotation reaction proceeds. The transition state has C_s symmetry which resembles to the C_{4v} structure of the simple penta-coordinated molecule such as PH_5 and PF_5. The energy diagram of the pseudorotation is shown in Figure 12-(a). A low potential barrier is found in the pseudorotation reaction. The relative energy of the transition state to the ground state is calculated to be only 2.32 kcal/mol (SCF) and 1.83 kcal/mol (MP4), respectively. Thus it is expected that the isomerization easily occurs by the

pseudorotation reaction.

We also studied another cyclic phosphorane $P(OC_3H_6)H_3$ in which one oxygen atom of ethyleneglycoxyphosphorane is replaced by a methylene group. There is only one stable energy minimum structure in which the oxygen occupies the apical position and the carbon atom is placed in the equatorial plane. We calculated the energy change when the angle <O2P1H3 is changed. The results are shown in Figure 12-(b) as an potential energy curve. There is no second stable isomer in which the carbon atom occupies the apical position and the oxygen atom occupies the equatorial one. The calculated energy barrier for the pseudorotation is about 9 kcal/mol in the SCF level. Thus the pseudorotation reaction is not expected to occur easily. When the correlation energy is taken into account, the potential barrier is reduced to 7.77 kcal/mol. The potential energy barrier became low, but the pseudorotated isomer will return to the ground state because of the shape of the potential surface. In the process of the pseudorotation reaction the methylene group which forms covalent bond with the central phosphorus cannot keep the equatorial position. This bond is transferred to the apical position and stretched, and the molecule becomes unstable.

3B. Equatoriphilicity

Here we explain the relation between the structure and the stability of the penta-coordinated phosphorous compound. Let having five atoms (ligands) around P with a large distant apart. If we suppose that those atoms (ligands) are able to form a stable penta-coordinated molecule, we shall obtain a stabilization energy. It will be convenient to divide this into

two processes, of which the first one corresponds to forming the equatorial plane and the second one to forming a penta-coordinated whole molecule. The results on PF_3H_2 and $PF_3(CH_3)_2$ are summarized in Table IV. In this table when the ligand are far apart we speak of the separated ligand. We name the process in which the equatorial plane part as the equatorial plane formation. The process of the whole penta-coordinated molecule formation is called as a whole molecule formation. E(stable) and E(unstable) of Table IV mean the total energy of the stable and unstable isomers, respectively. The value in E(A)-E(b) is the difference between E(stable) and E(unstable), that is the relative stability to the stable isomer. The structures of stable and unstable molecules are shown in Figure 13. The energy of the separated ligand is the sum of the energies of all separated ligands and that of the phosphorus atom. The energy of the equatorial plane formation is the sum of the total energy of the equatorial part and those of the separated apical ligands.

In the case of PF_3H_2, the stable isomer is 12.03 kcal/mol stabler than the pseudorotated unstable one. When the stabilization energies are compared in the formation of the equatorial plane (PH_2F and PF_2H), the stabilization energy of the PH_2F which is a equatorial plane of the stable isomer is 31.64 kcal/mol greater than that of PF_2H. In the apical bond formation E(stable) of the PF_2H + FH process obtains more stabilization by 19.61 kcal/mol than E(unstable) of the PH_2F + F_2. The total stabilizations are obtained by adding up all stabilization energies. The stability of the equatorial plane mainly determines the total stabilization of the penta-coordinated whole molecule. There is a same tendency in the case of $PF_3(CH_3)_2$, in which the total stabilization is mainly determined by

the stability of the equatorial plane.

These results come from the fact that the ligands such as hydrogen, methyl group and methylene group which form the covalent bonds with the central phosphorus prefer to coordinate on the equatorial positions. If such a group is contained only one in the molecule, it is able to remain near the equatorial position through the pseudorotation reaction occupying the pivotal position and its bond length remains almost constant. But when there are more than one such ligands, one ligand at least must be moved to the apical position and the covalent bond is lengthened in the reaction process. Thus the pseudorotated isomer becomes less stable. These process determine the possibility of the pseudorotation reaction. This explains the relationship between the ligand position and the stability of the molecule in the different view point from the known apicophilicity, which says that more electronegative ligand prefers to occupy the apical position. We name this concept as an ***equatoriphilicity*** .

We present some predictions of the relation between the possibility of the pseudorotation and the number of equatoriphilic groups in Table V. In acyclic molecules when the number of the equatoriphilic group is zero or one, the reaction is expected to occur as shown in PF_5, PF_4H and PF_4CH_3. In the case of two, three and four equatoriphilic groups, the progress of the pseudorotation reaction brings the equatoriphilic group to the apical position and so the reaction is prohibited. When all the ligands are replaced by the equatoriphilic group, the energy change before and after the pseudorotation reaction is remains zero and thus the reaction will not be hindered. But because both of the two apical positions are

occupied by the equatoriphilic ligands in this case, the resultant penta-coordinated molecule would become less stable. For example PH_5 is a metastable molecule not a global one. In cyclic molecules when the number of the equatoriphilic end of the ring is zero or two the reaction is expected to proceed. On the other hand if the number is one, the reaction will be prohibited.

We applied the equatoriphilicity to the pseudorotation reaction of $PO_5H_4^-$. This molecule is a prototype of the penta-coordinated intermediate of the hydrolysis reaction of phosphates. There are two possible structures. One is that the phosphoryl oxygen atom is placed in the equatorial plane. The phosphoryl oxygen occupies an axial position in the other isomer. The energy relation given by our studies is showed in Figure 14 with the transition state between two isomers. The energy of the isomer **A** relative to the isomer **B** is considerably high, i.e. 11.52 kcal/mol at the SCF level and 9.57 kcal/mol even at the MP4 level. The transition state energy between these stable isomers is calculated to be 13.53 kcal/mol (SCF) and 11.64 kcal/mol (MP4), respectively. The relative energy of the transition state to the isomer **A** is computed as 2.01 kcal/mol (SCF) and 2.07 kcal/mol (MP4). If the isomer **A** is formed in the reaction of PO_4H_3 with OH^- anion, this isomer isomerizes easily to the very stable product **B**. The phosphoryl PO bond is in the apical position in the isomer **A**. In this structure the covalent bond is in the apical position and is lengthened. Thus the necessity of the equatoriphilicity is not satisfied in this structure. So it isomerizes to the most stable isomer **B** through the pseudorotation to transfer the phosphoryl PO bond to the equatorial position. We also consider the pseudorotation reaction between

the isomers **B** and its 90° pseudorotated **B′**. The transition state between them is C_4 symmetry structure. The transition state energy is 6.90 kcal/mol (SCF) and 6.19 kcal/mol (MP4) higher than that of the isomer **B**. This result implies that the intermediate of the hydrolysis reaction of the phosphate will easily isomerize by the pseudorotation.

3C. Apical Bonding Character

We divided a whole molecule to an equatorial plane and an apical ligand part as shown in Figure 15-(a) and drew molecular orbital energy correlation diagrams between them in order to study the character of the apical bond and the origin of the well-known apicophilicity. (see Figure 15-(b)) Here an orbital which is symmetric about the equatorial plane is called as a symmetric orbital. An antisymmetric orbital means an antisymmetric one about the equatorial plane. When a whole molecule **A-B** is formed from two parts **A** and **B**, their orbitals φ_a and φ_b having the orbital energies ε_a and ε_b ($\varepsilon_a<\varepsilon_b$), respectively, interact to yield two new orbitals φ_a' and φ_b'. Through the orbital interaction the energy level of the orbital φ_a' is lowered relative to that of the initial orbital φ_a by the value $\Delta\varepsilon_a$ estimated with the second-order perturbation theory

$$\Delta\varepsilon_a = \varepsilon_a' - \varepsilon_a = \frac{(\mathbf{H}_{ab} - \varepsilon_a \mathbf{S}_{ab})^2}{\varepsilon_a - \varepsilon_b}$$

where $\mathbf{H}_{ab}$ is the interaction energy and $\mathbf{S}_{ab}$ is the overlap integral for these orbitals.[51] The factors affecting to the orbital stabilization are the orbital overlapping and the energy level closeness of the interacting two orbitals φ_a and φ_b.

The graph on Figure 16 shows the stabilization of the total energy,

symmetric and antisymmetric orbital energies in the formation of the penta-coordinated molecule. The stabilization energies are plotted to the change of the number of the equatorial fluorine. Both of the two apical ligands are fixed to fluorine atoms. The symbols in the parenthesis mean the equatorial plane parts. We can easily see that the close relation between the equatorial substituent effect on the symmetric orbital and that on the whole molecule. On the other hand the stabilization of the antisymmetric orbitals are almost same for every case. There are little substituent effect on the antisymmetric orbital from the equatorial fluorines. Thus we can discuss the molecular stabilization by using only the symmetrical orbital stabilization.

This result can be explained as follows. The electrons in the antisymmetric orbital concentrate on $3p_z$ lone-pair of the central phosphorus before the orbital interaction. The orbital interaction stabilizes it by the extension of the orbital space. Therefore if the same apical ligands are coordinated, the stabilization with an almost same level will be given by the orbital interaction. This corresponds to the known apicophilicity. If the electronegative and electron withdrawing group is placed in the apical position, the electrons concentrated on $3p_z$ lone-pair of the phosphorus can begin to move to the apical bond region effectively and strong ionic bond is formed with the great stabilization. On the other hand, the symmetric electron is on the stretched apical ligands before the orbital interaction. The $3dz^2$ AO of the central phosphorus bridges two apical fluorines through the symmetric orbital interaction, and thus its contribution is essentially important for the stabilization of the axial bond. Thus there are obvious difference in the stabilization of the symmetric

orbital due to the difference in the ability to participate in the three-center bond.

The orbital energy correlation diagrams of PH_5, PH_3F_2 and PF_5 are shown in Figure 17-(a), (b) and (c), respectively.

In PH_5 the symmetric orbital is characterized by 1s AO of the apical hydrogen and $3dz^2$ orbital of the central phosphorus atom mixed into it. This orbital is very slightly stabilized because the $3dz^2$ AO of the central phosphorus is in high energy level. There is a difficulty of charge transfer from the donor H_2 to the acceptor PH_3.

In PH_3F_2 the stabilization of the **A** orbital is much larger than that of PH_5. This means that the fluorine is more apicophilic ligand. The stabilization of **S** orbital mainly comes from the interaction of 2p AO of the apical fluorine and $3dz^2$ AO of the central phosphorus. The charge transfer from HOMO of fluorine to LUMO of phosphorus atom is induced fairly strongly by this contribution of $3dz^2$ AO. The larger stabilization of the antisymmetric orbital induces the great charge transfer from the lone-pair HOMO of PH_3 to the LUMO of F_2, as the difference of the electronegativity is large (2.19 for P and 3.98 for F by Pauling's definition).[52] According to the great charge transfer, almost all the charge on phosphorus HOMO flows to the apical LUMO and the coefficients of $3p_z$ AO of the central phosphorus in the whole PH_3F_2 molecule become small and the bond with ionic character is formed in P - F regions.

In PF_5 there is a very strong substituent effect on the LUMO of the equatorial plane because all equatorial positions are substituted by fluorines. So the stabilization of symmetric orbital becomes much larger

than that of PH_5. The stabilization of the antisymmetric orbital is almost same level with PH_3F_2 as the apical ligand is fluorine for both molecules, i.e. the apicophilicity is fixed.

3D. Substituent Effects

The orbital energy level of the equatorial plane parts of the penta-coordinated molecule have an important contribution to the stabilization of the apical bond. We studied the substituent effect on the apical orbital of the equatorial plane part.

The results of the substituent effects on HOMO and LUMO of equatorial part are shown in Figure 18. The bond angles in the triangle plane are fixed to be 120 °. All combinations of equatorial ligands are considered by using the following bond lengths; R(P-H)=1.40 Å, R(P-F)=1.55 Å and $R(P-CH_3)$=1.81 Å. When a fluorine atom coordinates as an equatorial ligand, the orbital energy of LUMO becomes lower. On the other hand, there is not an obvious effect of an equatorial ligand in methyl group and hydrogen atom. The substituent effect on LUMO comes from the σ-type attracting interaction by the ligands. When great electronegative ligands like fluorine coordinate, the strong σ-type interaction is induced and the orbital energy of LUMO becomes lower. Thus if the apical ligands are fixed, there is much stabilization of the axial orbital in molecules having fluorine as an equatorial ligand. The axial bond becomes strong in such molecules. The influence of the substituent to HOMO of the equatorial part comes from the π-type donating interaction to the $3p_z$ lone-pair of central phosphorus atom. When methyl group coordinates, its effect is given through the

hyperconjugation. The orbital energy of HOMO becomes higher as the antibonding nature through the π-type interaction increases, though this effect is smaller than that of the σ-type interaction between substituents and LUMO.

We showed the variation of the orbital energies of the apical LUMO according to the difference of the apical ligand in Figure 19. In this study one dummy atom is defined at a middle point of the apical bond. The bond lengths from a dummy atom(X) to each apical ligands are as follows; R(X-H)=1.45 Å R(X-F)=1.60 Å, R(X-CH_3)=1.84 Å and R(X-OH)=1.74 Å. The interaction between $3p_z$-HOMO of central phosphorus and LUMO of the apical ligand becomes greater when the electronegative ligands participate in the interactions because of their low orbital energy LUMO. If the equatorial part is same, the molecule having fluorines as apical ligand is most stable and that having hydrogen atoms or methyl groups is less stable. The difference of the orbital energy level of the apical ligand is the origin of the apicophilicity.

4. Conclusions

The implications of this study can be summarized as follows;

1. By analyzing the energy relation between the stable isomer and the unstable one in the pseudorotation reaction, we found that the stabilization of the equatorial plane part of the penta-coordinated molecule determines the stability of the whole molecule. The groups forming the covalent bonds with P such as H, CH_3 and CH_2 prefer to coordinate in the equatorial position, i.e. ***equatoriphilicity*** . If the whole molecule was formed from completely separate atoms, the equatorial plane part would

be formed first by the groups which make covalent bonds with P and then the remained ligands would coordinate at the apical positions.

2. We drew orbital energy correlation diagrams for some molecules and considered the stability of apical bonds. The apical bond is three-center four-electron character. When the apical ligands are fixed, the special orbital is related with the stabilization of the molecule. We can discuss the strength or nature of the apical bond by using the special orbital.

3. The potential energy barrier of the pseudorotation for the model phosphate molecule is fairly low, and it is considered that the reaction proceeds easily in gas phase.

4. From the study of the substituent effect on the equatorial plane part, it is shown that the fluorine has a significant effect on the 3d AO of the central phosphorus.

5. The correlation effect is necessary but not essential in determining the potential barrier height. The MP2 level of energy correction seems to be adequate for some explanations of the nature of pseudorotation reactions.

Acknowledgments

The SCF and MP4 calculations were carried out using the Gaussian-80[42], Gaussian-82[43] and Gaussian-86[34] programs. The calculations were carried out on FACOM M782 and VP200 computers at Nagoya University Computational Center and on a HITAC S810 computer at Institute for Molecular Science. This study was supported in part by a Grant-in-Aid for Scientific Research from the Japanese Ministry of

Education, Science and Culture.

References

1. H. Dugas and C. Penney, Bioorganic Chemistry : A Chemical Approach to Enzyme Action, Chapter 3, Springer-Verlag, New York
2. F. H. Westheimer, Acc. Chim. Res., **1968** , *1*, 70
3. I. Ugi, F. Ramirez, D. Marquarding, H. Klusacek, G. Gokel and P. Gillespie, Angew. Chem., **1970** , *82*, 766
4. R. S. Berry, J. Chem. Phys., **1960** , *32*, 933
5. R. Hoffmann, J. M. Howell and E. L. Muetterties, J. Am. Chem. Soc., **1972** , *94*, 3047
6. J. B. Florey and L. C. Cusachs, J. Am. Chem. Soc., **1972** , *94*, 3040
7. A. Strich and A. Veillard, J. Am. Chem. Soc., **1973** , *95*, 5574
8. F. Keil and W. Kutzelnigg, J. Am. Chem. Soc., **1975** , *97*, 3623
9. R. R. Holmes, J. Am. Chem. Soc., **1978** , *100*, 433
10. W. Kutzelnigg and H. Wallmeier, Theoret. Chim. Acta **1979** , *51*, 261
11. G. Trinquier, J. -P. Daudey, G. Caruana and Y. Madaule, J. Am. Chem. Soc., **1984** , *106*, 4794
12. C. J. Marsden, J. Chem. Soc. Chem. Comm., **1984** , Number 7, 401
13. A. E. H. de Keijzer, L. H. Koole and H. M. Buck, J. Am. Chem. Soc., **1988** , *110*, 5995
14. J. A. Deiters, R. R. Holmes and J. M. Holmes, J. Am. Chem. Soc., **1988** , *110*, 7672
15. E. Anslyn and R. Breslow, J. Am. Chem. Soc., **1989** , *111*, 4473
16. L. S. Bartell and K. W. Hansen, Inorganic Chemistry, 1965, *4*, 1777

17. E. L. Muetterties, W. Mahler and R. Schmutzler,
Inorganic Chemistry, **1963** , *2*, 613
18. E. L. Muetterties, W. Mahler, K. J. Packer and R. Schmutzler,
Inorganic Chemistry, **1964** , *3*, 1298
19. R. Schmutzler and G. S. Reddy, Inorganic Chemistry, **1965** , 4, 191
20. R. Schmutzler, J. Am. Chem. Soc., **1964** , *86*, 4500
21. A. Rauk, L. C. Allen and K. Mislow, J. Am. Chem. Soc.,
1972 , *94*, 3035
22. W. Kutzelnigg and J. Wasilewski, J. Am. Chem. Soc., **1982** , *104*, 953
23. R. S. McDowell and A. Streitwieser Jr., J. Am. Chem. Soc.,
1985 , *107*, 5849
24. R. J. Gillespie, "Molecular Geometry", Van Nostrand-Rheinhold,
London, **1972**
25. R. E. Rundle, J. Am. Chem. Soc., **1963** , *85*, 112
26. R. E. Rundle, Progr. Chem., **1963** , *1*, 81
27. R. J. Hach and R. E. Rundle, J. Am. Chem. Soc., **1951** , *73*, 4321
28. R. Hoffmann, J. M. Howell and A. R. Rossi, J. Am. Chem. Soc.,
1976 , *98*, 2484
29. J. M. Howell, J. Am. Chem. Soc., **1977** , *99*, 7447
30. M. -B. Krogh-Jespersen, J. Chandrasekhar, E. U. Wurthwein,
J. B. Collins and P. V. R. Schleyer, J. Am. Chem. Soc.,
1980 , *102*, 2263
31. R. R. Holmes, J. Am. Chem. Soc., **1984** , *106*, 3745
32. R. R. Holmes, "Pentacoordinated Phosphorus", American Chemical
Society, Washington D. C., **1980** , vol.1 and 2, ACS Monographs
No. 175 and 176

33. T. H. Dunning Jr., J. Chem. Phys., **1970** , *53*, 2823

34. M J. Frisch, J. S. Binkley, H. B. Schlegel, K. Raghavachari, C. F. Melius, R. L. Martin, J. J. P. Stewart, F. W. Bobrowicz, C. M. Rohlfing, L. R. Kahn, D. J. Defrees, R. Seeger, R. A. Whiteside, F. J. Fox, E. M. Fluder, S. Topiol and J. A. Pople, "Gaussian-86", Carnegie-Mellon Quantum Chemistry Publishing Unit, Carnegie-Mellon University, Pittsburgh PA 15213

35. T. H. Dunning Jr. and P. J. Hay, "Modern Theoretical Chemistry", p. 1, vol. 3, edited by H. F. Schaefer III, Plenum Press, New York, **1977**

36. R. F. W. Bader, Can. J. Chem., **1962** , *40*, 1164

37. R. G. Pearson, J. Am. Chem. Soc., **1969** , *91*, 1252

38. R. G. Pearson, J. Am. Chem. Soc., **1969** , *91*, 4947

39. R. G. Pearson, J. Chem. Phys., **1970** , *52*, 2167

40. C. J. Ballhausen, J. Chem. Phys., **1970** , *53*, 2986

41. R. G. Pearson, J. Am. Chem. Soc., **1972** , *94*, 8287

42. J. A. Pople et al., QCPE #406 and #437

43. J. S. Binkley, M. J. Frisch, D. J. Defrees, K. Raghavachari, R. A. Whiteside, H. B. Schlegel and J. A. Pople, **1984** , "Gaussian-82", Carnegie-Mellon Chemistry Publishing Unit, Pittsburgh.

44. E. Magnusson, J. Comput. Chem., **1984** , *5*, 612

45. P. V. R. Schleyer, Pure Appl. Chem., **1987** , **59**, 1647

46. P. Lemmen, R. Baumgartner, I. Ugi and F. Ramirez, Chem. Scr., **1988** , *28*, 451

47. T. P. E. Auf der Heyde and H. -B. Bürgi, Inorganic Chemistry,

1989 , *28*, 3982

48. W. Kutzelnigg and J. Wasilewski, J. Am. Chem. Soc., **1982** , *104*, 953
49. J. A. Altmann, K. Yates and I. G. Csizmadia, J. Am. Chem. Soc., **1976** , *98*, 1450
50. M. S. Gordon, T. L. Windus, L. W. Burggraf and L. P. Davis, J. Am. Chem. Soc., **1990** , *112*, 7167
51. V. I. Minkin, B. Ya. Simkin and R. M. Minyaev, "Quantum Chemistry of Organic Compounds", Springer-Verlag, New York, 1990
52. P. W. Atkins, "Physical Chemistry ", third edition, Oxford University Press, Oxford, 1987
53. C. S. Ewig and J. R. Van Wazer, J. Amer. Chem. Soc., **1989** , *111*, 4172

Table I The calculated energies in some levels

PH_5 TZP Basis Set

Methods	Ground State (a.u.)	Transition State (a.u.)	Relative energy (kcal/mol)
SCF	-343.528616	-343.524348	2.68
MP2	-343.693636	-343.690815	1.77
MP3	-343.720720	-343.718088	1.65
MP4(DQ)	-343.724957	-343.722374	1.62
MP4(SDQ)	-343.725823	-343.723284	1.59
MP4(SDTQ)	-343.728719	-343.726277	1.53
SDCI	-343.715483	-343.712706	1.74
SDCI(Davidson's correction)	-343.728684	-343.726360	1.46
Coupled Cluster	-343.725743	-343.723208	1.59

PF_5 DZP Basis Set

Methods	Ground State (a.u.)	Transition State (a.u.)	Relative energy (kcal/mol)
SCF	-838.184055	-838.175975	5.07
MP2	-839.145335	-839.138455	4.32
MP3	-839.134876	-839.127467	4.65
MP4(DQ)	-839.141543	-839.134182	4.62
MP4(SDQ)	-839.157117	-839.150024	4.45
MP4(SDTQ)	-839.183257	-839.176493	4.24
SDCI	-838.999488	-838.991797	4.83
SDCI(Davidson's correction)	-839.149570	-839.142333	4.54

PF_4H DZP Basis Set

Methods	Ground State (a.u.)	Transition State (a.u.)	Relative energy (kcal/mol)
SCF	-739.339311	-739.251810	7.38
MP2	-740.066801	-740.057365	5.92
MP3	-740.062518	-740.052423	6.33
MP4(DQ)	-740.069250	-740.059178	6.32
MP4(SDQ)	-740.082283	-740.072611	6.07
MP4(SDTQ)	-740.103597	-740.094516	5.70
SDCI	-739.962596	-739.952088	6.59
SDCI(Davidson's correction)	-740.076286	-740.066540	6.12

PF_3H_2 DZP Basis Set
Calculated energies (a.u.)

Methods	Isomer A	Transition State	Isomer B
SCF	-640.339311	-640.319940	-640.320136
MP2	-640.983482	-640.966482	-640.965907
MP3	-640.986074	-640.968355	-640.967983
MP4(DQ)	-640.992684	-640.974932	-640.974537
MP4(SDQ)	-641.002782	-640.985444	-640.984945
MP4(SDTQ)	-641.019130	-641.002503	-641.001888
SDCI	-640.917403	-640.899434	-640.899221
SDCI(Davidson's correction)	-640.998586	-640.981249	-640.980803

Relative energies to Isomer A (kcal/mol)

Methods	Transition State	Isomer B
SCF	12.16	12.03
MP2	10.67	11.03
MP3	11.12	11.35
MP4(DQ)	11.14	11.39
MP4(SDQ)	10.88	11.19
MP4(SDTQ)	10.43	10.82
SDCI	11.28	11.41
SDCI(Davidson's correction)	10.88	11.16

PF_4CH_3 DZP Basis Set
Calculated energies (a.u.)

Methods	Ground State (a.u.)	Transition State (a.u.)	Relative energy (kcal/mol)
SCF	-778.317482	-778.309098	5.26
MP2	-779.243283	-779.236814	4.06
MP3	-779.249062	-779.241875	4.51
MP4(DQ)	-779.256377	-779.249252	4.47
MP4(SDQ)	-779.270468	-779.263708	4.24
MP4(SDTQ)	-779.295633	-779.289336	3.95

$PF_3C_2H_6$ DZP Basis Set
Calculated energies (a.u.)

Methods	Ground State (a.u.)	122.5 degree (a.u.)	Relative energy (kcal/mol)
SCF	-718.444972	-718.420999	15.04
MP2	-719.335317	-719.313707	13.56
MP3	-719.357558	-719.334828	14.26
MP4(DQ)	-719.365328	-719.342659	14.23
MP4(SDQ)	-719.377661	-719.355332	14.01

$PO_5H_4^-$ DZP+diffuse(on phosphonyl O) Basis Set
The calculated energies (a.u.)

Methods	A	TS1	B	TS2
SCF	-717.543764	-717.540558	-717.562121	-717.551127
MP2	-718.577403	-718.574347	-718.592420	-718.582677
MP3	-718.576367	-718.573054	-718.592565	-718.582292
MP4(DQ)	-718.584464	-718.581140	-718.600412	-718.590297
MP4(SDQ)	-718.596275	-718.592979	-718.611530	-718.601662

Relative energies to Isomer B State (kcal/mol)

Methods	A	TS1	TS2
SCF	11.52	13.53	6.90
MP2	9.42	11.34	6.11
MP3	10.16	12.24	6.36
MP4(DQ)	10.01	12.09	6.35
MP4(SDQ)	9.57	11.64	6.19

$P(O_2C_2H_4)H_3$ DZP Basis Set
Calculated energies (a.u.)

Methods	Ground State (a.u.)	Transition State (a.u.)	Relative energy (kcal/mol)
SCF	-570.259906	-570.256207	2.32
MP2	-571.006186	-571.003244	1.85
MP3	-571.036013	-571.033022	1.88
MP4(DQ)	-571.043240	-571.040223	1.89
MP4(SDQ)	-571.051341	-571.048432	1.83

$P(OC_3H_6)H_3$ DZP Basis Set
Calculated energies (a.u.)

Methods	Ground State (a.u.)	120.0 degree (a.u.)	Relative energy (kcal/mol)
SCF	-534.399504	-534.384867	9.18
MP2	-535.103777	-535.091700	7.58
MP3	-535.146680	-535.133687	8.15
MP4(DQ)	-535.153406	-535.140562	8.06
MP4(SDQ)	-535.159715	-535.147335	7.77

Table II The potential energy change with SCF calculations for PF_3H_2, $PF_3C_2H_6$ and $P(OC_3H_6)H_3$

1. PF_3H_2 Potential Energy Change with SCF

degree	Total Energy (a.u.)	Relative Energy (a.u.)	Relative Energy (kcal/mol)
178.8 (Minimum 1)	-640.339311	0.000000	0.00
160.0	-640.327938	0.011373	7.14
145.0	-640.320708	0.018603	11.67
136.0 (TS)	-640.319940	0.019371	12.16
130.0	-640.320064	0.019247	12.08
125.8 (Minimum 2)	-640.320136	0.019175	12.03
120.0	-640.319871	0.019440	12.20

2. $PF_3C_2H_6$ Potential Energy Change with SCF

degree	Total Energy (a.u.)	Relative Energy (a.u.)	Relative Energy (kcal/mol)
175.3 (Minimum)	-718.444974	0.000000	0.00
155.0	-718.430836	0.014138	8.87
135.0	-718.422170	0.022804	14.31
130.0	-718.421659	0.023315	14.63
125.0	-718.421252	0.023722	14.89
122.5	-718.421002	0.023972	15.04

3. $P(OC_3H_6)H_3$ Potential Energy Change with SCF

degree	Total Energy (a.u.)	Relative Energy (a.u.)	Relative Energy (kcal/mol)
177.8 (Minimum)	-534.399504	0.000000	0.00
150.0	-534.388692	0.010812	6.78
140.0	-534.386962	0.012542	7.87
130.0	-534.385960	0.013544	8.50
120.0	-534.384867	0.014637	9.18

Table III-(a) The change of the bond length of PH_5 (Å)

	before reaction	transition state	after reaction
pivotal length	1.415 (100)	1.394 (98.5)	1.415 (100)
equatorial length	1.415 (100)	1.451 (102.5)	1.477 (104.4)

Table III-(b) The change of the bond length of PF_5 (Å)

	before reaction	transition state	after reaction
pivotal length	1.537 (100)	1.524 (99.2)	1.537 (100)
equatorial length	1.537 (100)	1.562 (101.6)	1.577 (102.6)

TableIV

(1) The total energy change of PF_3H_2 (hartree)

	separated ligand	equatorial plane formation (PH_2F[(b)] and PF_2H[(c)])	whole molecule formation
A. E(stable)	-639.877916	-640.003001	-640.320136
B. E(unstable)	-639.877916	-640.053428	-640.339311
E(A)-E(B) [(a)]	0.000000 (0.00)	0.050427 (31.64)	0.019175 (12.03)

(2) The total energy change of $PF_3(CH_3)_2$ (hartree)

	separated ligand	equatorial plane formation ($P(CH_3)_2F$[(d)] and PF_2CH_3[(e)])	whole molecule formation
A. E(stable)	-717.992666	-718.110894	-718.420999
B. E(unstable)	-717.992666	-718.131585	-718.444972
E(A)-E(B) [(a)]	0.000000 (0.00)	0.020691 (12.98)	0.023973 (15.04)

(a) The values in the parenthesis are shown in kcal/mol.
(b) equatorial plane part of the stable isomer of PF_3H_2
(c) equatorial plane part of the unstable isomer of PF_3H_2
(d) equatorial plane part of the stable isomer of $PF_3(CH_3)_2$
(e) equatorial plane part of the unstable isomer of $PF_3(CH_3)_2$

Table V. The relationship between the possibility of the pseudorotation and the number of the equatoriphilic groups

(a) acyclic molecule

Number of the equatoriphilic groups	Pseudorotation	Some examples (acyclic molecule)
0	Yes	PF_5
1	Yes	PF_4CH_3, PF_4H
2	No	$PF_3(CH_3)_2$, PF_3H_2
3	No	$PF_2(CH_3)_3$
4	No	$PF(CH_3)_4$
5	Yes	PH_5, $P(CH_3)_5$

(b) cyclic molecule

Number of the equatoriphilic groups	Pseudorotation	Some examples (cyclic molecule)
0	Yes	$P(O_2C_2H_2)H_3$
1	No	$P(OC_3H_6)H_3$
2	Yes	$P(C_4H_8)H_3$

Figure Captions

Figure 1 (a) : The schematic structure of D_{3h} trigonal bipyramid. (b) : The schematic explanation for Berry's pseudorotation reaction.

Figure 2 The experimental results of some pseudorotation reactions.

Figure 3 The optimized structure of PH_5. (a) : The ground state structure. (b) : The transition state structure of the pseudorotation reaction. The bond length is shown in Å and the angle is shown in degrees.

Figure 4 The energy diagram for the pseudorotation reaction of PH_5. **TS** means the transition state with C_{4v} symmetry. The energies are relative to that of **A** in kcal/mol. The SCF energy of the ground state **A** is -343.528616 hartree.

Figure 5 (a) : The contour map of the highest occupied molecular orbital of PH_5. (b) : The calculated transition density from HOMO to LUMO of PH_5 molecule along the apical axis. (c) : The transition density in the equatorial plane. The expected intramolecular movements of atoms are shown by arrows.

Figure 6 The vibrational modes of PH_5 molecule. (a) and (b) are e' modes of the ground state and (c) is the transition vector.

Figure 7 The optimized structures of PF_5 molecule. (a) is the ground state structure, and (b) is the transition state structure. The values in the parenthesis are experimental values.[16] The bond length is shown in Å and the angle is shown in degrees.

Figure 8 The energy diagram for the pseudorotation reaction of PF_5. The SCF energy of the ground state **A** is -838.184055 hartree.

Figure 9 The vibrational modes of PF_5 molecule. (a) is e' modes of the ground state and (c) is the transition vector.

Figure 10 (a) : The energy diagram for the pseudorotation reaction of PF_4H. The SCF energy of the ground state A is -739.339311 hartree. (b) : The potential energy curve of PF_3H_2 for the pseudorotation reaction. One fluorine atom occupies an equatorial position in the ground state and

two fluorine atoms occupy equatorial positions in the pseudorotated isomer. The SCF energy of the ground state is -640.339311 hartree.

Figure 11 (a) : The energy diagram for the pseudorotation reaction of PF_4CH_3. The SCF energy of the ground state **A** is -778.317482 hartree. (b) : The potential energy curve of $PF_3(CH_3)_2$ for the pseudorotation reaction. The SCF energy of the ground state is -718.444972 hartree.

Figure 12 (a) : The energy diagram of the pseudorotation reaction of $P(O_2C_2H_4)H_3$ model molecule. The SCF energy of the ground state **A** is -570.259906 hartree. (b) : The potential energy curve of $P(OC_3H_6)H_3$ molecule for the pseudorotation reaction. The SCF energy of the ground state is -534.399504 hartree.

Figure 13 The structures of the stable (A) and unstable (B) isomers of PF_3H_2 and $PF_3(CH_3)_2$.

Figure 14 The energy diagram of the pseudorotation reaction of $PO_5H_4^-$. The phosphoryl oxygen occupies the apical position in the isomer **A** and it is contained in the equatorial plane in the isomer **B**. The SCF energy of the isomer B is -717.562121 hartree.

Figure 15 (a) : The explanation of the method of division of a whole molecule into an apical part and an equatorial plane. (b) : The schematic explanation of the orbital interaction of D_{3h} trigonal bipyramidal molecule.

Figure 16 The stabilization energy of the whole molecule (full line), antisymmetric (dotted line) and symmetric (broken line) orbitals. The symbols in the parenthesis mean the equatorial plane part of the penta-coordinated molecule.

Figure 17 (a) : The orbital energy correlation diagram of PH_5. (b) : The orbital energy correlation diagram of PH_3F_2. (c) : The orbital energy correlation diagram of PF_5. The **S** and **A** mean the symmetric and antisymmetric orbitals about the equatorial plane.

Figure 18 The substituent effect on HOMO and LUMO of the equatorial part. The orbital energy is shown in atomic unit.

Figure 19 The orbital energy variations of some apical ligands part. The orbital energy is shown in atomic unit.

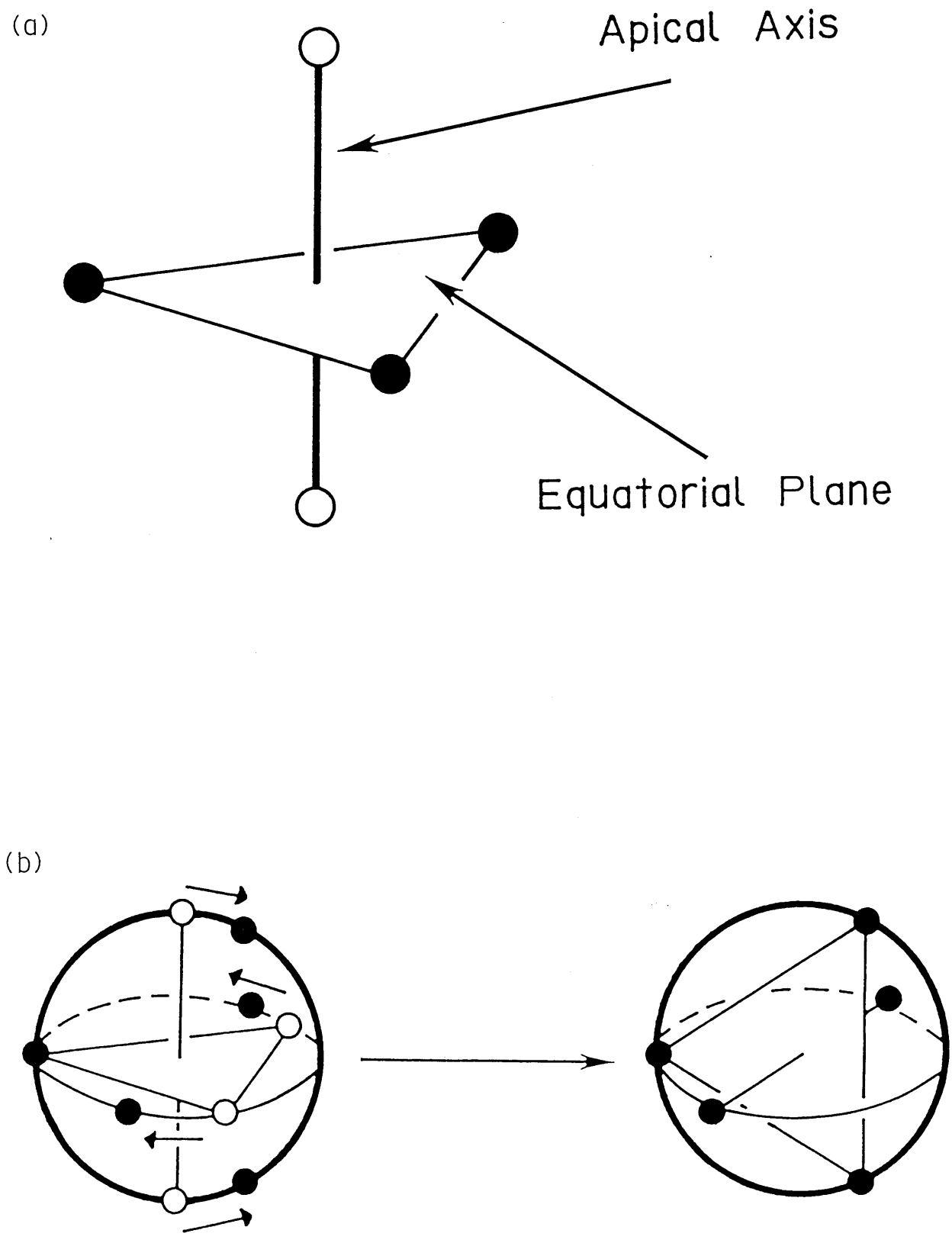

 Figure 1

(a)
F
F
F
CH3
F
F
F
CH3
F
(b)
F
CH3
CH3
F
CH3
CH3
F
F
(c)
CH2
O
CH2
CH3O
H
O
O
OH2
CH2
O
CH2
CH3O
H
O
O
OH2
(d)
CH3O
O
O
CH2
CH2
CH2
OH2
CH2
O
CH2
CH3O
CH2
O
OH2
CH2
O
CH2
CH2
CH3O
O
OH2

Figure 2

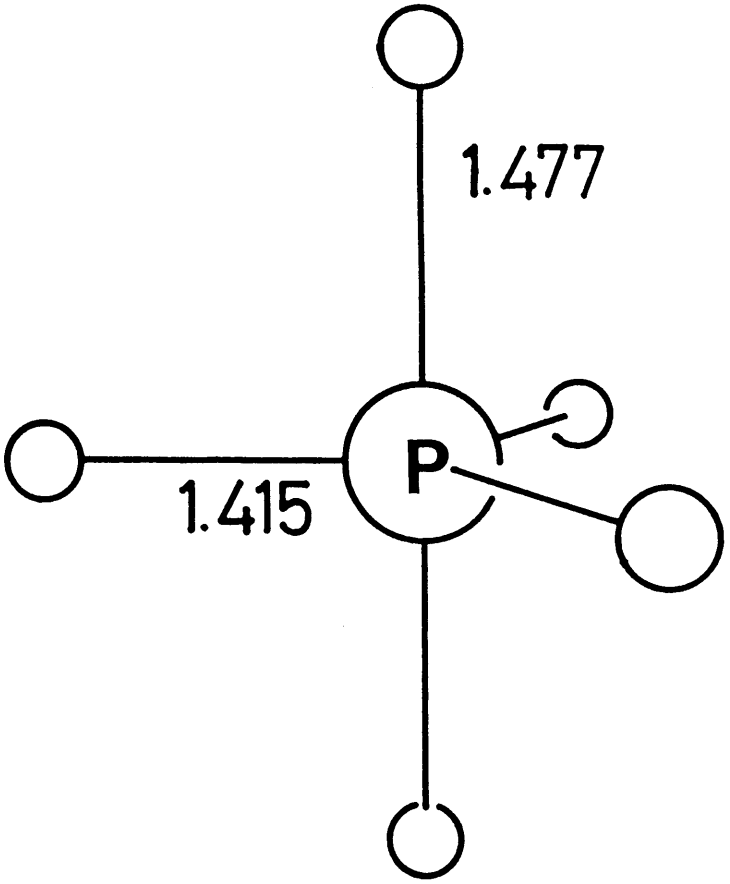

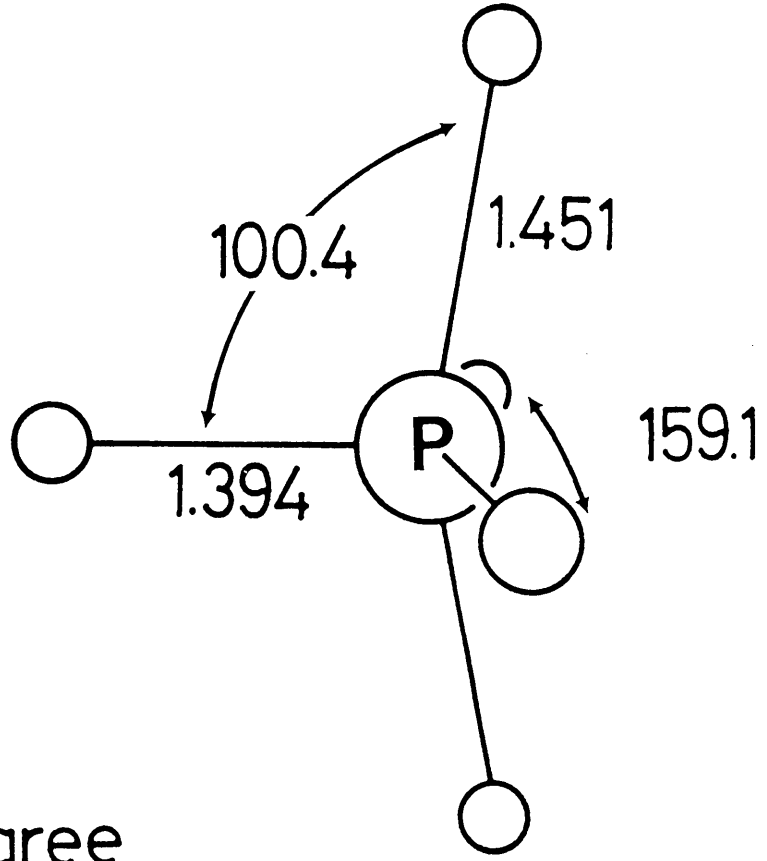

Å and degree

(a) D_{3h} GROUND STATE

(b) C_{4v} TRANSITION STATE

Figure 3

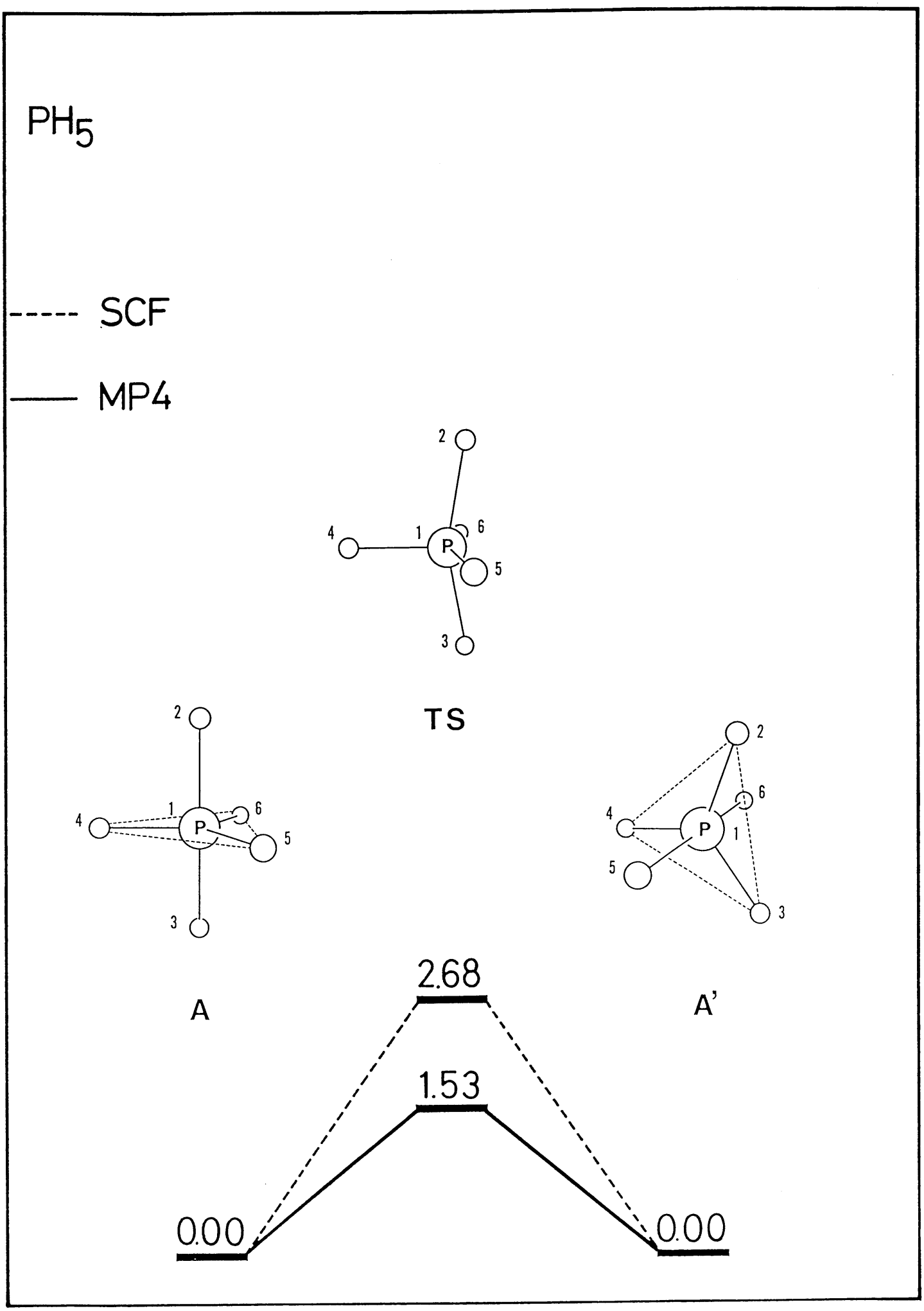

40 Figure 4

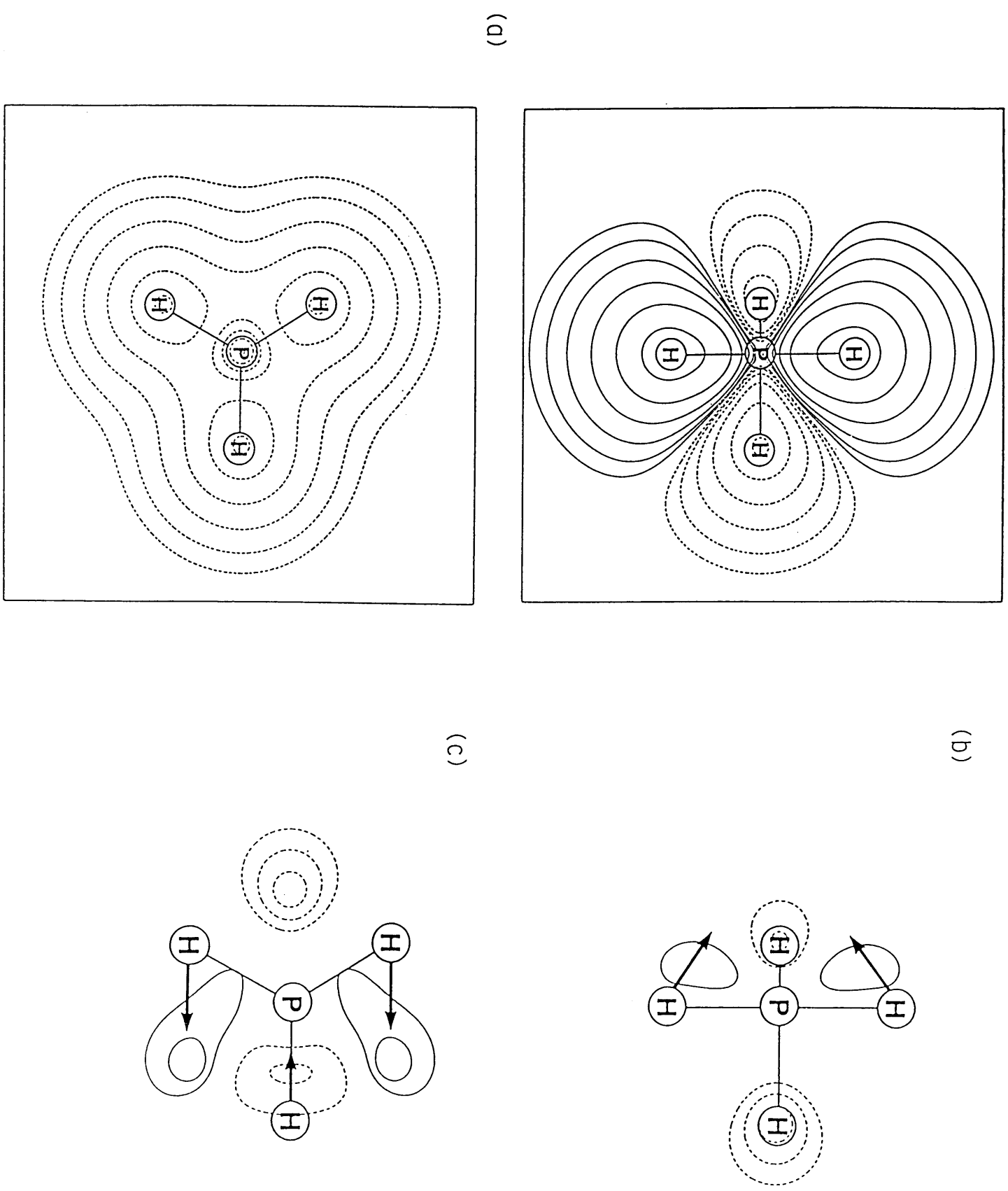

 Figure 5

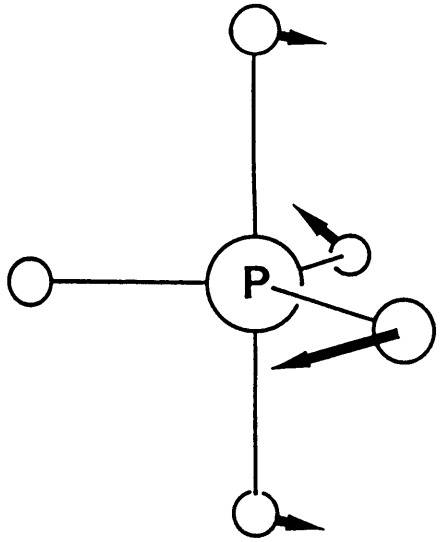

629.0 cm^{-1}

(a)

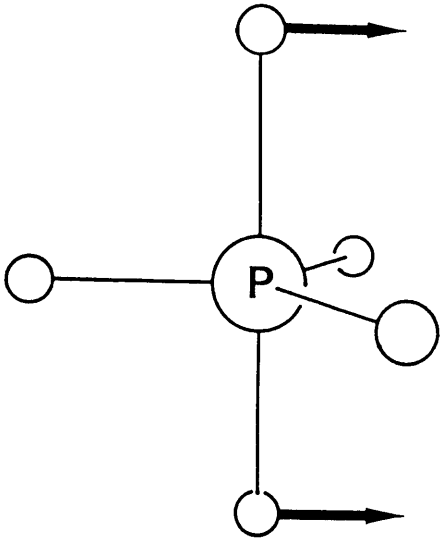

1373.8 cm^{-1}

(b)

D_{3h} GROUND STATE

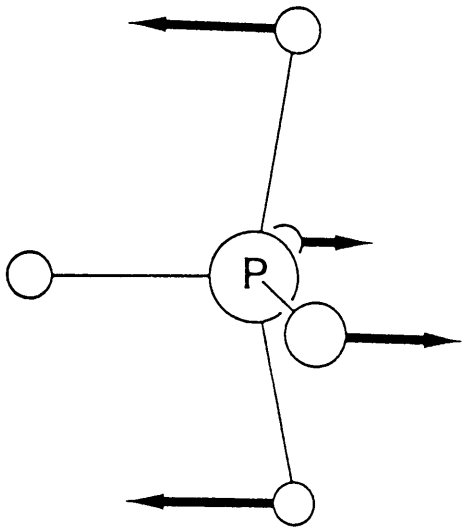

429.9 *i* cm^{-1}

Transition Vector

(c)

C_{4V} TRANSITION STATE

Figure 6

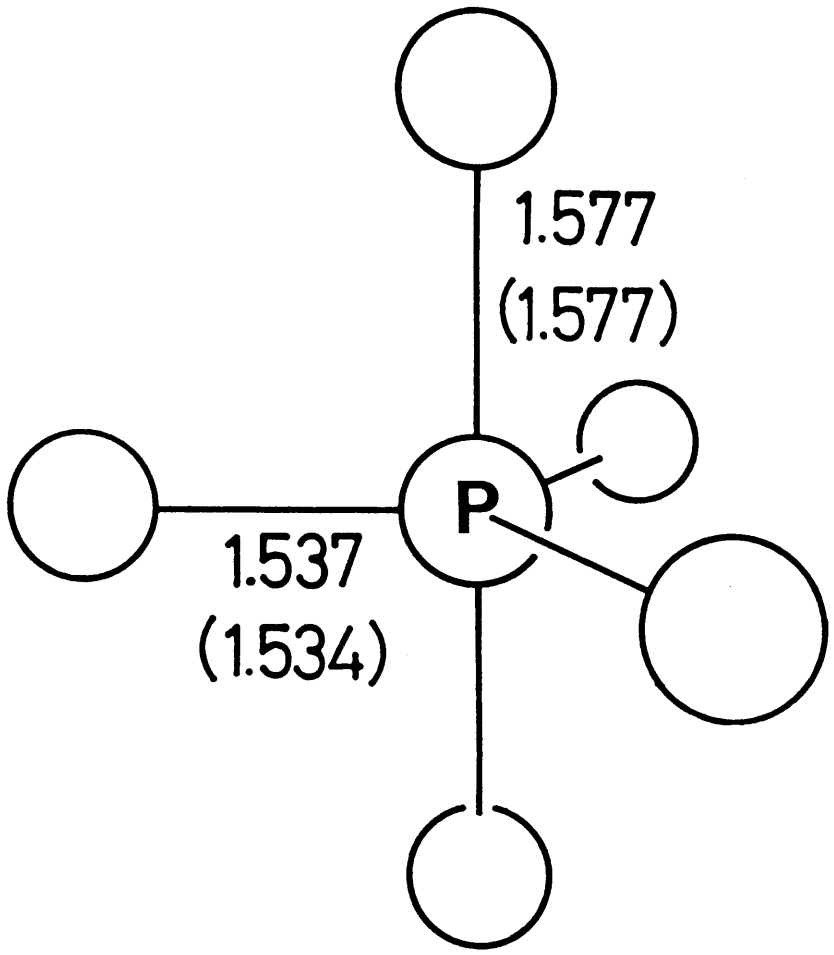

(a) D_{3h} GROUND STATE

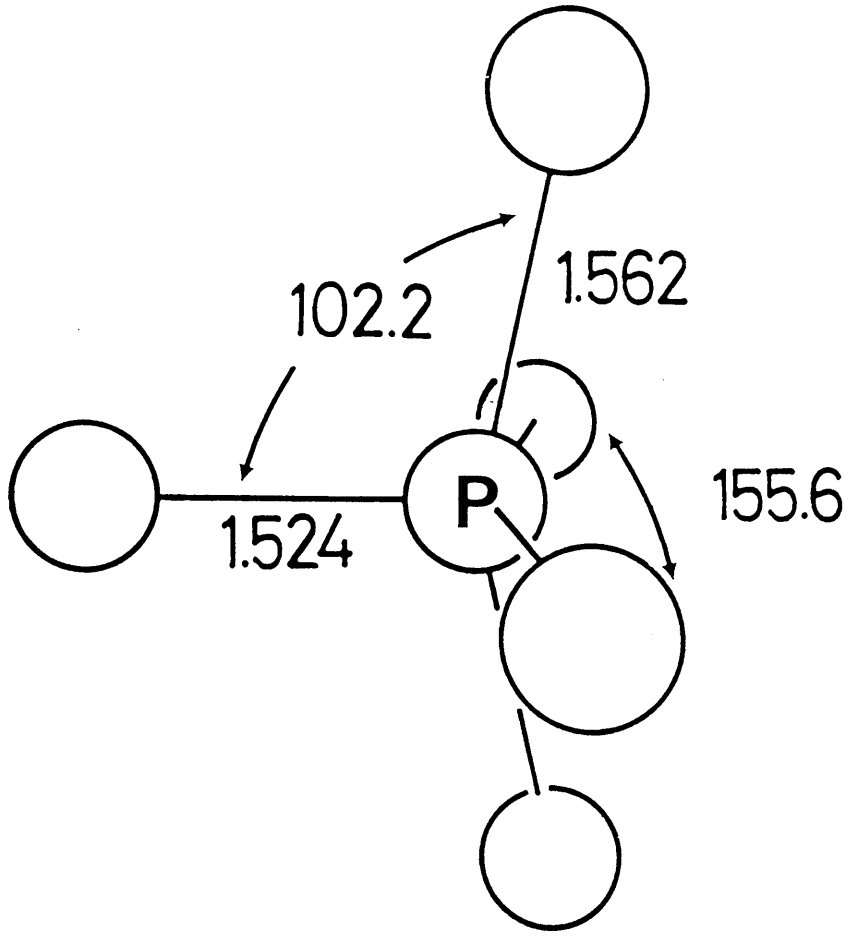

(b) C_{4v} TRANSITION STATE

43 Figure 7

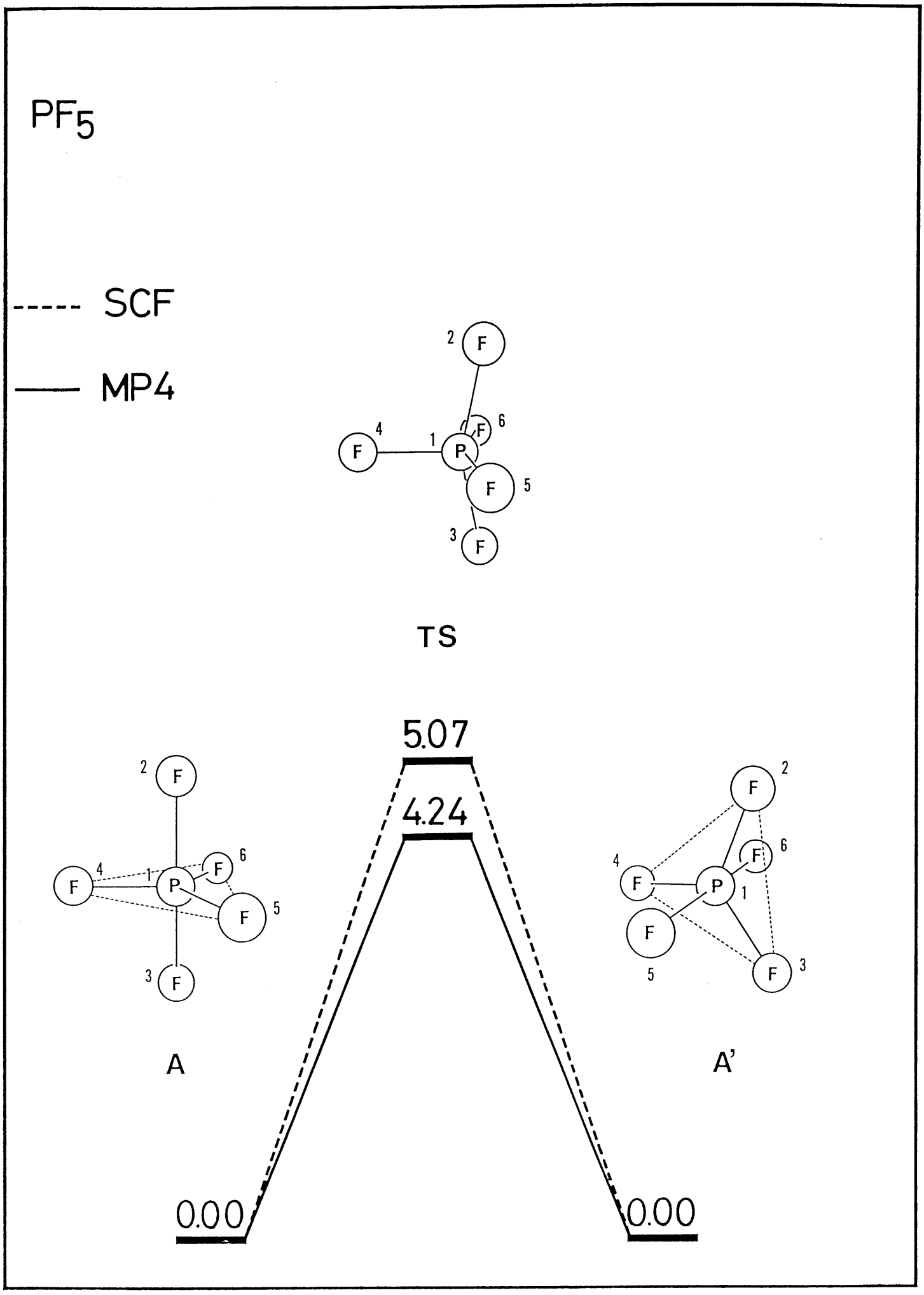

44 Figure 8

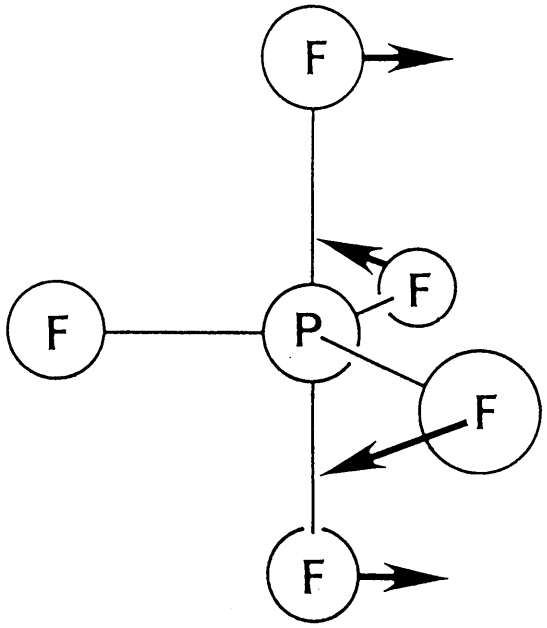

185.3 cm^{-1}

(a) D_{3h} Ground State

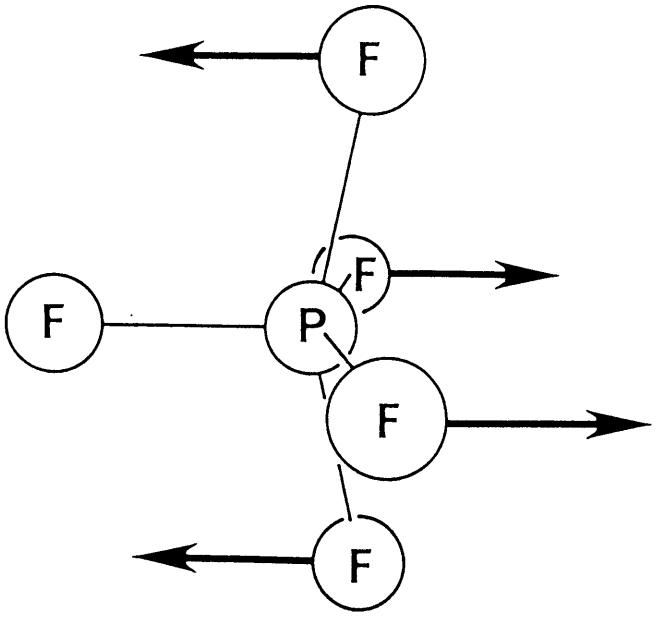

137.9 *i* cm^{-1}

Transition Vector

(b) C_{4v} Transition State

45 Figure 9

(a)

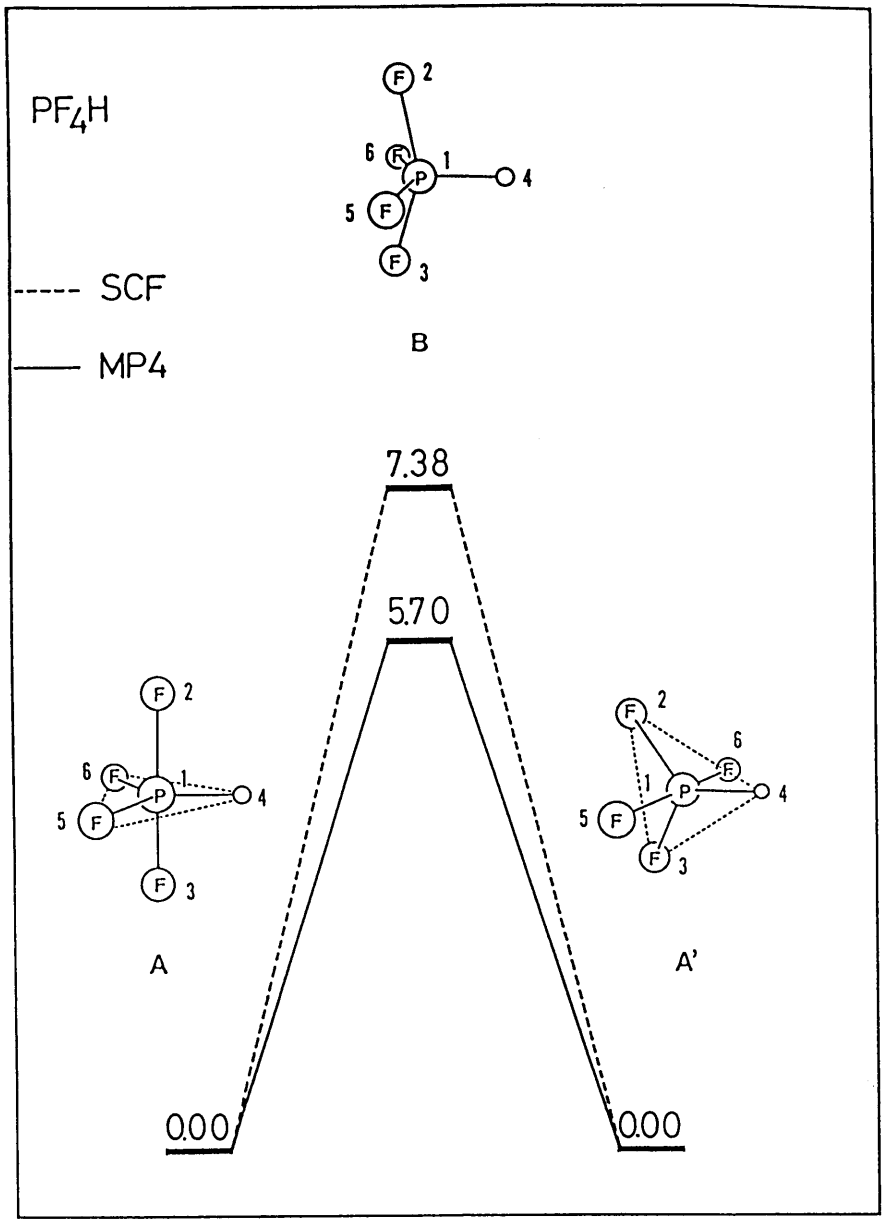
PF4H
SCF
MP4
B
7.38
5.70
A
A'
0.00
0.00

(b)

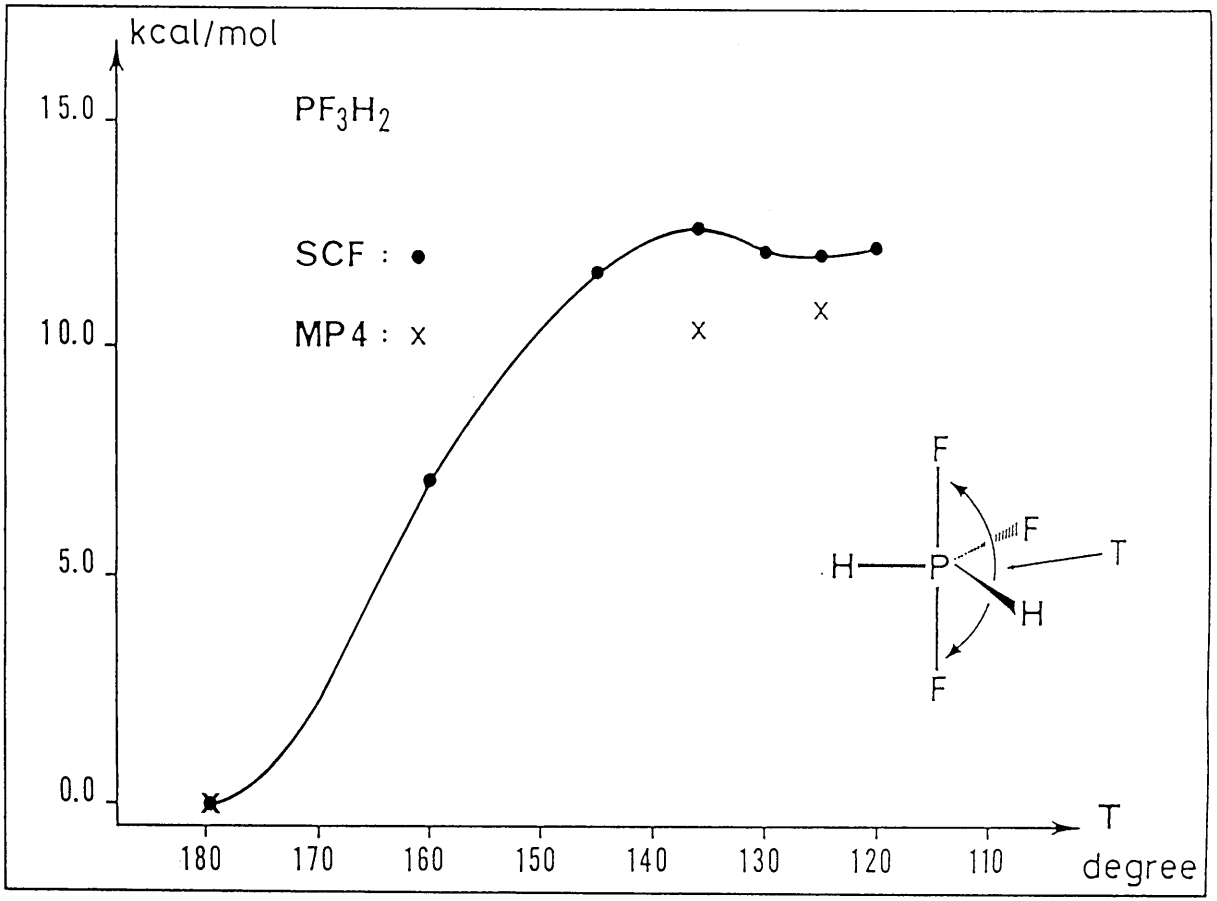
kcal/mol
PF3H2
SCF : •
MP4 : x
15.0
10.0
5.0
0.0
180
170
160
150
140
130
120
110
T
degree

Figure 10

(a)

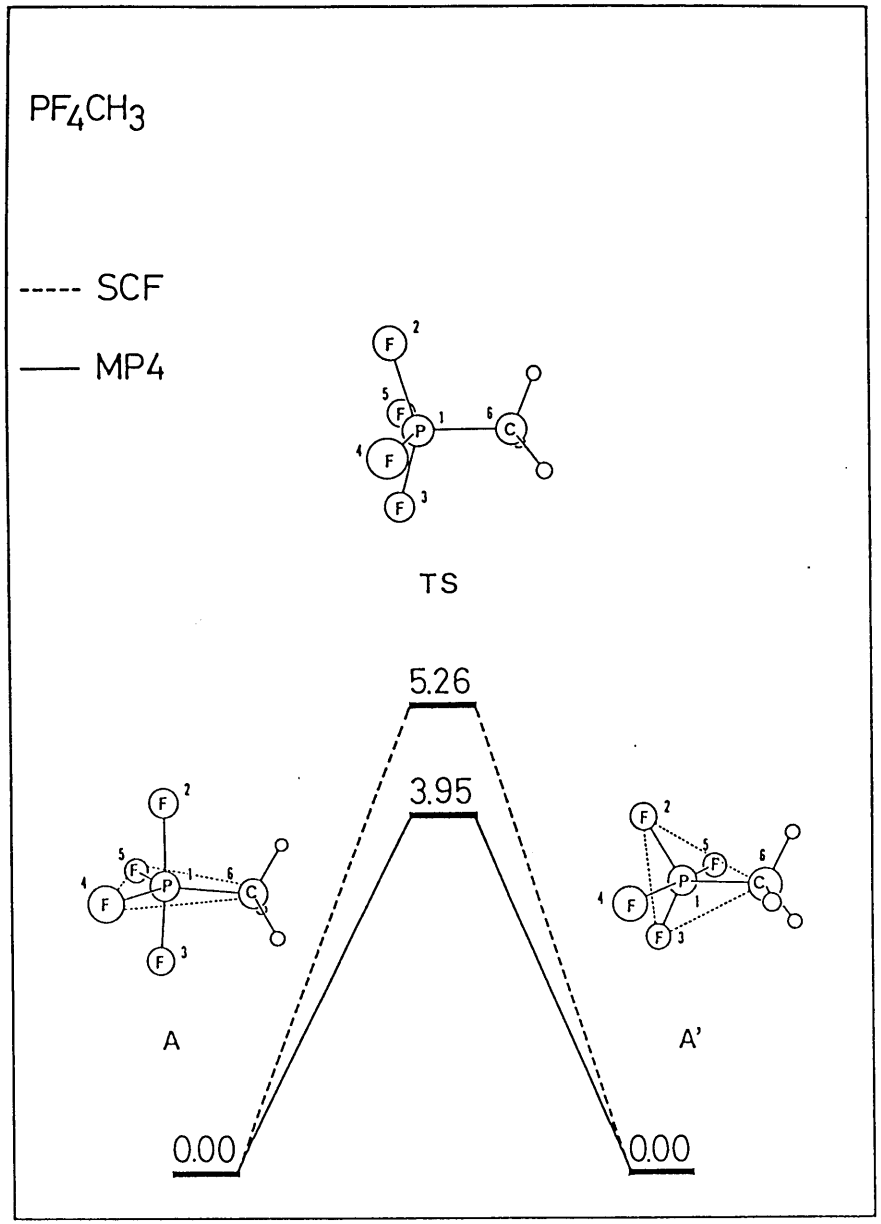
PF4CH3
----- SCF
—— MP4
TS
5.26
3.95
A
A'
0.00
0.00

(b)

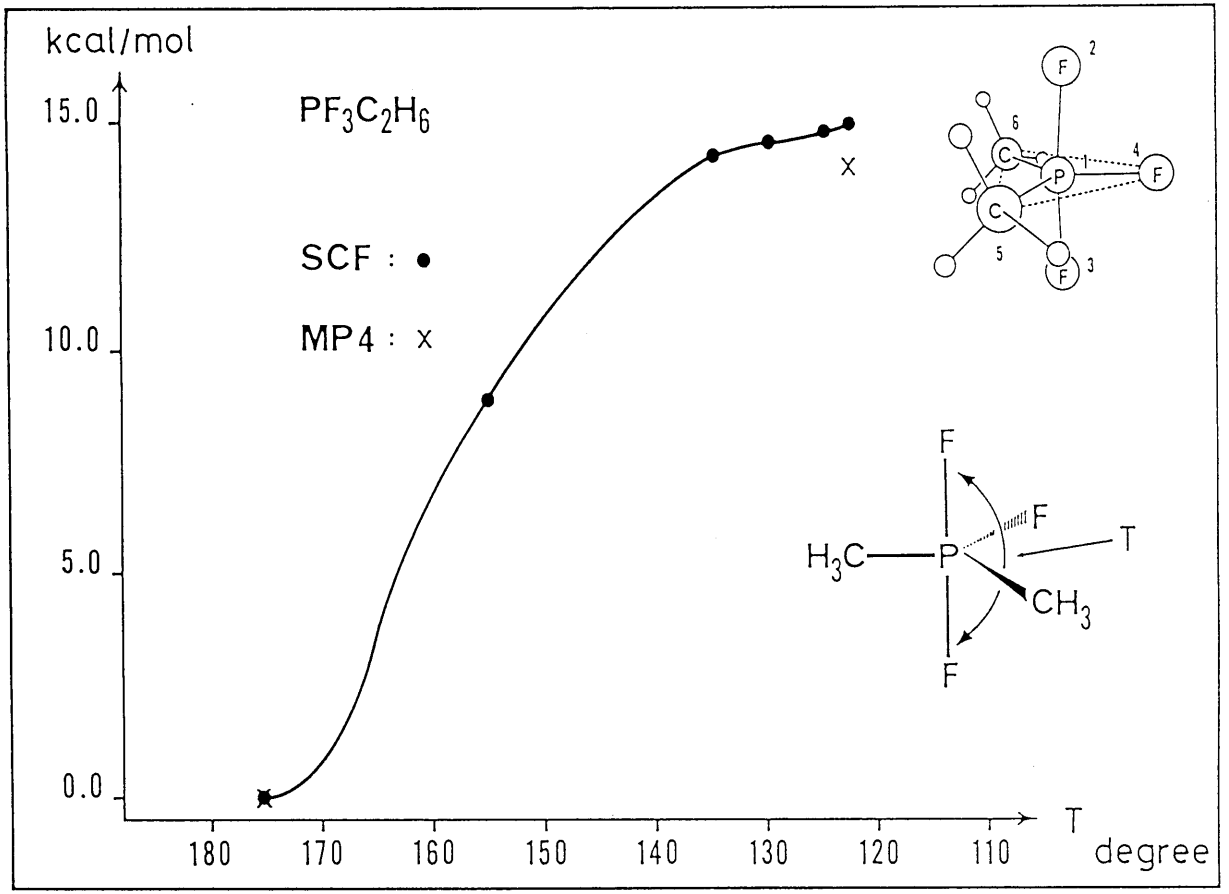
kcal/mol
15.0
10.0
5.0
0.0
PF3C2H6
SCF : •
MP4 : x
x
T
180
170
160
150
140
130
120
110
degree
H3C
CH3

Figure 11

(a)

$P(O_2C_2H_4)H_3$

----- SCF

—— MP4

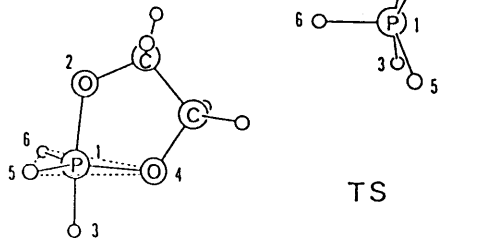

A

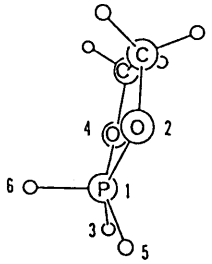

TS

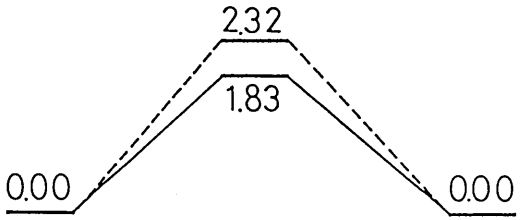

(b)

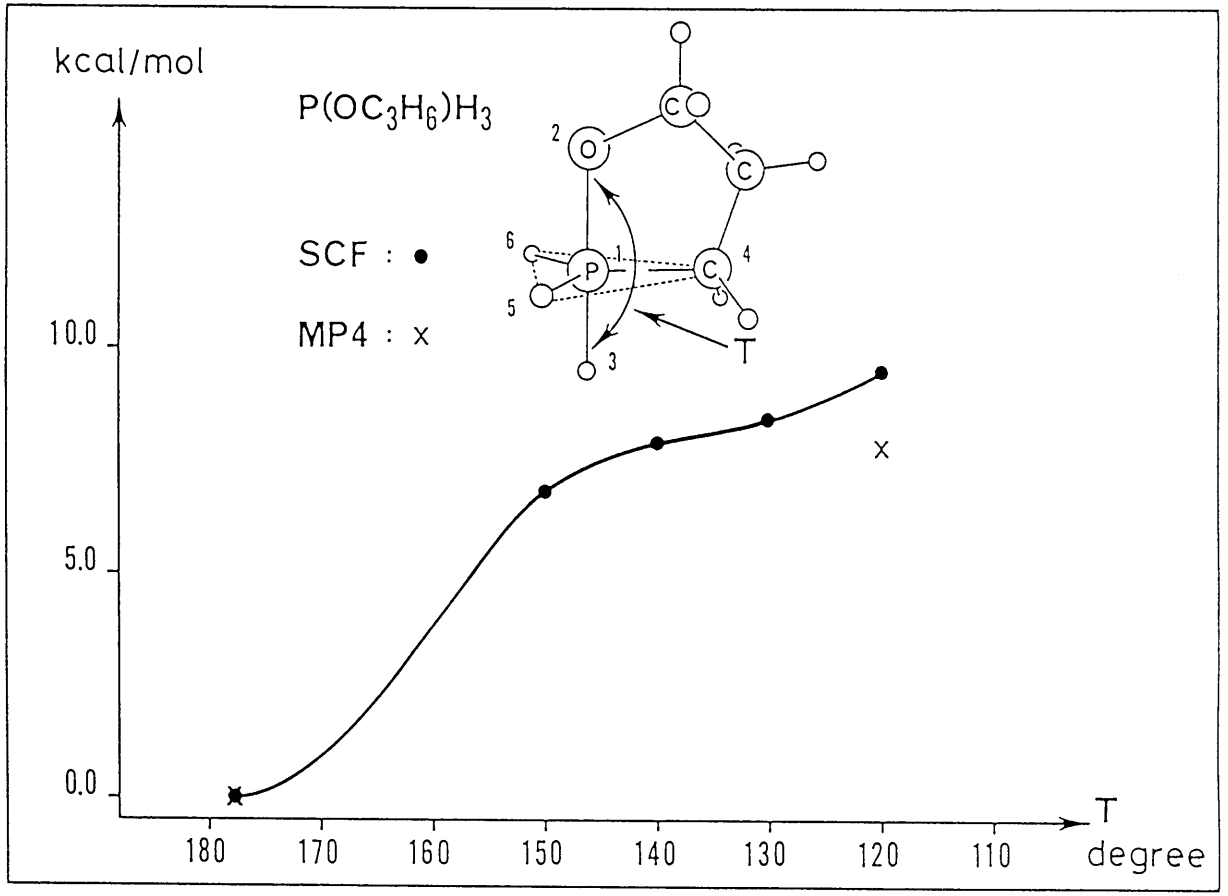

Figure 12

A. Stable isomer

B. Unstable isomer

PF_3H_2

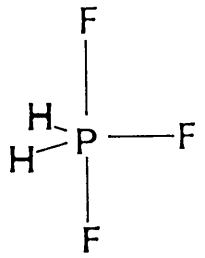

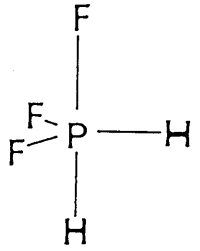

$PF_3(CH_3)_2$

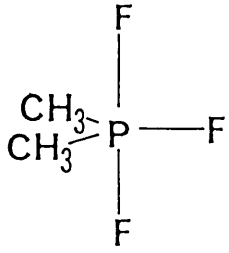

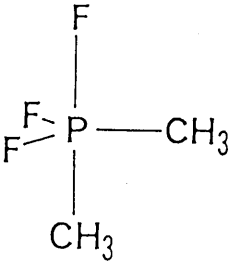

Figure 13

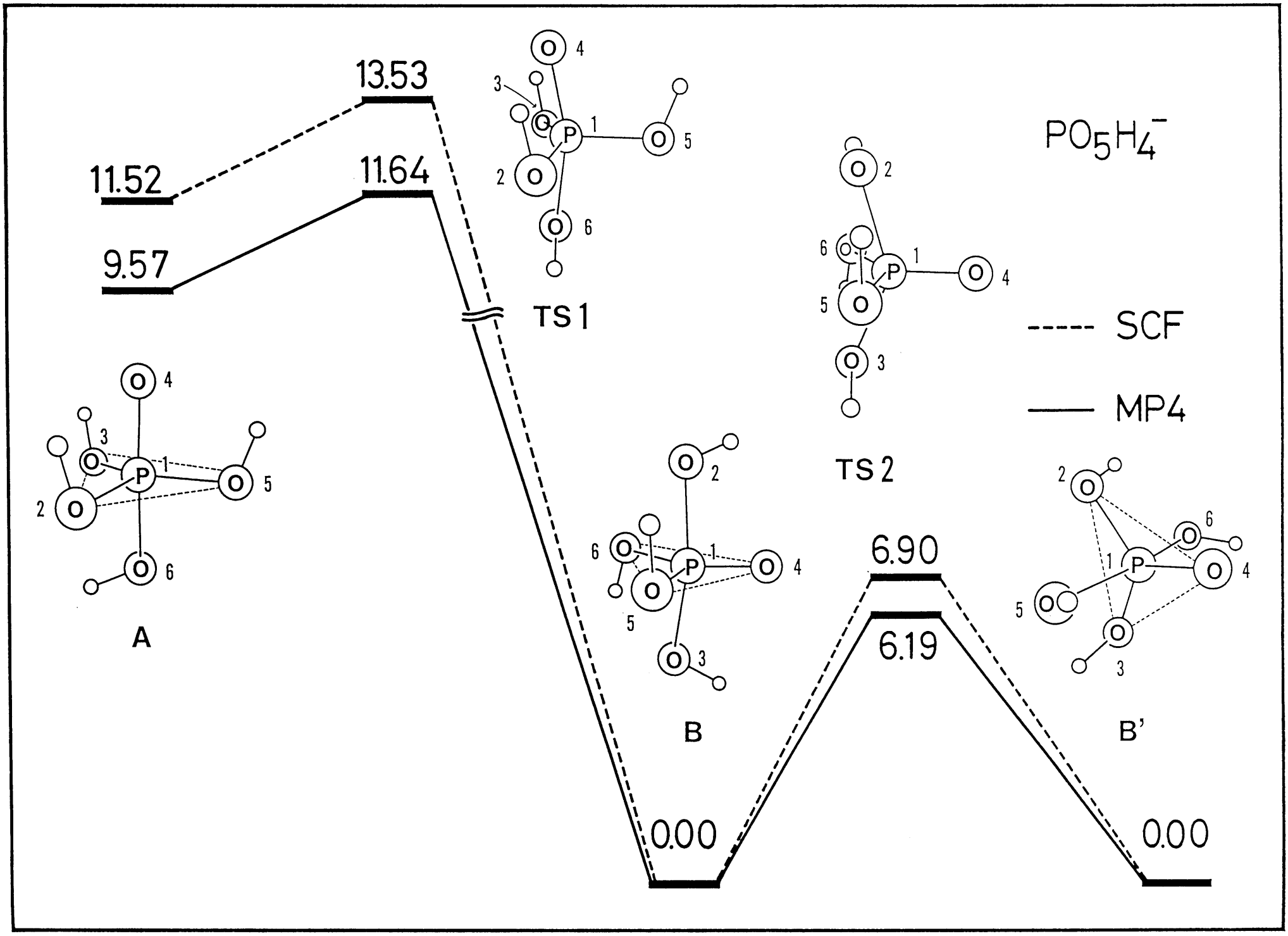

Figure 14

(a)

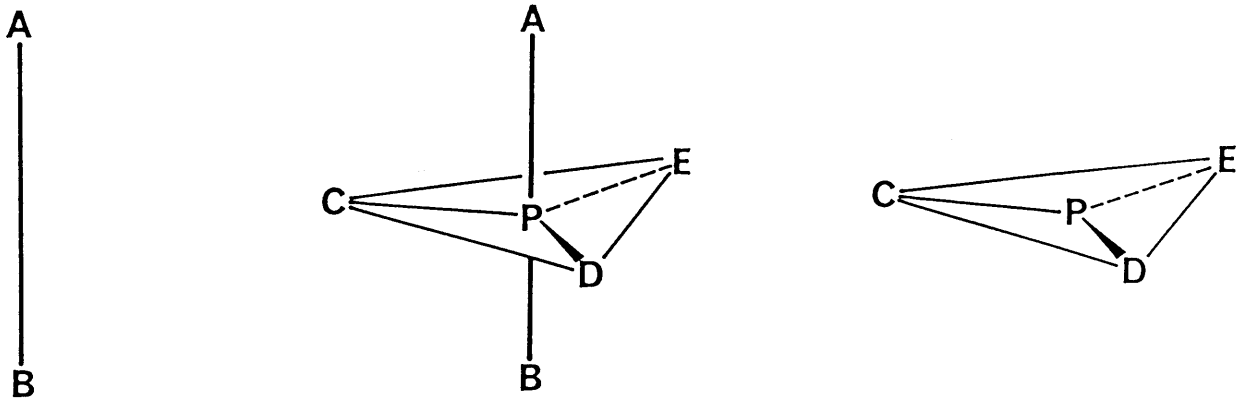

Apical ligand part Whole molecule Equatorial plane part

(b)

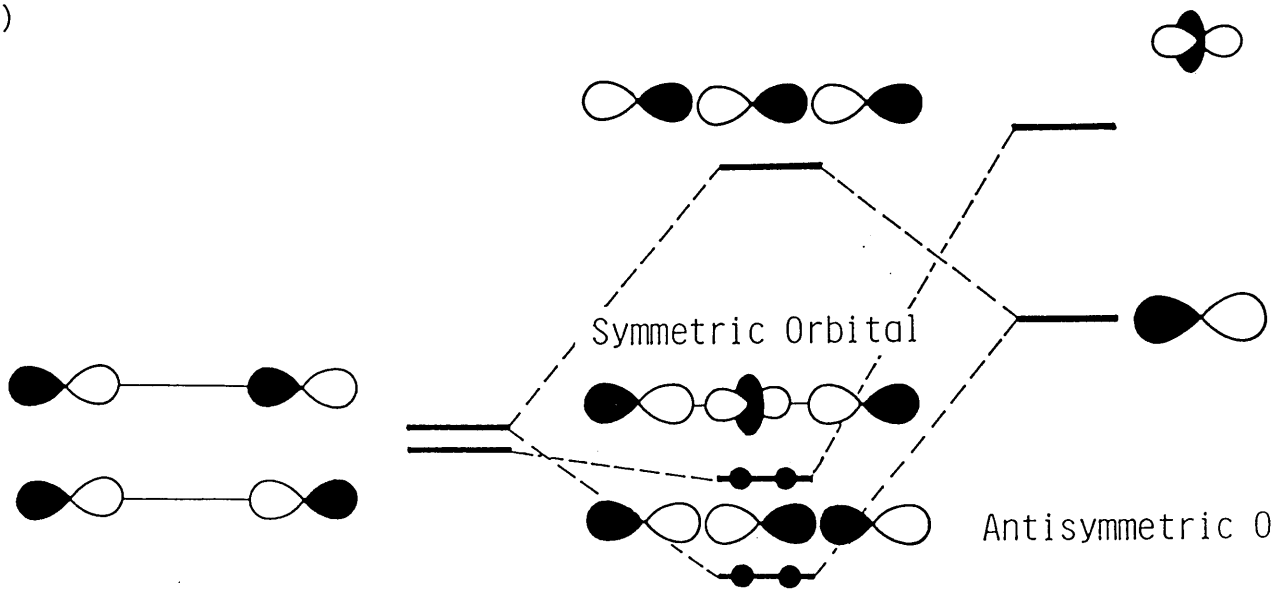

Apical ligand part Whole molecule Equatorial plane part

 Figure 15

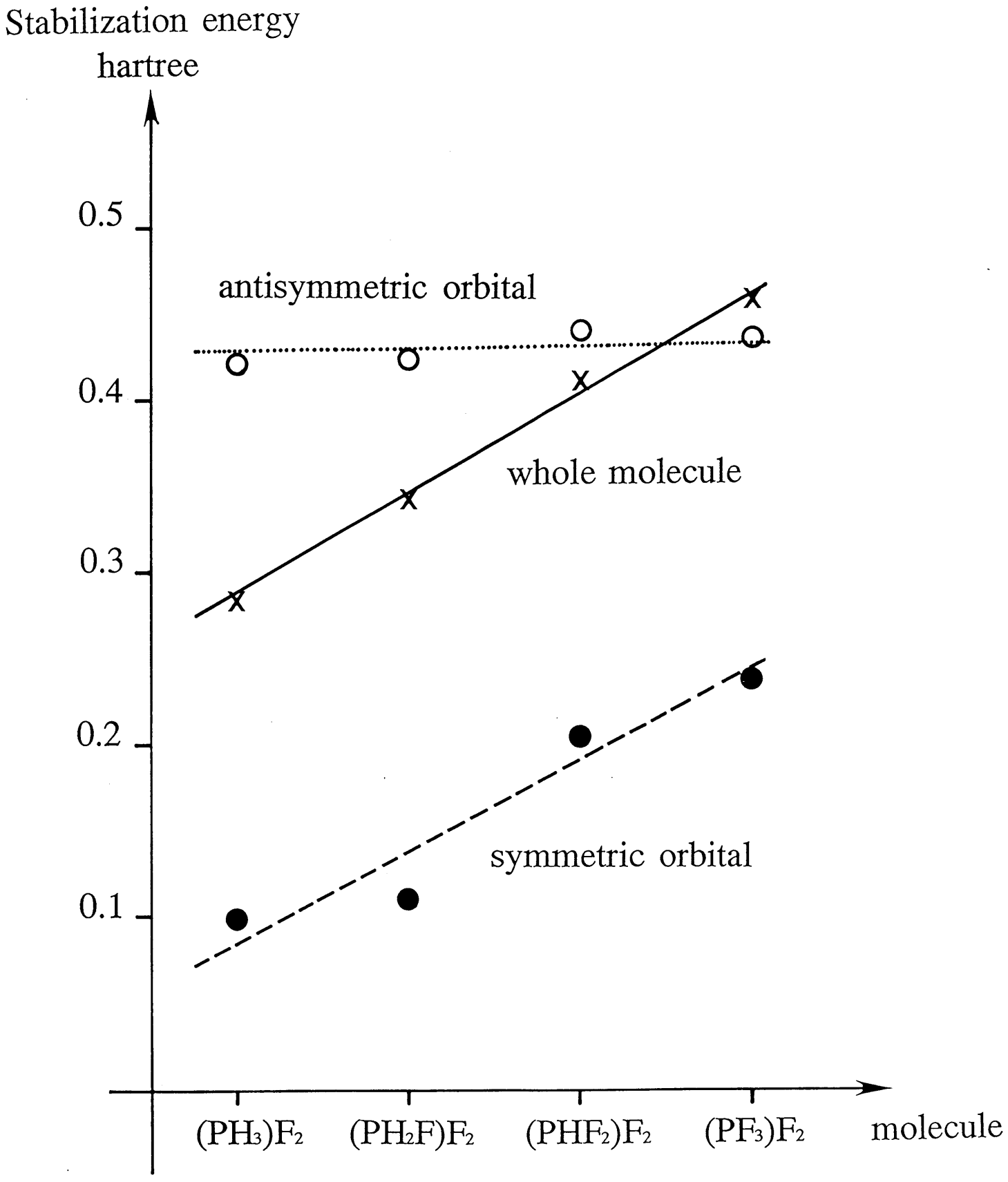
Stabilization energy
hartree
0.5
0.4
0.3
0.2
0.1
antisymmetric orbital
whole molecule
symmetric orbital
(PH3)F2
(PH2F)F2
(PHF2)F2
(PF3)F2
molecule

52 Figure 16

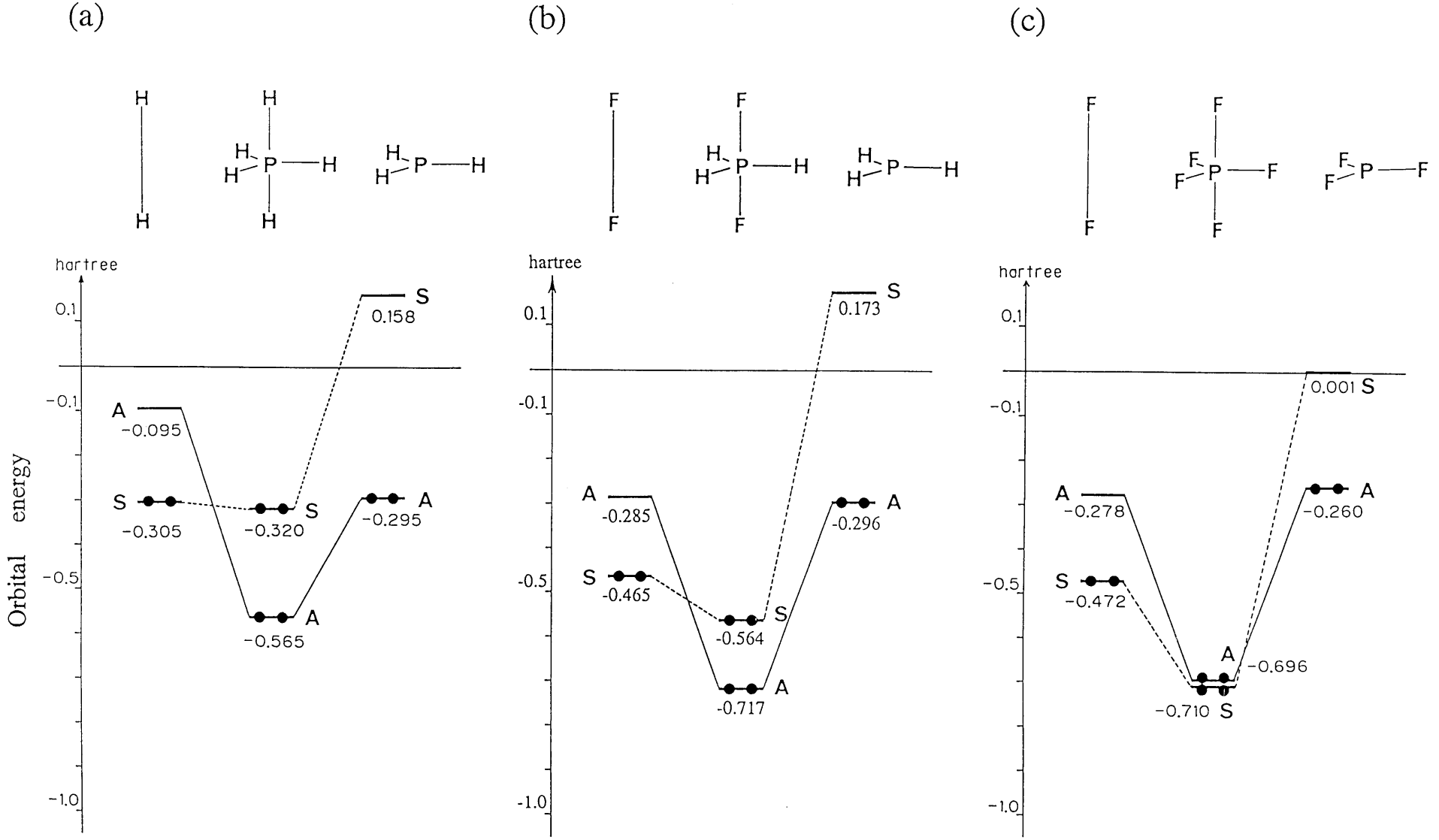
(a)
(b)
(c)
Orbital energy
hartree
0.1
-0.1
-0.5
-1.0
A
S
-0.095
-0.305
-0.320
-0.565
0.158
-0.295
-0.285
-0.465
-0.564
-0.717
0.173
-0.296
-0.278
-0.472
-0.710
-0.696
0.001
-0.260

Figure 17

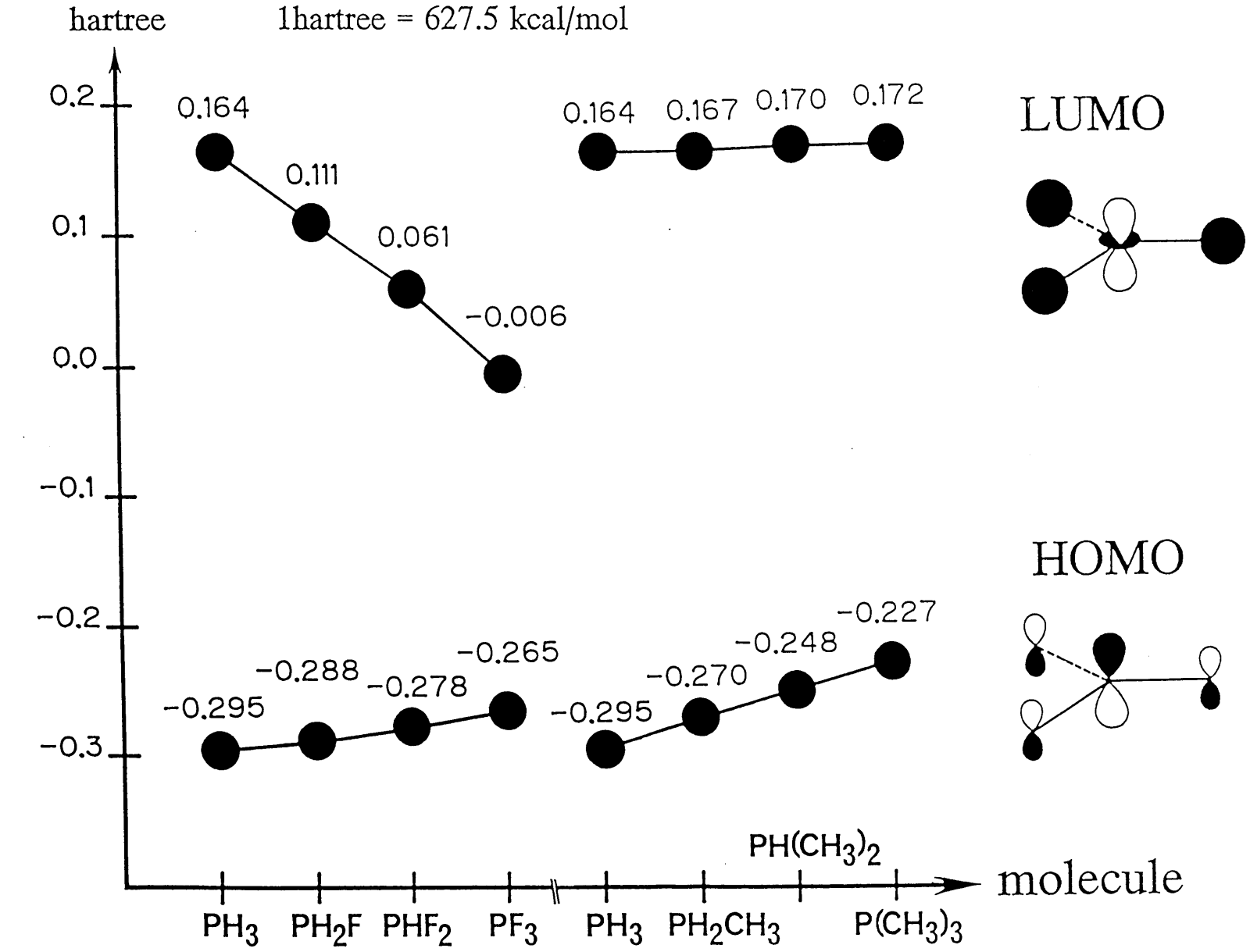
Orbital energy
hartree
1hartree = 627.5 kcal/mol
0.2
0.1
0.0
-0.1
-0.2
-0.3
0.164
0.111
0.061
-0.006
0.164
0.167
0.170
0.172
LUMO
HOMO
-0.295
-0.288
-0.278
-0.265
-0.295
-0.270
-0.248
-0.227
PH3
PH2F
PHF2
PF3
PH3
PH2CH3
PH(CH3)2
P(CH3)3
molecule

54 Figure 18

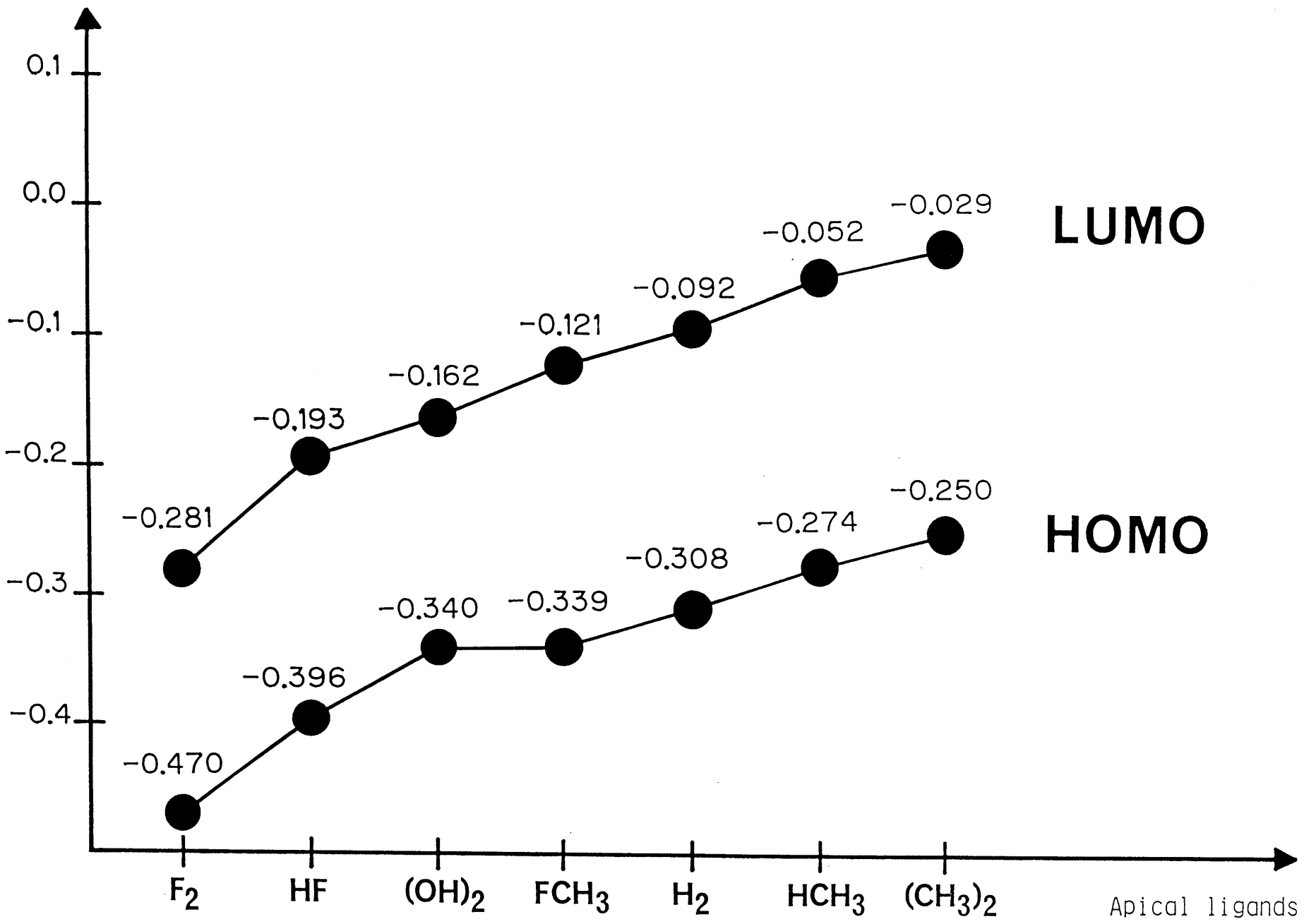
orbital energy (a.u.)
0.1
0.0
-0.1
-0.2
-0.3
-0.4
-0.029
-0.052
-0.092
-0.121
-0.162
-0.193
-0.281
LUMO
-0.250
-0.274
-0.308
-0.339
-0.340
-0.396
-0.470
HOMO
F2
HF
(OH)2
FCH3
H2
HCH3
(CH3)2
Apical ligands

Figure 19

Theoretical study on N_2O··· HF Complexes

K. Mogi, and T. Komine
Department of Chemistry, Faculty of Science, Nagoya University, Nagoya, Japan
and
K. Hirao
Department of Chemistry, College of General Education, Nagoya University, Nagoya, Japan
and
Institute for Molecular Science, Okazaki, Japan

Abstract

The stability and structure of bent and linear N_2O···HF complexes are studied by *ab initio* method. It is shown that the N_2O dipole moment is very sensitive to two bond lengthes and to the electron correlation. The theory predicts a minimum difference of 273 cm^{-1} between the isomers with the bent isomer more stable. The interconversion path connecting two isomers is also calculated. There is a low energy conversion path between linear and bent complexes. The barrier between two minima is estimated to be 497 cm^{-1} .

I. Introduction

The study of the weakly bound molecular complexes is of importance to a variety of chemical phenomena including inelastic energy transfer, photofragmention dynamics, theories of hydrogen bonding and transition between gas and condensed phase. A considerable research effort has been done to elucidate the full potential energy surfaces which govern these weak but important intermolecular forces.[1)]

Largely by virtue of their simplicity, complexes involving hydrogen fluoride have been the focus of many investigations both experimentally and theoretically.[2)] One of these is the study of HF complexes with CO_2 and N_2O. Aside from being isoelectronic, N_2O and CO_2 display many other similarities and both are important atmospheric compounds. However, N_2O has a small dipole moment of 0.160880 debye. Unlike CO_2, N_2O has a liquid phase at atmospheric pressure. N_2O is sweet tasting but CO_2 is tasteless.

It is well established both theoretically and experimentally that $CO_2 \cdots HF$ is a linear hydrogen bound species.[3)] On the other hand, in the $N_2O \cdots HF$ complexes, two distinct isomers are observed. This complex was first studied by Klemperer et al [4)] in a molecular beam electric resonance apparatus and indicated a decidedly bent structure, with the HF hydrogen bonding on the oxygen atom. High-resolutional IR spectroscopy by Lovejoy et al[5)] on the ν_1 HF stretch mode in $N_2O \cdots HF$, however, yields a spectrum of a linear hydrogen fluoride-nitrous oxide complex, red shifted by 61.4 cm^{-1} from the monomer. Subsequent investigation of complexes labeled with ^{15}N nitrous oxide unambiguously demonstrated that the hydrogen bond in these complexes was forming on the nitrogen atom.[6)] This behavior in $N_2O \cdots HF$ complexes constituted the first demonstration of two stable geometric isomers in a

hydrogen bonded system. The linear isomer has been observed and verified experimentally in a FT microwave spectrometer.[7] The bent isomer has also been observed by Miller et al [8] with a band origin red shifted by 83.2347 cm^{-1}.

How has *ab initio* calculation responded to the challenge posed by the new evidence? The earlier works assumed a bent structure rather than performing a completely free optimization. The SCF calculations of Sapse et al [9] with 6-31G and 6-31G** conformed the bent structure. Rendell et al [10] studied the nature of the SCF binding energy and concluded that the electrostatic term dominates. The first theoretical observation of two isomers was done by Handy et al.[11] They optimized two isomer at MP2 level, predicting that the linear structure to be more stable than the bent structure by 320 cm^{-1}. It is surprizing since the monomer dipoles are opposed in the linear structure. BSSE was calculated but did not change this conclusion.

Frisch and Del Bene [12] studied nitrous oxide and showed that the severe oscillation occurs in dipole moment and protonation energies with the perturbation series. The oscillation with order of perturbation theory includes a change of direction at each order. They further studied the binding energies of N_2O and HF using the various correlation method and demonstrated that the convergence of the MP expansion is erratic, predicting that the terminal nitrogen is the preferred binding site for the complexes at the MP2 and MP4 levels, in disagreement with SCF and MP3 and other models. They concluded that the bent structure is more stable by 0.6-1.1 kcal/mol than the linear structure.

N_2O and hydrogen bond formation with HF are still a challenging problem for theory. The difference in the structural and dynamical behavior

of these complexes make them attractive for further theoretical study. The binding energy in these complexes is dominated by electrostatic term caused by the dipole moments of two molecules. It is suggested that the N_2O dipole moment is even more sensitive to the electron correlation than that of CO. The most interesting is to study how the N_2O dipole moments depends on the two bond lengths in the region of minima.

The $N_2O\cdots HF$ is the only weakly bound complexes for which the microwave spectrum has been observed for two different structural isomers. The possible interpretation of this is that the binding energies of two isomers must be very close and the barrier to interconversion should be higher than 200 cm^{-1}. The relative well depths for these two isomers and the barrier to interconversion between them are still of considerable interest.

In this paper we will report the structures and energetics of the weakly bound hydrogen complexes formed from N_2O and HF. The dependence of N_2O dipole moment on the bond lengths is also studied from the theoretical point of view.

II. Computational Methods

The geometries were fully optimized at SCF level. The basis sets used in this study are Dunning's [4s2p] contraction for N, O and F, with [2s] contraction for H. [13] These are augmented by a polarization function on each atom (α_N=0.864, α_O=1.154, α_F=1.496, α_H=1.0). The calculations were also performed with [5s3p] augmented by double polarization functions (α_N=1.35, 0.45 , α_O=1.35, 0.45, α_F=2.0, 0.67, α_H= 1.5, 0.5) . [14] The electron correlation effect was estimated by single and double CI (SDCI) and MP2, MP3, MP4 methods. To compensate for the lack of size consistency of SDCI method, the

Davidson's corrections were included (SD(Q)CI).

III. Results and Discussions

A. N_2O dipole moment

Energies, bond lengths, and the dipole moments of N_2O computed using the two basis sets and various levels of electron correlation can be found in Table 1. The dipole moment values in parentheses are those calculated at the experimental geometry. Geometry optimization at the SCF/DZp level yields NN bond length (R_{NN}) of 1.096 Å and NO bond length (R_{NO}) of 1.187 Å. The CISD/DZp calculation gives R_{NN}=1.128 Å and R_{NO}= 1.198 Å. These have to be compared to the reported experimental values of R_{NN}=1.1282 Å and R_{NO} = 1.1842 Å. Thus, the SCF computes shorter bond lengths, which can be remedied by the inclusion of the correlation effect. The MP2 values differ markedly from the SDCI and the experimental results. Especially MP2 increases the SCF optimized R_{NN} by 0.0875 Å. The similar tendency can be found in the calculations with TZ2p basis sets.

The calculated dipole moments are more sensitive to the method employed. The SCF and SDCI give the correct sign $^{+}NNO^{-}$ although the computed dipole moments are too large compared to the experiment. The MP2, however, produces incorrect sign. The dipole moments at the experimental geometry did not change the tendency. Clearly the perturbation series oscillates badly for N_2O dipole moment as pointed by Del Bene. [12]

A simple resonance hydrid pictures of N_2O is

$$\textbf{(A)}\ N{\equiv}N^{+}\text{-}\ O^{-} \qquad \textbf{(B)}\ N^{-}{=}\ N^{+}{=}O$$

where (A) is the n-oxide valence bond formula and (B) is the germinal double bond formula. N_2O is best described by (A) with contribution of (B). The calculated geometries and dipole moments suggest that the SCF underestimates the contribution of (B) and MP2 overestimates the contribution of (B). The CISD includes (B) to a reasonable extent although still not sufficient.

To understand the dependence of the dipole moment both on the geometry of a molecule and on the correlation effect, we showed in Fig.1 by the contours which are for the energies and the dipole moments of N_2O. They show how these proprieties change with the two bond stretching coordinates. We can easily see how the minimum point changes due to the correlation effect. The SCF and SDCI gives similar energy contour maps while the MP2 gives quite different map. The SCF and SDCI optimized geometries lie in thee positive region of the dipole moment but the MP2 geometry is embedded in the negative region. The dipole moments has zero contours passing through regions not too distant from the optimized geometry. This indicates that the dipole moment if N_2O may change sign in the course of some low-energy vibrational excision. We can also see from the fact that the contour lines are nearly vertical that there is a greater sensitivity of the dipole moment to the R_{NO} than to the R_{NN}. The SCF contour lines are more denser than of MP2 and SDCI. The inclusion of the electron correlation make the dipole moment less sensitive to the geometry. The sign reversal of the MP2 dipole moment is undoubtedly a reflection of the poor MP2 geometry.

B. $N_2O\cdots HF$ Complexes

The total energies and the hydrogen bond energies for the complexes NNO-HF and FH-NNO computed relative to the isolated monomers and

relative to the supermolecule are summarized in table 2. The MP binding energies converge poorly leading to a change in the preferred site for hydrogen bond formation with HF. At second (MP2) and fourth (MP4) order, the nitrogen site is predicted to be the more basic site, whereas oxygen is favored at SCF, third order (MP3) and SDCI. The MP2 and MP4 overestimated the contribution of the germinal double bond formula (B). The bent form is more stable than the linear by 1.77 kcal/mol a the SCF level and by 0.77 kcal/mol at the SD(Q)CI level. The correlation effect to the binding energy is quite large. The MP3 increases the binding energy of NNO-HF by 0.34 kcal/mol while SD(Q)CI by 0.15 kcal/mol. The MP3 leads to stabilization of the FH-NNO by 1.00 kcal/mol and SD(Q)CI by 1.14 kcal/mol, compared to the SCF results. Obviously correlation effect is considerably greater in the linear form than in the bent form. It is interesting that the significant binding of the linear complex does not occur until correlation is included in theory.

The optimized geometries of both isomers are given in Fig.2. As the HF approaches to the oxygen end of N_2O, the N-oxide valence bond structure $\mathbf{N{\equiv}N^{+}\text{-}\,O^{-}}$ **(A)** will be favored over the germinal double bond structure $\mathbf{N^{-}{=}\,N^{+}{=}O}$ **(B)** . Thus, it is expected that hydrogen bonding leads to the structural shift of a shortening of the R_{NN} and a lengthening of the R_{NO}. It is also seen from the contour plots of dipole moments in Fig.2 that this structural shift corresponds to the increase of the dipole moments of N_2O. The calculated R_{NN} and R_{NO} are shortened (0.03 Å) and lengthened (0.07Å), respectively by forming a complex at oxygen. The geometrical change of R_{NO} bond is larger in magnitude than that of R_{NN}. This is consistent with the fact that the dipole moment of N_2O is more sensitive to the R_{NO} than the R_{NN}.

Analogous reasoning suggests that as HF approaches N_2O collinearly from the nitrogen end, the resonance structure (B) will be favored over (A), leading that the R_{NO} should be shorter. This shift decreases the dipole moment of N_2O. They confirms the prediction, with the R_{NO} decrease upon forming the hydrogen bond at oxygen being 0.007 Å. The hydrogen bond length is calculated to be 2.003 Å for the bent NNO-HF isomer and 2.181 Å for the linear FH-ONN isomer.

To examine the change in the charge distribution on complex formation, two difference density maps are drawn in Fig.3. The increase of the density around the oxygen in the bent complex and around the nitrogen in the linear complex and the decrease around the hydrogen in both complexes are all caused by the polarization interactions. The figure also gives the correct trend for the polarization and structural results as discusses above based on the resonance structures. The dipole moments of the complexes are listed in Table 3. The N_2O shows increases polarization in the complexes under the influence of the HF molecule.

Table 4 shows the harmonic frequencies for two isomers calculated at the SCF with DZp basis set. The experimental frequencies are obtained in an Ar matrix for the bent structure. The SCF overestimates the frequencies and we multiplied 0.88 to the computed frequencies to improve the agreement with the experiment. We see that the shifts are in reasonable agreement. The HF stretch in the bent complex is calculated to be 3891 cm^{-1} red-shifted 70 cm^{-1} from the calculated monomer frequency as compared to an experimental red shift of 83 cm^{-1}. The corresponding red shift for the linear complex is calculated to be 20 cm^{-1} and can be compared with the experimental red shift of 61 cm^{-1}. The stretching modes ν_3 of N_2O are blue shifted 59 and 7 cm^{-1} in

the bent and linear complexes, respectively. This suggests a stronger perturbation of N_2O by forming the bent complex than the linear complex.

In Fig. 4, the interconversion path connecting two isomers are shown schematically. The θ is the angle between the line of the NNO and HF centers of mass and the NNO axis. The θ=140 and θ=0 correspond to NNO-HF and FH-NNO isomers, respectively. The θ is varied from the 0 to 180 and each fixed θ all other geometric parameters are optimized. As can be seen from Fig.4, there is a low energy conversion path between linear and bent complexes. We found six stationary points in the range of θ=0-180. Vibrational analysis indicates that three correspond to the minima and three to the transition states. Two minima correspond to the linear and bent isomers and the remaining minimum corresponds to the meta-stable state. The three transition states connect these minima, respectively. The energies and geometries of these stationary points are given in Table 5 and Fig.5. In the linear and bent isomers, the negatively charged fluorine will tend to positive itself as far apart as possible from the negatively charged terminal nitrogen and oxygen since the main effect in the formation of the complex is electrostatic. Between two isomers, the fluorine attaches to the more positive central nitrogen. The complex, bound by electrostatic attraction, exhibits a meta-stable in energy at a distance of 3.094 Å between the fluorine and the positive nitrogen to which it is bound. The positive hydrogen in HF tends to positive itself closer to the negatively charges atoms. In the interconversion path, the motion of HF is rather complicated as shown in Fig.5. This arises primarily from the motion of hydrogen atom due to the small mass of the hydrogen compared to the fluorine atom. The hydrogen rotates around the fluoride involving the out-of-plane displacement near the meta-stable region.

The bent is more stable by 0.78 kcal/mol (273 cm^{-1}) than the linear and the barrier between two minima is estimated to be 1.42 kcal/mol (497 cm^{-1}) from the unstable linear complex. This barrier to interconversion is sufficient to be observed as two structural isomers in the microwave spectrum.

The linear structure with HF hydrogen bonding on the oxygen atom corresponds to the transition state (TS1) connecting two bent isomers. The barrier height is calculated to be 0.97 kcal/mol (339 cm^{-1}) at the SD(Q)CI level. This is related to a picture of a floppy, nonrigid hydrogen bond to an oxygen atom in the bent NNO-HF complex. On the other hand, the linear FH - NNO complex has only a single well, which leads to a stiff, linear hydrogen bond to the nitrogen atom.

Acknowledgments

The SCF, MP and SDCI methods were carried out using the Gaussian-86 program [15] and MONSTERGAUSS program [16]. The calculations were carried out on FACOM M782 and VP200 computers at Nagoya University Computational Center and on a HITAC S820 computer at Institute for Molecular Science. This study was supported in part by a Grant-in-Aid for Scientific Research from the Japanese Ministry of Educations, Science and Culture. The authors thank Dr. H. Wasada for useful discussions on this study.

References

1 "Structure and Dynamics of Weakly Bond Molecular Complexes" ,edited by A. Weber ,NATO ASI Series C, Vol 212

2 a) D. J. Nesbitt, Chem.Rew, **1988** , *88*, 843

b) A. C. Logen, and D. J. Millen, J. Chem. Rev, **1986** , *86*, 635 and their in.

c) G. T. Fraser and A. S. Pine, J.Chem.Phys. **1989** , *91*, 637

3. C. M. Lovejoy, M. D. Schuder and D. J. Nesbitt , J. Chem. Phys. **1987** , *86*, 5337

4. a) C. H. Jonyer, T. A. Dixon, F. A. Baiocchi and W. Klemperer J. Chem. Phys. **1981** , *74*, 6550

b) L. Andrews, and G. L. Johnson, J. Chem. Phys, **1982** , *76*, 2875

5. C. M. Lovejoy and D. J. Nesbitt, J. Chem. Phys. **1987** , *87*, 1450

6. C.M.Lovejoy and D.J.Nesbitt, J.Chem.Phys, **1989** , *90*, 4671

7. a) S. G. Kukolich, R. E. Bumgarner and D. J. Pauley, Chem. Phys. Lett, **1987** , *141*, 12

b) S.G.kukolich and D.J.Pauley, J.Chem.Phys, **1989** , *90*, 3458

c) S.G.Kukolich and D.J.Pauley, Chem.Phys.Letts, **1989** , *131*, 403

8. D. C. Dayton and R.E. Miller, Chem. Phys. Lett, **1988** ,*143*, 580

9. A. M. Sapse and J. M. Howell, J. Chem. Phys. **1983** , *78*, 5738

10. a)A.P.Rendell, G.B.Bacskay, and N.S.Hush, Chem.Phys.Lett, **1985** , *117*, 400

b) G. J. B. Hurst, P. W. Flowler, A. J. Stone, and A. D. Buckingham Int. J. Quant. Chem, **1986** , *24*, 1223

11. I. L. Alberts, N. C. Handy and E. D. Simandiras, Theor. Chim. Acta **1988** , *74*, 415

12. a) M. J. Frisch, and J. E. D. Bene, Int. J. Quant. Chem: Quant. Chem. Symposium, **1989** , *23*, 363

b) J. E. Del Bene, J. A. Stahlberg, and I. Shavitt, Int. J. Quant. Chem: Quant.Chem.Symposium, **1990** , *24*, 455

13. T. H. Dunning, Jr, J. Chem. Phys., **1970** , *53*, 2823

14. T.H.Dunning, Jr, J.Chem.Phys, **1971** ,*55*, 716

15. M.J.Frisch, J.S.Binkley, H.B.Schlegel, K.Raghavachari, C.F.Melius, R.L.Martin,J.J.P.Stewart, F.W.Bobrowicz, C.M.Rohlfing, L.R.Kahn, D.J.Defrees, R.Seeger, R.A.Whiteside, F.J.Fox, E.M.Fluder, S.Topiol, and J.A.Pople, "Gaussian-86", Carnegie-Mellon Quantum Chemistry Publishung Unit, Carnegie-Mellon University, Pittsburgh PA 15213

16. M. Peterson and R. Poirier, Universuty of Toronto Chemistry Department, Toronto, Ontario, Canada, Version: Aprol 1981

Table 1 Energies, bond lengths and dipole moments of N_2O at the optimized geometry

Method		Energy	R(N-N)	R(N-O)	dipole moment (debye) (A)	(B)
DZP	SCF	-183.715177	1.0956	1.1868	0.819 (0.661)	
	MP2	-184.269094	1.1831	1.2009		-0.135 (-0.064)
	CISD	-184.194723	1.1276	1.1983	0.395 (0.303)	0.473 (0.368)
TZ	SCF	-183.753388	1.0815	1.1712	0.709 (0.621)	
+DP	MP2	-184.390869	1.1557	1.1822		-0.173 (-0.070)
	CISD	-184.305255	1.1059	1.1776	0.346 (0.313)	0.387 (0.353)
experimentalvalue			1.1282	1.1842	0.161	

Values in parentheses are dipole moments calculated at the experimental geometry.

(A) calculated using electronic dipole operator

(B) calculated using first derivative methods

Table 2 Total energies of NNO-HF and FH-NNO

The calculated energies of NNO-HF

Methods	Total energy (a.u.)	Stabilization Energy (kcal/mol)
SCF	-283.820762	-2.98
MP2	-284.641780	-2.46
MP3	-284.616186	-3.32
MP4(SDTQ)	-284.680796	-2.50
SDCI	-284.519661	-3.19
SD(Q)CI	-284.636136	-3.13

The calculated energies of FH-NNO

Methods	Total energy (a.u.)	Stabilization Energy (kcal/mol)
SCF	-283.818396	-1.21
MP2	-284.643163	-3.04
MP3	-284.614873	-2.21
MP4(SDTQ)	-284.682021	-2.98
SDCI	-284.518450	-2.15
SD(Q)CI	-284.630820	-2.35

Table 3 Dipole moments of the complexes for NNO-HF, FH-NNO (debye)

	NNO-HF	FH-NNO	HF
SCF	3.040	1.791	1.95
CISD	2.453	1.702	1.87
experiment	2.069		1.91

The N_2O shows in creased polarization under the influence of the HF molecules.

Table 4 Vibrational frequencies of the complexes of HF with NNO at SCF/DZp

species	mode	calculated		shift	experiment	shift
HF	ν1	4505	(3961)		3961	
NNO	ν1	593			593	
	ν2	1198			1202	
	ν3	2284			2285	
NNO-HF	"bent"	30				
	"stretch"	126				
	"shear"	351,	439			
	"ν1(N_2O)"	577,	590	(-16,-3)	583	(-5)
	"ν2(N_2O)"	1170		(-27)	1307	(+24)
	"ν3(N_2O)"	2341		(+59)	2250	(+29)
	"ν1(HF)"	3891		(-70)	3878	(-68)
FH-NNO	"bent"	33				
	"stretch"	84				
	"shear"	268				
	"ν1(N_2O)"	600		(+7)		
	"ν2(N_2O)"	1228		(+31)		
	"ν3(N_2O)"	2289		(+7)		
	"ν1(HF)"	3941		(-20)	3900	(-61)

Table 5 Binding energies of the stationary points (kcal/mol)

Methods	TS1	NNO-HF	TS2	Meta-stable	TS3	FH-NNO
SCF	2.17	2.98	0.49	0.49	0.39	1.21
MP2	1.66	2.46	1.02	1.18	1.18	3.04
MP3	2.34	3.32	0.95	1.01	0.91	2.21
MP4(SDTQ)	1.63	2.50	0.98	1.13	1.14	2.98
SDCI	2.31	3.19	0.85	0.92	0.82	2.15
SD(Q)CI	2.16	3.13	0.93	1.01	0.94	2.35

Figure Captions

Fig.1

Contour plots of the energy and the dipole moment of N_2O as a function of the two bond lengths. The top figure is the energy. The relative energy count from the optimized structure in kcal/mol. The lower figure is the dipole moment. Magnitudes are quoted in debye(D).

Fig.2

Geometries of NNO-HF and FH-NNO with DZP basis sets. Bond lengths are Å. Bond angles are in degree. Value in parenthesis are Net charges of the complexes. The R(N-N) and R(N-O) bonds are shorten and lengthened, respectively, by forming a complex at oxygen. However, the R(N-N) bond is lengthened, and the R(N-O) bond is shortened by N-complex.

Fig.3

Differential density maps, supermolecule - isolated molecules, obtained with the DZP basis sets. Full lines show the increase of electronic density and broken lines the decrease. Values of contour lines are $\pm$ 0.0040, $\pm$ 0.0020, $\pm$ 0.0005, and $\pm$ 0.00025, respectively, from the inside out.

Fig.4

Interconversion path connecting two isomers NNO-HF and FH-NNO with SCF and SDCI method

Fig.5

Geometries of transition states and meta-stable state of the complexes of NNO-HF optimized with DZP basis sets. Bond lengths are Å. Bond angles are in degree. Value in parenthesis are Net charges of the complexes. The transition vectors indicate the reaction pass way of each transition states.

Fig.1 Contour plots of the energy and the dipole moment of N_2O

(a) Energy

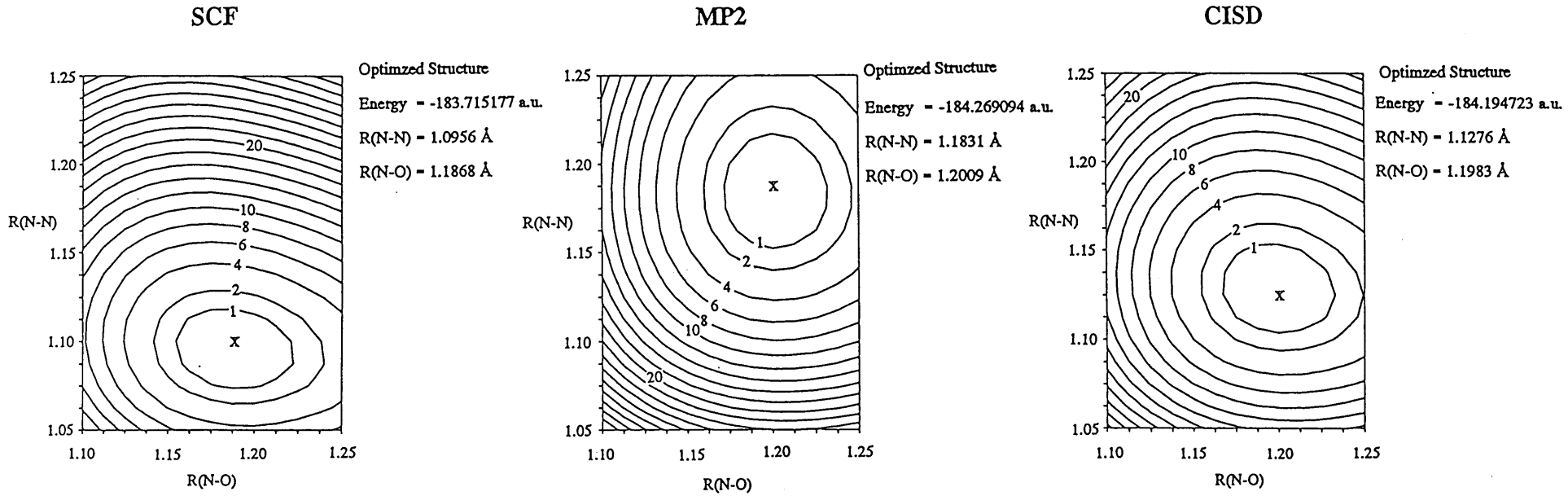

(b) Dipole Moment

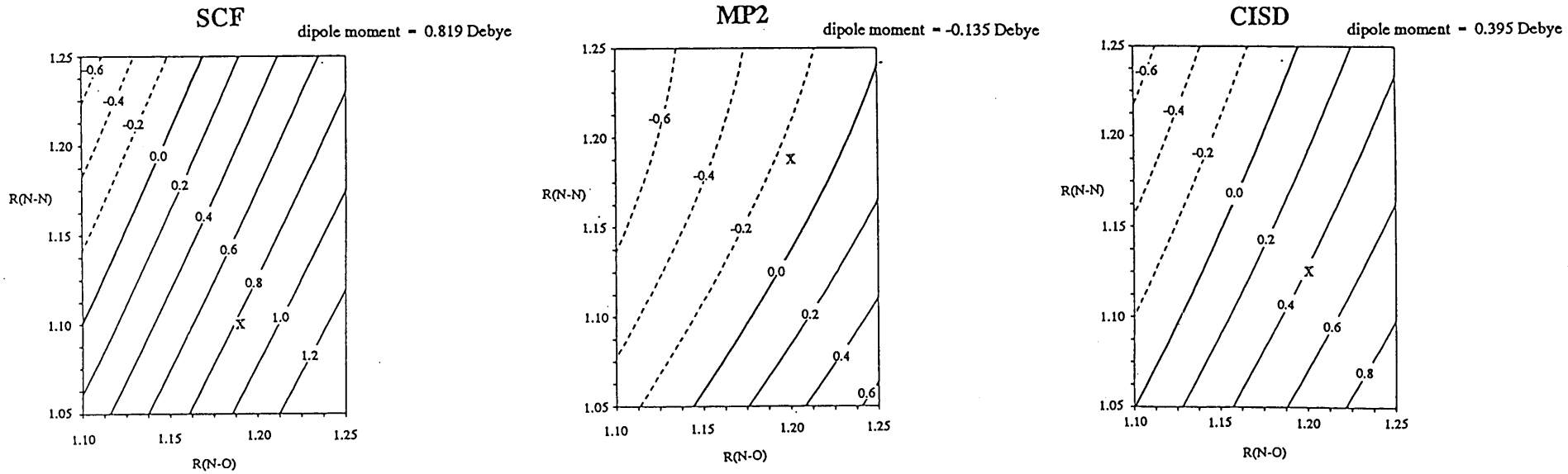

Fig.2 Geometries of NNO-HF and FH-NNO

(a) NNO-HF

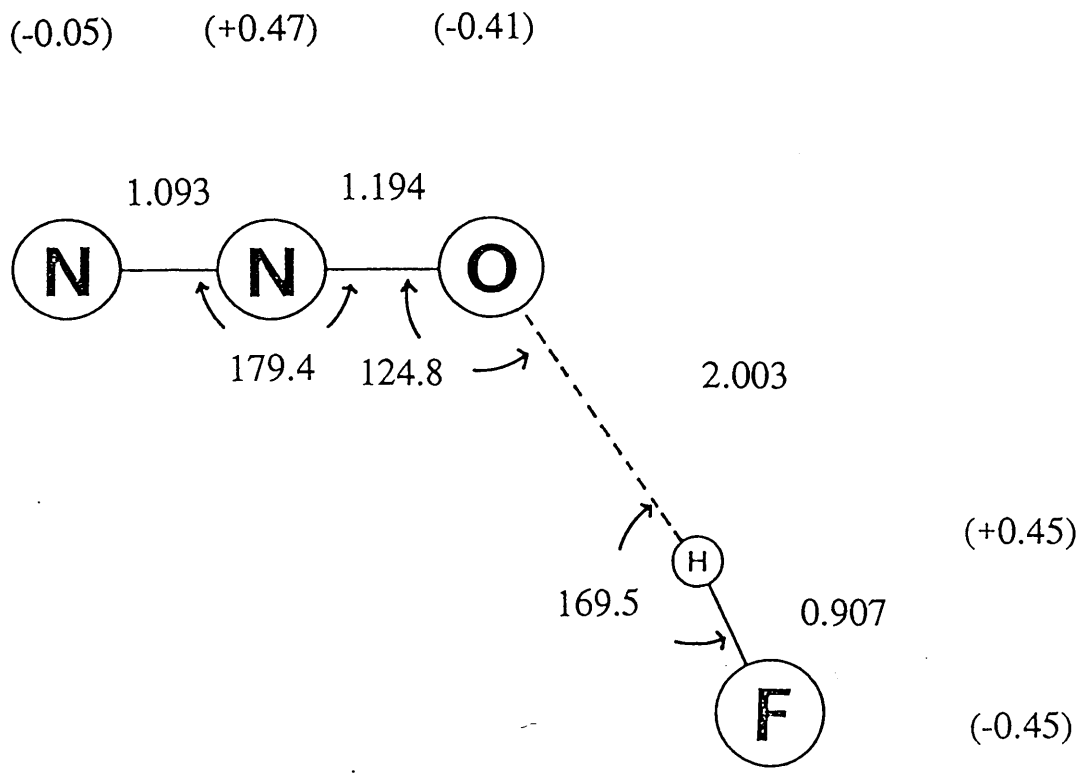

(b) FH-NNO

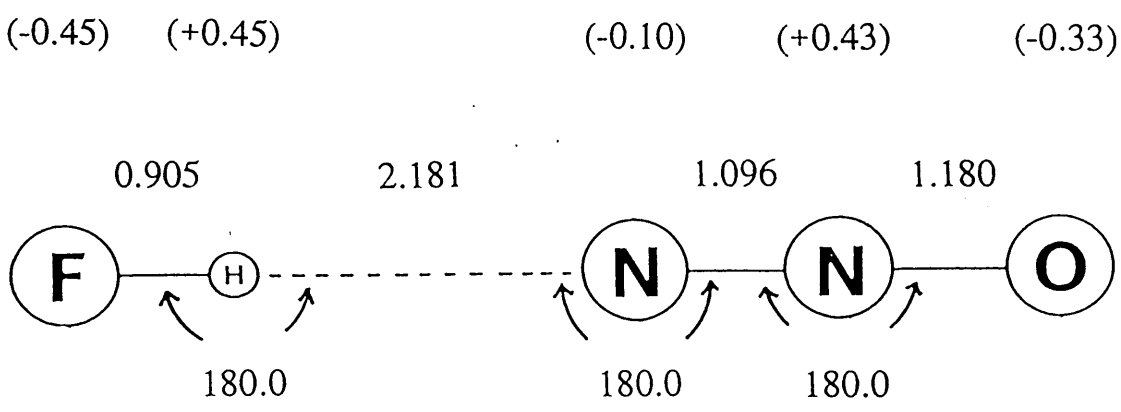

Fig.3 Differential density maps

NNO-HF

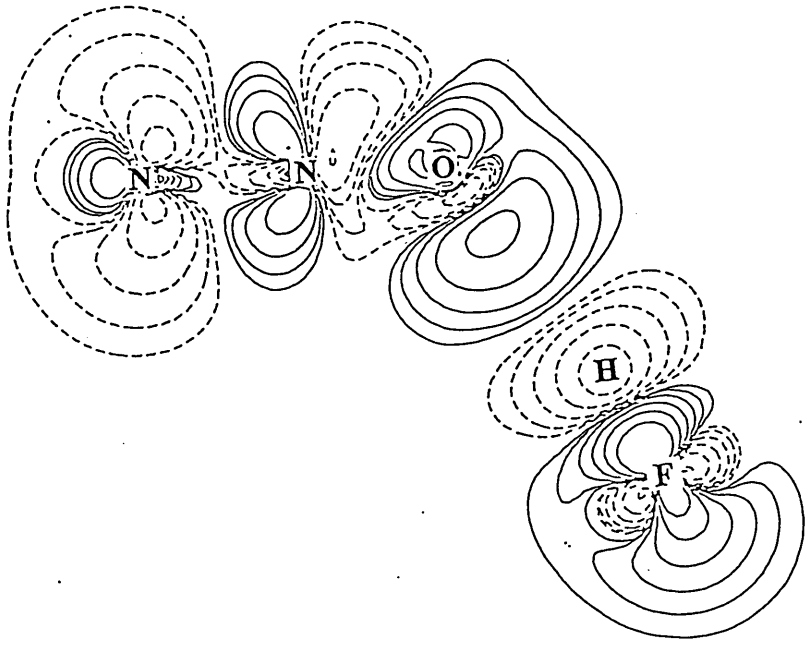

ONN-HF

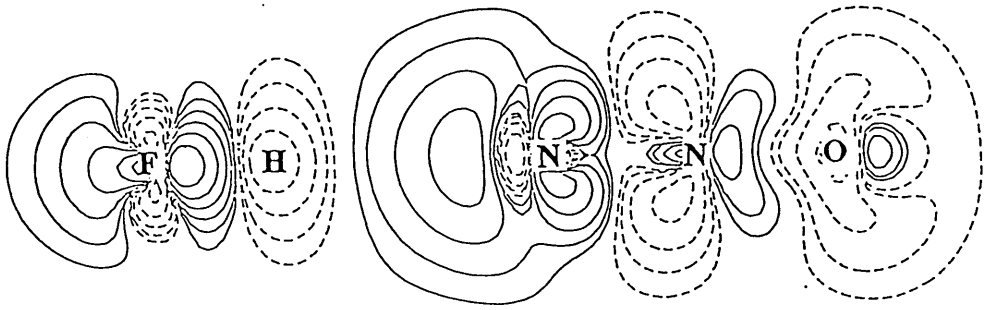

Fig. 4(a) **Isomerization reaction path of NNO-HF**

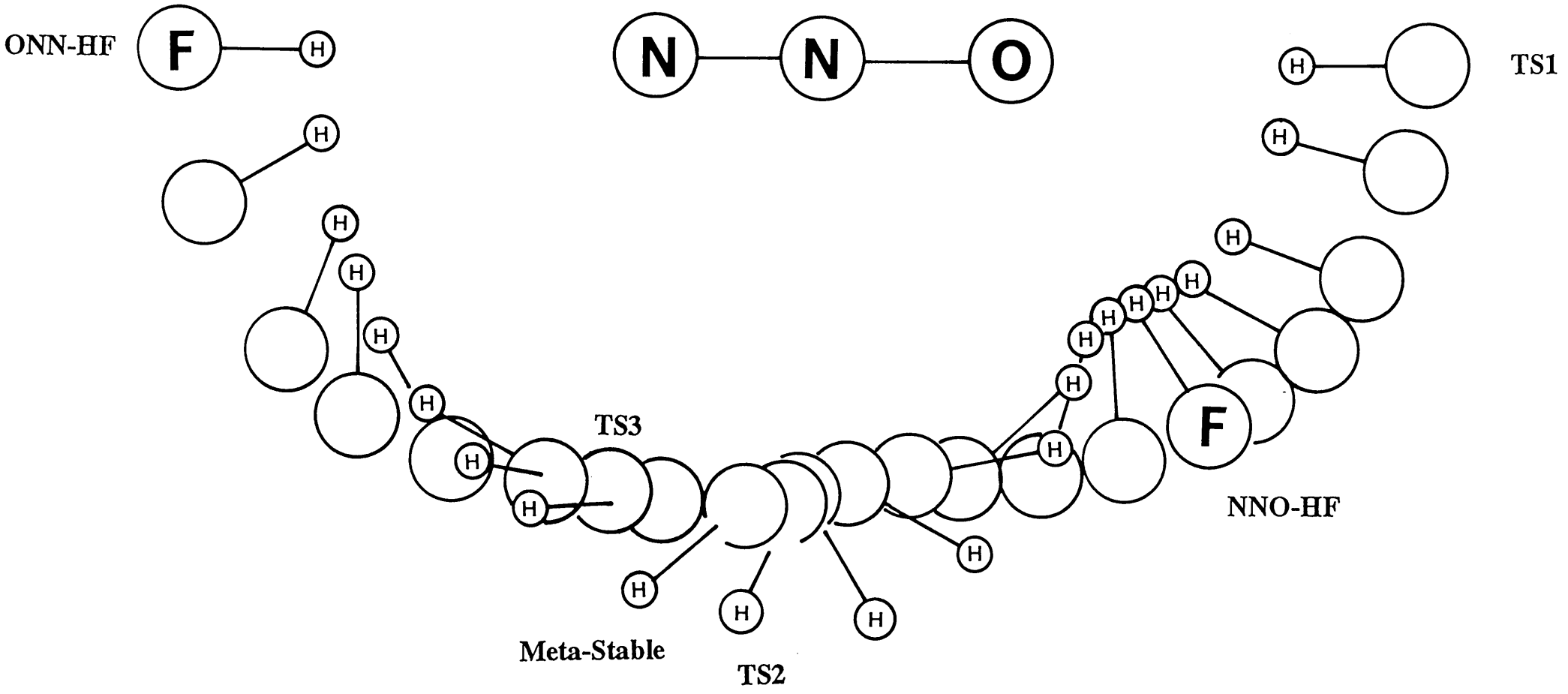

Fig. 4(b) Potential Energy Surface of NNO-HF

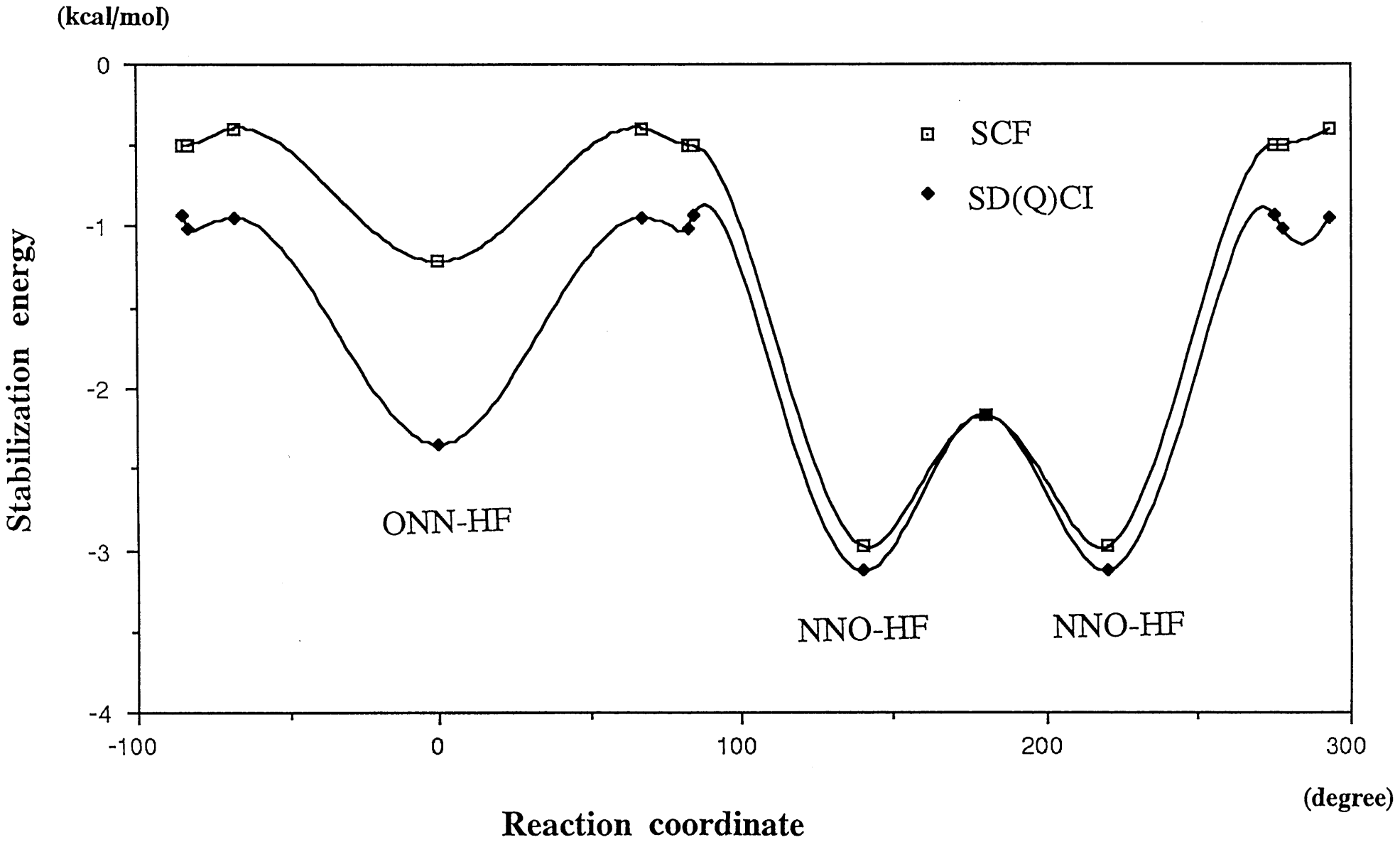

Fig. 5 Geometries of transition states and meta stable state

(a) Transition State No.1

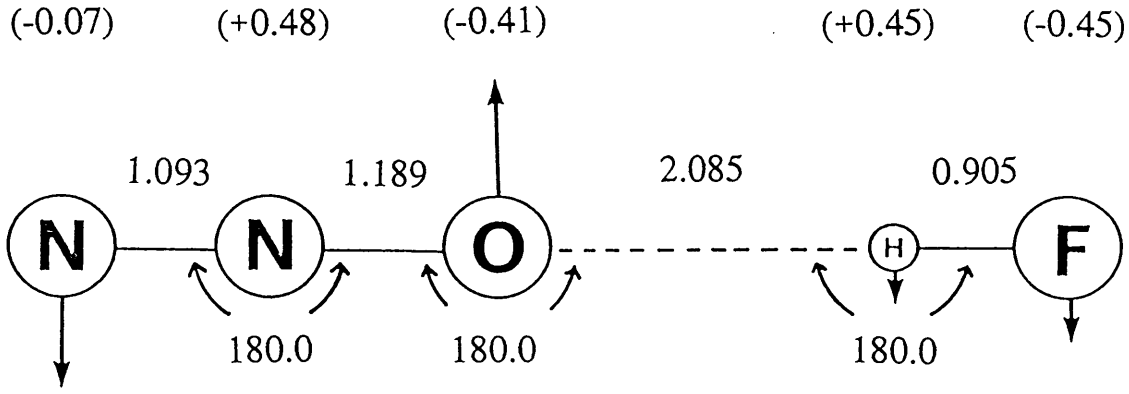

(b) Transition State No.2

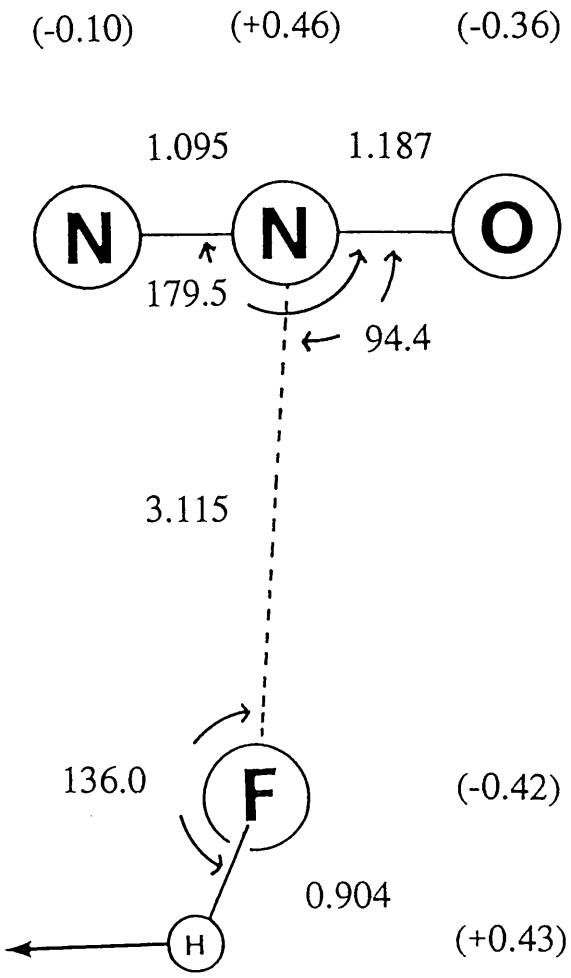

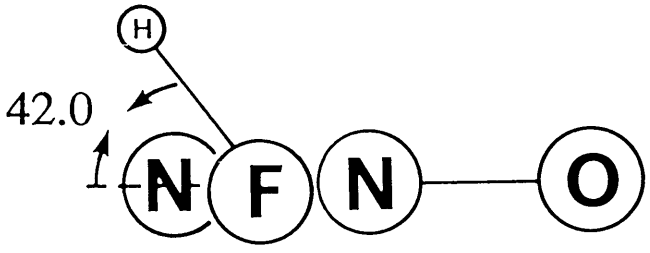

(c) Meta-stable state

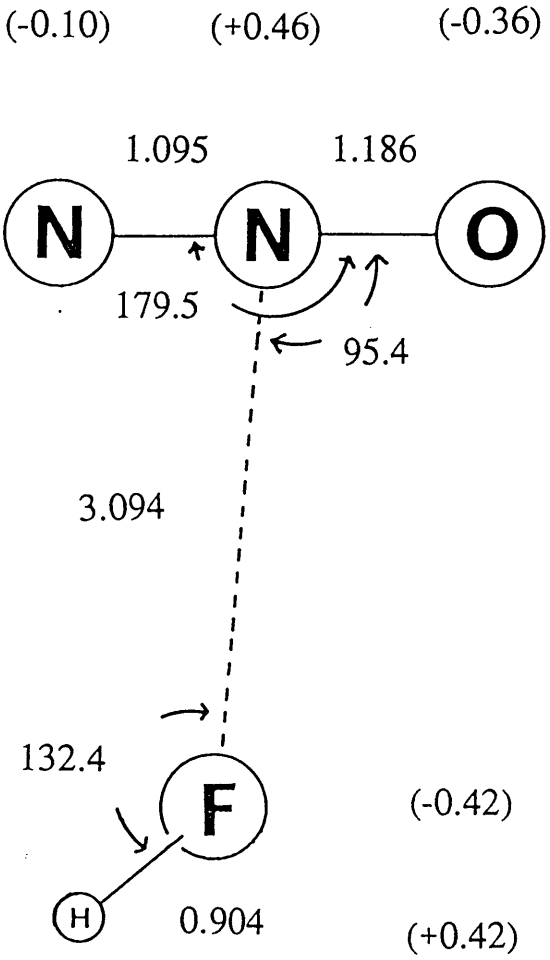

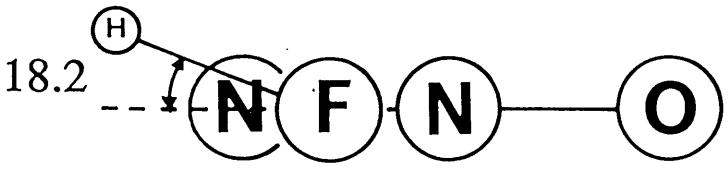

(d) Transition State No.3